UiT The Arctic University of Norway

Faculty of Biosciences, Fisheries and Economics

Department of Arctic and Marine Biology

Effect of light quality on the biosynthesis of flavonoids and sugars in bilberry (*Vaccinium myrtillus* L.)

Amos Samkumar Rajan Premkumar

A dissertation for the degree of *Philosophiae Doctor* - December 2021

Effect of light quality on the biosynthesis of flavonoids and sugars in bilberry (*Vaccinium myrtillus* L.)

Amos Samkumar Rajan Premkumar

A dissertation for the degree of *Philosophiae Doctor*

December 2021

Table of Contents

1 Acknowledgements

The study was carried out at Climate lab (Holt) that belongs to the Department of Arctic and Marine Biology (AMB), Faculty for Biosciences, Fisheries and Economics (BFE) at UiT The Arctic University of Norway under the supervision of Dr. Laura Jaakola, and Dr. Katja Karppinen, in addition to Dr. Inger Martinussen from the Norwegian institute of Bioeconomy Research (NIBIO). This PhD research project was funded by the BFE faculty.

First of all, I would like to thank Dr. Laura for providing me the opportunity to do my PhD studies in Norway and for her continuous supervision and support throughout the period of four years. Her constant motivation, enthusiasm, positive attitude and her immense expertise in berry research had helped me tremendously. Her support in the beginning of my PhD studies had helped me to settle-in and tackle the challenges faced. I also thank her for introducing me to excellent collaborators that allowed me to travel to the other part of the world as part of my research work.

I also thank Dr. Katja, my co-supervisor for all her inputs, guidance and support. The frequent discussions and team meetings with her helped me in fine-tuning the project findings. Her inputs on manuscript discussions had helped me a lot in writing and shaping up the final publications. I also thank Dr. Inger, my second co-supervisor for her support, cheerful attitude and sharing excellent ideas during manuscript discussion and team meetings.

I would like to thank Dr. Richard Espley for the excellent opportunity to work in Plant and Food Research (PFR), New Zealand. The stay played a very big part in this PhD journey. I thank his research group members, Dan for introducing me to the world of Bioinformatics, Andrew for helping me with chromatography and other members from color and health research group, PFR. I met some excellent researchers in anthocyanin research at PFR, which opened up new exciting ideas during my pandemic-hit research stay. The PhD student - travel grant from BFE faculty is greatly acknowledged for this stay.

I thank all the members of Microorganisms and Plants research group, especially Dr. Kirsten for her help during RNA-seq and allowed me to present in few plant-group seminars. Thanks to, Leidulf for all the technical help and setting up the experiments in the Phytotron facility. I thank all the student members who shared the office space in Holt, Priyanka, Joel, Florence, Bilal, Corine, Arpine and Maneh for the fantastic time together. I also enjoyed my time teaching basic molecular lab techniques to the incoming undergrad exchange students of Klimalab. I would like to thank other members of Klimalab, Jørgen for the excellent joint-review article and Ewelina, Tor, Anne-Linn for their friendly support.

A special thanks to my Karate club friends and my Indian friends in Tromsø, especially, Dr. Jessin & Dr. Sudhagar for all the care and affection, Dr. Swapnil & Nivedita for the fantastic time together and memorable trips. Thanks to all my friends back home in Chennai, Coimbatore (TNAU) and New Delhi (NRCPB), India. Thanks to the stress-busting weekly group calls from my best friends, Anbu, Mani and Pradeep. Thanks to my friends, Blessy, Finny, Shiny, Sruthi, Dr. Satheesh (Shanghai Center for plant stress biology), Dr. Jothikumar (Univ. Lund), Dr. Saminathan (GenØk), Shunmathi (NTNU) for their support and encouragement. The PhD journey wouldn't have been possible without the blessings, love and support of my parents, Visithira & Rajan, my late grandparents, my brother, Dr. Asher's family and my niece Brenda. I will really miss some of my loved ones who lost their lives in the pandemic and you all stayed in my thoughts. Last but not the least, I thank the Lord almighty for all the countless blessings in my life and it is God who arms me with strength and keeps my way secure (Psalms 18:32).

2 Abstract

Berries are abundant in bioactive compounds. Bilberry or European blueberry (*Vaccinium myrtillus* L.) is in particular gaining worldwide attention being one of the best natural sources of antioxidant rich phenolics that accumulate in both skin and flesh during fruit ripening. Alongside, the ubiquitous presence of anthocyanins and related flavonoids, it also contains other compounds such as carotenoids, stilbenes, terpenoids, vitamins and sugars. Especially flavonoids and sugars have major effect of fruit quality. Beside the genetic adaptation by the latitude-based cultivars and ecotypes, altering environmental conditions play a major role in determining the bioavailability of these compounds. Especially, the light quality impacts several secondary metabolic processes, thus by interacting with the number of known positive regulators and repressors of light signaling.

The thesis is focused on understanding the biosynthesis and regulatory mechanisms of the key quality compounds, flavonoids and sugars, in bilberry in response to different light qualities from the photosynthetically active radiation (PAR) spectrum. The light quality experiments were carried out in controlled conditions by mimicking single wavelength light spectra of red, blue and far-red using LED-light systems.

The promising results showed that indeed supplemental light wavelengths have a positive effect on anthocyanin and sugar biosynthesis in bilberries. Especially, delphinidins were found to be the most reactive class of anthocyanins in response to red light treatments, which increased the concentration several fold in fully ripe berries. The transcriptomic data revealed that the abscisic acid (ABA) biosynthesis and signaling was found to regulate the anthocyanin accumulation, where even the ABA degrading enzyme, ABA-8'-hydroxylase, acted as positive signaling factor. However, the results showed a differential effect or opposite response pattern towards red and blue light in berries which are ripening independently of mother plant to that of naturally attached ripening berries. Interestingly, the blue light influenced the anthocyanin biosynthesis in detached berries to the most, and resulted in highest anthocyanin levels quantified in fully ripe bilberries. The study also showed the effect of light quality on sugar metabolism from the differentially expressed genes (DEGs) data, where both red and blue light influenced the starch and sucrose metabolism. Supplemental red light also increased the amount of sugars in ripe bilberry.

The findings of this study will drive-forward the plant research communities towards better understanding on the effect of light on fruit ripening and improving quality. The results can also be further utilized in future commercial breeding programs or cultivation practices of wild *Vaccinium* berries with improved value-added properties.

Keywords: *Vaccinium myrtillus* L., bilberry, anthocyanins, flavonoids, sugar, transcriptome, light quality, LED lights, spectrum, abscisic acid

3 List of Papers

The thesis is based on papers (I-III). Paper I is reprinted from the journal publisher, John Wiley & Sons Ltd. under creative commons attributions license CC-BY.

Paper I

Red and blue light treatments of ripening bilberry fruits reveal differences in signalling through abscisic acid-regulated anthocyanin biosynthesis

Amos Samkumar, Dan Jones, Katja Karppinen, Andrew P. Dare, Nina Sipari, Richard V. Espley, Inger Martinussen, Laura Jaakola

Plant, Cell & Environment, 44(10), 3227-3245. https://doi.org/10.1111/pce.14158

Paper II

Flavonoid biosynthesis is differentially altered in detached and naturally ripening attached bilberries in response to spectral light quality

Amos Samkumar, Katja Karppinen, Tony K. McGhie, Richard V. Espley, Inger Martinussen, Laura Jaakola

Prepared for submission to ***Journal of Photochemistry and Photobiology B:Biology***

Paper III

Insights into sugar metabolism during bilberry (*Vaccinium myrtillus* L.) fruit development

Amos Samkumar, Katja Karppinen, Binita Dhakal, Inger Martinussen, Laura Jaakola

Prepared for submission to ***Physiologia Plantarum*** (Special issue*: Plant sugar metabolism, transport and signaling in a challenging environment*)

4 Abbreviations

ABA- Abscisic acid

HPLC- High performance liquid chromatography

LC-MS- Liquid chromatography coupled with mass spectrometry

FW- Fresh weight

DW- Dry weight

CHS- Chalcone synthase

ANS- Anthocyanidin synthase

PAL- Phenylalanine ammonia-lyase

DFR- Dihydro-flavanol reductase

F3H- Flavanone 3-hydroxylase

F3′H- Flavanone 3′ hydroxylase

F3′5′H - Flavanone 3′5′ hydroxylase

UFGT- UDP glucose: flavonoid-3-O-glucosyltransferase

Dp- Delphinidins

Cy- Cyanidins

DEG- Differentially expressed genes

MBW- MYB, bHLH, WD-40

MYB- Myeloblastosis

bHLH- basic helix-loop-helix

TF- Transcription factors

SNARE- Soluble N-ethylmaleimide-sensitive factor attachment protein receptor

ABC- ATP-binding cassette transporters

MATE- Multidrug and toxic compound extrusion transporters

5 Introduction

The demand for 'super-foods' in human diet rich in bioactive compounds is increasing among consumer markets, including fresh fruits. Berries in general are widely regarded as one of the best sources of health-beneficial compounds. They are consumed as either fresh during the season or in processed form and desired by health-conscious consumers worldwide. Among the small berries, a US market study shows that the blueberries (*Vaccinium* spp.) are the second-most popular in consumption after strawberries (*Fragaria* spp.), followed by blackberries and raspberries (*Rubus* spp.) in minor demand (Sobekova et al., 2013). These small berries are abundant in anti-oxidant rich phenolic compounds such as anthocyanins, a wide range of organic acids, vitamins (ascorbic acid), and taste enhancing compounds such as volatiles and sugars (Skrovankova et al., 2015; Zorzi et al., 2020). The berry phenolic compounds are majorly attributed to many human health benefits such as protection against degenerative and cardiovascular diseases (Paredes-López et al., 2010). Several studies have shown that abiotic factors, specifically light conditions play a major role in the determination of concentration and composition of phenolics (Teixeira et al., 2013; Bian et al., 2015; Sharma et al., 2019) Hence, the knowledge and understanding on regulatory mechanisms against specific spectral light qualities is important in improving the bioavailability of berry phytochemicals.

5.1 *Vaccinium* berries

The family of Ericaceae consists of around 120 genus and over 4000 species of flowering plants (Stevens et al., 2004). They are distributed from the subarctic tundra to the temperate, tropical regions and usually thrive on open barren lands as shrubs or small trees, and many are characterized as cultivated species (Fang et al., 2007). The fused petals in the shape of an urn are a very common feature of Ericaceae family flowers (Glimn-Lacy et al., 2006). The *Vaccinium* genus of this family consists of more than 400 species of wild and cultivated species that produce small to medium-sized fleshy berries (Hancock et al., 2003). The important commercial species are coming from the sections *Cyanococcus* (blueberries) and *Oxycoccus* (cranberries). Other important species include lingonberries (*V. vitis-idaea),* lowbush blueberries (*V. angustifolium),* highbush blueberries (*V. corymbosum),* rabbiteye blueberry (*V. virgatum)* and bilberries (*V. myrtillus)* (Song & Hancock, 2011; Debnath & Goyali, 2020). All the berries from this genus are edible and easily palatable. The skin color ranges from pink to blue and even the flesh is deeply colored in some species. The taste of berries begins to develop in late ripening stages and differs slightly between sweet to tart flavor (Milivojevic et al., 2012). The ploidy levels vary from diploid to hexaploid across these species, and new genome datasets have been made publicly available recently (Genome database for *Vaccinium*, https://www.vaccinium.org/). All the cultivars of above mentioned *Vaccinium* species differ widely in the amount and composition of phenolic compounds

(Moyer et al., 2012; Li et al., 2017). These berries are utilized mostly in the human diet but the commercial aspect also depends of interest on nutraceutical and cosmetic industries.

5.2 Wild bilberry (*Vaccinium myrtillus* L.)

Bilberries are regarded as one of the best natural sources of anthocyanins. The perennial deciduous, dwarf shrub is native to Northern Eurasian regions and typically grows in spruce, birch and mountainous forests of arctic alpine region. The plant thrives to grow up to 30 cm (≈1 foot) high mostly in acidic moist soil and prefers semi-shade under tree covers (Chu et al., 2011; Nestby et al., 2011). A peculiar feature in bilberries among Ericaceae family is that it possesses green stems and branches, and it continues the photosynthetic process even when leaves fall off in autumn (Fig.1a). The flowers start to bloom from April-June and the fruits develop during July-September depending of the growth location. The pollination is naturally facilitated for example by the bumble bees. The ripe berries are small (5-9 mm) and have a distinct deep blue/purple coloration due to higher amounts of anthocyanin compounds that accumulate during ripening. The berries are also protected by a waxy layer coat that avoids dehydration of fruits.

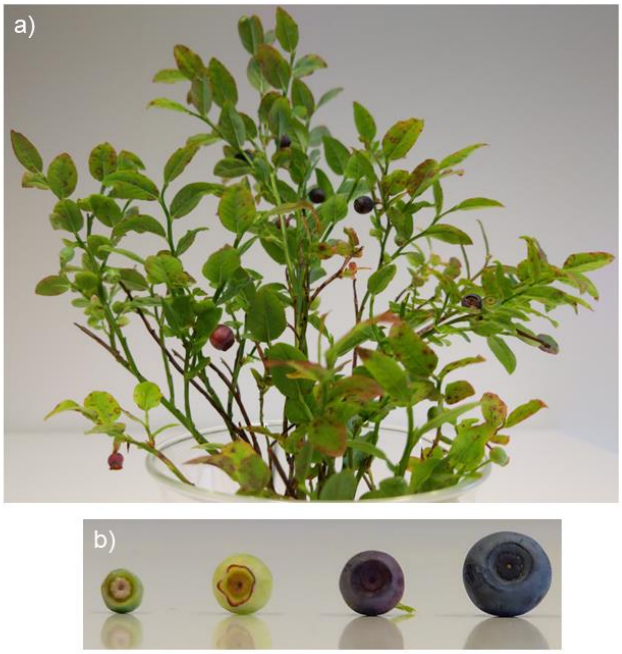

Fig. 1 A fully-grown bilberry plant yielding fruits **(a)**, major developmental stages of bilberry fruit from small green to fully matured blue-colored ripe berries **(b)**.

The berry ripening can be classified into four major developmental stages after the flower maturation; small green berries to reddish medium-sized and fully ripe blue/purple-colored berries (Fig. 1b). The duration between each developmental stage also often varies based on temperature and local weather

conditions, but usually the fruit set from the flower falls anywhere between 25-40 days. Bilberries are one of the most commonly found wild plants in Norway and found throughout the country even at altitudes as high as 1500 masl. They have a high commercial value in the market, despite of which tons of berries are left unpicked in Nordic forests every year. Berry picking is a traditional leisure activity among the Nordic public during late summer. The growing interest on bilberries in non-native markets could potentially lead to better cultivation or sustained farming practices in future (Nestby et al 2011).

5.3 Bioactive compounds in bilberries

Bilberries contain high levels of antioxidant compounds (phenolics, flavonoids, tannins), color pigments such as anthocyanins and carotenoids, vitamins (ascorbic acid) and sugars (Michalska & Łysiak, 2015; Pires et al., 2020). Flavonoids, which represent the larger part of bilberry bioactive compounds, in general are a group of polyphenolic-class secondary metabolites that represent over 4,000 low molecular weight compounds. Flavonoids can be further divided into six subclasses such as flavonols, flavones, isoflavones, anthocyanins, catechins and flavonones (Fang et al., 2013; Panche et al., 2016). These flavonoids are conjugated to sugar molecules and occur naturally in plant tissues, such as fruits, nuts, seeds and other storage tissues.

The nutritional components in fully ripe *Vaccinium* berries can be categorized into carbohydrates (15.3%), protein (0.7%), dietary fibers (1.5%), lipids (0.5%) and with water content of 85% (Hancock et al., 2003; Rowland et al., 2011). The predominantly found sugars in bilberries are fructose and glucose, whereas sucrose and galactose are found in low amounts. A fully matured blueberry contains 3.5% cellulose and 0.7% pectin which are sugar constituents of the cell wall (Akšić et al., 2019). In addition to these essential nutrients, these berries contain a wide range of organic acids, non-nutritive phytosterols such as sitosterol and stigmasterol (Koponen et al., 2001). Anthocyanins alone constitute more than 60% of the total polyphenolics of *Vaccinium* berries. They are water soluble pigments that give deep red or purple coloration to the fruits or flowers (Krga, & Milenkovic, 2019). Apart from being colorants to the berry skin and flesh, anthocyanins are possessing excellent antioxidant properties that could scavenge free radicals and chelate metal ions in biological system (Kalt et al., 2003; Kalt et al., 2020). Numerous studies have been demonstrated on several model organisms, however, solid evidence in human studies is still lacking. But in general, it is understood that consumption of bilberries on a regular basis have numerous health benefits such as prevention of cardio-vascular diseases, cancer obesity, aging, improving vision, immunity and used as performance booster supplement in sports. Bilberries have been also traditionally been used in folklore medicines since ancient times (Erlund et al., 2008; Qin et al., 2009; Gaspar et al., 2021).

5.3.1 Anthocyanins

There are more than 700 anthocyanins found in nature from all the glycosylated, hydroxylated or amino acid group attached derivatives from 27 anthocyanidin classes. However, only six major anthocyanidins; cyanidin (Cy), delphinidin (Dp), pelargonidin (Pg), peonidin (Pe), malvidin (Mv) and petunidin (Pt) are commonly found in plants (Andersen & Jordheim 2013; Fang, 2014). They are aglycone end products from the flavonoid pathway and are glycosylated by glucose, galactose, rhamnose or arabinose at the end of the biosynthetic pathway. Sugars are attached to anthocyanidins mainly at the C3-position of the C-ring or the C5, C7-position of the A-ring (Bueno et al., 2012).

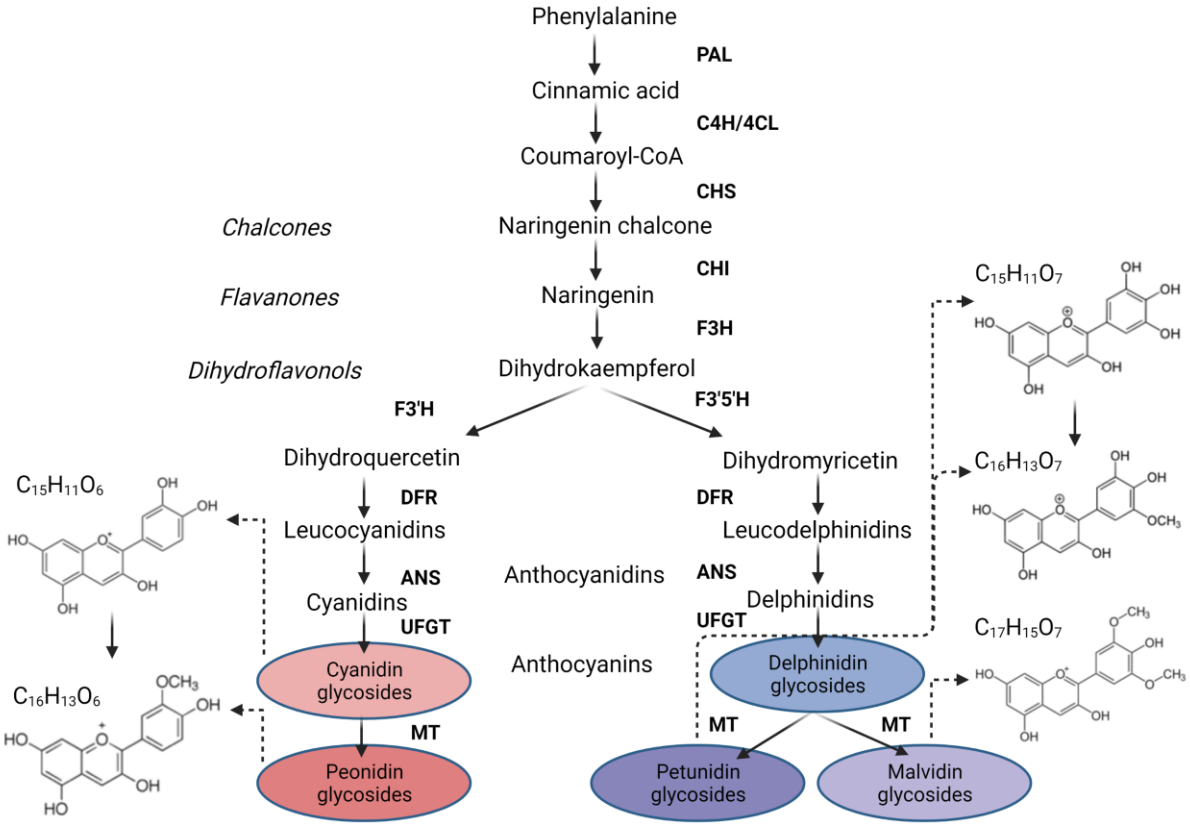

Fig. 2 Schematic representation of the anthocyanin biosynthesis highlighting the major anthocyanin compounds and structures commonly found in *Vaccinium* species. *PAL*, Phenylalanine ammonia lyase; *4CL*, 4-coumarate: CoA ligase; *CHS*, chalcone synthase; *CHI*, chalcone isomerase; *F3H*, flavanone 3 hydroxyase; *F3'H*, flavanone 3′ hydroxyase; *F3'5'H*, flavanone 3′ 5′ hydroxyase; *FLS*, flavonol synthase; *DFR*, dihydroflavonol reductase; *ANS*, anthocyanidin synthase; *MT*, 3-O-methyl transferase; *UFGT*, UDP glucose-flavonoid 3-O- glucosyl transferase.

The anthocyanin biosynthesis initiates from the well-studied phenylpropanoid pathway, with phenylalanine as a starting point, which comes from the shikimate pathway (Fig. 2). It is converted to

cinnamic acid and further to 4-coumaroyl- CoA by phenylalanine ammonia lyase (*PAL*) and 4-coumaroyl- CoA ligase (*4CL*). Chalcone synthase (*CHS*) condenses one molecule of 4-coumaroyl-CoA into naringenin chalcone. These chalcones are isomerized to flavanones, such as naringenin by chalcone flavanone isomerase (*CHI*). Then the pathway cleaves into different branches yielding types of dihydroflavnols, each resulting in a different class of flavonoids. Flavanone 3-hydroxylase (*F3H*) catalyzes naringenin to dihydroflavonols such as dihydrokaempferol, dihydroquercetin and dihydromyricetin. For the biosynthesis of anthocyanins, dihydroflavonol reductase (*DFR*) catalyzes the reduction of dihydroquercetin and dihydromyricetin to leucocyanidins and leucodelphinidins, which are converted further to anthocyanidins by anthocyanidin synthase (*ANS*) and glycosylated by UDP glucose-flavonoid 3-O-glucosyl transferase (*UFGT*) (Jaakola et al., 2002; Jaakola et al., 2013) (Fig. 2).

The direct regulation of flavonoid biosynthesis is well understood and characterized from various plant species. (Zoratti et al., 2014). The coordinated expression of genes in this pathway is regulated by a complex consists of R2R3-MYB, bHLH transcription factors and WD-40 repeat proteins, which form so called MBW complex and determines the spatio-temporal patterns and downstream accumulation of anthocyanins (Xie et al., 2020; Yan et al., 2021).

5.3.2 Flavonols and flavan-3-ols

Flavonols are another important class of flavonoids also known for their potent antioxidant activities. They are usually colorless or appear in pale color. Flavonol synthase (*FLS*) is the key enzyme in flavonol biosynthesis that converts all the dihydroflavonols produced from the flavonoid biosynthesis such as dihydroquercetin and dihydromyricetin to quercetin and myricetin. Glycosyl-groups are further added by 3-O-glucosyl transferases (*3GT*). Myricetin is methylated at 3' site to form laricitrin and further methylated at 5' into syringetin by the 3′-O-methyltransferase and 5'-O-methyltransferase, respectively (Davies et al., 2003) (Fig 3).

Studies in grape have shown that flavonols such as myricetin and kaempferol were found in high levels at veraison stage, whereas quercetin was detected highest during the early fruit development (Fang et al., 2013). Anthocyanidins can be diverted into proanthocyanidins via anthocyanidin reductase (*ANR*), to produce catechin-type or epicatechin-type flavan-3-ols which are produced from leucocyanidins by leucoanthocyanidin reductase (*LAR*) (Määttä-Riihinen et al., 2005).

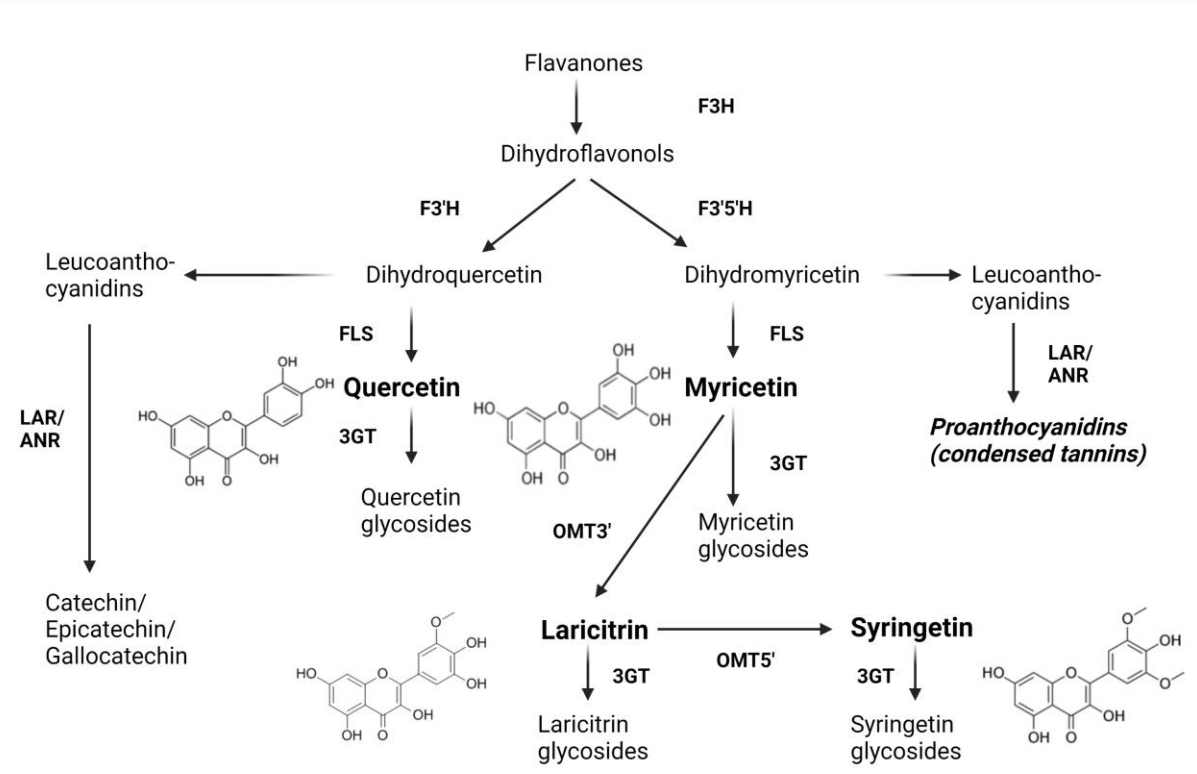

Fig. 3 Schematic representation of the flavonols biosynthesis highlighting the major flavonol compounds (quercetin, myricetin, laricitrin, syringetin) and its structures commonly found in *Vaccinium* species. *F3H*, flavanone 3 hydroxyase; *F3'H*, flavanone 3′ hydroxyase; *F3'5'H*, flavanone 3′ 5′ hydroxyase; *FLS*, flavonol synthase; *OMT*, 3-O-methyl transferase, 5-O-methyl transferase; *3GT*, flavonol 3-O glucosyl transferase; *LAR*, leucoanthocyanidin reductase; *ANR*, anthocyanidin reductase.

5.3.3 Sugars

Sugars are biosynthesized in photosynthetic source tissues such as leaves, and transported to the sink tissues such as roots and fleshy fruits by sucrose transporters and through sieve elements of phloem in most plant species (Lemoine et al., 2013). *Vaccinium* berries accumulate different kinds of soluble sugars, mainly sucrose, glucose and fructose during fruit development and ripening, the latter two being the two predominantly found sugars (Forney et al., 2012). The starch metabolism is a complex process and differs across species.

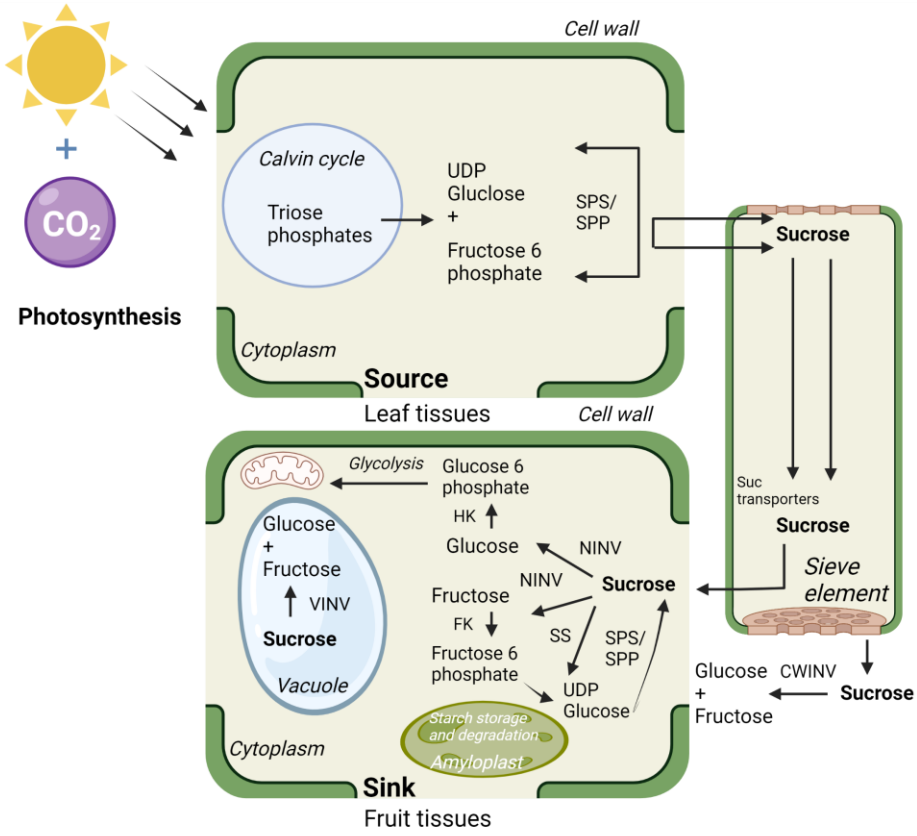

Fig. 4 Schematic representation of sucrose synthesis and transport from source tissues to sink tissues highlighting the major enzymes involved in plant sugar metabolism. SPS/SPP, sucrose phosphate synthase, sucrose phosphate phosphatase; SS, sucrose synthase: NINV, neutral invertase; CWINV, cell wall invertase; VINV, vacuolar invertase; HK, hexokinase; FK, fructokinase.

Generally, starch synthesis and degradation occur in amyloplasts, a type of storage plastids. Starch represents an important intermediate in the general sugar metabolism in the fruit development by serving as reserve energy source in plastids that can be utilized to produce glucose and fructose when needed (Lloyd & Kötting, 2016). The utilization of sucrose for metabolism in sink tissues starts with the cleavage of sucrose into its hexose monosaccharides, glucose and fructose, by acid and neutral invertases. Sucrose cleavage is carried out either by neutral invertase (NINV) in the cytoplasm, acid invertases in vacuoles (VINV) or by cell wall invertases (CWINV) to yield glucose and fructose, or by sucrose synthase (SS) to yield UDP-Glucose and fructose (Salerno & Curatti, 2003). The free hexoses (glucose and fructose) are phosphorylated by hexokinases (HK) or fructokinases (FK) that produces glucose-6-phosphate or fructose-6-phosphate, which are key precursors for energy yielding processes such as glycolysis (Stein & Granot, 2018) (Fig 4).

5.4 Light spectral quality: perception and its significance

Light being the main energy source for plants is an important environmental factor that affects several physiological processes including fruit development (Yavari et al., 2021). Photosynthetically active radiation (PAR) stretches from 400-700 nm ranging from blue to far-red light (Wu et al., 2019). The visible PAR light spectrum varies across different latitudes and changes daily along with the radiation doses that reaches the surface (Chiang et al., 2019). Along with chlorophylls that perceive solar light for photosynthesis, specific classes of plant photoreceptors, such as phytochromes and cryptochromes, perceive light wavelengths to enable plants to sense and respond to high or low light environments. Phytochrome (PHY) photoreceptors sense red and far-red light, cryptochromes (CRY) perceive blue light and UVR8 photoreceptor respond to UV light (Moglich et al., 2010).

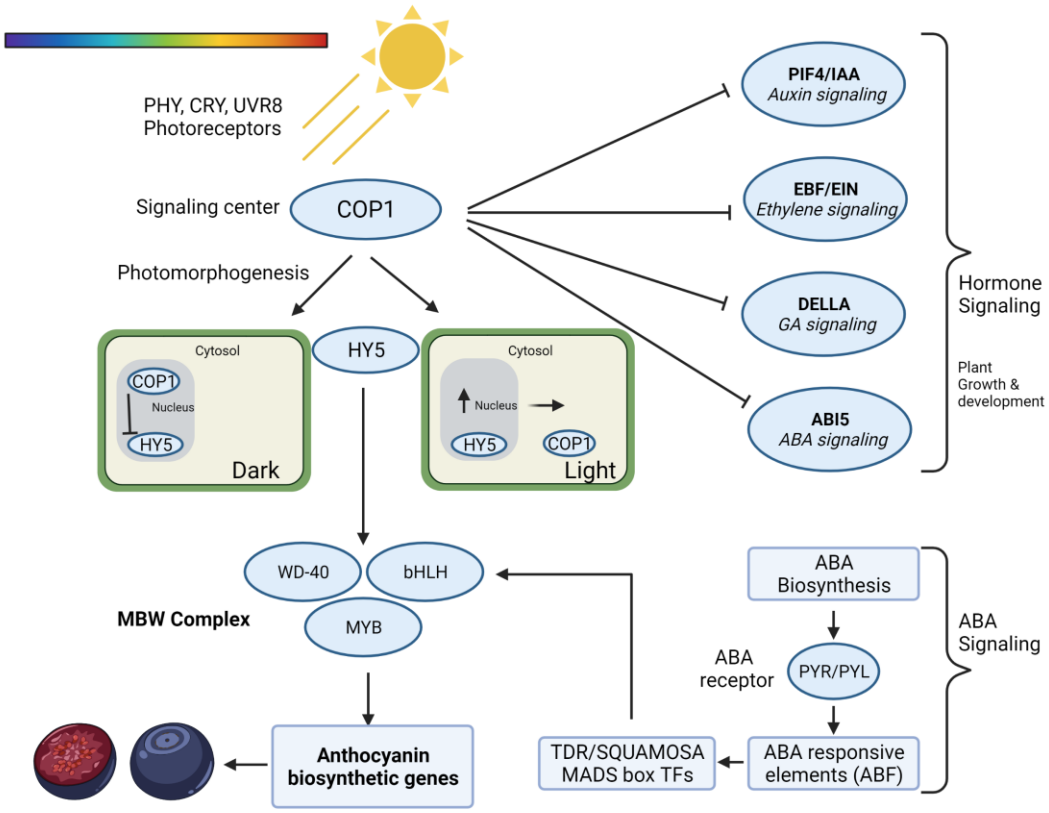

Fig. 5 Schematic representation of light perception mediated by COP1 and its response towards anthocyanin biosynthesis and hormone signaling during fruit development. COP1, constitutive photomorphogenic 1; HY5, elongated hypocotyl 5; PHY, phytochrome; CRY, cryptochrome photoreceptors; MBW complex, MYB, bHLH, WD-40; bHLH, basic helix-loop-helix; WD-40 repeat domains; ABA, abscisic acid; *PYR/PYL*, pyrabactin resistance/like ABA receptors; *PIF*, phytochrome interacting factor; IAA, indole acetic acid; *EBF*, ethylene binding factor; *EIN*, ethylene insensitive, *ABI5*, ABA-insensitive.

The light signal perception induces either photomorphogenesis or skotomorphogenesis, changes in circadian rhythm flux and importantly affects the biosynthesis of secondary metabolites. The central light signal processing is mediated by the constitutive photomorphogenic 1 (COP1) regulator. Photoreceptor activation by light suppresses the activity of COP1 which is an E3 ubiquitin ligase that ubiquitinates a number of positive transcriptional regulators, thus repressing photomorphogenesis. COP1 is active in dark growth conditions accumulating in the nucleus, while light induces its export out of the nucleus and move to the cytosol, leading to the accumulation of transcription factors, and thus promoting photomorphogenesis (Wang et al., 2019) (Fig 5). Light-induced activation of photoreceptors initiates downstream signal elements like elongated hypocotyl 5 (HY5) resulting in light-induced physiological responses including anthocyanin accumulation. HY5 also tends to positively react with MBW complex which consists of MYB, bHLH and WD-40 repeat proteins transcription factors. (Zhao et al., 2010) (Fig 5). Although bHLH and WD-40 might not be directly involved in response to light quality and intensity and play only a secondary role from the complex, MYBs are more directly involved in light-mediated regulation of flavonoid biosynthesis (Matus et al., 2009).

COP1 being the central repressor of photomorphogenesis, recent studies have shown that it is also likely to be involved in different plant hormone signalling pathways. In auxin signalling, COP1/SPA complex can regulate phytochrome interacting factor (*PIF5*) stability under red light (Pacin et al., 2016). It has also been reported that COP1 may promote ethylene insensitive gene (*EIN3*) stability through ubiquitination of ethylene binding factors (*EBF1/2*) (Shi et al., 2016), although the mechanism controlling the ubiquitination of *EBF1/2* by COP1, in ethylene signaling is not clear. In abscisic acid (ABA) signalling, COP1 appears to participate in two ABA-regulated processes, seed germination and ABA-induced stomatal closure (Khanna et al., 2014). In dark conditions, skotomorphogenesis is mediated by COP1/HY5 with signalling from gibberellic acid (GA) with the suppression of DELLA proteins (Mazzella et al., 2014). All likely interaction of COP1 with different hormone signaling factors is depicted in Fig 5. Plant hormones respond to environmental signals such as light and COP1 could be the connecting link between light and hormone signaling pathways (Liang et al., 2012).

5.5 Role of light qualities in flavonoid biosynthesis and sugar metabolism

Light conditions perceived by the plants are categorized into duration (photoperiod), intensity and quality. Among them, light quality is the most important factor that affects both plant primary and secondary metabolism. In the past, photo-selective nets and bagging methods have been commonly used to selectively increase the sensitivity of fruits to solar light intensities towards anthocyanin accumulation as shown in fruit crops such as apple, litchi and tomato (Liu et al., 2013; Tinvane et al., 2013; Zhang et al., 2016). In order to study the effect of light quality by selectively inducing, it is now possible to

flexibly simulate specific wavelengths using light emitting diodes (LEDs), which are already widely used in indoor horticulture in the commercial production of vegetables (Bian et al., 2015; Nassarawa et al., 2021). From the wide range of PAR spectra, mostly blue (460 nm) and red (660 nm) light wavelengths have the maximal effect on the biosynthesis of secondary metabolites. Several studies have shown that blue light actively promotes anthocyanin biosynthesis in fruit crops such as pear, strawberries and bayberries (Shi et al., 2014; Xu et al., 2014; Nadalini et al., 2017; Tao et al., 2018). Some studies have also highlighted the possible role of red light in increasing the anthocyanin content in fruits (Zhou & Singh, 2002; Miao et al., 2016). The light qualities interact via the photoreceptors and signalling pathways with the specific regulatory and structural genes. For example, in cherries, blue light promoted anthocyanin accumulation by increasing the expression of PAL activity (Kokalj et al., 2019). Likewise, in sugar metabolism, the composition and accumulation can also be affected by the light conditions as reported in tomato (Beckles, 2012). Both red and blue light could be involved in photo-regulation of sugar metabolism and sucrose transport (Girault et al., 2010). In bilberries, it was shown earlier that the plants that are growing exposed to high PAR range had increased phenolic compounds and sugar content (Zoratti et al., 2014; Mikulic-Petkovsek et al., 2015). Further understanding of the mechanisms behind the effect of individual light wavelengths on the accumulation of both anthocyanins and sugars in berries still needs to be addressed.

6 Aim of the study

The main objective of the study was to investigate the effect of spectral light qualities on biosynthesis and accumulation of major bioactive compounds in bilberry such as anthocyanins, flavonols and sugars, and shed light on the mechanisms controlling the light quality mediated related signalling. Therefore, the study was further widened up to see if the light quality perception and its effect on anthocyanin profile is different or not in independently ripening berries without involvement of plant signals, compared to that of naturally ripening berries.

The research work was carried out:

1. To study the effect of light quality, specifically the red and blue light on anthocyanin biosynthesis through high throughput RNA-seq transcriptomics and metabolite analyses **(Paper I)**;
2. To study if the light quality responses (red, blue and far-red) are different across naturally ripening berries and in detached conditions on flavonoid biosynthesis through gene expression and metabolite analyses **(Paper II)**;
3. To study the sugar-metabolism in bilberry during fruit development and under supplemental light through related gene expression, enzyme activity analyses and quantification of sugar content **(Paper III)**.

7 Summary of Papers

7.1 Paper I

Red and blue light treatments of ripening bilberry fruits reveal differences in signaling through ABA regulated anthocyanin biosynthesis

Amos Samkumar[1]*, Dan Jones[2], Katja Karppinen[1], Andrew P. Dare[2], Nina Sipari[3], Richard V. Espley[2], Inger Martinussen[4], Laura Jaakola[1,4]

Published in ***Plant, Cell & Environment***, 44(10), 3227-3245. https://doi.org/10.1111/pce.14158

The response to supplemental red and blue light irradiation between mid to late ripening stages of bilberry was investigated in this study. We found out that anthocyanin content was increased by both red and blue light treatments when compared to control natural light conditions. The highest elevation of anthocyanins was found under red light with a 12-fold increase. Further, transcriptome libraries were constructed from the 6-day old supplemental light-irradiated ripening berries using RNA-sequencing. Both red and blue light treated berries had similar up-regulation of all the key early and late anthocyanin biosynthetic genes, but the major difference was found in light signaling and perception, in addition to ABA metabolism and catabolism. The highest accumulation of delphinidin glycosides under red light was well correlated with increased expression of *F3'5'H* and *UFGT* genes. We also showed that the ABA biosynthesis was positively linked to increased anthocyanin accumulation under red light. Hence, alongside common ABA receptors, *PYR/PYL, ABF, ABI5*, the catabolic enzyme, *ABA-8'-hydroxylase* was highly up-regulated under red light alone, suggesting that all these ABA-linked genes act as positive signaling factors of anthocyanin biosynthesis in bilberry. Also, the regulatory genes alongside *MYBA1, MYBPA1.1* were found to be upregulated under red light. In addition, we showed an alternative model of vesicle-mediated trafficking and transport of anthocyanins by *SNARE* domain transporters towards vacuolar storage, which could likely explain the sequestration in stress-induced anthocyanin accumulation in berry tissues and needs further investigation.

7.2 Paper II

Flavonoid biosynthesis is differentially altered in detached and naturally ripening attached bilberries in response to spectral light quality

Amos Samkumar*, Katja Karppinen, Tony K. McGhie, Richard V. Espley, Inger Martinussen, Laura Jaakola

Prepared for submission to ***Journal of Photochemistry and Photobiology B:Biology***

In this manuscript, we further extended our previous study to see how the light perception and signalling is different in independently ripening bilberries on detached conditions. The early harvest at premature stage is unusual in this non-climacteric berry species by theory at least, where it lacks independent ethylene-burst mechanisms and the fruit quality tends to deteriorate over time. We have documented interesting findings, where the bilberries continued to ripe over two weeks in detached conditions accumulating high yield of anthocyanins. Above all, the highest elevated anthocyanin content was detected in detached conditions, but unlike the red light which had positive influence on natural bushes, the detached berries interestingly responded to blue light instead. The metabolite quantification was supported by gene expression studies of biosynthetic and regulatory genes over the course of time, where in particular, the key regulatory gene *MYBA1* was found to be regulating the biosynthesis in response to blue light in detached conditions. On the other hand, red light increased accumulation of both the anthocyanin and flavonols in naturally ripening berries on the bushes. We also analyzed the key photomorphogenesis regulators COP1 and HY5 expression trends to support our findings. Our results indicate that there could be independent hormone signalling network in the developing berries, and possibly fruit-localized photoreceptors behind the independent light-mediated regulatory mechanisms. This finding could open up new avenues to non-climacteric berry ripening, hormone signaling and related light regulation.

7.3 Paper III

Insights into sugar metabolism during bilberry (*Vaccinium myrtillus* L.) fruit development

Amos Samkumar*, Katja Karppinen, Binita Dhakal, Inger Martinussen, Laura Jaakola

Prepared for submission to ***Physiologia Plantarum*** (Special issue*: Plant sugar metabolism, transport and signaling in a challenging environment*)

Alongside anthocyanins and other phenolic compounds contributing for human health-beneficial properties, sugars are also attributed toward the berry fruit quality by enhancing the taste or flavour. Sugar metabolism in bilberries is not explored earlier in detail. In this study, we have identified 25 genes categorized into acid and neutral invertases, sucrose phosphatases, sucrose synthases, and interconverting hexokinases and fructokinases. Most of the isoforms were differentially expressed across berry developmental stages suggesting they all might have different functions. The enzyme activity analyses strongly suggested that sucrose is converted and resynthesized mostly at the beginning of ripening. A similar trend was also seen in vacuolar acid invertases. Starch degrading-amylases were not detected in early stages and were found only in minor levels in late ripening stages. We have also estimated the sugar content across the developmental stages and the highest content was found in ripe berries with fructose and glucose dominating the sugar composition. Sucrose was detected only in low levels in all berry developmental stages. We have also further mined the bilberry light-treated transcriptome dataset to see if the spectral light quality has a positive influence on sugar metabolism. We observed a very similarly differentially expressed gene pattern on kinases but the sucrose coding-genes were down-regulated under blue light. The most interesting response was found in starch degradation by amylases being highly up-regulated by both light treatments. Considering the earlier result, that the amylase activity was found on very low levels in all stages, it seems that the degradation of starch into hexoses is triggered by light quality. This is the first study of on bilberry sugar metabolism and could open up new insights on sugar signaling, transport and its regulation towards other bioactive compounds.

8 General discussion from main findings

8.1 Supplemental light irradiation promotes anthocyanin biosynthesis in bilberry

Light is one of the most important external factors which drastically affects the fruit ripening process. Some of the key changes impacted by light during fruit ripening include changes in texture, firmness, accumulation of phytochemicals, and most importantly the pigmentation (Feng et al., 2013; Henwood et al., 2018). The development of colored compounds such as anthocyanins is an important parameter in evaluating fruit quality. The changes in the composition of anthocyanins determine the fruit color in both skin and flesh, as well as their bioavailability upon consumption (Routray & Orsat, 2011; Fang, 2014). Several studies over the past decades have shown that abiotic stress signals largely influence the biosynthesis of anthocyanins during fruit development and ripening (Zhou & Singh., 2004; Zoratti et al., 2014; de Rosas et al., 2017). The results from the paper I showed that the bilberry anthocyanin composition is strongly regulated by the light spectral qualities such as red and blue wavelengths. The study quantified 15 anthocyanin compounds from five major aglycone classes detected in light-treated and control samples. These were mostly glucoside, galactoside and arabinoside derivatives of cyanidin, delphinidin, petunidin, peonidin or malvidin class of anthocyanins, which were found in agreement with previous studies in bilberry (Lätti et al., 2008; Zoratti et al., 2014). The effect of light to anthocyanin pigmentation has been investigated in several studies in many commercial fruit crops (Dussi & Sugar, 1995; Zhou & Singh., 2004; Kokalj et al., 2019). For example, shading and bagging experiments in such crops showed that exposure to solar light intensities could stimulate up-regulation of both early and late anthocyanin biosynthesis-related genes by interacting upon with regulatory elements (Fukuoka et al., 2014). Short-term bagging treatment technique has been used widely in crops such as apple, litchi and pear, in which the exposure to light at certain ripening stages leads to accumulation of anthocyanins in fruit pericarp. (Ju, 1998; Zhang et al., 2016; Liu et al., 2019). Also, it has to be noted that the mechanisms are not similar across cultivars as shown in grapes, where the light exclusion treatment differentially regulated the anthocyanin accumulation in skin of berries (Zheng et al., 2013). Hence, in general, it is clearly understood that light from perceivable solar spectra of whole range (UV to far-red light) enhances anthocyanins, and dark/shadiness affects in an opposite manner. Nevertheless, plants with their specialized specific photoreceptors are able to perceive and segregate wavelengths from the visible spectral range (400-700 nm) and are able to respond to individual light qualities. Thus, enhancing the radiation of such specific range of light wavelengths could lead to responses in accumulation of certain classes of phytochemicals (Holopainen et al., 2018).

In paper I, delphinidin glycosides, which dramatically increased under red light and showed significant correlation with all the major flavonoid biosynthetic genes, were considered to be the most light-induced class of anthocyanins in bilberries. Likewise, cyanidin and petunidin glycosides also showed a significant increase under both red and blue light, respectively. However, levels of peonidin and malvidin glycosides were not affected by supplemental light treatments in the same manner like other anthocyanin classes. Therefore, these results indicate that the specific light qualities can change the composition and concentration of specific anthocyanins in berries by interacting with light-inducible biosynthetic and regulatory genes (Ma et al., 2019). Specifically, delphinidins being one of the most abundant class of anthocyanins found in northern clones and responsible for the distinct blue color appearance in ripe bilberries (Lätti et al., 2008; Uleberg et al., 2012), also happened to be the most light-reactive class of anthocyanins accumulated in our simulated and controlled light-quality experiments (paper I & paper II).

The anthocyanin biosynthetic process in bilberries is quite similar to the well-studied flavonoid metabolic pathways from other blue-colored fruits. The pathway involves a series of enzymatic reactions ultimately resulting in different classes and glycoside derivatives of anthocyanins. Light qualities target specifically upon certain key genes of this pathway by the inducible-transcription factors such as MYBs interacting with their promoters. Earlier studies have shown that *PAL* and *DFR*, some of the early structural genes of the flavonoid pathway, are highly responsive to light (Plunkett et al., 2018; Zhu et al., 2018). Similarly, the results of the present study revealed that the expression levels of most structural genes were up-regulated under both red and blue light, which also positively correlated with the concentrations of delphinidin-3-O-galactosides and arabinosides (paper I). A previous study by Zhang et al., (2017) showed that over-expression of *CHS*, the key enzyme gene in the flavonoid pathway, enhanced high-light resistance by accumulating more anthocyanins in leaves of *Arabidopsis thaliana*. In the present study, the expression of *CHS* was positively correlated with the concentration of delphinidins. Other important genes leading to the branching of leucoanthocyanidins, *F3'H*, *F3'5'H* and the last glycosylating gene of anthocyanin pathway, *UFGT*, were highly up-regulated under red light and also showed strong positive correlation with the concentration of delphinidin glycosides (paper I). From the current study, we consolidate that the late biosynthetic genes *F3'5'H*, branching point towards delphinidins biosynthesis, and *UFGT* were considered to positively regulate the synthesis of light-inducible anthocyanins, specifically correlating with the increased concentration of delphinidins under red light (paper I).

Several key members of the MYB transcription factor family particularly, *MYBA1*, *MYB5*, *MYBC2*, *MYBPA1.1*, *MYBPA2* and *MYBPA3* were involved in regulating red light-induced accumulation of anthocyanins in bilberries (paper I). Some of these MYBs have earlier been shown to regulate expression of structural genes of the anthocyanin biosynthesis such as *DFR* and *UFGT* by interacting with their

promoters (Cavallini et al., 2014). For instance, MYB10, the homolog of MYBA, has been shown to be one of the most responsive MYB genes to light, and the main regulator of anthocyanin biosynthesis in cultivable fruit crops such as strawberry and apple (Feng et al., 2013; Lin-Wang et al., 2014). In blue-colored *Vaccinium* berries, MYBA-type and MYBPA-type gene family members are identified to be the major regulators of anthocyanin biosynthesis (Plunkett et al., 2018; Karppinen et al., 2021). In this study, supplemental light-inducible anthocyanin synthesis was positively correlated with *MYBA1*, but also with *MYBPA1.1*, suggesting the co-regulation of the biosynthesis of delphinidin-type anthocyanins in bilberries as suggested by Karppinen et al. (2021). In an earlier study with wine grape, both *MYBPA1* and *MYBPA2* were identified as positive modulators of both anthocyanin and abscisic acid (ABA) levels in berry skin (Azuma et al., 2012). The current findings will strengthen our understanding in anthocyanin regulatory mechanisms, specifically showing that both *MYBA1/MYBPA1.1*, as key regulatory genes identified in bilberry, have a major role in mediating the expression of structural genes such as *CHS, DFR, F3'5'H* and *UFGT* towards delphinidin biosynthesis also as response to red and blue light treatments (paper I).

8.2 Red light induces biosynthesis of delphinidin branch anthocyanins mediated by abscisic acid metabolism

Plant hormones have synergistic effects on anthocyanin biosynthesis during fruit development (Ferrero et al., 2018). The accumulation of secondary metabolites in plants has been shown to be influenced by endogenous hormones and signaling (Belhadj et al., 2008). The hormonal responses are also altered by biotic and abiotic signals, and the responses of both synergistic and antagonistic effects in the plants are well documented. Some hormones that are involved in response to light environmental stimuli include ethylene, jasmonic acid, salicylic acid, indoleacetic acid and ABA (Zhu, 2016). Our findings indicated that anthocyanin accumulation was mediated through ABA by enhancing the expression of both ABA signaling and metabolism-related genes in light irradiated ripening bilberries (paper I). The past studies haven't ruled out the possible role of ABA signaling and metabolism in flavonoid biosynthesis under enhanced light environments. For instance, in strawberries the flavonoid regulatory gene, MYB10 was affected in response to light as well as to exogenous ABA and showed additive effects when both were combined (Kadomura-Ishikawa et al., 2014). Earlier, ABA has been reported to be central driving factor of ripening in bilberries because of its rise in endogenous concentration at the onset of berry ripening (Karppinen et al., 2016). Exogenous application of ABA in unripe bilberries also promoted anthocyanin biosynthesis (Karppinen et al., 2018). The similar effect of ABA regulatory mechanisms has been shown towards anthocyanins accumulation in grape berries (Wheeler et al., 2009; Sandhu et al., 2011). Thus,

the present results have shown further evidence on the link between the ABA metabolism and anthocyanin biosynthesis in fruits, especially under specific light wavelengths (paper I).

From the findings of current study, red light up-regulated the expression of key ABA biosynthetic and catabolic pathway genes (*NCED & ABA-8′ hydroxylase*), in addition to the genes involved in ABA signal transduction mechanisms. A similar regulatory model was shown under drought stress in a recent study in tomato (González-Villagra et al., 2017). To determine whether red light promoted anthocyanin accumulation through ABA signaling, we analyzed the expression of ABA binding receptors and downstream signal transducers including the MADS-box transcription factors. Firstly, the expression of *NCED*, the rate-limiting key ABA biosynthetic gene, was increased in light-treated berries, further triggering the downstream signaling cascade (paper I) (Zhang et al., 2015). Later on, ABA transported from the apocarotenoid pathway binds to pyrabactin/like resistance (*PYR/L*) receptors. The bound *ABA-PYR* complex is essential for inducing downstream regulators such as *TDR*, and other *SQUAMOSA*-type MADS-box transcription factor family genes affecting further towards associated regulatory elements from the MBW complex (Chung et al., 2019). At least five MADS-box transcription factor family of genes including AGAMOUS-type and TDR have earlier identified to be directly involved in bilberry fruit ripening (Jaakola et al., 2010; Nguyen et al., 2018). Under supplemental red light, all the above-mentioned ABA binding receptors and regulatory elements were up-regulated (paper I). Contrastingly, blue light down-regulated *PYL* expression, further resulting in lowered expression levels of most downstream positive regulators, such as AGAMOUS and other MADS-box transcription factors, leading to the significant decrease in total anthocyanin content (paper I).

The expression level of ABA-biosynthetic *NCED* gene was increased under both red and blue light treatments. However, the ABA-catabolizing gene, *ABA-8'-hydroxylase* was found increased under red and down-regulated under blue light (paper I). *ABA-8'-hydroxylase* activity is usually involved in degradation of ABA to maintain its endogenous levels in tissues. These findings are in accordance with a previous study in grapes by Kondo et al. (2014) where it was demonstrated that this catabolizing gene could be involved in anthocyanin biosynthesis under red LED-light treatment. Hence, the maintenance of increased endogenous ABA levels as a response to red light have contributed more towards anthocyanin biosynthesis in bilberries than an irregular ABA homeostasis promoted by blue light. It has been shown earlier in grapes, that higher available cellular concentrations of ABA in stress-induced berry skins are vital in triggering fruit developmental and physiological responses (Ferrero et al., 2018).

8.3 Supplemental light wavelengths trigger anthocyanin transport in bilberries by vesicle-mediated trafficking

Generally, in plant vegetative tissues and in storage organs, anthocyanins are suggested to be transported to vacuolar depositions via two proposed models. The first model illustrates the involvement of membrane bound transporters such as ATP-binding cassette (ABCs), glutathione-S-transferases (GSTs) and multidrug and toxic compound extrusion (MATE) transporters, whereas the second model is through vesicle-mediated trafficking via endosomes (Grotewold & Davies, 2008). Earlier studies proposed that anthocyanins and proanthocyanidins could be also possibly transported from cytosol to vacuoles through vesicular trafficking (Pourcel et al., 2010; Zhao et al., 2010). Another study in *Arabidopsis* characterized and evidenced the involvement of *SNARE* protein complex in the transport of secondary metabolites to cellular organelles via endosomes (Kwon et al., 2008). Simultaneously, membrane transporters can be involved and assist the vesicle-trafficking process during sequestration before depositing as anthocyanic vacuolar inclusions (AVIs) (Kaur et al., 2021). In our study, we have shown that a group of SNARE (Syntaxin/SNAP type) domain proteins are highly up-regulated under red light and likely sequestered via endosomes. In addition, GST and MATE membrane transporters were also found likely to be associated with the vesicle-trafficking process in bilberry fruit (paper I). Our results led to possible speculations, on why and how the SNARE assisted vesicle-mediated trafficking was triggered in bilberries under enhanced-light environments instead of usual membrane bound transport by MATEs, ABCs and GST transporters. Our findings were backed up by some recent literatures, suggesting that the enhanced red light (an external abiotic stimuli) or high levels of inter-cellular cargo (anthocyanins) in the organelles could trigger such phagosome-mediated complex (Gu et al., 2020; Kwon et al., 2020). However, further investigations are needed to consolidate this interesting finding from paper I.

8.4 Blue and red light affect flavonoid biosynthesis in an opposite manner in detached and naturally ripening bilberries

Naturally ripening bilberries could take up to 4 weeks for complete anthocyanin pigmentation to appear on the skin, from green to deep-blue color in mature berries under controlled conditions. Whereas in detached conditions, anthocyanin accumulation in bilberry skins occurs at a slow rate in the beginning (S2-S3 stage up to 4 days), followed by a rapid increase (S3-S4 stage within 8 days), and finally a stabilization (S4-S5 stage up to 14 days) (paper II), before a decline at the end of ripening stages, similar

to a pattern observed in grape berries (Gholami, 2004). In the current study, both naturally-ripening attached berries and detached berries, which were allowed to ripe until coloration appears, were tested for their differential responses to spectral light qualities such as red, far-red and blue light. Both detached berries and berries in bushes started developing pigmentation in skins between 5-7 days of enhanced irradiation. Metabolite analysis of fully-ripe bilberries confirmed that blue light promoted even higher anthocyanin accumulation in detached conditions than the positive influence of red light in attached berries (paper II). Based on these interesting results, we have concluded that supplemental lights responsible for the elevated anthocyanin levels were totally contrasting and could adapt different regulatory routes, when the berries were allowed to ripen independently (paper II).

In a previous study in grapevine, detached berries under controlled light and temperature conditions continued to develop color even after removal from the vine (Lurie et al., 2015). It is generally understood that a photoperiodic signal is perceived by the leaves and transferred to shoot apexes at the initiation of flowering and later to fruit set (Levy & Dean 1998). For instance, in brightly colored flowers like petunia, sepals appear to have the same role as leaves when the leaves are covered or when the flowers are illuminated independently towards anthocyanin accumulation (Moscovici et al., 1996). However, in our experiments, detaching the bilberries, and exposing green, unripe berries to individual light qualities without the involvement of signals from leaves, still strongly regulated the expression of key structural and regulatory genes of the anthocyanin pathway, resulting in highest anthocyanin accumulation under blue light (paper II). Moscovici et al. (1996) proposed that in flowers, corolla tissues may contain low levels of photoreceptors because the anthocyanin concentration induced by light was much higher in the attached corollas than in detached ones. In contrast, our results showed that light-induced anthocyanin accumulation was highest in detached berries, suggesting that the fruit-localized photoreceptors could have been more reactive towards light quality in an independent manner and when the berries are detached (Gonzalez et al., 2015). Likewise, high expression levels of all major flavonoid-biosynthesis related genes showed a similar trend in attached berries between 4-6 days of irradiation with red light. Interestingly, the MYBA1-driven anthocyanin accumulation in detached berries under blue light had slightly more even distribution of different classes of anthocyanins unlike the berries in bushes, which mostly increased the delphinidin-type anthocyanins under light treatments. These results suggest that berry tissue itself is the sensor site for the photoreceptors and responsible for the photocontrol of pigmentation in bilberries, not being dependent on photoperiodic signals from other source tissues such as leaves (paper II).

Unlike anthocyanins, the accumulation of flavonols was found to be higher in both attached and detached conditions under red light compared to control and other light treatments (paper II). Similarly, the highest concentration of total flavonols was found in detached berries, compared to the quantified amounts in attached berries. Far-red light (730 nm) also influenced on flavonol biosynthesis in both

experimental conditions (paper II). Far-red light, which is found outside the PAR spectra and are mostly reflected by the plant canopy, is still an important component that can increase the photosynthetic efficiency. Far-red is generally known to be involved in inducing taller canopy with broad leaf sizes during plant development (Demotes-Mainard et al., 2016). Some studies have shown that wavelengths ranging above 700 nm are likely to be involved in promotion of phenolic compounds, when combining in proportion with red light because of its dependency on interaction with same phytochrome A/red light photoreceptor (Dorokhov et al., 2021). In current study, far-red was found to be actively promoting colorless flavonols, after red light in the current study (paper II). A recent finding suggested that flavonol profile is a reliable indicator to assess canopy architecture and exposure of vines leaning towards solar radiation (Martínez-Lüscher et al., 2019). In non-climacteric berries, quercetin-3-*O*-glucoside and quercetin-3-*O*-glucuronide were the commonly found flavonol glycosides (Castillo-Muñoz et al., 2009). From our results, we have quantified quercetin-3-*O*-glucoside as the most abundant flavonol in bilberries and found in concordant with the previous study by Stanoeva et al (2017) (paper II).

Earlier studies have reported that shading and exposing to light had impacted flavonol glucosides either at harvest or during berry development (Spayd et al., 2002; Downey et al., 2004). A higher exposure to UV-light also tends to increase flavonol levels for the photoprotection mechanisms (Downey et al., 2003). Based on earlier studies, it is assumed that the flavonol concentration and content are dependent on the light quality especially between the UV range and higher PAR range (above 600nm). Our results are in agreement with these studies showing that fruit exposed to such light wavelength ranges had higher accumulation of flavonol glucosides irrespective of ripening conditions (attached or detached). This also indicates that flavonol biosynthesis is independent from anthocyanin accumulation during bilberry ripening and protects the epidermal tissues of the berry from high light environments (Singh Brar et al., 2008; Agati & Tattini, 2010).

8.5 Sugar metabolism in bilberries with emphasis on response to red and blue light qualities

Sucrose metabolism is the backbone for sugar accumulation during fruit ripening and three major enzyme categories such as invertases, sucrose phosphatases and sucrose synthases are actively involved (Lingle & Dunlap, 1987; Nguyen-Quoc & Foyer 2001;). The sucrose futile cycles in sink tissues can be also influenced by altering environmental conditions including light and thus the resulting sugar composition in mature fruits could be affected (Lattanzi et al., 2012). The import of sucrose, which is responsible for the carbon source in berry ripening and development, is generally driven from source tissues to sink organs (Ward et al., 1998; Koch, 2004). It has been documented that the light quality not

only affects the flavonoid biosynthesis but also a wide array of secondary metabolic pathways including sugar metabolism (Li et al., 2017). Soluble sugars such as sucrose, glucose and fructose are the major sugars found in fruits. They are also the main source for energy yielding by-products and substrates for primary metabolism, which are the backbone for plant growth and development (Lastdrager et al., 2014). We have characterized all the major genes involved in sugar metabolism in bilberries, including the invertases, hexokinases, fructokinases, sucrose synthases and phosphatases (paper III). We also showed that red and blue light can influence almost all the different sugar metabolic pathways such as glucose, fructose, galactose metabolic routes, as well as starch biosynthesis and degradation occurring in storage plastids (paper III). In bilberries, it has been shown mainly that both red and blue wavelengths could influence the starch metabolism by up-regulating the amylases, where the starch will be converted to primary hexose sugars. Previous studies have shown that the soluble sugar contents in crops such as tomato, lettuce and celery increased significantly when treated with combination of red and blue light ratios (Liu et al. 2010; Gao et al. 2015; Chen et al., 2019). Invertases, which are the primary enzymes involved in the conversion of sucrose in different cellular spaces and organelles, maintain the sugar homeostasis but also respond mainly to abiotic signals (Zhang et al. 2017). In the present results, the vacuolar invertases were up-regulated and contributed to the increase in total sugar content under red and blue light, whereas, cell wall acid invertases reacted opposite way and were down-regulated by both wavelengths. These dynamic characteristics of invertases are related with some previous studies. For instance, the abundance of invertases was found to be lower after combination of red and blue light treatment in tomato fruit, which indicated that light quality could affect starch and sucrose metabolism and increase the soluble sugar content in fruit (Dong et al., 2019). The current study also found opposite regulation of some hexose interconverting genes such as phosphoglucomutase (*PGM*) and *α-galactosidase* from the galactose metabolism between red and blue light treatments (paper III).

Likewise, previous studies have shown that the fructo- and hexokinases are other key genes involved in metabolism of sugars and contribute toward the soluble sugar accumulation in ripe fruit (Yu et al. 2016). The up-regulation of *PFK*, *FK* and *HK* genes under red and blue light in our study resulted in higher amount of soluble hexoses. These hexose end products can be also further utilized in energy yielding processes such as glycolysis (Yao & Wu, 2016). The related gene expression from some isoforms and enzyme activities was found consistent with the quantification of soluble sugars in fully ripe bilberries. Whereas, the up-regulation of vacuolar invertases, amylases and hexose-kinases were responsible for the increase in sugar content under red light (paper III).

9 Conclusions and future perspectives

The current study combines transcriptomics and metabolite analyses to reveal the effect of light quality to anthocyanin and sugar biosynthesis in ripening bilberries. The findings concluded highest accumulation of anthocyanins under red light in naturally ripening bilberry fruit, which seems to be mediated via ABA metabolism and signaling. A parallel study showed differences in light quality perception between berries ripening detached and naturally attached in the plants, and concluded that both ripening conditions are positively regulated by red and blue light, and that the regulation mechanisms are not similar. Finally, the study was concluded with deciphering the role of light quality on sugar accumulation from the characterized sugar metabolism-encoding genes in bilberry. The key genes from starch and sucrose biosynthesis, which include the amylases, invertases and hexose-kinases were found to be differentially expressed under red light, and these results were further backed up by the increase in glucose and fructose amounts from the sugar content analysis.

The study also opened up new insights on anthocyanin transport mechanisms mediated by vesicular transport under light quality treatment, and documented the role of SNARE proteins in trafficking the several-fold increased anthocyanin accumulation response under red light. Therefore, the work provides a platform for hypothesis-building for the future research into the precise functions of these SNARE proteins during fruit development, especially with responses to the environmental signals. The independent detached ripening of bilberries that resulted in highest anthocyanin accumulation might further lead into studies unraveling autocatalytic hormonal signaling similar to that of climacteric fruits during ripening. The possible interlinking role of photomorphogenesis regulatory mechanisms with transduction pathways including ethylene and ABA signalling also needs to be investigated further in order to understand the hormonal regulation on independently ripening bilberries under enhanced light environments.

All these extensions of the current study will further provide deeper understanding on light-mediated physiological regulatory mechanisms on accumulation of major phytocompounds, such as anthocyanins and sugars in *Vaccinium* and other wild berries. The optimal supplemental light conditions could be also be applied in controlled indoor commercial berry cultivation practices to achieve the maximal berry quality with improved health beneficial and flavor properties.

10 Works cited

Agati, G., & Tattini, M. (2010). Multiple functional roles of flavonoids in photoprotection. *New Phytologist*, 186(4), 786-793.

Akšić, M. F., Tosti, T., Sredojevi´c, M., Milivojevi´c, J., Meland, M., Nati´c, M. (2019) Comparison of sugar profile between leaves and fruits of blueberry and strawberry cultivars grown in organic and integrated production system. *Plants*, 8, 205.

Andersen, Ø. M & Jordheim, M. (2013) Basic Anthocyanin Chemistry and Dietary Sources. In Anthocyanins in Health and Disease; Wallace, T., Giusti, M., Eds.; CRC Press: New York; pp 13−90.

Azuma, A., Yakushiji, H., Koshita, Y., & Kobayashi, S. (2012). Flavonoid biosynthesis-related genes in grape skin are differentially regulated by temperature and light conditions. *Planta*, 236(4), 1067-1080.

Beckles, D. M. (2012). Factors affecting the postharvest soluble solids and sugar content of tomato (*Solanum lycopersicum* L.) fruit. *Postharvest Biology and Technology*, 63(1), 129–140. https://doi.org/10.1016/j.postharvbio.2011.05.016

Belhadj, A., Telef, N., Saigne, C., Cluzet, S., Barrieu, F., Hamdi, S., & Mérillon, J. M. (2008). Effect of methyl jasmonate in combination with carbohydrates on gene expression of PR proteins, stilbene and anthocyanin accumulation in grapevine cell cultures. *Plant Physiology and Biochemistry*, 46(4), 493-499.

Bian, Z. H., Yang, Q. C., & Liu, W. K. (2015). Effects of light quality on the accumulation of phytochemicals in vegetables produced in controlled environments: A review. *Journal of the Science of Food and Agriculture*, 95(5), 869–877. https://doi.org/10.1002/jsfa.6789

Bueno, J. M., Sáez-Plaza, P., Ramos-Escudero, F., Jiménez, A. M., Fett, R., & Asuero, A. G. (2012). Analysis and Antioxidant Capacity of Anthocyanin Pigments. Part II: Chemical Structure, Color, and Intake of Anthocyanins. *Critical Reviews in Analytical Chemistry*, *42*(2), 126–151. https://doi.org/10.1080/10408347.2011.632314

Castillo-Muñoz, N., Gómez-Alonso, S., García-Romero, E., Gómez, M. V., Velders, A. H., & Hermosín-Gutiérrez, I. (2009). Flavonol 3-O-glycosides series of *Vitis vinifera* cv. Petit Verdot red wine grapes. *Journal of Agricultural and Food Chemistry*, 57(1), 209-219.

Cavallini E, Zenoni S, Finezzo L, Guzzo F, Zamboni A, Avesani L, Tornielli GB. (2014). Functional diversification of grapevine MYB5a and MYB5b in the control of flavonoid biosynthesis in a petunia anthocyanin regulatory mutant. *Plant and Cell Physiology*, 55(3):517:534. DOI: https://doi.org/10.1093/pcp/pct190.

Chen, X. li, Wang, L. chun, Li, T., Yang, Q. chang, & Guo, W. zhong. (2019). Sugar accumulation and growth of lettuce exposed to different lighting modes of red and blue LED light. *Scientific Reports*, 9(1), 1–10. https://doi.org/10.1038/s41598-019-43498-8

Chiang, C., Olsen, J. E., Basler, D., Bånkestad, D., & Hoch, G. (2019). Latitude and weather influences on sun light quality and the relationship to tree growth. *Forests*, *10*(8), 1–12. https://doi.org/10.3390/f10080610

Chu, W., Cheung S.C.M. & Lau, R.A.W. (2011). Bilberry (*Vaccinium myrtillus* L.) In: Benzie IFF, Wachtel-Galor S, editors. Herbal Medicine: Biomolecular and Clinical Aspects. 2nd edition. Boca Raton (FL): CRC Press/Taylor & Francis.

Chung, S. W., Yu, D. J., Oh, H. D., Ahn, J. H., Huh, J. H., & Lee, H. J. (2019). Transcriptional regulation of abscisic acid biosynthesis and signal transduction, and anthocyanin biosynthesis in 'Bluecrop'highbush blueberry fruit during ripening. *PLoS One*, 14(7), e0220015.

Davies, K.M., Schwinn, K.E., Deroles, S.C., Manson, D.G., Lewis, D.H., Bloor, S.J., Bradley, J.M. (2003) Enhancing anthocyanin production by altering competition for substrate between flavonol synthase and dihydroflavonol 4-reductase. *Euphytica* 131(3):259–268

de Rosas, I., Ponce, M. T., Malovini, E., Deis, L., Cavagnaro, B., & Cavagnaro, P. (2017). Loss of anthocyanins and modification of the anthocyanin profiles in grape berries of Malbec and Bonarda grown under high temperature conditions. *Plant Science*, 258, 137–145. https://doi.org/10.1016/j.plantsci.2017.01.015

Debnath, S. C & Goyali, J. C. (2020). In vitro propagation and variation of antioxidant properties in micropropagated vaccinium berry plants - A review. *Molecules*, *25*(4), 1–26. https://doi.org/10.3390/molecules25040788

Demotes-Mainard, S., Péron, T., Corot, A., Bertheloot, J., Le Gourrierec, J., Pelleschi-Travier, S., ... & Sakr, S. (2016). Plant responses to red and far-red lights, applications in horticulture. *Environmental and experimental Botany*, 121, 4-21.

Dong, F., Wang, C., Sun, X., Bao, Z., Dong, C., Sun, C., … Liu, S. (2019). Sugar metabolic changes in protein expression associated with different light quality combinations in tomato fruit. *Plant Growth Regulation*, 88(3), 267–282. https://doi.org/10.1007/s10725-019-00506-1

Dorokhov, A. S., Smirnov, A. A., Semenova, N. A., Akimova, S. V., Kachan, S. A., Chilingaryan, N., … Yu Podkovyrov, I. (2021). The effect of far-red light on the productivity and photosynthetic activity of tomato. IOP Conference Series: *Earth and Environmental Science*, 663(1). https://doi.org/10.1088/1755-1315/663/1/012044

Downey, M. O., Harvey, J. S., & Robinson, S. P. (2003). Synthesis of flavonols and expression of flavonol synthase genes in the developing grape berries of Shiraz and Chardonnay (*Vitis vinifera* L.). *Australian Journal of Grape and Wine Research*, 9(2), 110-121.

Downey, M. O., Harvey, J. S., & Robinson, S. P. (2004). The effect of bunch shading on berry development and flavonoid accumulation in Shiraz grapes. *Australian Journal of Grape and Wine Research*, 10(1), 55-73.

Dussi, M., Sugar, D., & Wrolstad, R. (1995). Characterizing and quantifying anthocyanins in red pears and the effect of light quality on fruit color. *Journal of the American society for Horticultural Science*, 120(5), 785-789. doi: 10.21273/jashs.120.5.785

Erlund, I., Koli, R.., Alfthan, G., Marniemi, J., Puukka, P., Mustonen, P., Mattila, P., Jula. (2008). A. favorable effects of berry consumption on platelet function, blood pressure, and HDL cholesterol. *The American. Journal of clinical nutrition*, *87*, 323– 331, DOI: 10.1093/ajcn/87.2.323

Fang, F., Tang, K., & Huang, W. D. (2013). Changes of flavonol synthase and flavonol contents during grape berry development. *European Food Research and Technology*, 237(4), 529–540. https://doi.org/10.1007/s00217-013-2020-z

Fang, J. (2014). Bioavailability of anthocyanins. *Drug Metabolism Reviews*, 46(4), 508–520. https://doi.org/10.3109/03602532.2014.978080

Fang, J. (2014). Bioavailability of Anthocyanins. *Drug metabolism reviews*. 46 (4), 508−520.

Fang, M., Fang R., He, M., Hu, L., Yang, H., Qin, H., Min, T., David, F. C., Peter, F. S., Gary D. W., Arne, A. (2007). Ericaceae. In: Wu, Z-Y., P. H. Raven & D. Y. Hong (eds.), Flora of China, Missouri Botanical Garden press, St. Louis and science press, Beijing.

Feng, F., Li, M., Ma, F., & Cheng, L. (2013). Phenylpropanoid metabolites and expression of key genes involved in anthocyanin biosynthesis in the shaded peel of apple fruit in response to sun exposure. *Plant Physiology and Biochemistry*, 69, 54–61. https://doi.org/10.1016/j.plaphy.2013.04.020

Ferrero, M., Pagliarani, C., Novák, O., Ferrandino, A., Cardinale, F., Visentin, I., & Schubert, A. (2018). Exogenous strigolactone interacts with abscisic acid-mediated accumulation of anthocyanins in grapevine berries. *Journal of experimental botany*, 69(9), 2391-2401.

Forney, C. F., Kalt, W., Jordan, M. A., Vinqvist-Tymchuk, M. R., & Fillmore, S. A. E. (2012). Blueberry and cranberry fruit composition during development. *Journal of Berry Research*, *2*(3), 169–177. https://doi.org/10.3233/JBR-2012-034

Fukuoka, N., Suzuki, T., Minamide, K., & Hamada, T. (2014). Effect of shading on anthocyanin and non-flavonoid polyphenol biosynthesis of Gynura bicolor leaves in midsummer. *HortScience*, 49(9), 1148–1153. https://doi.org/10.21273/hortsci.49.9.1148

Gao, B., Yang, Z. C., Li, W. Q., Wang, X. X., Ding, J. J., Geng, F. Z., ... & Wang, D. F. (2015). Effects of three different red and blue LED light ratio on growth and quality of celery. *Acta Agric Boreali-occident Sin*, 24, 125-132.

Gaspar, D. P., Lechtenberg, M., & Hensel, A. (2021). Quality assessment of bilberry fruits (*Vaccinium myrtillus*) and bilberry-containing dietary supplements. *Journal of Agricultural and Food Chemistry*, *69*(7), 2213-2225.

Gholami, M., 2004. Biosynthesis of anthocyanins in Shiraz grape berries. *Acta Horticulturae*. 640,472 353-360.

Girault, T., Abidi, F., Sigogne, M., Pelleschi-Travier, S., Boumaza, R., Sakr, S., & Leduc, N. (2010). Sugars are under light control during bud burst in *Rosa* sp. *Plant, Cell and Environment*, 33(8), 1339–1350. https://doi.org/10.1111/j.1365-3040.2010.02152.x

Glimn-Lacy, J., & Kaufman, P. B. (2006). Heath family (Ericaceae). Botany Illustrated: Introduction to Plants, Major Groups, Flowering Plant Families, 97-97.

Gonzalez, C. V., Fanzone, M. L., Cortés, L. E., Bottini, R., Lijavetzky, D. C., Ballare, C. L., & Boccalandro, H. E. (2015). Fruit-localized photoreceptors increase phenolic compounds in berry skins of field-grown *Vitis vinifera* L. cv. Malbec. *Phytochemistry*, 110, 46-57.

González-Villagra, J., Kurepin, L. V., & Reyes-Díaz, M. M. (2017). Evaluating the involvement and interaction of abscisic acid and miRNA156 in the induction of anthocyanin biosynthesis in drought-stressed plants. *Planta*, 246(2), 299-312.

Grotewold, E., & Davies, K. (2008). Trafficking and Sequestration of Anthocyanins. *Natural Product Communications*. https://doi.org/10.1177/1934578X0800300806

Gu, X., Brennan, A., Wei, W., Guo, G., & Lindsey, K. (2020). Vesicle Transport in Plants: A Revised Phylogeny of SNARE Proteins. Evolutionary *Bioinformatics*, 16. https://doi.org/10.1177/1176934320956575

Hancock, J.F.; Luby, J.J.; Beaudry, R. (2003). Fruits of temperate climates/Fruits of the Ericaceae. In Encyclopedia of Food Science, Food Technology and Nutrition, 2nd ed.; Trugo, L., Finglas, P.M., Caballero, B., Eds.; Academic Press: London, UK; pp. 2762–2768.

Henwood, R. J. T., Wargent, J. J., Black, M., & Heyes, J. A. (2018). Environmental and management factors contributing to variability in flesh colour of a red kiwifruit cultivar in New Zealand. *Scientia Horticulturae*, 235(November 2017), 21–31. https://doi.org/10.1016/j.scienta.2017.12.009

Holopainen, J. K., Kivimäenpää, M., & Julkunen-Tiitto, R. (2018). New light for phytochemicals. *Trends in biotechnology*, 36(1), 7-10.

Jaakola L., Poole, M., Jones, M., Kämäräinen-Karppinen, T., Koskimäki, J.J., Hohtola, A., Häggman, H., Fraser, P., Manning, K., King, G.J. Thomson, H. & Seymour, G.B. (2010) A SQUAMOSA MADS-box gene involved in the regulation of anthocyanin accumulation in bilberry fruits. Plant Physiology, 153, 1619-1629. https://doi.org/10.1104/pp.110.158279

Jaakola, L. (2013). New insights into the regulation of anthocyanin biosynthesis in fruits. *Trends in Plant Science*, *18*(9), 477–483. https://doi.org/10.1016/j.tplants.2013.06.003

Jaakola, L., Määttä, K., Pirttilä, A. M., Törrönen, R., Kärenlampi, S., & Hohtola, A. (2002). Expression of genes involved in anthocyanin biosynthesis in relation to anthocyanin, proanthocyanidin, and flavonol levels during bilberry fruit development. *Plant Physiology*, *130*(2), 729–739. https://doi.org/10.1104/pp.006957

Ju, Z. (1998). Fruit bagging, a useful method for studying anthocyanin synthesis and gene expression in apples. *Scientia Horticulturae*, 77(3–4), 155–164. https://doi.org/10.1016/S0304-4238(98)00161-7

Kadomura-Ishikawa, Y., Miyawaki, K., Takahashi, A., Masuda, T., & Noji, S. (2014). Light and abscisic acid independently regulated FaMYB10 in *Fragaria* × *ananassa* fruit. *Planta*, 241(4), 953-965. doi: 10.1007/s00425-014-2228-6

Kalt, W., Cassidy, A., Howard, L. R., Krikorian, R., Stull, A. J., Tremblay, F., & Zamora-Ros, R. (2020). Recent Research on the Health Benefits of Blueberries and Their Anthocyanins. *Advances in Nutrition*, *11*(2), 224–236. https://doi.org/10.1093/advances/nmz065

Kalt, W., Lawand, C., Ryan, D.A.J., McDonald, J.E., Forney, C.F. (2003) Oxygen radical absorbing capacity, anthocyanin and phenolic content of highbush blueberries (*Vaccinium corymbosum* L.) during ripening and storage. *Journal of the American society for Horticultural Science*. 128, 917–23.

Karppinen, K., Lafferty, D. J., Albert, N. W., Mikkola, N., McGhie, T., Allan, A. C., ... & Jaakola, L. (2021). MYBA and MYBPA transcription factors co-regulate anthocyanin biosynthesis in blue-coloured berries. *New Phytologist*, 232 (3), 1350-1367 doi: https://doi.org/10.1111/nph.17669

Karppinen, K., Tegelberg, P., Häggman, H., & Jaakola, L. (2018). Abscisic acid regulates anthocyanin biosynthesis and gene expression associated with cell wall modification in ripening bilberry (*Vaccinium myrtillus* L.) fruits. *Frontiers in Plant Science*, 9(August), 1–17. https://doi.org/10.3389/fpls.2018.01259

Karppinen, K., Zoratti, L., Sarala, M., Carvalho, E., Hirsimäki, J., Mentula, H., … Jaakola, L. (2016). Carotenoid metabolism during bilberry (*Vaccinium myrtillus* L.) fruit development under different light conditions is regulated by biosynthesis and degradation. *BMC Plant Biology*, 16(1), 95. https://doi.org/10.1186/s12870-016-0785-5

Kaur, S., Sharma, N., Kapoor, P., Chunduri, V., Pandey, A. K., & Garg, M. (2021). Spotlight on the overlapping routes and partners for anthocyanin transport in plants. *Physiologia Plantarum*, 171(4), 868–881. https://doi.org/10.1111/ppl.13378

Khanna, R., Li, J., Tseng, T. S., Schroeder, J. I., Ehrhardt, D. W., and Briggs, W. R. (2014). COP1 jointly modulates cytoskeletal processes and electrophysiological responses required for stomatal closure. *Moecular Plant* 7, 1441–1454. doi: 10.1093/mp/ssu065

Koch, K. (2004). Sucrose metabolism: Regulatory mechanisms and pivotal roles in sugar sensing and plant development. *Current Opinion in Plant Biology*, 7(3), 235–246. https://doi.org/10.1016/j.pbi.2004.03.014

Kokalj, D., Zlatić, E., Cigić, B., & Vidrih, R. (2019). Postharvest light-emitting diode irradiation of sweet cherries (*Prunus avium* L.) promotes accumulation of anthocyanins. *Postharvest Biology and Technology*, 148, 192–199. https://doi.org/10.1016/j.postharvbio.2018.11.011

Kondo, S., Tomiyama, H., Rodyoung, A., Okawa, K., Ohara, H., Sugaya, S., ... & Hirai, N. (2014). Abscisic acid metabolism and anthocyanin synthesis in grape skin are affected by light emitting diode (LED) irradiation at night. *Journal of plant physiology*, 171(10), 823-829

Koponen, J., Kallio, H., Yang, B., & Tahvonen, R. (2001). Plant sterols in Finnish blueberry (*Vaccinium myrtillus* L.) and lingonberry (*Vaccinium vitis-idaea* L.) seed oils. In Biologically-active phytochemicals in food: analysis, metabolism, bioavailability and function. Proceedings of the EUROFOODCHEM XI Meeting, Norwich, UK, 26-28 September 2001 (pp. 233-236). Royal Society of Chemistry.

Krga, I., & Milenkovic, D. (2019). Anthocyanins: From Sources and Bioavailability to Cardiovascular-Health Benefits and Molecular Mechanisms of Action. *Journal of Agricultural and Food Chemistry*, *67*(7), 1771–1783. https://doi.org/10.1021/acs.jafc.8b06737

Kwon, C., Lee, J. H., & Yun, H. S. (2020). Snares in plant biotic and abiotic stress responses. *Molecules and Cells*, 43(6), 501–508. https://doi.org/10.14348/molcells.2020.0007

Kwon, C., Neu, C., Pajonk, S., Yun, H. S., Lipka, U., Humphry, M., … Schulze-Lefert, P. (2008). Co-option of a default secretory pathway for plant immune responses. *Nature*, 451(7180), 835–840. https://doi.org/10.1038/nature06545

Lastdrager, J., Hanson, J., & Smeekens, S. (2014). Sugar signals and the control of plant growth and development. *Journal of Experimental Botany*, 65(3), 799–807. https://doi.org/10.1093/jxb/ert474

Lattanzi, F., Ostler, U., Wild, M., Morvan-Bertrand, A., Decau, M., & Lehmeier, C. et al. (2012). Fluxes in central carbohydrate metabolism of source leaves in a fructan-storing C3 grass: rapid turnover and futile cycling of sucrose in continuous light under contrasted nitrogen nutrition status. *Journal Of Experimental Botany*, 63(6), 2363-2375. doi: 10.1093/jxb/ers020

Lätti, A., Riihinen, K., & Kainulainen, P. (2008). Analysis of Anthocyanin Variation in Wild Populations of Bilberry (*Vaccinium myrtillus* L.) in Finland. *Journal of agricultural and food chemistry*, 56(1), 190-196. doi: 10.1021/jf072857m

Lemoine, R., La Camera, S., Atanassova, R., Dédaldéchamp, F., Allario, T., Pourtau, N., … Durand, M. (2013). Source-to-sink transport of sugar and regulation by environmental factors. *Frontiers in Plant Science*, *4*(JUL), 1–21. https://doi.org/10.3389/fpls.2013.00272

Levy, Y.Y & Dean. (1998) The Transition to Flowering, *The Plant Cell*, 10 (12) 1973–1989, https://doi.org/10.1105/tpc.10.12.1973

Li, D., Li, B., Ma, Y., Sun, X., Lin, Y., & Meng, X. (2017). Polyphenols, anthocyanins, and flavonoids contents and the antioxidant capacity of various cultivars of highbush and half-high blueberries. *Journal of Food Composition and Analysis*, *62*, 84-93.

Li, Y., Xin, G., Wei, M., Shi, Q., Yang, F., & Wang, X. (2017). Carbohydrate accumulation and sucrose metabolism responses in tomato seedling leaves when subjected to different light qualities. *Scientia Horticulturae*, 225(August), 490–497. https://doi.org/10.1016/j.scienta.2017.07.053

Liang, X., Wang, H., Mao, L., Hu, Y., Dong, T., Zhang, Y., et al. (2012). Involvement of COP1 in ethylene- and light-regulated hypocotyl elongation. *Planta* 236, 1791–1802. doi: 10.1007/s00425-012-1730-y

Lin-Wang, K., McGhie, T. K., Wang, M., Liu, Y., Warren, B., Storey, R., ... & Allan, A. C. (2014). Engineering the anthocyanin regulatory complex of strawberry (*Fragaria vesca*). *Frontiers in plant science*, 5, 651.

Liu, B., Wang, L., Wang, S., Li, W., Liu, D., Guo, X., & Qu, B. (2019). Transcriptomic analysis of bagging-treated 'Pingguo' pear shows that MYB4-like1, MYB4-like2, MYB1R1 and WDR involved in anthocyanin biosynthesis are up-regulated in fruit peels in response to light. *Scientia Horticulturae*, 244, 428–434. https://doi.org/10.1016/j.scienta.2018.09.040

Liu, X., Chang, T., Guo, S., Xu, Z., & Chen, W. (2010). Effect of irradiation with blue and red LED on fruit quality of cherry tomato during growth period. *China vegetables*, (22), 21-27.

Liu, Y., Zhang, X., & Zhao, Z. (2013). Effects of fruit bagging on anthocyanins, sugars, organic acids, and color properties of "Granny Smith" and "Golden Delicious" during fruit maturation. *European Food Research and Technology*, 236(2), 329–339. https://doi.org/10.1007/s00217-012-1896-3

Lloyd, J., & Kötting, O. (2016). Starch Biosynthesis and Degradation in Plants. *eLS*, 1-10. doi: 10.1002/9780470015902.a0020124.pub2

Lurie, S., Ovadia, R., Nissim-Levi, A., Oren-Shamir, M., Kaplunov, T., Zutahy, Y., … Lichter, A. (2009). Abscisic acid improves colour development in "Crimson Seedless" grapes in the vineyard and on detached berries. *Journal of Horticultural Science and Biotechnology*, 84(6), 639–644. https://doi.org/10.1080/14620316.2009.11512579

Ma, Z. H., Li, W. F., Mao, J., Li, W., Zuo, C. W., Zhao, X., … Chen, B. H. (2019). Synthesis of light-inducible and light-independent anthocyanins regulated by specific genes in grape “Marselan” (*V. Vinifera* L.). *PeerJ*, 2019(3), 1–24. https://doi.org/10.7717/peerj.6521

Määttä-Riihinen, K. R., Kähkönen, M. P., Törrönen, A. R., & Heinonen, I. M. (2005). Catechins and procyanidins in berries of Vaccinium species and their antioxidant activity. *Journal of Agricultural and Food Chemistry*, *53*(22), 8485–8491. https://doi.org/10.1021/jf050408l

Martínez-Lüscher, J., Brillante, L., & Kurtural, S. K. (2019). Flavonol profile is a reliable indicator to assess canopy architecture and the exposure of red wine grapes to solar radiation. *Frontiers in plant science*, 10, 10.

Matus, J. T., Loyola, R., Vega, A., Peña-Neira, A., Bordeu, E., Arce-Johnson, P., et al. (2009). Post-veraison sunlight exposure induces MYB-mediated transcriptional regulation of anthocyanin and flavonol synthesis in berry skins of *Vitis vinifera*. *Journal of Experimental. Botany*. 60, 853–867. doi: 10.1093/jxb/ern336

Mazzella, M. A., Casal, J. J., Muschietti, J. P., and Fox, A. R. (2014). Hormonal networks involved in apical hook development in darkness and their response to light. *Frontiers in Plant Sci.* 5:52. doi: 10.3389/fpls.2014.00052

Miao, L., Zhang, Y., Yang, X., Xiao, J., Zhang, H., Zhang, Z., … Jiang, G. (2016). Colored light-quality selective plastic films affect anthocyanin content, enzyme activities, and the expression of flavonoid genes in strawberry (*Fragaria* × *ananassa*) fruit. *Food Chemistry*, 207, 93–100. https://doi.org/10.1016/j.foodchem.2016.02.077

Michalska, A., & Łysiak, G. (2015). Bioactive compounds of blueberries: post-harvest factors influencing the nutritional value of products. International Journal of Molecular Sciences, 16(8), 18642–18663. https://doi.org/10.3390/ijms160818642

Mikulic-Petkovsek, M., Schmitzer, V., Slatnar, A., Stampar, F., & Veberic, R. (2015). A comparison of fruit quality parameters of wild bilberry (*Vaccinium myrtillus* L.) growing at different locations. Journal of the Science of Food and Agriculture, 95(4), 776–785. https://doi.org/10.1002/jsfa.6897

Milivojevic, J., Maksimovic, V., Maksimovic, J. D., Radivojevic, D., Poledica, M., & ERCİŞLİ, S. (2012). A comparison of major taste-and health-related compounds of Vaccinium berries. *Turkish Journal of Biology*, *36*(6), 738-745.

Möglich, A., Yang, X., Ayers, R. A., & Moffat, K. (2010). Structure and function of plant photoreceptors. *Annual Review of Plant Biology, 61*, 21–47. https://doi.org/10.1146/annurev-arplant-042809-112259

Moscovici, S., Moalem-Beno, D., & Weiss, D. (1996). Leaf-mediated light responses in petunia flowers. *Plant physiology*, 110(4), 1275-1282.

Moyer, R. A., Hummer, K. E., Finn, C. E., Frei, B., & Wrolstad, R. E. (2002). Anthocyanins, phenolics, and antioxidant capacity in diverse small fruits: Vaccinium, Rubus, and Ribes. *Journal of agricultural and food chemistry*, *50*(3), 519-525.

Nadalini, S., Zucchi, P., & Andreotti, C. (2017). Effects of blue and red led lights on soilless cultivated strawberry growth performances and fruit quality. *European Journal of Horticultural Science*, 82(1), 12–20. https://doi.org/10.17660/eJHS.2017/82.1.2

Nassarawa, S. S., Abdelshafy, A. M., Xu, Y., Li, L., & Luo, Z. (2021). Effect of Light-Emitting Diodes (LEDs) on the Quality of Fruits and Vegetables During Postharvest Period: a Review. *Food and Bioprocess Technology*, 14(3), 388–414. https://doi.org/10.1007/s11947-020-02534-6

Nestby, R., Percival, D., Martinussen, I., Opstad, N., & Rohloff, J. (2011). The European blueberry (*Vaccinium myrtillus* L.) and the potential for cultivation. *European Journal of Plant Science and Biotechnology*, 5(January), 5–16.

Nguyen, N., Suokas, M., Karppinen, K., Vuosku, J., Jaakola, L., & Häggman, H. (2018). Recognition of candidate transcription factors related to bilberry fruit ripening by de novo transcriptome and qRT-PCR analyses. *Scientific Reports*, 8(1), 1–12. https://doi.org/10.1038/s41598-018-28158-7

Nguyen-Quoc, B., & Foyer, C. H. (2001). A role for 'futile cycles' involving invertase and sucrose synthase in sucrose metabolism of tomato fruit. *Journal of experimental botany*, 52(358), 881–889. https://doi.org/10.1093/jexbot/52.358.881

Pacin, M., Semmoloni, M., Legris, M., Finlayson, S. A., and Casal, J. J. (2016). Convergence of constitutive photomorphogenesis 1 and phytochrome interacting factor signalling during shade avoidance. *New Phytologist.* 211, 967–979. doi: 10.1111/nph.13965

Panche, A. N., Diwan, A. D., & Chandra, S. R. (2016). Flavonoids: An overview. *Journal of Nutritional Science*, 5, E47. https://doi.org/10.1017/jns.2016.41

Paredes-López, O., Cervantes-Ceja, M. L., Vigna-Pérez, M., & Hernández-Pérez, T. (2010). Berries: Improving Human Health and Healthy Aging, and Promoting Quality Life-A Review. *Plant Foods for Human Nutrition*, 65(3), 299–308. https://doi.org/10.1007/s11130-010-0177-1

Pires, T. C. S. P., Caleja, C., Santos-Buelga, C., Barros, L., & Ferreira, I. C. F. R. (2020). *Vaccinium myrtillus* L. Fruits as a Novel Source of Phenolic Compounds with Health Benefits and Industrial Applications - A Review. *Current Pharmaceutical Design*, 26(16), 1917–1928. https://doi.org/10.2174/1381612826666200317132507

Plunkett, B. J., Espley, R. V., Dare, A. P., Warren, B. A., Grierson, E. R., Cordiner, S., ... & Schwinn, K. E. (2018). MYBA from blueberry (*Vaccinium* section Cyanococcus) is a subgroup 6 type R2R3MYB transcription factor that activates anthocyanin production. *Frontiers in plant science*, 9, 1300.

Pourcel, L., Irani, N. G., Lu, Y., Riedl, K., Schwartz, S., & Grotewold, E. (2010). The formation of anthocyanic vacuolar inclusions in *Arabidopsis thaliana* and implications for the sequestration of anthocyanin pigments. *Molecular Plant*, 3(1), 78–90. https://doi.org/10.1093/mp/ssp071

Qin, Y., Xia, M., Ma, J., Hao, Y., Liu, J., Mou, H., Cao, L., & Ling, W. (2009) Anthocyanin supplementation improves serum LDL- and HDL-cholesterol concentrations associated with the inhibition of cholesteryl ester transfer protein in dyslipidemic subject. *The American Journal of Clinical Nutrition, 90*, 485– 492, DOI: 10.3945/ajcn.2009.27814

Routray, W., & Orsat, V. (2011). Blueberries and Their Anthocyanins: Factors Affecting Biosynthesis and Properties. *Comprehensive Reviews in Food Science and Food Safety*, 10(6), 303–320. https://doi.org/10.1111/j.1541-4337.2011.00164.x

Rowland, L.J.; Hancock, J.F.; Bassil, N.V. (2011). Blueberry. In Genetics, Genomics and Breeding of Berries; Folta, K.M.,Kole, C., Eds.; CRC Press: Boca Raton, FL, USA; pp. 1–39.

Salerno, G. L., & Curatti, L. (2003). Origin of sucrose metabolism in higher plants: When, how and why? *Trends in Plant Science*, *8*(2), 63–69. https://doi.org/10.1016/S1360-1385(02)00029-8

Sandhu, A. K., Gray, D. J., Lu, J., & Gu, L. (2011). Effects of exogenous abscisic acid on antioxidant capacities, anthocyanins, and flavonol contents of muscadine grape (*Vitis rotundifolia*) skins. *Food Chemistry*, 126(3), 982-988.

Sharma, A., Shahzad, B., Rehman, A., Bhardwaj, R., Landi, M., & Zheng, B. (2019). Response of phenylpropanoid pathway and the role of polyphenols in plants under abiotic stress. *Molecules*, 24(13), 1–22. https://doi.org/10.3390/molecules24132452

Shi, H., Shen, X., Liu, R., Xue, C., Wei, N., Deng, X. W., et al. (2016). The red-light receptor phytochrome B directly enhances substrate-E3 ligase interactions to attenuate ethylene responses. *Developmental Cell* 39, 597–610. doi: 10.1016/j.devcel.2016.10.020

Shi, L., Cao, S., Chen, W., & Yang, Z. (2014). Blue light induced anthocyanin accumulation and expression of associated genes in Chinese bayberry fruit. *Scientia Horticulturae*, 179, 98–102. https://doi.org/10.1016/j.scienta.2014.09.022

Singh Brar, H., Singh, Z. and Swinny, E. (2008). Dynamics of anthocyanin and flavonol profiles in the 'Crimson Seedless' grape berry skin during development and ripening. *Scientia Horticulturae*, 117, 349–356.

Skrovankova, S., Sumczynski, D., Mlcek, J., Jurikova, T., & Sochor, J. (2015). Bioactive compounds and antioxidant activity in different types of berries. *International Journal of Molecular Sciences*, 16(10), 24673–24706. https://doi.org/10.3390/ijms161024673

Sobekova, K., Thomsen, M. R., & Ahrendsen, B. L. (2013). Market trends and consumer demand for fresh berries. *Applied Studies in Agribusiness and Commerce*, 7(2–3), 11–14. https://doi.org/10.19041/apstract/2013/2-3/1

Song, G.Q & Hancock, J.F (2011) *Vaccinium*. In: Kole C (ed) Wild crop relatives: genomic and breeding resources, temperate fruits. Berlin Heidelberg, Springer: 197-221.

Spayd, S., Tarara, J., Mee, D., & Ferguson, J. (2002). Separation of sunlight and temperature effects on the composition of *Vitis vinifera* cv. Merlot berries. *American journal of enology and viticulture*, 53, 171.

Stanoeva, J. P., Stefova, M., Andonovska, K. B., Vankova, A., & Stafilov, T. (2017). Phenolics and mineral content in bilberry and bog bilberry from Macedonia. *International Journal of Food Properties*, 20(1), S863–S883. https://doi.org/10.1080/10942912.2017.1315592

Stein, O., & Granot, D. (2018). Plant fructokinases: Evolutionary, developmental, and metabolic aspects in sink tissues. *Frontiers in Plant Science*, *9*(March), 1–12. https://doi.org/10.3389/fpls.2018.00339

Stevens, P. F., Luteyn, J., Oliver, E. G. H., Bell, T. L., Brown, E. A., Crowden, R. K., ... & Weiller, C. M. (2004). Ericaceae. In *Flowering Plants· Dicotyledons* (pp. 145-194). Springer, Berlin, Heidelberg.

Tao, R., Bai, S., Ni, J., Yang, Q., Zhao, Y., & Teng, Y. (2018). The blue light signal transduction pathway is involved in anthocyanin accumulation in 'Red Zaosu' pear. *Planta*, 248(1), 37–48. https://doi.org/10.1007/s00425-018-2877-y

Teixeira, A., Eiras-Dias, J., Castellarin, S. D., & Gerós, H. (2013). Berry phenolics of grapevine under challenging environments. *International Journal of Molecular Sciences*, 14(9), 18711–18739. https://doi.org/10.3390/ijms140918711

Tinyane, P. P., Sivakumar, D., & Soundy, P. (2013). Influence of photo-selective netting on fruit quality parameters and bioactive compounds in selected tomato cultivars. *Scientia Horticulturae*, 161, 340–349. https://doi.org/10.1016/j.scienta.2013.06.024

Uleberg, E., Rohloff, J., Jaakola, L., Trôst, K., Junttila, O., Häggman, H., & Martinussen, I. (2012). Effects of temperature and photoperiod on yield and chemical composition of northern and southern clones of bilberry (*Vaccinium myrtillus* L.). *Journal of Agricultural and Food Chemistry*, 60(42), 10406–10414. https://doi.org/10.1021/jf302924m

Wang, W., Chen, Q., Botella, J. R., & Guo, S. (2019). Beyond light: Insights into the role of constitutively photomorphogenic1 in plant hormonal signaling. *Frontiers in Plant Science*, *10*(May). https://doi.org/10.3389/fpls.2019.00557

Ward, J. M., Kühn, C., Tegeder, M., & Frommer, W. B. (1998). Sucrose transport in higher plants. *International Review of Cytology*, 178(ii), 41–71. https://doi.org/10.1016/s0074-7696(08)62135-x

Wheeler, S., Loveys, B., Ford, C., & Davies, C. (2009). The relationship between the expression of abscisic acid biosynthesis genes, accumulation of abscisic acid and the promotion of *Vitis vinifera* L. berry ripening by abscisic acid. *Australian Journal of Grape and Wine Research*, 15(3), 195-204.

Wu B.S., Rufyikiri A.S., Orsat, V., & Lefsrud. M. G. (2019). Re-interpreting the photosynthetically action radiation (PAR) curve in plants. *Plant Science*, vol. 289, p. 110272.

Xu, F., Cao, S., Shi, L., Chen, W., Su, X., & Yang, Z. (2014). Blue light irradiation affects anthocyanin content and enzyme activities involved in postharvest strawberry fruit. *Journal of Agricultural and Food Chemistry*, 62(20), 4778–4783. https://doi.org/10.1021/jf501120u

Xu, P., Zawora, C., Li, Y., Wu, J., Liu, L., Liu, Z., … Lian, H. (2018). Transcriptome sequencing reveals role of light in promoting anthocyanin accumulation of strawberry fruit. *Plant Growth Regulation*, 86(1), 121–132. https://doi.org/10.1007/s10725-018-0415-3

Yao, K., & Wu, Y. Y. (2016). Phosphofructokinase and glucose-6-phosphate dehydrogenase in response to drought and bicarbonate stress at transcriptional and functional levels in mulberry. *Russian Journal of Plant Physiology*, 63(2), 235-242.

Yavari, N., Tripathi, R., Wu, B. Sen, MacPherson, S., Singh, J., & Lefsrud, M. (2021). The effect of light quality on plant physiology, photosynthetic, and stress response in Arabidopsis thaliana leaves. *PLoS ONE*, *16*(3 March), 1–19. https://doi.org/10.1371/journal.pone.0247380

Yu, L., Liu, H., Shao, X., Yu, F., Wei, Y., Ni, Z., ... & Wang, H. (2016). Effects of hot air and methyl jasmonate treatment on the metabolism of soluble sugars in peach fruit during cold storage. *Postharvest Biology and Technology*, 113, 8-16.

Zhang XH, Zheng XT, Sun BY, Peng CL, Chow WS. (2017). Over-expression of the CHS gene enhances resistance of Arabidopsis leaves to high light. *Environmental and Experimental Botany* 154:33-43.

Zhang, H. N., Li, W. C., Wang, H. C., Shi, S. Y., Shu, B., Liu, L. Q., … Xie, J. H. (2016). Transcriptome profiling of light-regulated anthocyanin biosynthesis in the pericarp of litchi. *Frontiers in Plant Science*, 7(JUNE), 1–15. https://doi.org/10.3389/fpls.2016.00963

Zhang, H., Li, W., Wang, H., Shi, S., Shu, B., & Liu, L. et al. (2016). Transcriptome Profiling of Light-Regulated Anthocyanin Biosynthesis in the Pericarp of Litchi. Frontiers In Plant Science, 07. doi: 10.3389/fpls.2016.00963

Zhang, L., Wang, Y., Gao, Q., & Duan, K. (2017). The phylogeny, expression patterns of alkaline/neutral invertase genes (Fa. A/N-Invs) family and their influence on sugar accumulation in strawberry fruit. *Acta Horticulturae Sinica*, 44(6), 1049-1060.

Zhang, X. L., Jiang, L., Xin, Q., Liu, Y., Tan, J. X., & Chen, Z. Z. (2015). Structural basis and functions of abscisic acid receptors PYLs. *Frontiers in Plant Science*, 6, 88.

Zhao, J., Pang, Y., & Dixon, R. A. (2010). The mysteries of proanthocyanidin transport and polymerization. *Plant Physiology*, 153(2), 437–443. https://doi.org/10.1104/pp.110.155432

Zhao, Y., Dong, W., Wang, K., Zhang, B., Allan, A. C., Lin-Wang, K., … Xu, C. (2017). Differential sensitivity of fruit pigmentation to ultraviolet light between two peach cultivars. *Frontiers in Plant Science*, *8*(September), 1–15. https://doi.org/10.3389/fpls.2017.01552

Zheng, Y., Li, J., Xin, H., Wang, N., Guan, L., Wu, B., & Li, S. (2013). Anthocyanin profile and gene expression in berry skin of two red *Vitis vinifera* grape cultivars that are sunlight dependent versus sunlight independent. *Australian Journal of Grape and Wine Research*, 19(2), 238-248. doi: 10.1111/ajgw.12023.

Zhou, Y., & Singh, B. R. (2004). Effect of light on anthocyanin levels in submerged, harvested cranberry fruit. *Journal of Biomedicine and Biotechnology*, 2004(5), 259.

Zhu, J. K. (2016). Abiotic stress signaling and responses in plants. *Cell*, 167(2), 313-324.

Zhu, Y.F., Su, J., Yao, G.F., Liu, H.N., Gu, C., Qin, M.F., Bai, B., Cai, S.S., Wang, G.M., Wang, R.Z., Shu, Q, Wu, J. (2018). Different light-response patterns of coloration and related gene expression in red pears (*Pyrus* L.). *Scientia Horticulturae* 229:240-251
DOI: https://doi.org/10.1016/j.scienta.2017.11.002.

Zoratti, L., Karppinen, K., Luengo Escobar, A., HÃ¤ggman, H., & Jaakola, L. (2014). Light-controlled flavonoid biosynthesis in fruits. *Frontiers in Plant Science*, *5*(October), 1–16. https://doi.org/10.3389/fpls.2014.00534

Zoratti, L., Sarala, M., Carvalho, E., Karppinen, K., Martens, S., Giongo, L., … Jaakola, L. (2014). Monochromatic light increases anthocyanin content during fruit development in bilberry. *BMC Plant Biology*, 14(1), 1–10. https://doi.org/10.1186/s12870-014-0377-1

Zorzi, M., Gai, F., Medana, C., Aigotti, R., Morello, S., & Peiretti, P. G. (2020). Small Berries. *Foods*, 9, 623, 1–13.

Publications and Manuscripts

Paper 1

Received: 24 May 2021 | Revised: 19 July 2021 | Accepted: 19 July 2021

DOI: 10.1111/pce.14158

ORIGINAL ARTICLE

Plant, Cell & Environment WILEY

Red and blue light treatments of ripening bilberry fruits reveal differences in signalling through abscisic acid-regulated anthocyanin biosynthesis

Amos Samkumar[1] | Dan Jones[2] | Katja Karppinen[1] | Andrew P. Dare[2] | Nina Sipari[3] | Richard V. Espley[2] | Inger Martinussen[4] | Laura Jaakola[1,4]

[1]Department of Arctic and Marine Biology, UiT The Arctic University of Norway, Tromsø, Norway

[2]The New Zealand Institute for Plant and Food Research Ltd., Auckland, New Zealand

[3]Viikki Metabolomics Unit, Organismal and Evolutionary Biology Research Programme, University of Helsinki, Helsinki, Finland

[4]Norwegian Institute of Bioeconomy Research, Ås, Norway

Correspondence
Amos Samkumar, Department of Arctic and Marine Biology, UiT The Arctic University of Norway, Tromsø, Norway.
Email: amos.s.premkumar@uit.no

Funding information
New Zealand Ministry for Business, Innovation, and Employment (MBIE) Endeavour programme - 'Filling the Void: boosting the nutritional content of NZ fruit, Grant/Award Number: C11X1704; Nord Plant - NordForsk, Grant/Award Number: 84597; UiT- BFE faculty's mobility grant- University of Tromsø

Abstract

The biosynthesis of anthocyanins has been shown to be influenced by light quality. However, the molecular mechanisms underlying the light-mediated regulation of fruit anthocyanin biosynthesis are not well understood. In this study, we analysed the effects of supplemental red and blue light on the anthocyanin biosynthesis in non-climacteric bilberry (*Vaccinium myrtillus* L.). After 6 days of continuous irradiation during ripening, both red and blue light elevated concentration of anthocyanins, up to 12- and 4-folds, respectively, compared to the control. Transcriptomic analysis of ripening berries showed that both light treatments up-regulated all the major anthocyanin structural genes, the key regulatory *MYB* transcription factors and abscisic acid (ABA) biosynthetic genes. However, higher induction of specific genes of anthocyanin and delphinidin biosynthesis alongside ABA signal perception and metabolism were found in red light. The difference in red and blue light signalling was found in 9-*cis*-epoxycarotenoid dioxygenase (*NCED*), ABA receptor pyrabactin resistance-like (*PYL*) and catabolic *ABA-8'hydroxylase* gene expression. Red light also up-regulated expression of soluble *N*-ethylmaleimide-sensitive factor attachment protein receptor (SNARE) domain transporters, which may indicate involvement of these proteins in vesicular trafficking of anthocyanins during fruit ripening. Our results suggest differential signal transduction and transport mechanisms between red and blue light in ABA-regulated anthocyanin and delphinidin biosynthesis during bilberry fruit ripening.

KEYWORDS
bilberry (*Vaccinium myrtillus* L.), LED light, SNARE, transcriptome

1 | INTRODUCTION

Light is among the most important environmental factors modifying plant growth and development. Higher plants have evolved sophisticated mechanisms to perceive light signals through specialized photoreceptors that respond to various light properties, such as light intensity, light spectral quality and photoperiod (Briggs & Olney, 2001; Zoratti, Karppinen, Luengo Escobar, Häggman, & Jaakola, 2014). Different

visible light photoreceptors and UV-B receptors can sense light signals from a broad range of solar spectrum between 280 and 750 nm (Möglich, Yang, Ayers, & Moffat, 2010). Most of the transducible wavelengths absorbed by plants fall within 400–700 nm (from blue to red), which is also commonly referred to as photosynthetically active radiation (PAR; Chen, Chory, & Fankhauser, 2004). Within this range, phytochrome B has a specialized function towards red light while cryptochromes sense blue light to promote photomorphogenesis (Li & Yang, 2007; Lu et al., 2015).

After light perception, phytochrome and cryptochrome interact with the E3 ubiquitin ligase constitutive photomorphogenesis protein 1 (COP1), which is the key light signalling regulator (Lau & Deng, 2012). In the dark, COP1 directly interacts and represses the action of elongated hypocotyl 5 (*HY5*) gene inhibiting light signal transmittance and circadian clock genes, also the flowering regulators, such as CONSTANS (CO) via the proteasomal degradation complex (Bhatnagar, Singh, Khurana, & Burman, 2020; Zoratti, Karppinen, et al., 2014). Under light, COP1 activity is repressed, allowing the expression of *HY5* and positive transcriptional regulators in a number of developmental processes and metabolic pathways, including anthocyanin biosynthesis (Wu et al., 2019).

Light quality has a significant influence on plant secondary metabolism (Ouzounis, Rosenqvist, & Ottosen, 2015). For example, biosynthesis of polyphenols, anthocyanins, glucosinolates, terpenes, and carotenoids in plant tissues are responsive to light quality, and they have important roles, for example, in photoprotection (Ballaré, 2014; Holopainen, Kivimäenpää, & Julkunen-Tiitto, 2018). Light quality also influences the metabolite accumulation in fruits and berries, as shown by several pre- and postharvest light treatments in different fruit crops (Koyama, Ikeda, Poudel, & Goto-Yamamoto, 2012; Tao et al., 2018; Kokalj et al., 2019). High light intensity has generally been reported to increase anthocyanin accumulation in fruits, but it is also affected by light quality (Jaakola, 2013; Ma et al., 2019). For instance, red light has been reported to increase anthocyanin content in strawberry (*Fragaria* × *ananassa*), and blue light radiation increased anthocyanin levels after selective bagging treatment in pear (*Pyrus communis* L.) fruit (Miao et al., 2016; Tao et al., 2018). In bilberry, Zoratti et al. (2014) showed that short-term treatment with supplemental monochromatic light affected the anthocyanin profile during bilberry fruit development. However, the regulatory mechanisms behind the effect of red and blue light wavelengths on anthocyanin biosynthesis are not well understood.

Anthocyanins are prominent phenolic compounds in plants that are biosynthesized from the well-studied flavonoid pathway, which branches from phenylpropanoid biosynthesis (Tohge, de Souza, & Fernie, 2017). The major early biosynthetic enzymes involved in flavonoid biosynthesis are phenylalanine ammonia lyase (PAL), chalcone synthase (CHS) and chalcone isomerase (CHI). At the branchpoint of flavonoid biosynthesis, flavonoid 3′ hydroxylase (F3′H) and flavonoid 3′5′ hydroxylase (F3′5′H) direct biosynthesis to cyanidin and delphinidin compounds, respectively (Jaakola et al., 2002). The six major anthocyanin aglycone end-products, namely cyanidin, delphinidin, pelargonidin, petunidin, malvidin and peonidin, are biosynthesized by the late biosynthetic enzymes, dihydroflavonol 4-reductase (DFR) and anthocyanin synthase (ANS), and further glycosylated by UDP-glucose: flavonoid-*O*-glycosyltransferase (UFGT) as the last step in anthocyanin biosynthesis (Wu, Gong, Ni, Zhou, & Gao, 2017). Anthocyanins are transported to the vacuole after their biosynthesis. The mechanisms of anthocyanin transport are not fully understood, but common transporter proteins, such as ATP-binding cassettes (ABCs), multidrug and toxic extrusion (MATEs) and glutathione-S-transferases (GSTs), are commonly believed to be responsible for transportation to vacuolar membrane and lumen (Behrens, Smith, Iancu, Choe, & Dean, 2019). Another proposed model has been vesicular trafficking by phagosomes involving engulfment of anthocyanin bodies by endosomes before reaching the vacuole (Chanoca et al., 2015). The vesicular transportation is mediated by soluble *N*-ethylmaleimide-sensitive factor attachment protein receptor (SNARE) protein complexes, which are proposed to have a role in cellular transport in higher plants under stress responses (Pečenková, Marković, Sabol, Kulich, & Zárský, 2017).

The biosynthesis of flavonoids is directly controlled by the transcriptional regulatory MYB, bHLH,WD-40' complex (MBW) complex, consisting of MYB and bHLH transcription factors (TFs) and WD-40 repeat proteins (Feller, MacHemer, Braun, & Grotewold, 2011; Xu, Dubos, & Lepiniec, 2015). R2R3 MYB TFs are known as the key regulators of anthocyanin biosynthesis and are responsive to shifts in light spectral quality (Zoratti, Karppinen, et al., 2014). In grapes, two R2R3 MYB TFs, *VvMYBA1* and *VvMYBA2*, controlling anthocyanin biosynthesis specifically regulate *UFGT* (Walker et al., 2007). In apple and peach, R2R3 MYBA-type TFs activate anthocyanin biosynthesis by interacting with both the *UFGT* and *DFR* promoters during fruit ripening (Ravaglia et al., 2013; Takos et al., 2006).

Abscisic acid (ABA), which is synthesized by the key cleavage enzyme 9-*cis*-epoxycarotenoid dioxygenase (NCED) in apocarotenoid pathway, has been shown to be a major regulator of ripening in non-climacteric fruits, such as strawberry, grapes and bilberry (Ferrara et al., 2015; Jia et al., 2011; Karppinen, Tegelberg, Häggman, & Jaakola, 2018) and in climacteric fruits, such as apple (An et al., 2021). The ABA signal transduction is known to be mediated by pyrabactin resistance/like (PYR/PYL) receptors and ABA-responsive element-binding factors (ABFs) through SQUAMOSA-MADS box (TDR-type) TFs leading to regulation of the MBW complex proteins (Chung et al., 2019). Another model has been proposed, illustrating that ABA interacts directly with PYR by inhibiting type 2C protein phosphatases subsequently binding with ABFs and transduces the ABA signalling pathway (Park et al., 2009).

Bilberry (*Vaccinium myrtillus* L.), also known as European blueberry, is one of the most important wild perennial berry species of *Vaccinium* genus and predominantly found in Northern Europe (Chu, Cheung, Lau, & Benzie, 2011; Karppinen, Zoratti, Nguyenquynh, Häggman, & Jaakola, 2016; Zoratti, Klemettilä, & Jaakola, 2016). The species has gained global interest due to its abundant health-beneficial bioactive compounds, including phenolic compounds, carotenoids and vitamins but especially anthocyanins, which constitutes 90% of total phenolics in these berries and give distinct deep blue colour to both skin and flesh (Karppinen, Zoratti, Nguyenquynh, et al., 2016). Several studies have reported consumption of bilberries to reduce risk of metabolic syndrome and various microbial and degenerative diseases (Bujor, Le

Bourvellec, Volf, Popa, & Dufour, 2016; Chu et al., 2011; Nile & Park, 2014). In bilberry, delphinidin and cyanidin glycosides are the major anthocyanins followed by malvidin and petunidin glycosides (Müller, Schantz, & Richling, 2012; Thornthwaite, Thibado, & Thornthwaite, 2020; Zoratti et al., 2016). In particular, delphinidins, which are abundant in northern clones alongside malvidins, have been recently linked to many biological and health-beneficial activities (Heysieattalab & Sadeghi, 2020; Nagaoka et al., 2019).

In the present study, we utilized the Illumina-based RNA-seq approach to produce transcriptome libraries from ripening bilberry fruit grown under supplemental red and blue light conditions. We specifically focused on the differences in red and blue light signal transduction in regulation of anthocyanin biosynthesis. The red and blue light-emitting diodes (LEDs) used in our study give an opportunity to provide high intensity spectral wavelengths to plants as source of light for studying the effect of light quality to biosynthesis of phytochemicals.

2 | MATERIALS AND METHODS

2.1 | Plant material and light treatments

Wild bilberry (*V. myrtillus* L.) ecotype from Tromsø, Norway (69° 75′N, 19° 01′E) was used for the experiments. The bilberry bushes were collected during early July after the fruit set at stage S2 when berries were small, unripe and green (Figure 1a). The plants were collected in

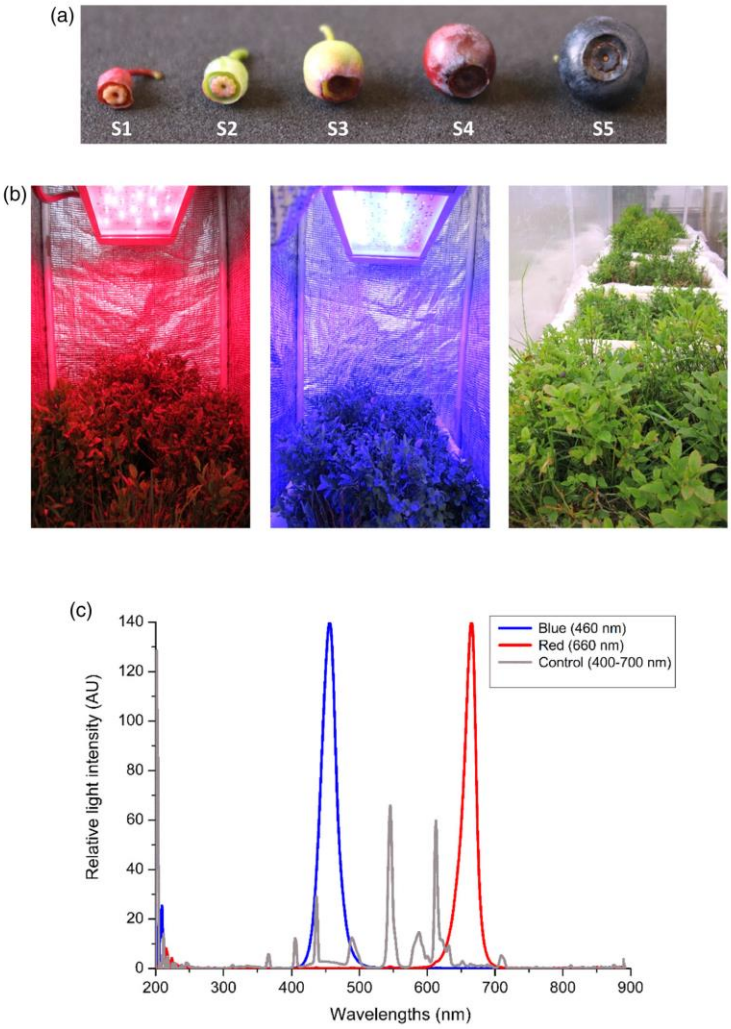

FIGURE 1 Spectral light treatments of bilberry plants. (a) Developmental stages of bilberry: S1, small unripe fruit after flowering; S2, small unripe green fruit; S3, large unripe green fruit; S4, ripening purple fruit; and S5, fully ripe blue fruit. (b) Supplemental blue (460 nm) and red (660 nm) light treatments provided for bilberry plants by Heliospectra LED lamps alongside control (400–700 nm). (c) Light spectra and relative light intensities in the light treatments expressed in arbitrary units (AU)

boxes (50 × 70 cm) with their root system intact in forest soil and watered well. The plants were kept in the phytotron conditions at 16°C for few days to acclimatize until they reached berry developmental stage S3 when berries were large, unripe and green (Figure 1a).

For light treatments, the plants were placed in chambers covered from sides with photo reflective sheets and irradiated from top with blue (460 nm) or red (660 nm) light wavelength provided by the Heliospectra RX30 lamps (Heliopspectra AB, Gothenburg, Sweden; Figure 1b). In addition to the specific spectral light wavelengths, the plants received continuous ambient white light (400–700 nm) from the top. The plants under the ambient white light (400–700 nm) served as control for the experiment. All plants were kept at 16°C, and the photon fluence rate (μmol m^{-2} s^{-1}) and irradiation energy flux (μW cm^{-2}) were measured using JAZ Spectrometer (Ocean Optics Inc., Orlando, FL, USA) and used to calculate the relative light intensity expressed as arbitrary units (AU; Figure 1c).

Berry samples were collected after 6 days from the beginning of the light treatments when berries had reached stage S4 and started to develop red colour on their skin (Figure 1a), and utilized for RNA sequencing and real-time qRT-PCR analyses. For metabolite analyses, light-treated S4 stage berries at 6 and 12 days and fully ripe berries after 4 weeks from the beginning of light treatments at stage S5 (Figure 1a) were collected. Approximately 20–25 berries were collected per treatment from three replicate bushes for RNA extraction and metabolite analyses. Immediately after collection, all the berry samples were frozen in liquid nitrogen and stored at −80°C until further used for analyses.

2.2 | RNA extraction and sequencing

The frozen berries were ground to a fine powder under liquid nitrogen using mortar and pestle. Total RNA was isolated from approximately 120 mg tissue powder by using Spectrum Plant Total RNA kit (Sigma-Aldrich, St. Louis, MO, USA) following the manufacturer's instructions. Contaminating DNA was removed with on-column digestion using DNase I (Sigma-Aldrich).

For constructing RNA libraries, the RNA was qualified with both NanoDrop 2000c UV–vis spectrophotometer (NanoDrop Technologies, Wilmington, DE, USA) and Experion Bioanalyzer (Bio-Rad laboratories, Hercules, CA, USA). To segregate the mRNA from total RNA, poly-A was captured using oligo (dT) Dynabeads (Invitrogen, Carlsbad, CA, USA). Before library preparation, all the samples were qualified by an Agilent 2100 Bioanalyzer (Agilent Technologies, Santa Clara, CA, USA). The libraries were prepared with NEBNext Ultra II RNA Library Prep Kit (New England Biolabs Inc., Ipswich, MA, USA). Sequencing of RNA libraries was performed using an Illumina Hiseq2000 platform (Illumina, San Diego, CA, USA) with paired-end sequencing strategy (PE-150 bp) at the Novogene sequencing services facility (Cambridge Science Park, UK). Libraries were prepared with three biological replicates for each blue, red and white (control) light treatments.

2.3 | Transcriptome assembly

The raw reads from Illumina were initially quality assessed using MultiQC software (Andrews, 2010; Ewels, Magnusson, Lundin, & Käller, 2016). The adapter contamination was removed using Trimmomatic tool specifically designed for Illumina Next generation sequencing data (Bolger, Lohse, & Usadel, 2014), followed by the removal of the residual rRNA reads by using sortMeRNA programme (Kopylova, Noé, & Touzet, 2012). The quality checking by MultiQC included assessment of sequence quality score (phred >30), adapter content and position, GC content and ambiguous bases (Ns). Only the clean filtered reads were used in our downstream analysis. A robust transcriptome was constructed with Trinity v2.9.0 software pipeline (Grabherr et al., 2011) by developing a combined redundant-over assembly from de novo and genome-guided assembly using a bilberry genome sequence of the same bilberry ecotype (Wu et al., 2021). The draft genome was indexed and align-mapped to the reads using STAR v2.6.1d software (Dobin et al., 2013). The genome-guided Trinity output was concatenated with de novo transcriptome to form a combined assembly. EvidentialGene tool (Gilbert, 2019) was used to remove the redundancy arising from assemblies. The reads were further mapped to the published highbush blueberry (*V. corymbosum* cv. Draper) v1.0 genome (Colle et al., 2019) using HISAT2 software to improve the annotation of assembly. The best possible coding regions were identified using TransDecoder tool (http://transdecoder.github.io), which identifies a minimal length of open reading frames (ORFs) within reconstructed Trinity transcripts. To assess the completeness of the transcriptome assemblies, BUSCO tool v3.0 (Simão, Waterhouse, Ioannidis, Kriventseva, & Zdobnov, 2015) was used to validate the single copy genes on an evolutionary perspective. Embryophyta orthologous database odb_v.10 (https://busco-archive.ezlab.org/v3/) was used to validate the assembled transcriptomes.

2.4 | Functional annotation of transcriptome

Functional annotation was performed by using Trinotate pipeline v3.2.1 (http://trinotate.github.io), which utilizes the homology search based on Swissprot, Pfam and NCBI-BLAST-nr (non-redundant) databases from the Cluster database at high identity with tolerance clustered trinity transcript IDs and TransDecoder-derived peptide sequences. The cut-off E-value for the BLAST search was adjusted between 1.0^{-5} and 1.0^{-100}, and the homology search was performed with default parameters. Additional tools, such as SignalP, tmHMM and RNAMMER (http://www.cbs.dtu.dk/services/), were integrated into the Trinotate pipeline to determine probable signal peptides, transmembrane helices and residual rRNA transcripts, respectively, in the assembled transcriptome. All the major TF families and transcriptional regulators were determined using the PlantTFcat tool (http://plantgrn.noble.org/PlantTFcat/).

2.5 | Differential gene expression and pathway analysis

To quantify the gene expression levels from the transcriptomes, we utilized Salmon tool (Patro, Duggal, Love, Irizarry, & Kingsford, 2017), which was able to identify and quantify the known gene isoforms. Differentially expressed genes (DEGs) between the light treatments (red vs. control and blue vs. control) were identified using DESeq2 v3.10 software package (Love, Huber, & Anders, 2014) with false discovery rate (FDR) adjusted *p*-value set to 0.05. Log_2 fold change ratio between ≥2 and ≤−2 was used to obtain the list of up- and down-regulated genes.

Gene Ontology (GO) terms for the transcripts were analysed using GOseq v3.11 software (https://bioconductor.org/packages/release/bioc/html/goseq.html) in R-package followed by enrichment analysis using Fisher's exact test. For validation and to improve the accuracy in GO determination, the top 500 DEGs from both the contrasts (red vs. control, blue vs. control) were extracted and annotated with Blast2GO suite (Gotz et al., 2008). Kyoto Encyclopedia of Genes and Genomes (KEGG) pathway enrichment analysis was performed in KOBAS v3.0 tool (Wu, Mao, Cai, Luo, & Wei, 2006) followed by interpreting the KEGG Orthology (KO) terms in KEGG Automated Annotation Server (KAAS) using *Vitis vinifera* as a reference organism for obtaining the KO identifiers. The original figures and pathway representations were created with www.biorender.com.

2.6 | qRT-PCR analysis

Total RNA was isolated from the berry samples using the same method as described earlier. First-strand cDNA was synthesized using Superscript IV reverse transcriptase (Invitrogen) from 1-μg total RNA according to manufacturer's instructions. MJ MiniOpticon Real-Time PCR System (Bio-Rad) was used for qRT-PCR analysis with SsoFast™ EvaGreen Supermix (Bio-Rad) in 15-μl volume reaction. The PCR conditions were as follows: initial denaturation at 95°C for 30 s followed by 40 cycles at 95°C for 5 s, and 60°C for 10 s. Subsequent melting curve analysis, ranging from 65°C to 95°C with an increment of 0.5°C per cycle, was used to assure amplification of only one product. All analyses were performed with three biological replicates and two technical replicates. The results were analysed using CFX Connect software (Bio-Rad) using $2^{(-\Delta\Delta Ct)}$ method, and the relative expression levels were normalized with glyceraldehyde-3-phosphate dehydrogenase (*GAPDH*) or *Actin*. Primer sequences of the genes are listed in Table S1.

2.7 | Analysis of anthocyanins

Bilberry (S4 stage) samples collected after 6 days of light treatment (equal time-point with transcriptomics samples) were ground and freeze-dried in a lyophilizer (Virtis benchtop-K; SP Scientific, Gardiner, NY, USA). Approximately 43-mg dry weight (DW) of freeze-dried bilberry powder from each sample was used in extraction. The samples were extracted twice with 500-μl MeOH:IPA:acetic acid (20:79:1) for anthocyanin analysis. The extracts were evaporated to dryness and resuspended in 100-μl MeOH. The extracts were analysed with ultra high performance liquid chromatography coupled to photodiode array (UPLC-PDA)-Synapt G2 Quadrupole time of flight/High-definition mass spectrometry (Waters, Milford, MA, USA) in positive (ESI+) resolution ion mode. Samples were analysed with capillary voltage at 3.0 kV. The source temperature was 120°C, and desolvation temperature was set to 360°C; cone gas flow rate was 20 L/h, and desolvation gas flow rate was 800 L/h. The compounds were separated on an Acquity UPLC-BEH C18 column (1.7 μm, 50 × 2.1 mm, Waters) in 40°C. The mobile phase consisted of (a) H_2O and (b) acetonitrile (Chromasolv grade, Sigma-Aldrich, Steinheim, Germany) both containing 0.1% HCOOH (Sigma-Aldrich). A gradient of eluents was used as follows: linear gradient of 95% of A to 5% in 10 min, and then back to 95% at 10.1 min and left to equilibrate for 1 min. The injection volume was 2 μl, and flow-rate of the mobile phase was 0.6 ml/min. Tray temperature was set to 10°C. Mass range was set from 100 to 1,500. Peak picking and integration of the peaks were executed with MassLynx V4.2 (Waters), and identification was performed by comparing the exact mass/chemical formula, retention time, UV-spectra, and/or previously published data of bilberry secondary metabolites. The relative content of the anthocyanins in AU was calculated by normalizing the analyte peaks area with the DW of the samples (AU/mg DW). Total anthocyanins from S4 stage berries after 12 days from light treatment were measured according to Karppinen et al. (2018).

To determine the anthocyanins from S5 stage fully ripe berries, 100 mg of samples were ground to a fine powder under liquid nitrogen using mortar and pestle and freeze-dried overnight to remove water content. The samples were further extracted with methanol acidified with 0.1% HCl (v/v) for 2 h at room temperature before being centrifuged and the supernatant vacuum spin dried. The pellet was resuspended in 500 μl 20% methanol and filtered using 0.45-μM PVDF syringe filter (Phenomenex, Torrance, CA, USA). The samples were diluted to 1:10 with 20% methanol before a 5-μl aliquot was injected into a C18 Acclaim Polar Advantage II column (150 × 2.1 mm i.d., 3-μm particle size; Dionex, Sunnyvale, CA, USA) in an high performance liquid chromatography (HPLC) system (Ultimate 3000; Thermo Fisher Dionex) coupled with a diode array detector (DAD). The column oven temperature was set to 35°C, and the flow rate was adjusted to 0.350 ml/min. The mobile phases consisted of 10% formic acid (A) and a mixture of 45% methanol, 45% acetonitrile and 10% formic acid (B). The gradient was as follows: 100% A followed by 9% B in A for 0–12 min, 35% B in A for 12–25 min, 50% B in A for 25 min and 9% B in A for 30–35 min. The identified anthocyanin peaks were compared with that of known authentic standards and monitored at 254, 280, 320 and 520 nm. The samples were quantified using a calibration curve and expressed as cyanidin 3-O-galactoside equivalents. All analyses were performed with three biological replicates.

2.8 | Statistical analysis

The statistical analysis of LC–MS profiling data was performed with MetaboAnalyst 5.0 tool (Chong, Wishart, & Xia, 2019). Differences in anthocyanin levels among the light treatments were analysed by one-way analysis of variance (ANOVA) followed by Tukey's post-hoc test. Statistically significant differences between the light treatments analysed by qRT-PCR were determined by independent samples *t*-test in SPSS Statistics programme v26 (IBM corporation, New York, NY, USA). Pearson's correlation matrices were used to visualize the statistical relationship from correlation coefficients between selected gene expression levels and dominant anthocyanin concentrations (delphinidin 3-galactoside and delphinidin 3-arabinoside) with *p*-value set to <0.05. ANOVA and Pearson's correlation analysis were performed using OriginPro software v2020b (OriginLab Corporation, Northampton, MA, USA).

3 | RESULTS

3.1 | Elevated anthocyanin content under red and blue supplemental light

Metabolite profiling with UPLC-HDMS was performed from light-treated berry samples after 6 days (same time-point for transcriptome libraries). The red, blue and control samples from the metabolite analysis were separated in the first component in the principal component analysis (PCA), explaining 32.3% of the variation (Figure S1). The heatmap analysis of metabolite profiling data shows large number of significantly different metabolites (407 metabolites of total 700, ANOVA, $p < 0.05$); anthocyanins localized in the middle part of the clusters (Figure S2). The results showed consistent and significant increase in all the anthocyanin compounds under both the red and blue light treatments when compared with control (Figure 2a). Delphinidin galactosides/glucosides were detected 12-fold higher in red light when compared to other light treatments followed by significant increase in all the cyanidin, petunidin and malvidin glycosides (Figure 2a). In addition, the total anthocyanins quantified in ripening berries (S4 stage) after 12 days of light treatment showed higher amounts of anthocyanin accumulation in red light followed by blue light treatments compared with ambient white light control (Figure 2b).

Similar trend was also observed in S5 stage fully ripe berries although the difference was not as apparent (Table S2). Quantitative analysis with HPLC confirmed that the two major delphinidin glycosides, delphinidin-3-galactoside and delphinidin 3-arabinoside, were found at significantly higher amounts in red light treatment, contributing to the increase in total anthocyanin content (4,760 mg 100 g^{-1} DW) compared to that of blue light and the control samples. The trend is followed by the increase in levels of cyanidin and petunidin glycosides in red light treated berries. A very low amount of peonidin-3-glucoside was detected in all the samples, which was not generally influenced by different light treatments (Table S2).

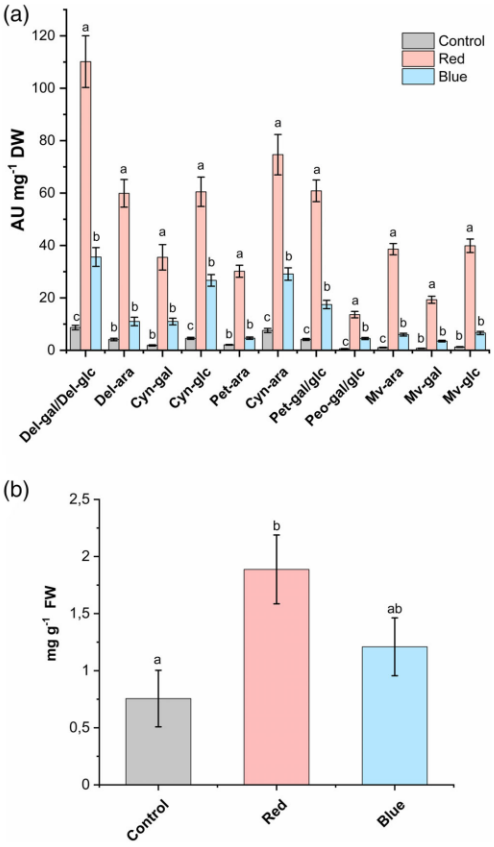

FIGURE 2 Determination of anthocyanin content. (a) Anthocyanin content after 6 days of spectral light treatment of bilberries determined by LC–MS. The relative content is expressed in arbitrary units (AU) and was calculated by normalizing the analyte peaks area with the dry weight of the samples (AU mg^{-1} DW). Ara-arabinoside; Cyn-cyanidins; Del-delphinidins; gal-galactoside; glu-glucoside; Mv-malvidins; Pet-petunidins. (b) Total anthocyanins in bilberries after 12 days of spectral light treatment expressed in mg g^{-1} FW of cyanidin 3-glucoside equivalents. Different letters denote significant differences among groups analysed by one-way ANOVA followed by Tukey's post-hoc test (p-value < 0.05) [Colour figure can be viewed at wileyonlinelibrary.com]

3.2 | Bilberry transcriptome sequencing and functional annotation

The raw sequencing reads of the bilberry transcriptomes yielded approximately 56 GB of data and reached approximately 8 GB per sample data. The read number for control samples was 70,627,656 bases, whereas it was 82,253,205 bases for the red light-treated samples and 78,192,227 bases for the blue light-treated samples

TABLE 1 Statistics of combined Trinity transcriptome assembly after concatenating de novo and genome-guided assemblies

Assembly		Transcripts	Unigenes
Total counts		671,952	472,876
Contig N50 (bp)		1,567	1,122
Contig N30 (bp)		2,431	2035
Average contig length (bp)		910.78	720.23
Median contig length (bp)		508	408
Total assembled bases		611,998,789	340,578,754
Average read length	150 bp		
Percent GC	41.71%		

(Table S3). MultiQC analysis proved that the processed reads were of good quality with Phred score >36 (Table S2). Read-mapping to a recently published *V. corymbosum* genome (Colle et al., 2019) resulted in 75–77% of total reads mapped including ~50% uniquely mapped to the genome. Using a draft genome of bilberry (Wu et al., 2021), representing the same bilberry ecotype as our samples, enabled unique mapping of 83.5% of the filtered reads. A total of 671,952 transcripts and 472,876 unigenes were generated from the combined transcriptome assembly with mean contig lengths of 911 and 720 bp, respectively (Table 1). BUSCO analysis revealed that the combined assembly had 97.4% complete sequences when searched within 1,375 orthologous groups of embryophyta_odb9 lineage (Table S4). The scores were slightly improved compared to genome-guided assembly, indicating that the combined transcriptome in our analysis is a robust assembly and was subsequently used in this study.

In total, around 25,316 (61%) of putative protein IDs of bilberry transcripts showed significant hits in Swissprot and 25,280 (61%) in Pfam databases (Figure 3a). Around 60% of the sequences had hits with eggNOG (clusters of orthologous groups) and relatively high number of hits (65%) obtained from the KEGG database (Figure 3a). BLAST hits distribution among the top-25 species showed the highest homology in *Rhododendron williamsianum* (33%) followed by *Camelia sinensis* var. (25%) and *Actinidia chinensis* var. (16%). The top-hit species with some considerable matches obtained from the top DEGs (0.2–2.6%) showed sequence similarities with *V. myrtillus*, *V. macrocarpon* and *V. corymbosum* (Figure S3).

There were 49,105 commonly co-expressed genes detected among the transcriptomes of the three different light treatments (Figure 3b). The distribution between the different light treatments is visualized in a venn diagram showing that 1,816 and 1,686 genes were uniquely expressed among the red and blue light treatments, respectively (Figure 3b). The BLAST sequence similarity distribution within the query sequences (E-value cut-off 1.0^{-5}) showed high number of positives to that of aligned reads length in the range of 70–90% suggesting a strong match between query and assembled known sequences from databases (Figure S4).

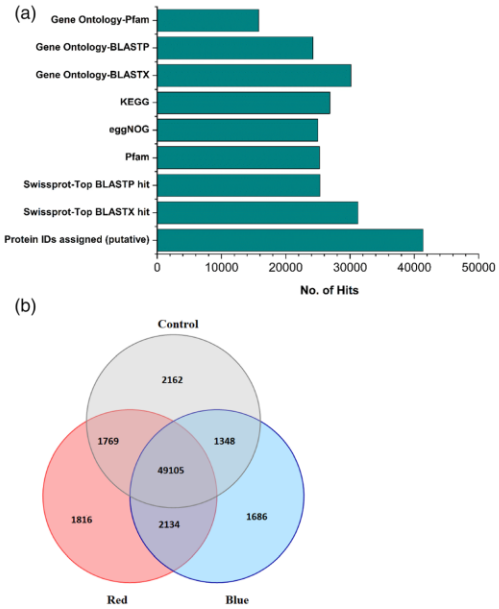

FIGURE 3 Functional annotation of bilberry transcriptome. (a) Summary of functional annotation from Trinotate pipeline. The number of hits from the unigenes has been denoted in *x*-axis, whereas *y*-axis denotes the different databases utilized for search. (b) Co-expression of genes among red, blue and control light treatments represented as venn diagram [Colour figure can be viewed at wileyonlinelibrary.com]

3.3 | Differential expression analysis between light treatments and enrichment (GO, KEGG) analysis

The gene expression levels quantified from the read counts generated from the transcriptomes showed 14,105 DEGs. The fragments per kilobase of transcript per million mapped reads (FPKM) counts (fragments per kilobase of transcript per million mapped reads) were aggregated from three replicates of each light treatment (Figures S5 and S6). Hierarchical clustering analysis showed clear differences in the expression patterns between the light treatments (Figure 4a). In red light-treated berries, high number of DEGs corresponding to 7,327 up-regulated genes and 1,545 down-regulated genes (Figure 4b) were detected when compared with blue light treatment yielding 3,686 up-regulated and 1,547 down-regulated genes (Figure 4c) as visualized using volcano plots.

GO enrichment analysis classified the DEGs according to their functions and properties into three major categories: biological process (BP), molecular function (MF) and cellular component (CC) (Figure 5a). An average of 60–65% of unigenes was assigned GO terms either through one of the homology searches from Pfam, BLASTx and BLASTp databases. The top significantly enriched GO

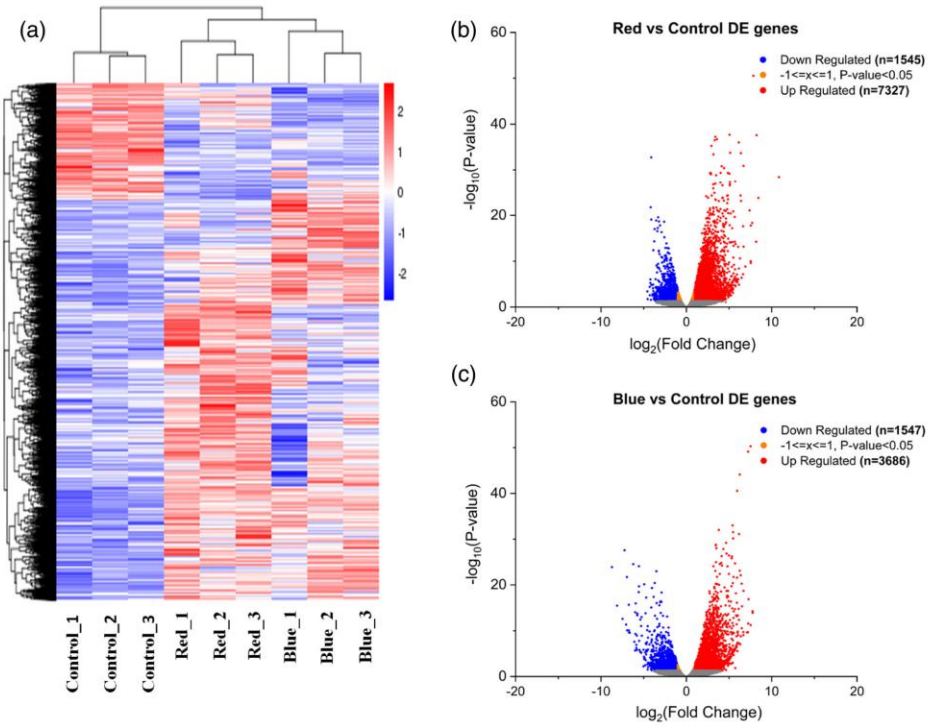

FIGURE 4 Differential gene expression analysis in the light-treated bilberries. (a) Clustered hierarchical heat-map of normalized differential gene expression among the samples (h-cluster). The scale bars from −2 to 2 represent the $\log_2$ fold change from fragments per kilobase of transcript per million mapped reads (FPKM) values. (b) Volcano plot of red versus control comparison. (c) Volcano plot of blue versus control comparison. Both the contrasts were FDR corrected/*p*-value adjusted to ≤ 0.05 for obtaining DEGs and plotted with the $\log_2$ fold changes against the adjusted $-\log_{10}$ *p*-values obtained [Colour figure can be viewed at wileyonlinelibrary.com]

terms across these three categories from our two comparison subsets showed that in CC, 'intracellular' and 'cellular anatomical entity' were the top sub-categories (Figure 5a). In the MF category 'catalytic activity', 'binding' and 'transporter' activities were found to be abundant (Figure 5a). Both these categories have similar number of GO terms assigned from the sequences but with two contrasting results. In the BP category, the sequences assigned to 'metabolic' and 'cellular' process were relatively higher in red light than blue light treatment. The GO terms assigned to 'localization', 'signalling' and 'response to stimulus' sub-categories were contrasting between the light treatments (Figure 5a). Some of the unigenes were also classified in 'rhythmic processes' and 'pigmentation' in the BP category. Hence, we further investigated the BP category by direct count of sequence distribution among the top DEGs. GO terms, such as 'oxidation–reduction process', 'protein phosphorylation' and 'regulation of transcription', were the top ones with relatively higher number of assigned sequences found in red light-treated samples than blue light treatment. Some annotated sequences related to sugar metabolism, shikimate, chorismate, lignin, cutin and sterol biosynthetic process were also determined with additional GO terms assigned to anthocyanin-containing compounds, and flavonoid biosynthetic process was obtained from red light treatment (Figure 5b). The KEGG pathways significantly enriched by adjusting FDR corrected/*p*-value to <.05 using the Benjamini–Hochberg method showed that a high number of gene ratio fell in both light treatments on metabolic pathways and secondary metabolite biosynthesis, followed by phenylpropanoid biosynthesis, and few primary metabolic pathways, such as amino acid biosynthesis, carbon metabolism and ribosome (blue vs. control) with considerable number of gene counts (Figure 5c,d). In addition, the red light treatment also positively enriched the fatty acid, galactose, starch and sucrose metabolism related pathways (Tables S5–S8). All the DEGs and corresponding unigene IDs analysed throughout this study are provided in Table S9.

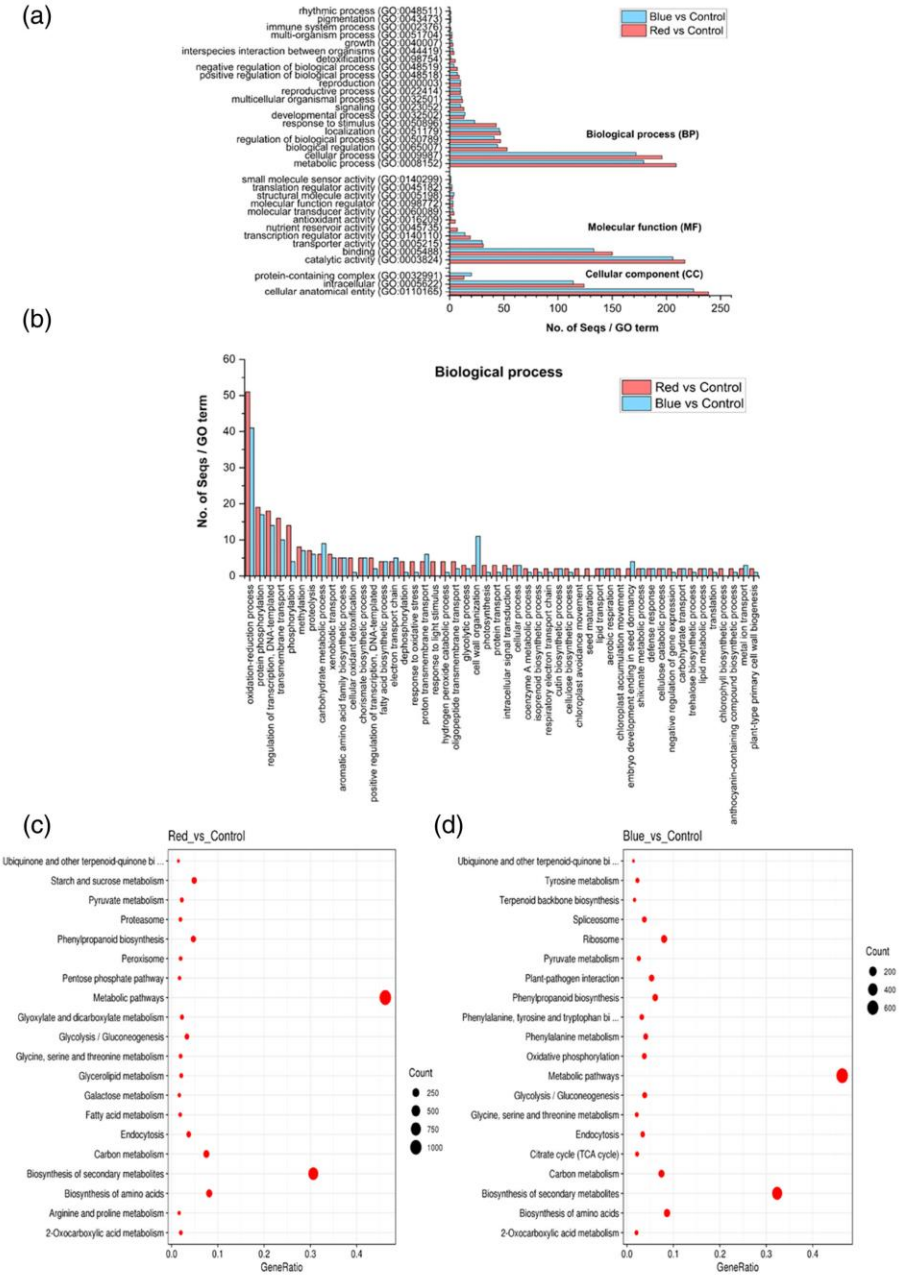

FIGURE 5 Enrichment analysis of Gene Ontology (GO) terms and KEGG pathways. (a) The number of significantly enriched GO terms obtained against the top 500 DEG sequences. The treatment contrasts are represented with similar colours. The GO terms are categorized into biological process (BP), molecular function (MF) and cellular component (CC). (b) Number of enriched GO terms obtained from direct count of sequences in BP category. The KEGG metabolic pathways significantly enriched in red versus control (c) and blue versus control (d). Circle sizes represent the counts of sequences with *p*-value <.01 [Colour figure can be viewed at wileyonlinelibrary.com]

3.4 | Identification of TF families

Blast2GO suite identified GO terms and protein domain signatures from top 500 DEGs utilizing InterproScan (IPS) database. The analysis indicated that the top category was a protein kinase domain followed by *MYB/SANT* domain, *AP2/ERF*, *NB-ARC* and *bHLH* domains (Figure S7). A total of 976 unigenes were identified as putative TFs and regulators from the transcriptome categorized into 72 TF families, which are likely to have a role in red and blue light-mediated transcriptional regulation in various metabolic pathways. Among them, *C2H2* was the most prominent TF family category with 117 unigenes followed by *CCHC(Zn)* (99 unigenes), *RR-A type* (42 unigenes), *MYB-HB* like (62 unigenes), *bHLH* (44 unigenes) and *WD-40* like TFs (40 unigenes) (Figure S8). Some of the earlier identified TFs known to be involved in bilberry ripening (Nguyen et al., 2018), such as *NAM* (*NAC* family TFs) with 13 unigenes, *WRKY* TFs with 17 unigenes and *MADS*-like TFs with 13 unigenes, were identified as differentially expressed in response towards red and blue light treatment. Another class of TFs called *AP2-EREBP* (*APETALA2/EF*), belonging to ethylene hormone responsive TF family, was also significantly expressed among the DEGs (38 unigenes).

3.5 | DEGs involved in red and blue light signalling

The unigenes corresponding to phytochrome B (*PHYB*) were found to be highly up-regulated in red light treatment, whereas cryptochrome (*CRY2*) transcripts were found in high levels under blue light (Figure 6). *COP1* expression level was found to be higher in red light treatment with blue light down-regulating its expression. The light treatments also showed similar trends on *HY5* expression, with red light increasing the expression and blue light having the opposite effect. *CK2α* and *PRR5*, which are key regulators in plant circadian rhythms, did not vary markedly in their expression levels between the

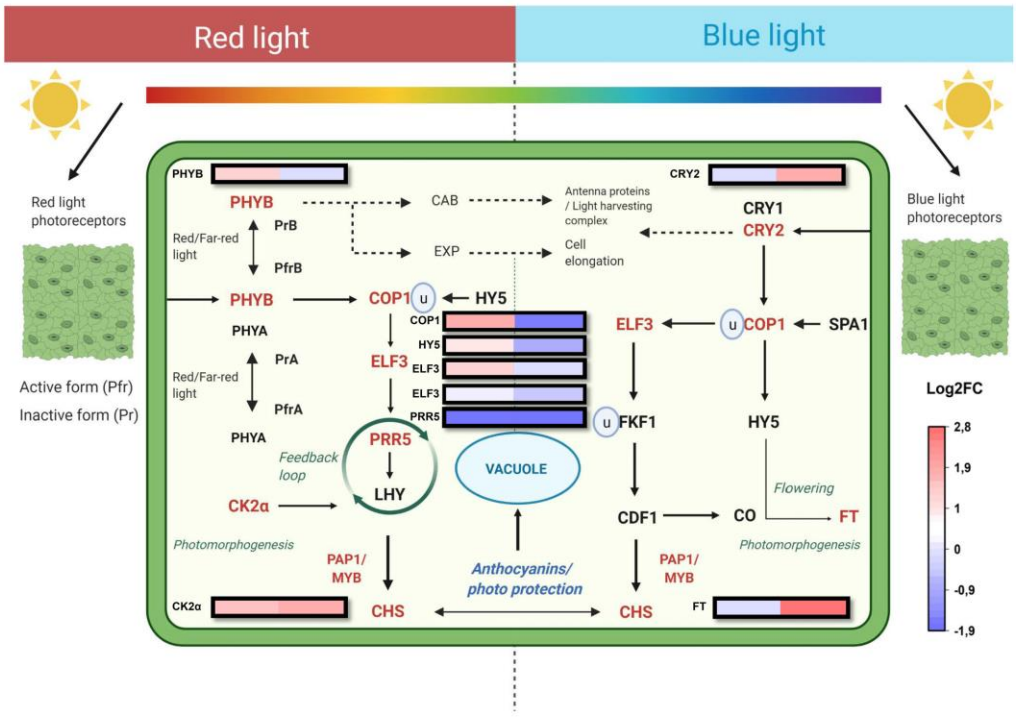

FIGURE 6 DEGs from light signalling and circadian rhythm. Schematic representation of red and blue light signal perception by higher plants, which are likely to be involved in light-regulated anthocyanin biosynthesis. The associated DEGs from red and blue light versus control contrasts are presented in colour code boxes based on $\log_2$ fold changes. Red light treatment is shown on left and blue light treatment on the right-hand side of the box. *Gene abbreviations*: Cab, chlorophyll *a*/*b* binding protein; CDF1, cycling DOF factor 1; CK2α, casein kinase II subunit alpha; Co, constans; COP1, constitutive photomorphogenic; CRY1/2, cryptochrome; Elf3, early flowering 3; Exp, expansin; FKF1, flavin-binding kelch domain F box protein; FT, flowering locus T; HY5, elongated hypocotyl 5; PHYA/B, phytochrome; PRR5, pseudo response regulator 5; SPA, suppressor of PhyA [Colour figure can be viewed at wileyonlinelibrary.com]

red and blue light treatments. Flowering locus gene-T (*FT*) involved in photoperiodism was highly up-regulated (2,8 $\log_2$ FC) upon blue light treatment (Figure 6).

3.6 | DEGs from anthocyanin biosynthesis and its associated regulatory complex

All the major identified unigenes involved in the phenylpropanoid pathway, such as *PAL*, cinnamate 4-hydroxylase (*C4H*) and 4-coumarate CoA ligase (*4CL*), were up-regulated upon both red and blue light treatments (Figure 7). Caffeoyl CoA *O*-methyltransferase (*cCoAoMT*) expression was found to be at a relatively high level in blue light compared to red light treatment also with similar expression levels identified in peroxidases and cationic peroxidases (*Prx*, *cPrx*) genes leading to lignin biosynthesis via the *p*-coumaryl alcohol branch pathways (Figure 7).

All the anthocyanin biosynthetic pathway structural genes were up-regulated both in red and blue light (Figure 7). The key biosynthetic enzyme gene *CHS* was found with a $\log_2$ fold increase of 3.3 and 3 between red and blue treatment, respectively. Expression of *CHI* and *F3H* was found to be at a higher level in red light treatment when compared with the blue light treatment. The changes in expression levels of *F3′H*, *DFR* and *ANS* genes were found to be slightly

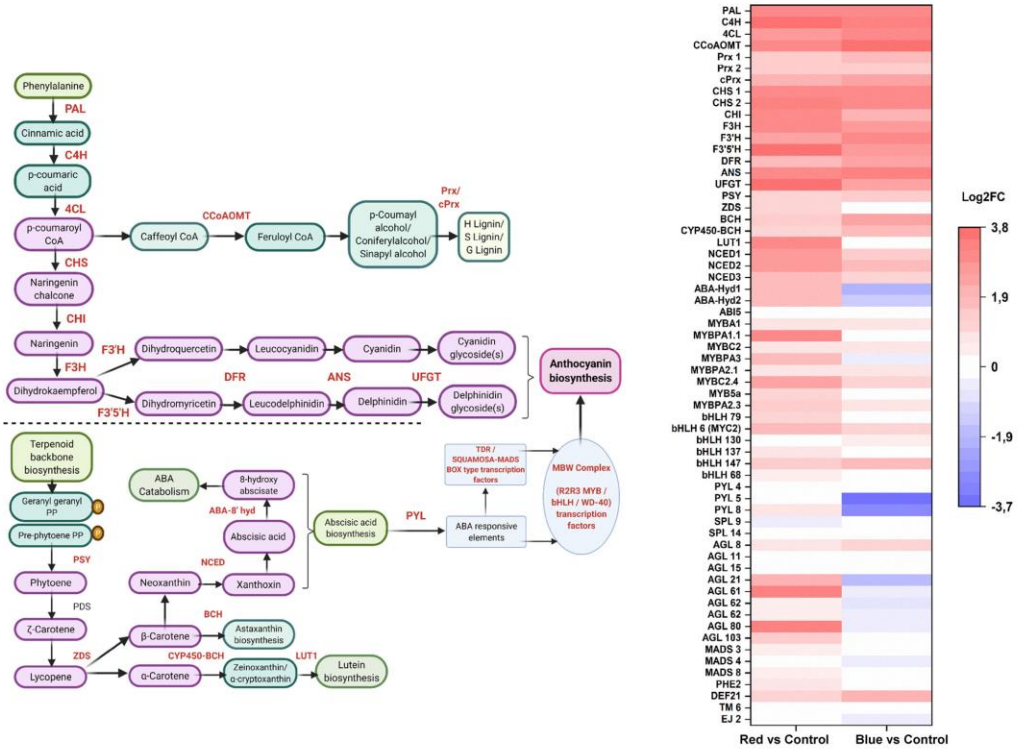

FIGURE 7 DEGs from anthocyanin, carotenoid and ABA biosynthesis. Schematic representation of anthocyanin biosynthetic pathway branching from phenylpropanoid biosynthesis (top) and representation of carotenoid biosynthetic pathway leading to abscisic acid (ABA) biosynthesis and catabolism. DEGs from flavonoid, carotenoid and ABA pathway genes and selected TFs visualized as heatmap based on $\log_2$ fold changes obtained from light treatments against the control samples. *Enzyme abbreviations*: 4CL, 4-coumarate:CoA ligase; ABA 8′ hyd, abscisic acid 8′ hydroxylase, PYR/PYL, pyrabactin-resistance like; ANS, anthocyanidin synthase; BCH, beta-carotene hydroxylase; C4H, cinnamate 4-hydroxylase; CCoAOMT, caffeoyl-CoA O-methyltransferase; CHI, chalcone isomerase; CHS, chalcone synthase; CYP 450-BCH, carotenoid β-ring hydroxylase of cytochrome P450 family; DFR, dihydroflavonol 4-reductase; F3'5'H, flavonoid 3'5' hydroxylase; F3'H, flavonoid 3′ hydroxylase; F3H, flavanone 3-hydroxylase; LUT1, lutein deficient 1; NCED, 9-*cis*-epoxycarotenoid dioxygenase; PAL, phenylalanine ammonia-lyase; Prx, cPrx-peroxidases, cationic peroxidases; PSY, phytoene synthase; UFGT, UDP-glucose flavonoid 3-O-glucosyltransferase; ZDS, zeta-carotene desaturase [Colour figure can be viewed at wileyonlinelibrary.com]

higher in blue light treatment. The key gene involved in the delphinidin branch pathway, *F3′5′H*, and the specific gene for anthocyanin biosynthesis, *UFGT*, were found to be highly up-regulated in the response towards red light (Figure 7).

R2R3 MYBs (eight unigenes) and *bHLHs* (six unigenes) were found among the top 500 DEGs. All the identified TFs of MBW complex from top DEGs and corresponding gene ID with IPS domains are provided in Table S9. SQUAMOSA-MADS box (TDR-type) TFs, such as *AGAMOUS* (*AGL 15, 21, 61, 62, 80*) and *MADS* (*3,4,8*), were significantly up-regulated in red light treatment and down-regulated under blue light treatment (Figure 7). In contrast, blue light up-regulated *DEF2* and *PHE2* type MADS box TFs and red light down-regulated *SPL4* type TFs (Figure 7), which are all linked to regulating circadian rhythm and flowering. The expression level of *MYBA1*, the key regulatory gene of anthocyanin biosynthesis, was up-regulated by both red and blue light treatments, whereas *MYBPA1.1* was found comparatively higher level in red light treatment. Among the eight *R2R3 MYB* genes categorized as DEGs, three genes were up-regulated in similar levels under both the light treatments (Figure 7). Instead, *MYBPA1.1*, *MYBPA3*, *MYBC2.4*, *MYB5a* and *MYBPA2.3* were found to be expressed in higher levels in red light treatment compared to blue light treatment (Figure 7). All the *bHLH* TFs categorized under DEGs (*bHLH6 [MYC2]*, *bHLH130*, *bHLH137*, *bHLH147*, *bHLH68* and *bHLH79*) were found up-regulated in both light treatments and expressed in similar levels.

3.7 | DEGs from carotenoid and ABA metabolism

The carotenoid pathway genes, such as phytoene synthase (*PSY*), β-carotene hydroxylase (*BCH*) and carotenoid β-ring hydroxylase of cytochrome P450 family (*CYP450-BCH*), were up-regulated in both red and blue light treatments with the exception of ζ-carotene desaturase (*ZDS*) and lutein deficient 1-like (*Lut1*) with lower expression levels in blue light treatment (Figure 7). In addition, the important carotenoid cleavage gene *NCED*, the key cleavage gene in ABA biosynthesis, was up-regulated in both the light treatments but higher in red light treatment (Figure 7). On the other hand, *ABA-8′ hydroxylase*, which is the first step in the ABA catabolism route, was highly up-regulated only under red light treatment but down-regulated (to −1.88-fold change) in blue light treatment. There were three unigenes identified as ABA-receptors pyrabactin resistance-like gene

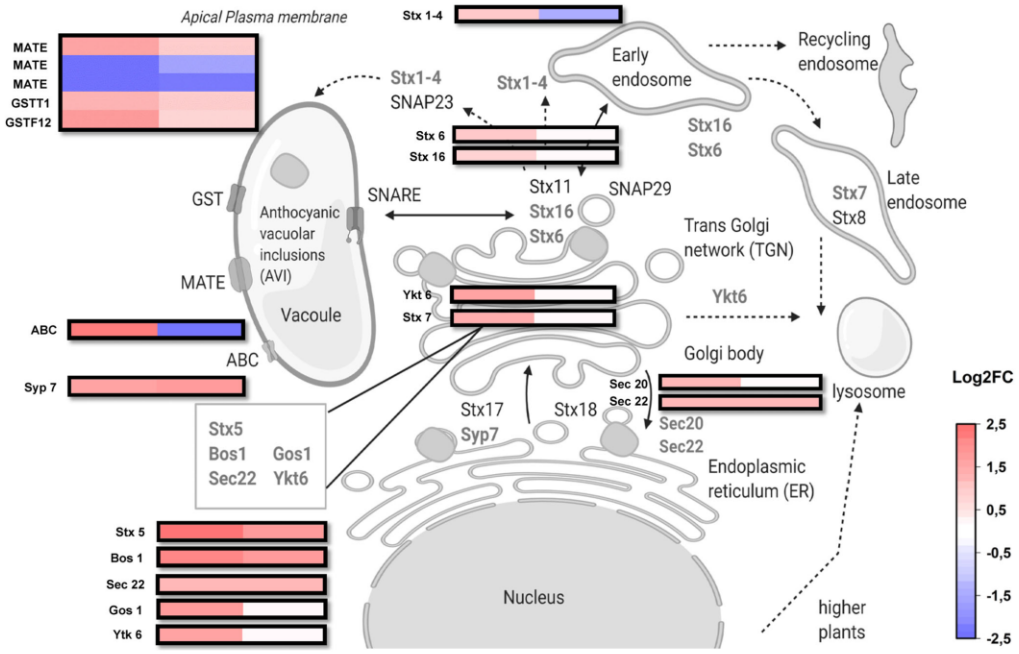

FIGURE 8 DEGs from SNARE mediated vesicular trafficking. Schematic representation of vesicular transport of anthocyanins mediated by SNARE proteins interaction through transmembrane—endoplasmic reticulum (ER)—golgi network. The associated transporter genes from red and blue light versus control contrasts DEGs were represented in colour code boxes based on $\log_2$ fold changes. Red light treatment is shown on left and blue light treatment on the right-hand side of the box. *Gene abbreviations*: Bos1, Gos, Qb type golgi SNAP receptor complex; SNAP, soluble NSF attachment protein; SNARE, 'SNAP REceptor'; Stx, syntaxin-like; Ykt6, Sec22, vesicle transporter/VAMP like protein [Colour figure can be viewed at wileyonlinelibrary.com]

(*PYL-4,5,8*) of which two of them (*PYL 5,8*) were down-regulated to two- to three-folds lower in response to blue light (Figure 7). ABA insensitive (*ABI5*) TF was found in similar levels in both the light treatments.

The relative gene expression for all the key anthocyanin and ABA biosynthetic genes discussed earlier (*CHS*, *F3'H*, *F3'5'H*, *DFR*, *ANS*, *UFGT*, *MYBA1*, *and NCED*) obtained from qRT-PCR analyses (Figure S9a) and identified unigenes from RNA-seq dataset were correlated, showing the higher correlation R^2 values of 0.9 with red versus control and 0.8 with blue versus control contrasts (Figure S9b).

3.8 | DEGs involved in vesicular trafficking

DEGs identified and annotated as group of genes related to SNARE-domain family of transporter proteins, such as *Stx 5,6,7* (syntaxin), *Sec 20,22* and *Ykt6*, were highly up-regulated in response towards the red light treatment (Figure 8). The syntaxin genes (*Stx1-4*), usually found in apical plasma membrane, were up-regulated in red light and down-regulated in blue light treatment. We also identified two unigenes from DEGs annotated as *ABC* family of transporter proteins (ATP-binding cassette sub-family B), which showed the same expression trend to syntaxin genes suggesting the involvement of ABCs in vesicular transport, possibly together with SNAREs (Figure 8). *GSTs F12* and *T1-like* transporter genes were up-regulated by both the light treatments, whereas a single unigene out of three annotated among the top DEGs corresponding to MATE efflux transporter protein family was found up-regulated by both treatments (Figure 8).

3.9 | Gene-metabolite interaction

Pearson's correlation matrices between the dominantly found anthocyanins quantified using HPLC (delphinidin 3-galactoside and delphinidin 3-arabinoside) and the transcript levels related to the flavonoid, carotenoid and ABA pathway genes, and ABA-receptors from both light treatments indicated strong links between ABA and anthocyanin biosynthesis, especially under red light (Figure 9). We also found statistically significant positive correlations among gene-metabolite interactions for red light compared to blue light treatment.

4 | DISCUSSION

It has been shown in many fruits that specific light spectral wavelengths from PAR spectrum can influence the biosynthesis of anthocyanins and other polyphenolic compounds (Jeong, Goto-Yamamoto, Kobayashi, & Esaka, 2004; Koyama et al., 2012; Tao et al., 2018; Kokalj et al., 2019). Beyond the PAR range spectral wavelengths, UV light can also positively regulate anthocyanin biosynthesis. Recent studies have shown that UV-B irradiation in pre-harvest and UV-A irradiation in post-harvest conditions promoted anthocyanin biosynthesis in blueberries (Li, Yamane, & Tao, 2021; Yang et al., 2018). However, the molecular mechanisms underlying the light quality-regulated fruit anthocyanin biosynthesis are not well understood. In this study, we used a comparative transcriptomics approach to analyse the effect of light quality on anthocyanin biosynthesis in ripening fruit of bilberry producing anthocyanins from both cyanidin and delphinidin branches. The light treatments were given to unripe green

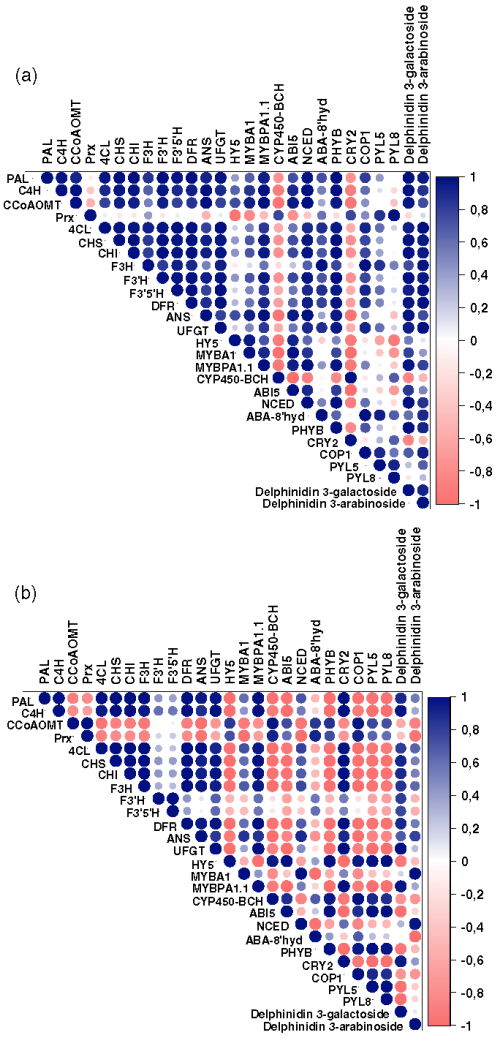

FIGURE 9 Metabolite-gene expression correlation analysis associated with anthocyanin, carotenoid and ABA metabolism. Pearson's coefficient-based correlation matrices from selected gene expression levels with two major identified delphinidin glycosides for control versus red (a) and control versus blue (b) contrasts. The sizes and colours of dots represent the strength of correlation from positive (blue) to negative (red) correlations arranged in an upper triangular matrix [Colour figure can be viewed at wileyonlinelibrary.com]

(S3 stage) bilberry fruits, as this stage has been shown earlier to be reactive towards changes in spectral light wavelengths affecting anthocyanin biosynthesis (Zoratti et al., 2014). Here, we showed that the anthocyanin concentration and profile in ripening berries was affected especially by red light but also blue light treatment, and our results indicate differences in light signalling pathways between red and blue light in regulation of anthocyanin biosynthesis.

4.1 | Light quality modulates light signal perception and transduction

In natural conditions, plants encounter varying light spectral conditions. For example, in the latitudes close to Arctic circle, the radiation flux from a distinct solar spectrum (UV-A/B ratio, blue and red/far-red wavelengths) changes compared to southern latitudes, and this has been shown to favour higher accumulation of flavonoids in northern vegetation, including wild bilberries (Jaakola & Hohtola, 2010; Zoratti, Karppinen, et al., 2014). Delphinidins are the major class of constituting anthocyanins found abundant in northern clones compared with higher cyanidin proportions found in southern clones (Zoratti et al., 2016). In addition, in forests, the top canopy absorbs most of the essential red and blue wavelengths, and only the green and far-red wavelengths are reflected by foliage to lower parts of the plant (Holopainen et al., 2018). In bilberry, populations grown under direct sunlight have demonstrated increased bioactive compounds and bioavailability compared with plants growing under forest canopy (Eckerter, Buse, Förschler, & Pufal, 2019). However, the even distribution through the foliage can be achieved by modern energy efficient LEDs, because the irradiation maxima from these supplemental lightings are often higher than plant's absorption peaks. Our study showed that during the red light LED treatment, *PHYB* expression was up-regulated together with *COP1* and *HY5*, the key genes involved in photomorphogenesis, alongside photoperiodism-related early flowering (*ELF3*) and *CK2α* genes (Figure 6). On the other hand, the blue light up-regulated cryptochrome (*CRY2*) but down-regulated *COP1* and *HY5* in tandem as its photoreactive mechanism, which might reveal that an early photomorphogenesis occurred upon light treatment as a spontaneous response but was found in low levels of expression at the time of our observation. It is also to be noted that *bHLH6 (MYC2)*, which is a negative regulator of blue light induced photomorphogenesis (Yadav, Mallappa, Gangappa, Bhatia, & Chattopadhyay, 2005) and was positively expressed in our study, might have played a crucial role in blue light signalling mechanism.

4.2 | Supplemental red and blue light irradiation positively affects anthocyanin biosynthesis and accumulation

Red and blue wavelengths have optimal chlorophyll absorption and photosynthetic efficiency (Massa, Kim, Wheeler, & Mitchell, 2008), and both appear to be effective in promoting anthocyanin biosynthesis in various horticultural crops (Bian, Yang, & Liu, 2014; Zhang et al., 2018). Our results showed that both the light treatments up-regulated all the anthocyanin biosynthetic genes in bilberry fruit, including all the bottleneck flavonoid biosynthetic genes *CHS*, *F3H* and *ANS* described in*Vaccinium* fruits (Günther et al., 2020; Primetta, Karppinen, Riihinen, & Jaakola, 2015; Zorenc et al., 2017). This led to the higher accumulation of anthocyanins under both red and blue light treatments compared to control fruits. Furthermore, the expression level of *UFGT*, the last gene in the anthocyanin pathway, and *F3'5'H*, the gene directing dihydroflavonol precursors to delphinidin biosynthesis, was found to be highly up-regulated under the red light treatment. Generally, blue light has been shown as a strong positive influencer of anthocyanin accumulation in many fruit crops, for example, in sweet cherries (Kokalj et al., 2019) and pear (Tao et al., 2018). However, red light can also promote in similar ways. A recent study in strawberry showed that both red and blue light were able to increase gene expression levels of flavonoid biosynthetic pathway with red light found to be slightly more effective in inducing anthocyanin accumulation (Zhang et al., 2018). For instance, also in a previous study in apple, red light has been shown to promote anthocyanin biosynthesis (Lekkham, Srilaong, Pongprasert, & Kondo, 2016), and red-shaded nets improved phytochemical contents in few vegetables (Ilić & Fallik, 2017). Our results suggest that *UFGT* and *F3'5'H* are separately regulated and highly responsive to red light in ripening bilberry fruit. This changed the anthocyanin profile towards delphinidin glycosides in fully ripe berries under red light.

Anthocyanin biosynthesis is directly regulated by the MBW complex and *R2R3 MYB* expression and to some extent *bHLH* expression. A high number of DEGs representing *MYB* and *bHLH* genes was found from our RNA-seq libraries, indicating that their regulation is strongly influenced by the light spectral quality. *MYBA*-type TFs have been identified as the key regulators activating anthocyanin biosynthesis in fruits including *Vaccinium* berries (Die, Jones, Ogde, Ehlenfeldt, & Rowland, 2020; Plunkett et al., 2018). In addition, *MYBPA1* has been suggested to have a regulatory role in anthocyanin biosynthesis based on our previous studies (Primetta et al., 2015; Günther et al., 2020; Karppinen et al., 2021). In this study, both *MYBA1* and *MYBPA1.1* were up-regulated by red and blue light. Especially, *MYBPA1.1* was induced by red light, which has been recently suggested as one of the key genes in regulating delphinidin branch during bilberry ripening (Karppinen et al., 2021). Other bilberry *MYB* sequences homologous to related *MYBPA2*, *MYB5* and *MYBC2* genes were also found among top 500 DEGs, which are likely to be involved in regulatory mechanisms during ripening and flavonoid biosynthesis. Some of the *bHLH* sequences, which were up-regulated in both red and blue light treatments, such as *bHLH79*, have been previously reported in grapes towards light-induced anthocyanin biosynthesis (Ma et al., 2019). In addition, *bHLH6* (*MYC2*) TF is reported to be commonly involved in light and ABA signalling pathways (Yadav et al., 2005).

4.3 | Differences in carotenoid biosynthesis and ABA metabolism suggest red light regulation through ABA

A significant increase in the expression of the carotenoid early biosynthetic genes and late cleavage gene, including *NCED*, has earlier been found in bilberry fruit ripening under red light (Karppinen et al., 2016). Our results are in agreement with this study but also showed that not only the red light but also blue light treatment up-regulated expression levels of many of the carotenoid biosynthetic genes. However, the expression of *ZDS* and *CYP450-BCH* genes branching towards α-carotene and further to lutein biosynthesis (*LUT1*) varied between the red and blue light treatments (Figure 7). It has also been shown in the previous study that the up-regulated expression levels of carotenoid biosynthetic genes in red light conditions led to low levels of carotenoids indicating elevated carotenoid cleavage reactions (Karppinen, Zoratti, Sarala, et al., 2016) that lead to production of plant hormone ABA.

The increase in ABA levels and the carotenoid cleavage reaction through action of the key enzyme *NCED* was found increased at the onset of bilberry ripening (Karppinen et al., 2013). Many studies have demonstrated the exogenous application of ABA increasing the anthocyanin levels of fruits when applied at the time of fruit ripening (Ferrero et al., 2018; Wheeler, Loveys, Ford, & Davies, 2009). The effect of exogenous application of ABA on inducing bilberry fruit anthocyanin biosynthesis has been demonstrated earlier (Karppinen et al., 2018). In *Fragaria* × *ananassa*, the positive effect of ABA as well as light has been reported to act independently through the activation of *FvMYB10*, the key gene in strawberry anthocyanin biosynthesis (Kadomura-Ishikawa, Miyawaki, Takahashi, Masuda, & Noji, 2015). In our study, the red light treatment induced higher expression of *NCED* compared to control and blue light treatment. In addition, we showed that expression levels of *ABA-8′ hydroxylase* gene, responsible for degradation of ABA, increased two-fold higher in red light treatment and were down-regulated in blue light treatment. It has been shown that the endogenous levels of ABA in plant cells are maintained only by the inhibition of this enzyme (Kondo et al., 2012). A similar trend of increase in expression of *NCED* and *ABA-8′ hydroxylase* genes alongside higher anthocyanin accumulation in response to red light irradiation was observed earlier in grapevine (Kondo et al., 2014). Rodyoung et al. (2016) have shown that in grapes, the expression of both of these genes was higher at veraison in response to red and blue light irradiation. In many fruits, the ABA catabolism might not directly coincide with anthocyanin biosynthesis but the upstream ABA biosynthesis and endogenous levels of ABA may be directly involved in interaction with the flavonoid pathway. Here, we show that in ripening bilberry fruit, the red light activates both the biosynthetic and catabolic ABA pathways and correlates with anthocyanin accumulation. Furthermore, the changes in delphinidin levels showing a strong correlation with anthocyanin biosynthesis and direct regulatory genes, ABA signalling and metabolism genes (Figure 9) suggest a well-orchestrated regulatory network of ABA-regulated anthocyanin biosynthesis occurring under supplemental red light.

The signal transduction from ABA to the regulation of anthocyanin biosynthesis has been reported earlier in other fruit species, such as *Lycium* fruits, where ABA was found to interact directly with the MBW complex and other key flavonoid genes (Li et al., 2019). In our study, we showed that light treatments during ripening process activated signal transduction cascade via ABA signalling leading to anthocyanin accumulation. It has been shown in one of the recent studies that red light increased the expression level of *AGAMOUS*-like (AGL) regulators in tomato (*Solanum lycopersicum* L.) during fruit ripening (Zhang et al., 2020). These AGL-like MADS box TFs are also orthologs to *VmTDR4* in bilberry, a key player in bilberry anthocyanin accumulation (Jaakola et al., 2010). This provides us with an understanding that red light might mediate ABA-regulated anthocyanin biosynthesis through SQUAMOSA-MADS box type TFs, ABA binding receptors such as pyrabactin resistance like (*PYR/PYL*), ABA insensitive (*ABI5*) gene, which all act as upstream regulators towards activating the MBW complex. A similar ABA signal transduction mechanism occurs via MADS box TFs was previously demonstrated in blueberry anthocyanin biosynthesis (Chung et al., 2019). It should also be noted that the *SPL* type TFs (SQUAMOSA promoter binding like) that were up-regulated in response to blue light in our study can be associated with the increase in expression of Flowering Locus-T (*FT*) gene involved in flowering and circadian clock-related mechanisms as the TF acts downstream to *FT* expression (Wang, Czech, & Weigel, 2009).

4.4 | Supplemental light triggers vesicular trafficking in ripening berry accumulating anthocyanins

The transportation of anthocyanins into vacuoles is usually trafficked intra-cellularly by different classes of transporter proteins, such as MATEs, ABCs and GSTs (Petrussa et al., 2013). The transporters involved in fruit anthocyanin transport in relation to light quality response have not been studied. However, our results demonstrated that a set of genes, including *Stx*, *Bos1*, *Gos1*, *Ykt6*, *Sec20*, *Sec 22* and *Syp7*, were highly up-regulated in response to red light treatment. These genes belonged to the SNARE-domain protein family, which includes the common syntaxin-like (*Stx*, *Syp*) genes. Interestingly, the unigenes annotated as *Stx*-like (1,4) type along with an ABC transporter were up-regulated in response to red light treatment and reacted in the opposite manner to that of blue light treatment. Hence, SNARE domain transporters are candidates to be involved in vesicular trafficking of anthocyanins or trans-membrane transport from endoplasmic reticulum (ER) to golgi and endosomes. It also indicates the potential role of syntaxin genes differentially responding to light-induced anthocyanin transport mechanisms. These different types of SNAREs, barring the ER-localized *Syp* and *Sec*, are usually localized in endosomes and in trans-golgi network (Kim & Brandizzi, 2012). Our results may indicate a new route for anthocyanin sequestration and transportation in fruit tissues. The proposed vesicular trafficking model of anthocyanins in fruits might be also co-regulated by other *GSTs*, *MATE* efflux transporters and *ABC* transporters, in addition to

the SNARE-domain type proteins before depositing as anthocyanic vacuolar inclusions (AVI) in the vacuole (Zhao, 2015). This mechanism could also relate to the plant tissues that accumulate higher anthocyanin levels under high intensity light and needs to be investigated further.

5 | CONCLUSION

Our RNA-seq analyses from the time of fruit ripening show that both red and blue wavelengths are capable of inducing a high number of up-regulated genes and metabolic pathways, including flavonoid, phenylpropanoid, carotenoid biosynthetic pathways and sugar metabolism. Blue and especially red light were effective in inducing anthocyanin and delphinidin accumulation but through different signal transduction routes. The blue light triggered early photomorphogenesis via *CRY2/COP1* interaction that potentially combined with positive regulators, such as *MYBA* and *HY5*, to induce the expression of anthocyanin biosynthetic genes during onset of ripening. Red light treatment instead positively up-regulated *PHYB* and all the major flavonoid genes, including the anthocyanin (*UFGT*) and delphinidin (*F3'5'H*) routes, key ABA biosynthetic gene (*NCED*) and ABA degrading *ABA-8'hydroxylase* genes. Our results provide an insight into the role of endogenous ABA accumulation and degradation as positive signalling factors leading to increased levels of anthocyanin accumulation via the ABA-signal transduction mechanism during the ripening process under red light. We also found the expression of SNARE complex-related vesicle trafficking genes to be highly expressed in red light treated berries, which might provide clues into the possible sequestration and transport mechanisms via endosomes in tissues with higher anthocyanin accumulation, but need further investigation. Our high-quality transcriptome dataset will be a useful genomics resource in future bilberry research and *Vaccinium* breeding programmes.

ACKNOWLEDGMENTS

The authors would like to thank Leidulf Lund for the help in setting up light experiments at the Phytotron facility at UiT The Arctic University of Norway. We are grateful for the UiT-BFE faculty's mobility grant to AS allowing the visit to Plant and Food Research, New Zealand. The research mobility was supported by the New Zealand Ministry for Business, Innovation and Employment (MBIE) Endeavour programme 'Filling the Void: boosting the nutritional content of NZ fruit' (contract C11X1704). The work was also financially supported by NordPlant (NordForsk grant no. 84597).

CONFLICT OF INTEREST

The authors declare that they have no conflict of interest.

AUTHOR CONTRIBUTIONS

L.J. conceptualized the project and along with K.K., I.M. and A.S. designed the experiment. A.S. performed the experiments, analysed the data and wrote the manuscript. D.J. contributed in RNA-seq bioinformatics pipeline and analysis. A.P.D. contributed with the HPLC analysis of anthocyanins. N.S. performed metabolic profiling with LC–MS. L.J., K.K., I.M. and R.V.E. contributed in the editing and proofreading of the manuscript draft. All authors have read and approved the manuscript.

DATA AVAILABILITY STATEMENT

The data that support the findings of this study are openly available in NCBI-SRA database at http://www.ncbi.nlm.nih.gov/bioproject/747684, reference number [PRJNA747684].

ORCID

Amos Samkumar https://orcid.org/0000-0002-2845-5301
Katja Karppinen https://orcid.org/0000-0002-5129-0656
Andrew P. Dare https://orcid.org/0000-0002-8973-9332
Nina Sipari https://orcid.org/0000-0002-0786-2493
Richard V. Espley https://orcid.org/0000-0002-1732-3688
Inger Martinussen https://orcid.org/0000-0001-8107-7787
Laura Jaakola https://orcid.org/0000-0001-9379-0862

REFERENCES

An, J. P., Zhang, X. W., Liu, Y. J., Wang, X. F., You, C. X., & Hao, Y. J. (2021). ABI5 regulates ABA-induced anthocyanin biosynthesis by modulating the MYB1-bHLH3 complex in apple. *Journal of Experimental Botany*, *72*(4), 1460–1472. https://doi.org/10.1093/jxb/eraa525

Andrews, S. (2010). FastQC: A quality control tool for high throughput sequence data. Retrieved from http://www.bioinformatics.babraham.ac.uk/projects/fastqc/

Ballaré, C. L. (2014). Light regulation of plant defense. *Annual Review of Plant Biology*, *65*, 335–363. https://doi.org/10.1146/annurev-arplant-050213-040145

Behrens, C. E., Smith, K. E., Iancu, C. V., Choe, J. Y., & Dean, J. V. (2019). Transport of anthocyanins and other flavonoids by the arabidopsis ATP-binding cassette transporter AtABCC2. *Scientific Reports*, *9*, 1–15. https://doi.org/10.1038/s41598-018-37504-8

Bhatnagar, A., Singh, S., Khurana, J. P., & Burman, N. (2020). HY5-COP1: The central module of light signaling pathway. *Journal of Plant Biochemistry and Biotechnology*, *29*(4), 590–610. https://doi.org/10.1007/s13562-020-00623-3

Bian, Z., Yang, Q., & Liu, W. (2014). Effects of light quality on the accumulation of phytochemicals in vegetables produced in controlled environments: A review. *Journal of the Science of Food and Agriculture*, *95*(5), 869–877.

Bolger, A., Lohse, M., & Usadel, B. (2014). Trimmomatic: A flexible trimmer for Illumina sequence data. *Bioinformatics*, *30*(15), 2114–2120. https://doi.org/10.1093/bioinformatics/btu170

Briggs, W. R., & Olney, M. A. (2001). Photoreceptors in plant photomorphogenesis to date. Five phytochromes, two cryptochromes, one phototropin, and one superchrome. *Plant Physiology*, *125*, 85–88. https://doi.org/10.1104/pp.125.1.85

Bujor, O., Le Bourvellec, C., Volf, I., Popa, V., & Dufour, C. (2016). Seasonal variations of the phenolic constituents in bilberry (*Vaccinium myrtillus* L.) leaves, stems and fruits, and their antioxidant activity. *Food Chemistry*, *213*, 58–68.

Chanoca, A., Kovinich, N., Burkel, B., Stecha, S., Bohorquez-Restrepo, A., Ueda, T., & Otegui, M. S. (2015). Anthocyanin vacuolar inclusions form by a microautophagy mechanism. *Plant Cell*, *27*(9), 2545–2559. https://doi.org/10.1105/tpc.15.00589

Chen, M., Chory, J., & Fankhauser, C. (2004). Light signal transduction in higher plants. *Annual Review of Genetics*, *38*(1), 87–117. https://doi.org/10.1146/annurev.genet.38.072902.092259

Chong, J., Wishart, D. S., & Xia, J. (2019). Using metaboanalyst 4.0 for comprehensive and integrative metabolomics data analysis. *Current Protocols in Bioinformatics*, *68*, e86. https://doi.org/10.1002/cpbi.86

Chu, W. K., Cheung, S. C. M., Lau, R. A. W., & Benzie, I. F. F. (2011). Bilberry (*Vaccinium myrtillus* L.). In I. F. F. Benzie & S. Wachtel-Galor, et al. (Eds.), *Herbal Medicine: Biomolecular and Clinical Aspects* (2nd ed.). Boca Raton, FL: CRC Press/Taylor & Francis.

Chung, S. W., Yu, D. J., Oh, H. D., Ahn, J. H., Huh, J. H., & Lee, H. J. (2019). Transcriptional regulation of abscisic acid biosynthesis and signal transduction, and anthocyanin biosynthesis in 'Bluecrop' highbush blueberry fruit during ripening. *PLoS One*, *14*(7), e0220015.

Colle, M., Leisner, C., Wai, C., Ou, S., Bird, K., Wang, J., … Edger, P. P. (2019). Haplotype-phased genome and evolution of phytonutrient pathways of tetraploid blueberry. *GigaScience*, *8*(3), giz012. https://doi.org/10.1093/gigascience/giz012

Die, J. V., Jones, R. W., Ogde, E. L., Ehlenfeldt, M. K., & Rowland, L. J. (2020). Characterization and analysis of anthocyanin-related genes in wild-type blueberry and the pink-fruited mutant cultivar 'Pink Lemonade': New insight into anthocyanin biosynthesis. *Agronomy*, *10*, 1296.

Dobin, A., Davis, C., Schlesinger, F., Drenkow, J., Zaleski, C., Jha, S., … Gingeras, T. R. (2013). STAR: Ultrafast universal RNA-seq aligner. *Bioinformatics*, *29*(1), 15–21. https://doi.org/10.1093/bioinformatics/bts635

Eckerter, T., Buse, J., Förschler, M., & Pufal, G. (2019). Additive positive effects of canopy openness on European bilberry (*Vaccinium myrtillus*) fruit quantity and quality. *Forest Ecology and Management*, *433*, 122–130. https://doi.org/10.1016/j.foreco.2018.10.059

Ewels, P., Magnusson, M., Lundin, S., & Käller, M. (2016). MultiQC: Summarize analysis results for multiple tools and samples in a single report. *Bioinformatics*, *32*(19), 3047–3048. https://doi.org/10.1093/bioinformatics/btw354

Feller, A., MacHemer, K., Braun, E. L., & Grotewold, E. (2011). Evolutionary and comparative analysis of MYB and bHLH plant transcription factors. *Plant Journal*, *66*(1), 94–116. https://doi.org/10.1111/j.1365-313X.2010.04459.x

Ferrara, G., Mazzeo, A., Matarrese, A. M. S., Pacucci, C., Punzi, R., Faccia, M., … Gambacorta, G. (2015). Application of abscisic acid (S-ABA) and sucrose to improve colour, anthocyanin content and antioxidant activity of cv. Crimson seedless grape berries. *Australian Journal of Grape and Wine Research*, *21*(1), 18–29. https://doi.org/10.1111/ajgw.12112

Ferrero, M., Pagliarani, C., Novák, O., Ferrandino, A., Cardinale, F., Visentin, I., & Schubert, A. (2018). Exogenous strigolactone interacts with abscisic acid-mediated accumulation of anthocyanins in grapevine berries. *Journal of Experimental Botany*, *69*(9), 2391–2401. https://doi.org/10.1093/jxb/ery033

Gilbert, D. (2019). Longest protein, longest transcript or most expression, for accurate gene reconstruction of transcriptomes? *bioRxiv*, 829184. https://doi.org/10.1101/829184

Gotz, S., Garcia-Gomez, J., Terol, J., Williams, T., Nagaraj, S. H., Nueda, M. J., … Conesa, A. (2008). High-throughput functional annotation and data mining with the Blast2GO suite. *Nucleic Acids Research*, *36*(10), 3420–3435. https://doi.org/10.1093/nar/gkn176

Grabherr, M., Haas, B., Yassour, M., Levin, J., Thompson, D., Amit, I., … Regev, A. (2011). Full-length transcriptome assembly from RNA-Seq data without a reference genome. *Nature Biotechnology*, *29*(7), 644–652. https://doi.org/10.1038/nbt.1883

Günther, C. S., Dare, A. P., McGhie, T. K., Deng, C., Lafferty, D. J., Plunkett, B. J., … Espley, R. V. (2020). Spatiotemporal modulation of flavonoid metabolism in blueberries. *Frontiers in Plant Science*, *11*, 545. https://doi.org/10.3389/fpls.2020.00545

Heysieattalab, S., & Sadeghi, L. (2020). Effects of delphinidin on pathophysiological signs of nucleus basalis of meynert lesioned rats as animal model of alzheimer disease. *Neurochemical Research*, *45*(7), 1636–1646. https://doi.org/10.1007/s11064-020-03027-w

Holopainen, J., Kivimäenpää, M., & Julkunen-Tiitto, R. (2018). New light for phytochemicals. *Trends in Biotechnology*, *36*(1), 7–10. https://doi.org/10.1016/j.tibtech.2017.08.009

Ilić, Z. S., & Fallik, E. (2017). Light quality manipulation improves vegetable quality at harvest and postharvest: A review. *Environmental and Experimental Botany*, *139*, 79–90. https://doi.org/10.1016/j.envexpbot.2017.04.006

Jaakola, L. (2013). New insights into the regulation of anthocyanin biosynthesis in fruits. *Trends in Plant Science*, *18*(9), 477–483. https://doi.org/10.1016/j.tplants.2013.06.003

Jaakola, L., & Hohtola, A. (2010). Effect of latitude on flavonoid biosynthesis in plants. *Plant, Cell and Environment*, *33*(8), 1239–1247. https://doi.org/10.1111/j.1365-3040.2010.02154.x

Jaakola, L., Määttä, K., Pirttilä, A. M., Törrönen, R., Kärenlampi, S., & Hohtola, A. (2002). Expression of genes involved in anthocyanin biosynthesis in relation to anthocyanin, proanthocyanidin, and flavonol levels during bilberry fruit development. *Plant Physiology*, *130*(2), 729–739.

Jaakola, L., Poole, M., Jones, M. O., Kämäräinen-Karppinen, T., Koskimäki, J. J., Hohtola, A., … Seymour, G. B. (2010). A SQUAMOSA MADS box gene involved in the regulation of anthocyanin accumulation in bilberry fruits. *Plant Physiology*, *153*(4), 1619–1629. https://doi.org/10.1104/pp.110.158279

Jeong, S. T., Goto-Yamamoto, N., Kobayashi, S., & Esaka, M. (2004). Effects of plant hormones and shading on the accumulation of anthocyanins and the expression of anthocyanin biosynthetic genes in grape berry skins. *Plant Science*, *167*(2), 247–252. https://doi.org/10.1016/j.plantsci.2004.03.021

Jia, H. F., Chai, Y. M., Li, C. L., Lu, D., Luo, J. J., Qin, L., & Shen, Y. Y. (2011). Abscisic acid plays an important role in the regulation of strawberry fruit ripening. *Plant Physiology*, *157*(1), 188–199. https://doi.org/10.1104/pp.111.177311

Kadomura-Ishikawa, Y., Miyawaki, K., Takahashi, A., Masuda, T., & Noji, S. (2015). Light and abscisic acid independently regulated FaMYB10 in *Fragaria* × *ananassa* fruit. *Planta*, *241*(4), 953–965. https://doi.org/10.1007/s00425-014-2228-6

Karppinen, K., Hirvelä, E., Nevala, T., Sipari, N., Suokas, M., & Jaakola, L. (2013). Changes in the abscisic acid levels and related gene expression during fruit development and ripening in bilberry (*Vaccinium myrtillus* L.). *Phytochemistry*, *95*, 127–134. https://doi.org/10.1016/j.phytochem.2013.06.023

Karppinen, K., Lafferty, D. J., Albert, N. W., Mikkola, N., McGhie, T., Allan, A. C., … Jaakola, L. (2021). MYBA and MYBPA transcription factors co-regulate anthocyanin biosynthesis in blue-coloured berries. *New Phytologist*. https://doi.org/10.1111/nph.17669.

Karppinen, K., Tegelberg, P., Häggman, H., & Jaakola, L. (2018). Abscisic acid regulates anthocyanin biosynthesis and gene expression associated with cell wall modification in ripening bilberry (*Vaccinium myrtillus* L.) fruits. *Frontiers in Plant Science*, *9*, 1–17. https://doi.org/10.3389/fpls.2018.01259

Karppinen, K., Zoratti, L., Nguyenquynh, N., Häggman, H., & Jaakola, L. (2016). On the developmental and environmental regulation of secondary metabolism in *Vaccinium* spp. berries. *Frontiers in Plant Science*, *7*, 655. https://doi.org/10.3389/fpls.2016.00655

Karppinen, K., Zoratti, L., Sarala, M., Carvalho, E., Hirsimäki, J., Mentula, H., … Jaakola, L. (2016). Carotenoid metabolism during bilberry (*Vaccinium myrtillus* L.) fruit development under different light conditions is regulated by biosynthesis and degradation. *BMC Plant Biology*, *16*(1), 95. https://doi.org/10.1186/s12870-016-0785-5

Kim, S. J., & Brandizzi, F. (2012). News and views into the SNARE complexity in Arabidopsis. *Frontiers in Plant Science*, *3*, 1–6. https://doi.org/10.3389/fpls.2012.00028

Kokalj, D., Zlatić, E., Cigić, B., Kobav, M. B., & Vidrih, R. (2019). Postharvest flavonol and anthocyanin accumulation in three apple cultivars in

response to blue-light-emitting diode light. *Scientia Horticulturae*, *257*, 108711.

Kokalj, D., Zlatić, E., Cigić, B., & Vidrih, R. (2019). Postharvest light-emitting diode irradiation of sweet cherries (*Prunus avium* L.) promotes accumulation of anthocyanins. *Postharvest Biology and Technology*, *148*, 192–199. https://doi.org/10.1016/j.postharvbio.2018.11.011

Kondo, S., Sugaya, S., Sugawa, S., Ninomiya, M., Kittikorn, M., Okawa, K., … Hirai, N. (2012). Dehydration tolerance in apple seedlings is affected by an inhibitor of ABA 8′-hydroxylase CYP707A. *Journal of Plant Physiology*, *169*(3), 234–241. https://doi.org/10.1016/j.jplph.2011.09.007

Kondo, S., Tomiyama, H., Rodyoung, A., Okawa, K., Ohara, H., Sugaya, S., … Hirai, N. (2014). Abscisic acid metabolism and anthocyanin synthesis in grape skin are affected by light emitting diode (LED) irradiation at night. *Journal of Plant Physiology*, *171*(10), 823–829. https://doi.org/10.1016/j.jplph.2014.01.001

Kopylova, E., Noé, L., & Touzet, H. (2012). SortMeRNA: Fast and accurate filtering of ribosomal RNAs in metatranscriptomic data. *Bioinformatics*, *28*(24), 3211–3217. https://doi.org/10.1093/bioinformatics/bts611

Koyama, K., Ikeda, H., Poudel, P. R., & Goto-Yamamoto, N. (2012). Light quality affects flavonoid biosynthesis in young berries of Cabernet Sauvignon grape. *Phytochemistry*, *78*, 54–64.

Lau, O. S., & Deng, X. W. (2012). The photomorphogenic repressors COP1 and DET1: 20 years later. *Trends in Plant Science*, *17*(10), 584–593. https://doi.org/10.1016/j.tplants.2012.05.004

Lekkham, P., Srilaong, V., Pongprasert, N., & Kondo, S. (2016). Anthocyanin concentration and antioxidant activity in light-emitting diode (LED)-treated apples in a greenhouse environmental control system. *Fruits*, *71*(5), 269–274. https://doi.org/10.1051/fruits/2016022

Li, G., Zhao, J., Qin, B., Yin, Y., An, W., Mu, Z., & Cao, Y. (2019). ABA mediates development-dependent anthocyanin biosynthesis and fruit coloration in *Lycium* plants. *BMC Plant Biology*, *19*(1), 1–13. https://doi.org/10.1186/s12870-019-1931-7

Li, Q.-H., & Yang, H.-Q. (2007). Cryptochrome signaling in plants. *Photochemistry and Photobiology*, *83*(1), 94–101. https://doi.org/10.1562/2006-02-28-ir-826

Li, T., Yamane, H., & Tao, R. (2021). Preharvest long-term exposure to UV-B radiation promotes fruit ripening and modifies stage-specific anthocyanin metabolism in highbush blueberry. *Horticulture Research*, *8*(1), 67. https://doi.org/10.1038/s41438-021-00503-4

Love, M., Huber, W., & Anders, S. (2014). Moderated estimation of fold change and dispersion for RNA-seq data with DESeq2. *Genome Biology*, *15*(12), 550. https://doi.org/10.1186/s13059-014-0550-8

Lu, X. D., Zhou, C. M., Xu, P. B., Luo, Q., Lian, H. L., & Yang, H. Q. (2015). Red-light-dependent interaction of phyB with SPA1 promotes COP1-SPA1 dissociation and photomorphogenic development in arabidopsis. *Molecular Plant*, *8*(3), 467–478. https://doi.org/10.1016/j.molp.2014.11.025

Ma, Z. H., Li, W. F., Mao, J., Li, W., Zuo, C. W., Zhao, X., … Chen, B. H. (2019). Synthesis of light-inducible and light-independent anthocyanins regulated by specific genes in grape 'Marselan' (*V. Vinifera* L.). *PeerJ*, *2019*(3), 1–24. https://doi.org/10.7717/peerj.6521

Massa, G. D., Kim, H. H., Wheeler, R. M., & Mitchell, C. A. (2008). Plant productivity in response to LED lighting. *HortScience*, *43*(7), 1951–1956.

Miao, L., Zhang, Y., Yang, X., Xiao, J., Zhang, H., Zhang, Z., … Jiang, G. (2016). Colored light-quality selective plastic films affect anthocyanin content, enzyme activities, and the expression of flavonoid genes in strawberry (*Fragaria* × *ananassa*) fruit. *Food Chemistry*, *207*, 93–100. https://doi.org/10.1016/j.foodchem.2016.02.077

Möglich, A., Yang, X., Ayers, R. A., & Moffat, K. (2010). Structure and function of plant photoreceptors. *Annual Review of Plant Biology*, *61*, 21–47. https://doi.org/10.1146/annurev-arplant-042809-112259

Müller, D., Schantz, M., & Richling, E. (2012). High performance liquid chromatography analysis of anthocyanins in bilberries (*Vaccinium myrtillus* L.), blueberries (*Vaccinium corymbosum* L.) and corresponding juices. *Journal of Food Science*, *77*(4), C340–C345.

Nagaoka, M., Maeda, T., Chatani, M., Handa, K., Yamakawa, T., Kiyohara, S., … Suzuki, K. (2019). A delphinidin-enriched maqui berry extract improves bone metabolism and protects against bone loss in osteopenic mouse models. *Antioxidants*, *8*(9), 386. https://doi.org/10.3390/antiox8090386

Nguyen, N., Suokas, M., Karppinen, K., Vuosku, J., Jaakola, L., & Häggman, H. (2018). Recognition of candidate transcription factors related to bilberry fruit ripening by *de novo* transcriptome and qRT-PCR analyses. *Scientific Reports*, *8*(1), 1–12. https://doi.org/10.1038/s41598-018-28158-7

Nile, S., & Park, S. (2014). Edible berries: Bioactive components and their effect on human health. *Nutrition*, *30*(2), 134–144. https://doi.org/10.1016/j.nut.2013.04.007

Ouzounis, T., Rosenqvist, E., & Ottosen, C. O. (2015). Spectral effects of artificial light on plant physiology and secondary metabolism: A review. *HortScience*, *50*(8), 1128–1135. https://doi.org/10.21273/hortsci.50.8.1128

Park, S. Y., Fung, P., Nishimura, N., Jensen, D. R., Fujii, H., Zhao, Y., … Cutler, S. R. (2009). Abscisic acid inhibits type 2C protein phosphatases via the PYR/PYL family of START proteins. *Science (New York, N.Y.)*, *324*(5930), 1068–1071. https://doi.org/10.1126/science.1173041

Patro, R., Duggal, G., Love, M., Irizarry, R., & Kingsford, C. (2017). Salmon provides fast and bias-aware quantification of transcript expression. *Nature Methods*, *14*(4), 417–419. https://doi.org/10.1038/nmeth.4197

Pečenková, T., Marković, V., Sabol, P., Kulich, I., & Zárský, V. (2017). Exocyst and autophagy-related membrane trafficking in plants. *Journal of Experimental Botany*, *69*(1), 47–57. https://doi.org/10.1093/jxb/erx363

Petrussa, E., Braidot, E., Zancani, M., Peresson, C., Bertolini, A., Patui, S., & Vianello, A. (2013). Plant flavonoids-biosynthesis, transport and involvement in stress responses. *International Journal of Molecular Sciences*, *14*(7), 14950–14973. https://doi.org/10.3390/ijms140714950

Plunkett, B. J., Espley, R. V., Dare, A. P., Warren, B. A. W., Grierson, E. R. P., Cordiner, S., … Schwinn, K. E. (2018). MYBA from blueberry (*Vaccinium* section *Cyanococcus*) is a subgroup 6 type R2R3MYB transcription factor that activates anthocyanin production. *Frontiers in Plant Science*, *9*, 1300.

Primetta, A. K., Karppinen, K., Riihinen, K. R., & Jaakola, L. (2015). Metabolic and molecular analyses of white mutant Vaccinium berries show down-regulation of MYBPA1-type R2R3 MYB regulatory factor. *Planta*, *242*(3), 631–643. https://doi.org/10.1007/s00425-015-2363-8

Ravaglia, D., Espley, R. V., Henry-Kirk, R. A., Andreotti, C., Ziosi, V., Hellens, R. P., … Allan, A. C. (2013). Transcriptional regulation of flavonoid biosynthesis in nectarine (*Prunus persica*) by a set of R2R3 MYB transcription factors. *BMC Plant Biology*, *13*, 68.

Rodyoung, A., Masuda, Y., Tomiyama, H., Saito, T., Okawa, K., Ohara, H., & Kondo, S. (2016). Effects of light emitting diode irradiation at night on abscisic acid metabolism and anthocyanin synthesis in grapes in different growing seasons. *Plant Growth Regulation*, *79*(1), 39–46. https://doi.org/10.1007/s10725-015-0107-1

Simão, F. A., Waterhouse, R. M., Ioannidis, P., Kriventseva, E. V., & Zdobnov, E. M. (2015). BUSCO: Assessing genome assembly and annotation completeness with single-copy orthologs. *Bioinformatics (Oxford, England)*, *31*(19), 3210–3212. https://doi.org/10.1093/bioinformatics/btv351

Takos, A. M., Jaffé, F. W., Jacob, S. R., Bogs, J., Robinson, S. P., & Walker, A. R. (2006). Light-induced expression of a *MYB* gene regulates anthocyanin biosynthesis in red apples. *Plant Physiology*, *142*, 1216–1232.

Tao, R., Bai, S., Ni, J., Yang, Q., Zhao, Y., & Teng, Y. (2018). The blue light signal transduction pathway is involved in anthocyanin accumulation in 'Red Zaosu' pear. *Planta*, *248*(1), 37–48.

Thornthwaite, J. T., Thibado, S. P., & Thornthwaite, K. A. (2020). Bilberry anthocyanins as agents to address oxidative stress. *Pathology* (pp. 179–187). London: Academic Press, Elsevier. https://doi.org/10.1016/b978-0-12-815972-9.00017-2

Tohge, T., de Souza, L. P., & Fernie, A. R. (2017). Current understanding of the pathways of flavonoid biosynthesis in model and crop plants. *Journal of Experimental Botany*, *68*, 4013–4028.

Walker, A. R., Lee, E., Bogs, J., McDavid, D. A. J., Thomas, M. R., & Robinson, S. P. (2007). White grapes arose through the mutation of two similar and adjacent regulatory genes. *Plant Journal*, *49*(5), 772–785. https://doi.org/10.1111/j.1365-313X.2006.02997.x

Wang, J. W., Czech, B., & Weigel, D. (2009). miR156-regulated SPL transcription factors define an endogenous flowering pathway in *Arabidopsis thaliana*. *Cell*, *138*(4), 738–749. https://doi.org/10.1016/j.cell.2009.06.014

Wheeler, S., Loveys, B., Ford, C., & Davies, C. (2009). The relationship between the expression of abscisic acid biosynthesis genes, accumulation of abscisic acid and the promotion of *Vitis vinifera* L. berry ripening by abscisic acid. *Australian Journal of Grape and Wine Research*, *15*(3), 195–204. https://doi.org/10.1111/j.1755-0238.2008.00045.x

Wu, C., Deng, C., Hilario, E., Albert, N., Lafferty, D., Grierson, E., … Chagné, D. (2021). A chromosome-scale assembly of the bilberry genome identifies a complex locus controlling berry anthocyanin composition. *Molecular Ecology Resources*. https://doi.org/10.1111/1755-0998.13467

Wu, J., Mao, X., Cai, T., Luo, J., & Wei, L. (2006). KOBAS server: A web-based platform for automated annotation and pathway identification. *Nucleic Acids Research*, *34*, W720–W724. https://doi.org/10.1093/nar/gkl167

Wu, M., Si, M., Li, X., Song, L., Liu, J., Zhai, R., … Wang, Z. (2019). PbCOP1.1 contributes to the negative regulation of anthocyanin biosynthesis in pear. *Plants*, *8*(2), 1–12. https://doi.org/10.3390/plants8020039

Wu, X., Gong, Q., Ni, X., Zhou, Y., & Gao, Z. (2017). UFGT: The key enzyme associated with the petals variegation in japanese apricot. *Frontiers in Plant Science*, *8*, 108. https://doi.org/10.3389/fpls.2017.00108

Xu, W., Dubos, C., & Lepiniec, L. (2015). Transcriptional control of flavonoid biosynthesis by MYB–bHLH–WDR complexes. *Trends in Plant Science*, *20*(3), 176–185.

Yadav, V., Mallappa, C., Gangappa, S. N., Bhatia, S., & Chattopadhyay, S. (2005). A basic helix-loop-helix transcription factor in Arabidopsis, MYC2, acts as a repressor of blue light-mediated photomorphogenic growth. *The Plant Cell*, *17*(7), 1953–1966. https://doi.org/10.1105/tpc.105.032060

Yang, J., Li, B., Shi, W., Gong, Z., Chen, L., & Hou, Z. (2018). Transcriptional activation of anthocyanin biosynthesis in developing fruit of blueberries (*Vaccinium corymbosum* L.) by preharvest and postharvest UV irradiation. *Journal of Agricultural and Food Chemistry*, *66*(42), 10931–10942. https://doi.org/10.1021/acs.jafc.8b03081

Zhang, J., Zhang, Y., Song, S., Su, W., Hao, Y., & Liu, H. (2020). Supplementary red light results in the earlier ripening of tomato fruit depending on ethylene production. *Environmental and Experimental Botany*, *175*, 104044. https://doi.org/10.1016/j.envexpbot.2020.104044

Zhang, Y., Jiang, L., Li, Y., Chen, Q., Ye, Y., Zhang, Y., … Tang, H. (2018). Effect of red and blue light on anthocyanin accumulation and differential gene expression in strawberry (*Fragaria* × *ananassa*). *Molecules*, *23*(4), 820. https://doi.org/10.3390/molecules23040820

Zhao, J. (2015). Flavonoid transport mechanisms: How to go, and with whom. *Trends in Plant Science*, *20*(9), 576–585. https://doi.org/10.1016/j.tplants.2015.06.007

Zoratti, L., Karppinen, K., Luengo Escobar, A., Haggman, H., & Jaakola, L. (2014). Light-controlled flavonoid biosynthesis in fruits. *Frontiers in Plant Science*, *5*, 534. https://doi.org/10.3389/fpls.2014.00534

Zoratti, L., Klemettilä, H., & Jaakola, L. (2016). Bilberry (*Vaccinium myrtillus* L.) ecotypes. *Nutritional Composition of Fruit Cultivars*, (pp. 83–99). Waltham, MA: Academic Press, Elsevier. https://doi.org/10.1016/b978-0-12-408117-8.0000

Zoratti, L., Sarala, M., Carvalho, E., Karppinen, K., Martens, S., Giongo, L., … Jaakola, L. (2014). Monochromatic light increases anthocyanin content during fruit development in bilberry. *BMC Plant Biol*, *14*, 377. https://doi.org/10.1186/s12870-014-0377-1

Zorenc, Z., Veberic, R., Slatnar, A., Koron, D., Miosic, S., Chen, M. H., … Mikulic-Petkovsek, M. (2017). A wild 'albino' bilberry (*Vaccinium myrtillus* L.) from Slovenia shows three bottlenecks in the anthocyanin pathway and significant differences in the expression of several regulatory genes compared to the common blue berry type. *PLoS One*, *12*, e019024.

SUPPORTING INFORMATION

Additional supporting information may be found in the online version of the article at the publisher's website.

How to cite this article: Samkumar, A., Jones, D., Karppinen, K., Dare, A. P., Sipari, N., Espley, R. V., Martinussen, I., & Jaakola, L. (2021). Red and blue light treatments of ripening bilberry fruits reveal differences in signalling through abscisic acid-regulated anthocyanin biosynthesis. *Plant, Cell & Environment*, *44*(10), 3227–3245. https://doi.org/10.1111/pce.14158

Paper 2

Flavonoid biosynthesis is differentially altered in detached and naturally ripening attached bilberries in response to spectral light quality

Amos Samkumar[1*], Katja Karppinen[1], Tony K. McGhie[2], Richard V. Espley[3], Inger Martinussen[4], Laura Jaakola[1,4]

[1]Department of Arctic and Marine Biology, UiT The Arctic University of Norway, Tromsø, Norway

[2]The New Zealand Institute for Plant & Food Research Ltd., Palmerston North, New Zealand

[3]The New Zealand Institute for Plant & Food Research Ltd., Auckland, New Zealand

[4]Norwegian Institute of Bioeconomy Research, Ås, Norway

*Corresponding author. E-mail: amos.s.premkumar@uit.no

Abstract

Light spectral quality is known to affect flavonoid biosynthesis during fruit ripening. However, it is unknown how non-climacteric fruits, which ripen autonomously and independent of the parent plant, respond to different spectral light. In this study, we have analyzed the effect of light quality from LED lights on detached and naturally ripening non-climacteric wild bilberry fruits (*Vaccinium myrtillus* L.) accumulating high amounts of anthocyanins and flavonols. Our results indicate differential opposing responses towards red and blue light treatments on phenolic compound accumulation in detached and naturally ripening berries. For detached berries, blue light resulted in the highest accumulation of total anthocyanins (>4400 mg $100g^{-1}$ DW) compared with attached berries which had higher accumulation of anthocyanins under red light treatment (3500 mg $100g^{-1}$ DW). Overall, both red and blue light treatments increased the expression levels of all the major regulatory and biosynthetic genes of the flavonoid pathway, between four to seven days of continuous exposure to mid-ripening stage berries, in both detached and non-detached conditions. The expression levels of *VmMYBA1,* one of the key regulatory genes of anthocyanin biosynthesis, was found to be 5-fold higher in response to blue light in detached berries compared to other treatments. The blue light-mediated increase in anthocyanin concentration in detached berries was due to similar increases in delphinidin, cyanidin, petunidin and malvidin classes of compounds. In addition, the differential response of light treatment was found in accumulation of flavonols, especially with myricetin, syringetin and laricitin glycoside derivatives. The elevated concentration of anthocyanins detected in detached berries under supplemental light opens up new insights in understanding the light-mediated and plant-independent regulatory mechanisms in non-climacteric fruit ripening.

Keywords: anthocyanins, LED light quality, bilberry (*Vaccinium myrtillus* L.), flavonoids, polyphenols

Highlights

- Detached ripening when the fruits are picked before maturity is atypical in non-climacteric species and could heavily reduce fruit quality and phytochemical accumulation.
- Bilberry fruits, a non-climacteric species accumulated the highest anthocyanin levels under blue-light and in detached conditions when picked at green, unripe stage.
- In contrast, red-light promoted flavonoid compounds accumulation including anthocyanins and flavonols in naturally ripening attached berries.
- Flavonoid biosynthesis is differentially regulated through the key photomorphogenesis regulator *COP1* and regulatory factors such as *MYBA1* and *HY5*.

1. Introduction

Fruit ripening is a complex process associated with determining various quality attributes, such as firmness, color, flavor and aroma development. Anthocyanins are a class of phenolic compounds that accumulate in high levels as pigments during ripening, providing distinct red or blue coloration to some fruits (Oh et al., 2018; Zifkin et al., 2012). Although anthocyanins majorly contribute to the phenolic composition, flavonols represent >30% in edible berries, in which quercetin and myricetin glycosides were the dominant compounds among flavonols (Wang et al., 2014; Häkkinen et al.,1999). These compounds are synthesized via the flavonoid pathway branching from the well characterized phenylpropanoid biosynthetic pathway and through a series of enzymatic reactions. This leads to the production of different anthocyanidin classes such as delphinidins, cyanidins, malvidins, petunidins and peonidins as end products of this metabolic pathway (Petroni et al., 2011). The key early enzymes involved in flavonoid biosynthesis are chalcone synthase (*CHS*) and flavonoid hydroxylases, *F3'H* and *F3'5'H*, that cleave the pathway into cyanidin and delphinidin branch, respectively. Flavonols, such as quercetin and myricetin derivatives, are synthesized from diverging enzymatic reaction from dihydroflavonols by flavonol synthase (*FLS*). The late anthocyanin biosynthetic enzymes, such as dihydroflavonol 4-reductase (*DFR*) and anthocyanidin synthase (*ANS*), are involved in production of cyanidins and delphinidins. UDP-glucose flavonoid 3-O-glucosyltrasnferase (*UFGT*) performs the last glycosylation steps to the 3-hydroxyl group of anthocyanidins (Zhai et al., 2014). Anthocyanin biosynthesis is also regulated by the *R2R3-MYB* transcription factors which have been shown to directly interact with promoters of key flavonoid biosynthetic genes such as *DFR*, *ANS* and *UFGT* (Plunkett et al., 2018; Die et al., 2020). *MYBA1* and *MYBPA1.1* were recently reported in *Vaccinium* berries and it has been shown that they actively promote anthocyanin biosynthesis in skin and flesh during ripening (Karppinen et al. 2021).

Light is known to be one of the major environmental factors controlling fruit ripening (Abeysinghe et al., 2019). Certain wavelengths from the photosynthetically active radiation range (PAR spectrum) are known to positively influence and alter plant secondary metabolism (Ouzounis et al., 2015). Light qualities and intensities can affect flavonoid biosynthesis and anthocyanin accumulation as reported in many plant species (Liu et al., 2018; Ma et al., 2019). The spectral wavelengths from the solar radiation are perceived by specific plant photoreceptors that interact upon constitutive photomorphogenic 1 (*COP1*) gene, which is one of the key photomorphogenesis controllers (Wu et al., 2019). It interacts with light-inducible genes such as *SPA1* (suppressor of phytochrome-A) and forms a complex, leading to a tightly regulated signal cascade mechanism resulting in changes in expression of both regulatory and structural genes of the flavonoid biosynthetic pathway (Miao et al., 2016). The *COP1* repressor specifically acts in degradation of positive regulators of anthocyanin biosynthesis, such as elongated

hypocotyl 5 (*HY5*) and *R2R3-MYB* transcription factors under altering light and dark conditions (Ma et al., 2021).

Supplemental light emitting diodes (LEDs) are widely used in pre- and postharvest fruits to improve the composition ofbioactive compounds (Kokalj et al., 2019; Panjai et al., 2019). Such high intensity light treatments can result in dramatic variation in accumulation of specific flavonoid end products such as flavonols, proanthocyanidins and anthocyanins. These low-heat dissipating lights can be also used to study the effect of single-wavelength spectral light qualities on plant primary and secondary metabolism. For example, blue and red light at different ratios has been shown to improve the biomass, photosynthesis and anthocyanin production in a medicinal plant (Silva et al., 2020). These two major light wavelengths have been widely shown in many fruit and vegetable crops for improved secondary metabolites production (Bian et al., 2014). The enhanced bioactive compounds biosynthesis is often associated with plant's own photoprotection mechanisms, developed against variable high light environments (Tran et al., 2021).

Non-climacteric fruits lack the independent ripening mechanisms when picked early before maturation, because, unlike climacteric species, they lack autocatalytic ethylene biosynthesis. Ripening in non-climacteric fruit is often associated with increases in another plant hormone, abscisic acid (ABA), where the levels tend to increase at the beginning of fruit maturation. However, the role of ABA has been equally documented in both climacteric and non-climacteric fruit ripening (Jia et al., 2011; Pilati et al., 2017). Determining the nature of fruit ripening based on hormonal release at onset is often misleading and varies across species as documented in a study on strawberry, where certain attributes mimicked climacteric fruit characteristics *in planta* (Iannetta et al., 2006). Thus, even if non-climacteric fruits were able to ripen independently of the mother plant or picked before maturation, it is important to investigate if the fruit quality or metabolic profile is affected. For example, the capability of strawberries to ripen when picked at the green stage was reported earlier but they were heavily devoid of fruit qualities such as aroma, mass and bioactive compounds (Van de Poel et al., 2012). Hence, the lack of photosynthesis (Das et al., 2011) and source-sink modulation from other tissues such as leaves are vital in determining the fruit quality of detached berries as shown in grapevine, where the leaf area and fruit composition are positively correlated (Kliewer & Dokoozlian, 2005).

Among the edible wild berries, bilberry (*Vaccinium myrtillus* L.), which is native to Northern Eurasian boreal regions, is gaining worldwide attention for its rich bioactive and nutritional properties (Pires et al., 2020). It is widely regarded as one of the richest sources of polyphenolic compounds, especially anthocyanins and other related flavonoids, which accumulate in both skin and flesh during ripening (Colak et al., 2018). In relation to bioactivity, the berry polyphenolic compounds are known to possess cardio-protective properties, anti-carcinogenic, anti-inflammatory and antioxidant activities (Korus et al., 2015; Seeram et al., 2008).

In our recent study, we have shown that supplemental light can regulate anthocyanin biosynthesis in naturally ripening bilberry, and especially red light promoted anthocyanin accumulation, mediated through ABA signaling and metabolism (Samkumar et al., 2021). But to our knowledge, studies on biosynthesis of flavonoids comparing natural and atypical ripening of detached, non-climacteric fruit in response to different light quality treatments has not been fully characterized and reported before. Therefore, the current study is aimed at understanding the biosynthesis of flavonoids, specifically anthocyanins and flavonols, in detached berries. These are picked at the green stage and allowed to ripen for comparison with berries ripening naturally on the plant and under supplemental light conditions. The outcome of this work will benefit the understanding of differential light responses in fruit ripening that could lead to better adaptation strategies in determining berry fruit quality and marketability.

2. Materials and methods

2.1 Plant material and light treatments

Wild bilberry (*Vaccinium myrtillus* L.) bushes with intact root systems and forest soil were collected in large boxes (50 x 70 cm) during mid-summer (July month) when the green berries started to appear from the flowers. The bilberry ecotype used throughout this experimental study were collected from the open vegetation covers near Tromsø, Norway (69° 75′N, 19° 01′E). The bilberry bushes were kept in phytotron conditions at 16°C for few days to acclimatize until they started to increase in size. For the experiments with detached berries, unripe green berries were picked from the same stand and kept in sterile distilled water until they were divided into samples for the light treatments. The berries were rinsed a few times with sterile water and 50 berries were placed into each petri dish with 20 ml of sterile water and closed with parafilm. The petri dishes were placed under the lamps in triplicates for each treatment.

The bushes in boxes and detached berries in petri plates were placed inside the chambers covered by photo reflective sheet with ambient natural light provided from the top. The temperature was maintained at 16°C inside the chamber. Heliospectra RX30 lamps (Heliopsectra AB., Gothenburg, Sweden) to irradiate blue (460 nm), red (660 nm) and far-red (735 nm) light wavelengths were inside the chambers. The plants and petri plates kept under the shaded dark chambers only received ambient light from the top, serving as a dark control. The plants and petri plates kept under normal greenhouse conditions with ample ambient light (400-700 nm) served as positive control (white) for this experimental setup. The photon fluence rate inside the chambers ranged from 8.0-10.0 μmol m^{-2} s^{-1}. The irradiation energy flux (μW cm^{-2}) and the distance from light source to plants from all the light treatments were measured using JAZ Spectrometer (Ocean Optics Inc., FL, USA). These parameters were used to calculate the relative light intensity (Fig S1). The changes in berry skin coloration were assessed and scored visually in

detached berries after 2, 5, 7 and 12 days from the beginning of light treatments. For RNA isolation, berry samples (5-6 berries) were collected on 0, 2, 4, 7 and 11 days. Leaves and ripening berry samples from the bushes were also collected at the same time-points. For metabolite screening, fully ripe berries (blue colored berries) were collected approximately after 4 weeks of light treatment from the bilberry bushes and until all the berries fully ripened in petri plates (12-14 days). A minimum of 20 berries per replicate were collected from detached berries experimental setup and bushes after 14 days for spectrophotometric analysis and FRAP antioxidant assays. All the berry and leaf samples were immediately frozen in liquid nitrogen and stored at -80°C until used for further analyses.

2.2 RNA extraction and cDNA synthesis

The frozen berries and leaves were ground to a fine powder under liquid nitrogen using mortar and pestle. Total RNA was isolated from approximately 120 mg tissue powder by using Spectrum Plant Total RNA kit (Sigma-Aldrich, St. Louis, MO, USA) following the manufacturer's instructions. The residual DNA was eliminated with on-column digestion using DNase I (Sigma-Aldrich). The RNA was qualified and quantified using a Nanodrop (Thermo Fischer Scientific, Waltham, MA, USA). First-strand cDNA was synthesized using Invitrogen Superscript IV reverse transcriptase (Thermo Fisher Scientific) using 1µg of total RNA according to manufacturer's instructions.

2.3 qRT-PCR analysis

Real-time quantitative reverse transcription PCR (qRT-PCR) analysis was performed in MJ MiniOpticon Real-time PCR system (Bio-Rad laboratories, Hercules, CA, USA) using SSOFast EvaGreen SYBR supermix (Bio-Rad) in 15 µl volume per reaction. The PCR conditions were 95°C for 30 sec (initial denaturation) followed by 40 cycles at 95°C for 5 sec, and 60°C for 10 sec. The program was further followed by a melt-curve analysis ranging from 65°C to 95°C with an increment of 0.5°C every cycle. All analyses were performed in three biological replicates and two technical replicates. The results were analyzed using CFX connect software (Bio-Rad) using $2^{(-\Delta\Delta Ct)}$ method. The relative expression levels were normalized with either *GAPDH* (glyceraldehyde-3-phosphate dehydrogenase) or *Actin*. Primer sequences for all genes used in this study are listed in Table S1.

2.4 Analysis of total polyphenols, total anthocyanins and total flavonoids

Berry samples collected after two weeks and at the end of light treatment from the bushes and petri plates were ground to a fine powder under liquid nitrogen and freeze dried in lyophilizer (Virtis benchtop-K, SP scientific, Gardiner, NY, USA). Approximately 100 mg of lyophilized berry powder was subsequently extracted in 1ml of 100% methanol+0.1% HCl (v/v) under constant shaking for 1 hour. The samples were centrifuged at maximum speed and the supernatant with suitable dilution used for analyses.

Total soluble polyphenols were spectrophotometrically determined according to Doumett et al., (2011) using Folin-Ciocalteau phenol reagent. The absorbance was measured at 740 nm and polyphenol concentrations were calculated based on a catechin calibration standard curve. The results were expressed as milligrams of catechin equivalent 100 g^{-1} dry weight (DW) of berries.

The aluminum chloride based spectrophotometric method was used for the determination of the total flavonoid content according to Chang et al. (2002). Quercetin was used for the standard calibration curve. The absorbance of the reaction mixtures was measured against blank at 420 nm. The total flavonoid content in the samples was calculated from the calibration curve and expressed as mg quercetin equivalent $100g^{-1}$ of dry weight (DW) of plant material.

Total monomeric anthocyanins were quantified using the pH differential method (Lee et al., 2005). The absorptions in reaction mixtures from the changes in pH of two buffer systems were measured at 520 nm and 700 nm. The anthocyanins were calculated based on the differential equation mentioned in Lee et al. (2005). The relative amounts were expressed as cyanidin 3-glucoside equivalents in mg $100g^{-1}$ of dry weight (DW). All the above analyses are performed with three independent biological replicates of samples from detached berries and berries attached to bush.

2.5 LC-MS analysis of polyphenols

For liquid chromatography-mass spectroscopy (LC-MS) analysis, 100 mg of lyophilized tissue powder per sample was used followed by extractions with 1ml of acidified methanol prepared as mentioned above and the collected supernatants were dried by vacuum spin to remove excess methanol. The extracts were resuspended in 500 µl of 20% methanol and filter sterilized using 0.45µm syringe filter (Phenomenex, Torrance, CA, USA). The samples were diluted to 1:10 before injecting into the chromatography column.

Polyphenols were separated using a Luna Omega C18 (100 × 2.1 mm, 1.6 µm) column maintained at 40°C. The mobile phase: A = 0.2% formic acid and B = 100% acetonitrile at a flow rate of 400 µL min^{-1}. The solvent gradient was: initial composition 95% A, 0-0.5 min; linear gradient to 60% A, 0.5–7 min; linear gradient to 5% A, 7-12 min; composition held at 5% A, 12-16 min; linear gradient to 95% A, 16–16.2 min. The injection volume for samples and standards was 1 µL. The micrOTOF QII parameters were: temperature 225°C; drying N_2 flow 6 L min^{-1}; nebulizer N_2 1.5 bar, endplate offset 500 V, mass range 100–1500 Da, data were acquired at 5 scans s^{-1}. Negative ion electrospray was used with a capillary voltage of 3500 V. Polyphenolic concentrations were calculated by comparison to external calibration curves of authentic compounds.

2.6 LC-MS analysis of anthocyanins

Anthocyanins were separated using a Luna Omega Polar C18 (100 × 2.1 mm, 1.6 µm) column maintained at 50°C. The mobile phase was composed of solvents: A = 5% formic acid in water and B = 100% acetonitrile at a flow rate of 300 µL min^{-1}. The solvent gradient was: initial composition 95% A, 0–0.5 min; linear gradient to 85% A, 0.5–10 min; linear gradient to 60% A, 10–20 min; linear gradient to 5% A, 20–25 min; composition held at 95% A, 25–28 min; linear gradient to 95% A, 28–28.2 min; to return to the initial conditions. The injection volume and the micrOTOF QII parameters were as above. Positive ion electrospray was used with a capillary voltage of 3000 V. All the anthocyanins were quantified as cyanidin 3-O-glucoside (Extrasynthese, Genay, France) equivalents 100 mg^{-1} of sample DW.

2.7 FRAP antioxidant activity assay

Ferric reducing antioxidant power (FRAP) assay was used to measure the antioxidant potential according to Benzie & Strain (1996). FRAP reagent was prepared with 10 volumes of 300 mM acetate buffer (pH = 3.6), 1 volume of 10 mM 2,4,6-tripyridyl-s-triazine in 40 mM HCl and 1 volume of 20 mM $FeCl_3$. Aliquots of 100 µL of test samples along with 300 µL of distilled water were added to 3 mL of FRAP reagent pre-warmed at 37°C. After two hours of incubation in the dark, absorbance was read at 593 nm. The results were calibrated from the standard curve prepared from different amounts of $FeCl_3$ (100-500 µg) with FRAP reagent and expressed as mmol Fe (II) $100g^{-1}$ of DW berries.

2.8 Statistical analysis

Statistically significant differences among gene expression levels obtained from qRT-PCR analysis between the control and light treatments were determined using independent t-test in IBM SPSS statistics v26 software package (IBM corporation, Armonk, NY, USA). Concentrations of anthocyanins and polyphenols between the light treatments and experimental setups were analyzed by ANOVA, comparison of means followed by Tukey's post-hoc test. All the visualizations and ANOVA were performed in Origin pro software v2020b (OriginLab Corporation, Northampton, MA, USA).

3. Results and Discussion

There are several earlier studies which have shown that specific spectral light wavelengths can stimulate the biosynthesis of flavonoids during ripening of fruits, including few species from the *Vaccinium* genus (Ma et al., 2019; Zhang et al., 2018; Zhou et al., 2002; Samkumar et al. 2021). So far, there have not been any comprehensive studies investigating the effect of spectral light qualities in ripening non-climacteric berries from both living plants and in detached conditions. Postharvest ripening, when the

fruit is picked before maturity, is unusual in non-climacteric species where many studies have previously reported that the fruit quality had deteriorated over time (Llorca et al., 2019; Van de Poel et al., 2012). Therefore, this study is one of the first to report the changes in the metabolite profiles and gene expression related to flavonoid biosynthesis from postharvest unripe green berries compared with berries ripening naturally under different spectral light qualities. Our results revealed dramatic differential changes in the composition of flavonoid compounds between the detached and naturally ripening bilberries (attached) under different light treatments.

3.1 Berry skin coloration in detached berries under light treatments

Under supplemental light irradiation and when compared with control, a rapid change in skin coloration of detached berries was observed, where all the berries appeared to be fully ripened after two weeks in petri plates. It has been shown in strawberries that detachment could accelerate stress related ripening process including rapid coloration (Chen et al., 2014). Red light had the highest effect of anthocyanin accumulation in berry skins that turned from green to blue-colored berries, as visually observed, between two and five days (Fig 1a, b). The clear difference in visual scoring of berry skin coloration (green to blue) can be seen after seven days of light treatment (Fig 1c). From our metabolite analyses, the anthocyanin content was found to be the highest under blue light in fully ripe detached berries after 14 days, but rapid blue coloration in berry skin was observed under red light (Fig 1). It suggests that the anthocyanin profile could differ in skin and flesh tissues even under altering light conditions as shown earlier in grape (Guan et al., 2016).

3.2 Effect of light treatment on total polyphenolic compounds

We estimated total polyphenols (TPH), total flavonoids (TF), total monomeric anthocyanins (TMA) and determination of antioxidant potential using FRAP assay (Figure 2). The highest TMA was quantified at 4615 and 4737 (mg $100g^{-1}$ DW cyanidin-3 glucoside equivalent) in ripe berries from bush and detached berries respectively. This significant increase is mainly due to red light in attached berries and blue light in detached berries when compared to control. A previous study in cranberry (*Vaccinium macrocarpon*) has shown that red light could selectively induce anthocyanin biosynthesis (Zhou et al., 2002). From our results, we have shown that the total monomeric anthocyanins, total polyphenols and total flavonoids were increased mainly by red light in attached berries that were ripening naturally on the bush (Fig 2a-d).

On the other hand, in bilberry, blue light was also promoting flavonoid biosynthesis to a certain extent in attached conditions but to the highest level in detached ripening berries (Fig 2a-d). Blue light has been previously reported in several studies as a positive influencer of anthocyanin biosynthesis in many

crops. For instance, blue irradiation promoted the bioactive compounds during pre-harvest conditions in kale and increased the anthocyanin content in postharvest strawberry fruit (Jiang et al., 2021; Xu et al., 2014). TF was found to be at almost similar levels at 8434 and 8905 (mg $100g^{-1}$ DW quercetin equivalent) between both the highly impacted light treated samples (red and blue light). Similarly, TPH was estimated at 9608 and 8838 (mg $100g^{-1}$ DW catechin equivalent) respectively. Both red and blue light treatment tend to significantly increase the phenolic compounds in general, but the trend is closely followed by far-red treatment in detached berries which yielded more flavonoids than control samples.

The polyphenolic compounds, which include flavonols and anthocyanins, contribute to the overall antioxidant capacity of these small berries (Zorzi et al., 2020). The relatively high concentration of phenolic compounds observed in red light (attached) and blue light (detached) treatments contributed to the overall antioxidant potential of the berries as estimated using FRAP assay (Fig 2d). However, this is not the same case, where the increased phenolic content under far-red light treated berries have lower antioxidant activity than control samples. Thus, we highlight the importance of environmental factors, such as external light irradiation, that could potentially determine the phenolic profile of the berry towards higher antioxidant potential. Also, the biochemical regulatory networks and signals from other source tissues could be altered in detached conditions when compared with non-detached fruits. Some of the major differences could be due to the limitation of photosynthesis, carbon-sugar homeostasis, lack of substrates flow from other tissues such as leaves (source-sink modulation) in detached berries when compared with attached berries from plants ripening under natural conditions (Yang et al., 2018).

3.3 Differential effect of light quality on anthocyanin accumulation in detached and attached berries

Anthocyanins were the prominent compounds affected by light quality treatments, mostly influenced by red light in naturally ripening bilberries and by blue light in detached berries (Fig 3, Table S2). Delphinidins were the most affected and reactive towards spectral light treatment, as similarly reported in a previous study (Zoratti et al., 2014). The delphinidin glycosides (glucoside, galactoside and arabinoside) were the most differentially accumulating anthocyanin compounds in response to light qualities as quantified by LC-MS (Table S2). The highest concentration of delphinidins was found in attached berries (1529 mg $100g^{-1}$ DW) and under the positive influence of red light followed by blue light treatment in detached berries (1290 mg $100g^{-1}$ DW) (Fig 3a, d). In both cases, delphinidins contributed as the major constituent towards the increase in total anthocyanins. Cyanidin, on the other hand, was not majorly influenced by supplemental light treatments in either of the ripening conditions. Interestingly, we found that in detached berries, blue light increased the total anthocyanins, even higher than in bilberries attached to the bush (Fig 3c, S2). This is interesting concerning the nature of non-climacteric fruit ripening, considering that detached berries lack hormonal signaling from leaf tissues

and have limited substrate flow. Also, the increase in overall anthocyanin composition in detached berries was evenly distributed among all the anthocyanin classes except peonidins (Fig 3d). The highest elevated total anthocyanin level detected in detached berries under the influence of blue light (4440 mg $100g^{-1}$ DW), was majorly contributed by delphinidins alongside an even distribution of cyanidins, malvidins and petunidins (Fig 3c). Interestingly, under the influence of red light in naturally ripening attached berries, the elevated total anthocyanin content (3500 mg $100g^{-1}$ DW) was mostly contributed by the delphinidin class of anthocyanins alone (43.4%) (Fig 3d). Both red and blue light treatments have earlier been shown to increase anthocyanin content in fruit and leaf tissues under controlled conditions (Lobiuc et al., 2017; Zhang et al., 2018). The most interesting finding in our study was how both the light qualities were perceived and differentially regulated regarding anthocyanin biosynthesis in detached and non-detached berries. An earlier similar study also showed that how UV A/B/C light could differentially regulate the anthocyanin accumulation by affecting the downstream biosynthetic genes such as *DFR* and *UFGT* in pre- and postharvest blueberries (*Vaccinium corymbosum*) (Yang et al., 2018).

3.4 Differential effect of light quality on accumulation of flavonols in detached and attached berries

Flavonols, on the other hand, were highly influenced by red light treatment in both naturally ripening berries as well as detached berries (Fig 4, Table S3). It was closely followed by far-red light, which is found to be much more effective in increasing flavonol compounds than other light treatments. LC-MS analysis showed that myricetin 3-glucoside and its derivate laricitin 3-glucuronide compounds were significantly increased in attached berries under red light treatment compared to control and other light treatments (Fig 4 a, b). Both blue and far-red light treatment also had a positive influence on these classes of compounds (Table S3). This is in accordance with a study which shows that quercetin compounds can be influenced directly by continuous far-red light and can be differentially regulated from anthocyanin content through phytochrome-induced biosynthesis (Beggs et al., 1987). Quercetin 3-arabinopyranoside did not show any significant increase under the influence of light treatments (Fig 4c). Syringetin 3-glucuronide was found to be significantly increased in detached berries by blue light followed by far-red light treatment (Fig 4d). Interestingly, gallocatechin, which was detected in very low levels in control and other treatments, increased almost 4-fold under red light treatment in attached berries (Fig 4e). The procyanidin dimers (B1, B2, C1) were not found to be significantly affected by the light treatments (Fig 4f, Table S3), but procyanidin C1, B2 was increased in attached berries under the influence of far-red light. Overall, the total flavonols concentration was found to be higher in red light treatment for berries ripening in bush (240 mg $100g^{-1}$ DW) compared with other light treatments (Table S3). In detached berries, red light (254 mg $100g^{-1}$ DW), followed by far-red light (246 mg $100g^{-1}$ DW),

increased the total flavonol concentration. The effect of far-red was also seen on caffoyl-4-glucoside concentration on both detached and attached berries (Table S2). Nandinaside-A ($C_{22}H_{22}O_{10}$) was detected in increased levels only in dark shaded control samples (Table S2). Leucocyanidin had a very similar trend in concentration levels to the observed total anthocyanin amounts with red light influencing in attached and blue light in detached berries (Table S2). Epicatechin and trans-p-coumaric acid were found in increased levels in our analysis under far-red light, whereas catechin concentrations were elevated by red light in naturally ripening berries (Table S3). A previous study in bilberry which quantified the total flavonol concentrations corresponding to the effect of monochromatic red, far-red light in ripe bilberries and was found in accordance with our metabolite analysis (Zoratti et al., 2014).

3.5 Expression profile of flavonoid biosynthesis genes

The relative expression of key flavonoid biosynthetic genes from berries of both attached and detached experimental setups was analyzed over the time course (from day zero to day 11) (Fig 5a, b). Red light increased the key early biosynthetic gene *VmCHS* expression on day 4 in detached berries and 7th day in attached berries under blue light, respectively. *VmDFR* expression was shown to steadily increase with the highest level observed under blue light treatment in both setups on the 7th day of the treatment. Interestingly, far-red light also tends to increase the *DFR* expression levels after seven days in detached berries (Fig 5 a, b). Expression of the cyanidin and delphinidin branchpoint enzyme genes, the flavonoid hydroxylases (*VmF3'H, VmF3'5'H*), was found at significantly higher level in attached berries from the bush under red light at 4th day, whereas the blue light appeared to increase the expression of these genes at later time points. In detached berries, red light was found to influence the *VmF3'H* expression only after 7 days whereas both red and blue light treatments significantly increased expression of *VmF3'5'H* after 7 days (Fig 5 a, b). In naturally ripening berries, flavonols and anthocyanin concentrations could be correlated with *VmF3'H, VmDFR* and *VmF3'5'H* expression, where red light increased the expression levels of these genes after four days of light treatment (Fig 5a). Whereas in detached berries, *VmF3'5'H* and *VmDFR* expression, which steadily increased after seven days under blue light, could be directly linked to increased anthocyanin accumulation. The positive influence of red light on *VmF3'H* and *VmDFR* gene expression levels could also be related to the accumulation of flavonols in detached berries (Fig 5b).

The expression of the late biosynthetic genes such as *VmANS* was found to show similar trends (Fig 6 a, b) in both experimental setups. *VmUFGT* transcript levels, on the other hand, increased under red light in berries attached to bushes after four days and under blue light in detached berries after seven days of irradiation. Interestingly, one of the key anthocyanin regulatory transcription factors, *VmMYBA1*, was found to be five-fold higher in detached berries under blue light (Fig 6 a, b). Under red

light, both *VmMYBA1* and *VmMYBPA1.1* had the highest expression levels after 4 days of treatment in attached berries (Fig 6a, b). A similar expression pattern was found in late biosynthetic genes, such as *VmANS* and *VmUFGT* expression in naturally ripening berries, which coincides with the anthocyanin accumulation under the red light with an increase in expression between four to seven days of light treatment (Fig 6a). In detached berries, *VmUFGT* was found to increase under blue light between seven to nine days, coinciding with the accumulation of anthocyanins (Fig 6b). It suggests that certain key biosynthetic genes perform the light-dependent regulation in both experimental setups in a totally different manner. The regulatory gene *VmMYBA1* expression was found to be the key component for highly elevated anthocyanin levels in detached berries under blue light (Fig 6b). This also indicates that it might be the key factor driving the blue light-mediated anthocyanin accumulation in detached, independently ripening berries by specifically interacting with the late biosynthetic genes. *MYBA1* has been earlier reported as one of the key regulators of anthocyanin biosynthesis in *Vaccinium* berries, activating the promoters of *DFR* and *UFGT* (Die et al., 2020; Plunkett et al., 2018). Whereas both *VmMYBA1* and *VmMYBPA1.1* showed very similar expression patterns in naturally ripening berries under the influence of red light, suggesting that both of these *MYB* transcription factors might co-regulate anthocyanin biosynthesis (Fig 6a, b). It has been recently reported that these two *MYBs* are the key regulators of anthocyanin biosynthesis during bilberry ripening (Karppinen et al., 2021).

We did not observe significant differences in expression levels of most of the flavonoid biosynthesis related genes in bilberry leaves between control and light treatments. Apparently, only *VmCHS* expression increased under red light treatment in leaves. It appeared to have a synergetic effect to that of expression in berries, with the highest level reached under blue light after 2 days, and red light increased the expression rapidly from 4th day onwards (Fig S2a). One of the major key regulatory gene in anthocyanin biosynthesis, *VmMYBPA1.1* also showed significantly higher expression levels early in response to blue light treatment (Fig S2b), but steadily increased towards higher levels after 7 days, under both red and blue light. The leaves are mostly regarded as waste by-product in fruit crops, but in some species such as blueberry, the polyphenolic constituents in leaves were often found to be higher than fruits (Li et al., 2012; Zhu et al., 2013). In terms of molecular regulation, the most important role of leaves in attached berry ripening conditions could be modulating the source-sink balance which could potentially affect the berry coloration and anthocyanin composition (Bobeica et al., 2015).

3.6 Expression profile of photomorphogenesis-related genes

The effect of spectral light qualities on the *VmCOP1*-related regulatory mechanisms was not vastly influenced in detached berries, including *VmHY5* expression. Bilberry has two characterized *COP1* genes (*VmCOP1a, VmCOP1b)* (Karppinen et al., unpublished), where both the genes, alongside *VmHY5*, had little effect in response to any light treatments in detached conditions (Fig 7 a, b). In contrary, in naturally ripening berries, photomorphogenesis seems to have occurred and mediated via

VmCOP1b, the repressor of anthocyanin biosynthesis. Generally, in high light conditions, *COP1* is exported to the cytosol which allows positive regulators, such as *HY5*, to accumulate in the nucleus, as its expression levels tend to increase after 7 days under red light treatment from our results (Fig 7b). In attached ripening berries under red light, the expression of both *VmHY5* and *VmCOP1b* increased after 7 days, whereas *VmCOP1a* expression was significantly increased under far-red light treatment after 2 days (Fig 7a, b). The key interaction between *COP* and *HY5* genes has been shown to determine the inhibitory effects and hyperaccumulation of anthocyanins under low and high light (Maier et al., 2014). Hence, detached berries ripening independently, and berries attached to the plant might have contrasted regulatory mechanisms and signaling routes to protect the tissues from high monochromatic light environments. The former showing a very strong systemic response by producing high levels of photoprotective anthocyanin compounds which also reflected in its overall antioxidant capacity.

In climacteric fruits such as banana, apple and mango, ripening is usually mediated by an ethylene burst causing changes in respiration rates, which allows ripening even when detached from the plant (Adams-Phillips et al., 2004; Symons et al., 2012). In contrary, non-climacteric fruits such as wine grapes and many other berries lack the autocatalytic ethylene biosynthesis in immature fruits, which prevents ripening on its own when picked and possible only with the involvement of plant signals or via exogenous hormonal regulation such as ABA (Cherian et al., 2014; Luo et al., 2014). The possibility of similar mechanisms found in climacteric fruits could exist, as documented by some of the studies that have shown the involvement of increased ethylene production before e véraison in grape (Chervin et al., 2004), and the autocatalytic ethylene biosynthesis-like response observed in young citrus fruits (Katz et al., 2004). However, knowledge concerning independent ripening in non-climacteric fruits is still scarce and widely varies across species. Further studies that compare fruit ripening with or without connection to mother plant will bridge the gap in understanding the independent ripening mechanisms and subsequent accumulation of the phytochemicals.

Conclusion

This study has shown that higher accumulation of anthocyanins and flavonols were achieved upon certain simulated light conditions even in green, detached non-climacteric species such as bilberry. Our results clearly show that flavonoid biosynthesis during ripening was positively influenced and differentially regulated in controlled experimental conditions. Blue light induced the highest anthocyanin accumulation in detached berries and red light stimulated anthocyanin biosynthesis in naturally ripening attached berries. The overall anthocyanin content was found to be highest and significantly elevated in blue-light treated detached berries with an even distribution of all the major anthocyanin classes of compounds. The current study has shown that *Vaccinium* berries could be used in further investigation of molecular mechanisms and hormonal regulation of independently ripening

non-climacteric fruits. Treatments with both supplemental blue and red light might be also considered in future cultivation practices for improved anthocyanin content in blue-colored berries.

Acknowledgments

The authors would like to thank Leidulf Lund for the technical help in setting up light experiments at the Phytotron facility at UiT The Arctic University of Norway. We are grateful for the UiT-BFE faculty's mobility grant to AS allowing the visit to Plant and Food Research, New Zealand. The research mobility was supported by the New Zealand Ministry for Business, Innovation, and Employment (MBIE) Endeavour programme 'Filling the Void: boosting the nutritional content of NZ fruit' (contract no. C11X1704). The work was also financially supported by NordPlant (NordForsk grant no. 84597).

Author contributions

LJ and KK conceptualized the project. AS performed the experiments, analyzed the data, and wrote the manuscript. TKM performed the anthocyanin and polyphenolic profiling with LC-MS. LJ, KK, IM and RVE contributed in the editing and proofreading of the manuscript draft. All authors have read and approved the manuscript.

Conflict of interest

The authors declare that they have no conflicts and competing interests.

References

Abeysinghe, S. K., Greer, D. H., & Rogiers, S. Y. (2019). The effect of light intensity and temperature on berry growth and sugar accumulation in *Vitis vinifera* "Shiraz" under vineyard conditions. *Vitis*, *58*(1), 7–16. https://doi.org/10.5073/vitis.2019.58.7-16

Adams-Phillips, L., Barry, C., & Giovannoni, J. (2004). Signal transduction systems regulating fruit ripening. *Trends in Plant Science*, *9*(7), 331–338. https://doi.org/10.1016/j.tplants.2004.05.004

Beggs, C. J., Kuhn, K., Böcker, R., & Wellmann, E. (1987). Phytochrome-induced flavonoid biosynthesis in mustard (*Sinapis alba* L.) cotyledons. Enzymic control and differential regulation of anthocyanin and quercetin formation. *Planta*, *172*(1), 121–126. https://doi.org/10.1007/BF00403037

Ben Ahmed, Z., Yousfi, M., Viaene, J., Dejaegher, B., Demeyer, K., Mangelings, D., & Heyden, Y. Vander. (2016). Determination of optimal extraction conditions for phenolic compounds from: *Pistacia*

atlantica leaves using the response surface methodology. *Analytical Methods*, *8*(31), 6107–6114. https://doi.org/10.1039/c6ay01739h

Bian, Z. H., Yang, Q. C., & Liu, W. K. (2015). Effects of light quality on the accumulation of phytochemicals in vegetables produced in controlled environments: A review. *Journal of the science of food and agriculture*, 95(5), 869–877. https://doi.org/10.1002/jsfa.6789

Bobeica, N., Poni, S., Hilbert, G., Renaud, C., Gomès, E., Delrot, S., & Dai, Z. (2015). Differential responses of sugar, organic acids and anthocyanins to source-sink modulation in Cabernet Sauvignon and Sangiovese grapevines. *Frontiers in plant science*, 6(May), 14. https://doi.org/10.3389/fpls.2015.00382

Chang, C. C., Yang, M. H., Wen, H. M., & Chern, J. C. (2002). Estimation of total flavonoid content in propolis by two complementary colometric methods. *Journal of Food and Drug Analysis*, *10*(3), 178–182. https://doi.org/10.38212/2224-6614.2748

Chen, J., Mao, L., Mi, H., Zhao, Y., Ying, T., & Luo, Z. (2014). Detachment-accelerated ripening and senescence of strawberry (*Fragaria* × *ananassa* Duch. cv. Akihime) fruit and the regulation role of multiple phytohormones. *Acta Physiologiae Plantarum*, 36(9), 2441–2451. https://doi.org/10.1007/s11738-014-1617-6

Cherian, S., Figueroa, C. R., & Nair, H. (2014). "Movers and shakers" in the regulation of fruit ripening: A cross-dissection of climacteric versus non-climacteric fruit. *Journal of Experimental Botany*, *65*(17), 4705–4722. https://doi.org/10.1093/jxb/eru280

Chervin, C., El-Kereamy, A., Roustan, J. P., Latché, A., Lamon, J., & Bouzayen, M. (2004). Ethylene seems required for the berry development and ripening in grape, a non-climacteric fruit. *Plant Science*, *167*(6), 1301–1305. https://doi.org/10.1016/j.plantsci.2004.06.026

Colak, A. M., Kupe, M., Bozhuyuk, M. R., Ercisli, S., & Gundogdu, M. (2018). Identification of some Fruit Characteristics in Wild Bilberry (*Vaccinium myrtillus* L.) Accessions from Eastern Anatolia. *Gesunde Pflanzen*, *70*(1), 31–38. https://doi.org/10.1007/s10343-017-0410-z

Das, P. K., Geul, B., Choi, S. B., Yoo, S. D., & Park, Y. Il. (2011). Photosynthesis-dependent anthocyanin pigmentation in Arabidopsis. *Plant Signaling and Behavior*, 6(1). https://doi.org/10.4161/psb.6.1.14082

Die, J. V., Jones, R. W., Ogden, E. L., Ehlenfeldt, M. K., & Rowland, L. J. (2020). Characterization and analysis of anthocyanin- related genes in wild-type blueberry and the pink-fruited mutant cultivar

"pink lemonade": new insights into anthocyanin biosynthesis. *Agronomy*, *10*(9). https://doi.org/10.3390/agronomy10091296

Doumett, S., Fibbi, D., Cincinelli, A., Giordani, E., Nin, S., & Del Bubba, M. (2011). Comparison of nutritional and nutraceutical properties in cultivated fruits of *Fragaria vesca* L. produced in Italy. *Food Research International*, *44*(5), 1209–1216. https://doi.org/10.1016/j.foodres.2010.10.044

Greco, M., Chiappetta, A., Bruno, L., & Bitonti, M. B. (2012). In Posidonia oceanica cadmium induces changes in DNA methylation and chromatin patterning. *Journal of Experimental Botany*, *63*(2), 695–709. https://doi.org/10.1093/jxb/err313

Guan, L., Dai, Z., Wu, B. H., Wu, J., Merlin, I., Hilbert, G., … Delrot, S. (2016). Anthocyanin biosynthesis is differentially regulated by light in the skin and flesh of white-fleshed and teinturier grape berries. *Planta*, *243*(1), 23–41. https://doi.org/10.1007/s00425-015-2391-4

Häkkinen, S. H., Kärenlampi, S. O., Heinonen, I. M., Mykkänen, H. M., & Törronen, A. R. (1999). Content of the flavonols quercetin, myricetin, and kaempferol in 25 edible berries. *Journal of agricultural and food chemistry*, 47(6), 2274–2279. https://doi.org/10.1021/jf9811065

Iannetta, P. P. M., Laarhoven, L. J., Medina-Escobar, N., James, E. K., McManus, M. T., Davies, H. V., & Harren, F. J. M. (2006). Ethylene and carbon dioxide production by developing strawberries show a correlative pattern that is indicative of ripening climacteric fruit. *Physiologia Plantarum*, 127(2), 247–259. https://doi.org/10.1111/j.1399-3054.2006.00656.x

Jia, H. F., Chai, Y. M., Li, C. L., Lu, D., Luo, J. J., Qin, L., & Shen, Y. Y. (2011). Abscisic acid plays an important role in the regulation of strawberry fruit ripening. *Plant Physiology*, *157*(1), 188–199. https://doi.org/10.1104/pp.111.177311

Jiang, H.; Li, X.; Tian, J.; Liu, H. (2021). Pre-Harvest Supplemental Blue Light Enhanced Antioxidant Activity of Flower Stalk in Chinese Kale during Storage. *Plants*, 10, 1177. https://doi.org/10.3390/plants10061177

Jovančević, M., Balijagić, J., Menkovič, N., šAvikin, K., Zdunić, G., Janković, T., & Dekić-Ivanković, M. (2011). Analysis of phenolic compounds in wild populations of bilberry (*Vaccinium myrtillus* L.) from montenegro. *Journal of Medicinal Plants Research*, *5*(6), 910–914.

Karppinen, K., Lafferty, D.J., Albert, N.W., Mikkola, N., McGhie, T., Allan, A.C., Afzal, B.M., Häggman, H., Espley, R.V. and Jaakola, L. (2021), MYBA and MYBPA transcription factors co-

regulate anthocyanin biosynthesis in blue-coloured berries. *New Phytologist*. 232:3:1350-1367. https://doi.org/10.1111/nph.17669

Katz, E., Lagunes, P. M., Riov, J., Weiss, D., & Goldschmidt, E. E. (2004). Molecular and physiological evidence suggests the existence of a system II-like pathway of ethylene production in non-climacteric Citrus fruit. *Planta*, *219*(2), 243–252. https://doi.org/10.1007/s00425-004-1228-3

Kliewer,W.M.,and Dokoozlian,N.K. (2005). Leaf area/crop weight ratios of grapevines: influence on fruit composition and wine quality. *American Journal of Enology and Viticulture*.56, 170–181.

Kokalj, D., Zlatić, E., Cigić, B., & Vidrih, R. (2019). Postharvest light-emitting diode irradiation of sweet cherries (*Prunus avium* L.) promotes accumulation of anthocyanins. *Postharvest Biology and Technology*, *148*(July 2018), 192–199. https://doi.org/10.1016/j.postharvbio.2018.11.011

Korus, A., Jaworska, G., Bernaś, E., & Juszczak, L. (2015). Characteristics of physico-chemical properties of bilberry (*Vaccinium myrtillus* L.) jams with added herbs. *Journal of Food Science and Technology*, *52*(5), 2815–2823. https://doi.org/10.1007/s13197-014-1315-9

Lee, J., Durst, R. W., & Wrolstad, R. E. (2005). Determination of total monomeric anthocyanin pigment content of fruit juices, beverages, natural colorants, and wines by the pH differential method: Collaborative study. *Journal of AOAC International*, *88*(5), 1269–1278. https://doi.org/10.1093/jaoac/88.5.1269

Li, C., Feng, J., Huang, W. Y., & An, X. T. (2013). Composition of polyphenols and antioxidant activity of rabbiteye blueberry (*Vaccinium ashei*) in Nanjing. *Journal of Agricultural and food chemistry*, 61(3), 523–531. https://doi.org/10.1021/jf3046158

Liu, Y., Fang, S., Yang, W., Shang, X., & Fu, X. (2018). Light quality affects flavonoid production and related gene expression in *Cyclocarya paliurus*. *Journal of Photochemistry and Photobiology B: Biology*, *179*(January), 66–73. https://doi.org/10.1016/j.jphotobiol.2018.01.002

Lobiuc, A., Vasilache, V., Pintilie, O., Stoleru, T., Burducea, M., Oroian, M., & Zamfirache, M. M. (2017). Blue and red LED illumination improves growth and bioactive compounds contents in acyanic and cyanic *Ocimum Basilicum* L. Microgreens. *Molecules*, *22*(12). https://doi.org/10.3390/molecules22122111

Luo, H., Dai, S. J., Ren, J., Zhang, C. X., Ding, Y., Li, Z., … Leng, P. (2014). The Role of ABA in the Maturation and Postharvest Life of a Nonclimacteric Sweet Cherry Fruit. *Journal of Plant Growth Regulation*, 33(2), 373–383. https://doi.org/10.1007/s00344-013-9388-7

Ma, A., Wang, D., Lu, H., Wang, H., Qin, Y., Hu, G., & Zhao, J. (2021). LcCOP1 and LcHY5 control the suppression and induction of anthocyanin accumulation in bagging and debagging litchi fruit pericarp. *Scientia Horticulturae*, *287*(May), 110281. https://doi.org/10.1016/j.scienta.2021.110281

Ma, Z. H., Li, W. F., Mao, J., Li, W., Zuo, C. W., Zhao, X., … Chen, B. H. (2019). Synthesis of light-inducible and light-independent anthocyanins regulated by specific genes in grape "Marselan" (*V. Vinifera* L.). *PeerJ*, *2019*(3), 1–24. https://doi.org/10.7717/peerj.6521

Maier, A., & Hoecker, U. (2015). COP1/SPA ubiquitin ligase complexes repress anthocyanin accumulation under low light and high light conditions. *Plant Signaling and Behavior*, *10*(1), e970440-1-e970440-3. https://doi.org/10.4161/15592316.2014.970440

Miao, L., Zhang, Y., Yang, X., Xiao, J., Zhang, H., Zhang, Z., … Jiang, G. (2016). Colored light-quality selective plastic films affect anthocyanin content, enzyme activities, and the expression of flavonoid genes in strawberry (*Fragaria* × *ananassa*) fruit. *Food Chemistry*, *207*, 93–100. https://doi.org/10.1016/j.foodchem.2016.02.077

Nin, S., Petrucci, W. A., Del Bubba, M., Ancillotti, C., & Giordani, E. (2017). Effects of environmental factors on seed germination and seedling establishment in bilberry (Vaccinium myrtillus L.). *Scientia Horticulturae*, *226*(September), 241–249. https://doi.org/10.1016/j.scienta.2017.08.049

Oh, H. D., Yu, D. J., Chung, S. W., Chea, S., & Lee, H. J. (2018). Abscisic acid stimulates anthocyanin accumulation in 'Jersey' highbush blueberry fruits during ripening. *Food Chemistry*, *244*(October 2017), 403–407. https://doi.org/10.1016/j.foodchem.2017.10.051

Ouzounis, T., Rosenqvist, E., & Ottosen, C. O. (2015). Spectral effects of artificial light on plant physiology and secondary metabolism: A review. *HortScience*, *50*(8), 1128–1135. https://doi.org/10.21273/hortsci.50.8.1128

Panjai, L., Noga, G., Hunsche, M., & Fiebig, A. (2019). Optimal red light irradiation time to increase health-promoting compounds in tomato fruit postharvest. *Scientia Horticulturae*, *251*(March), 189–196. https://doi.org/10.1016/j.scienta.2019.03.019

Pérez-Llorca, M., Muñoz, P., Müller, M., & Munné-Bosch, S. (2019). Biosynthesis, metabolism and function of auxin, salicylic acid and melatonin in climacteric and non-climacteric fruits. *Frontiers in Plant Science*, *10*(February), 1–10. https://doi.org/10.3389/fpls.2019.00136

Petroni, K., & Tonelli, C. (2011). Recent advances on the regulation of anthocyanin synthesis in reproductive organs. *Plant Science*, *181*(3), 219–229. https://doi.org/10.1016/j.plantsci.2011.05.009

Pilati, S., Bagagli, G., Sonego, P., Moretto, M., Brazzale, D., Castorina, G., … Moser, C. (2017). Abscisic acid is a major regulator of grape berry ripening onset: new insights into ABA signaling network. *Frontiers in plant science*, *8*(June), 1–16. https://doi.org/10.3389/fpls.2017.01093

Pires, T. C. S. P., Caleja, C., Santos-Buelga, C., Barros, L., & Ferreira, I. C. F. R. (2020). *Vaccinium myrtillus* L. Fruits as a Novel Source of Phenolic Compounds with Health Benefits and Industrial Applications - A Review. *Current Pharmaceutical Design*, *26*(16), 1917–1928. https://doi.org/10.2174/1381612826666200317132507

Plunkett, B.J., Espley, R.V., Dare, A.P., Warren, B.A.W., Grierson, E.R.P., Cordiner, S., Turner, J.L., Allan, A.C., Albert, N.W., Davies, K.M., Schwinn, K.E. (2018). MYBA from blueberry (*Vaccinium* section *Cyanococcus*) is a subgroup 6 type R2R3MYB transcription factor that activates anthocyanin production. *Frontiers in Plant Science* 9: 1300.

Samkumar, A., Jones, D., Karppinen, K., Dare, A.P., Sipari, N., Espley, R.V., Martinussen, I. and Jaakola, L. (2021), Red and blue light treatments of ripening bilberry fruits reveal differences in signaling through ABA regulated anthocyanin biosynthesis. *Plant Cell & Environment*.44:10: 3227-3245. https://doi.org/10.1111/pce.14158

Seeram, N. P. (2008). Berry fruits for cancer prevention: Current status and future prospects. *Journal of Agricultural and Food Chemistry*, *56*(3), 630–635. https://doi.org/10.1021/jf072504n

Silva, T. D., Batista, D. S., Fortini, E. A., Castro, K. M. de, Felipe, S. H. S., Fernandes, A. M., … Otoni, W. C. (2020). Blue and red light affects morphogenesis and 20-hydroxyecdisone content of in vitro Pfaffia glomerata accessions. *Journal of Photochemistry and Photobiology B: Biology*, 203(October 2019), 111761. https://doi.org/10.1016/j.jphotobiol.2019.111761

Tran, L. H., Lee, D. G., & Jung, S. (2021). Light quality-dependent regulation of photoprotection and antioxidant properties in rice seedlings grown under different light-emitting diodes. *Photosynthetica*, *59*(1), 12–22. https://doi.org/10.32615/ps.2020.082

Van de Poel, B., Vandendriessche, T., Hertog, M. L. A. T. M., Nicolai, B. M., & Geeraerd, A. (2014). Detached ripening of non-climacteric strawberry impairs aroma profile and fruit quality. *Postharvest Biology and Technology*, *95*, 70–80. https://doi.org/10.1016/j.postharvbio.2014.04.012

Wang, L. J., Su, S., Wu, J., Du, H., Li, S. S., Huo, J. W., … Wang, L. S. (2014). Variation of anthocyanins and flavonols in *Vaccinium uliginosum* berry in Lesser Khingan Mountains and its antioxidant activity. *Food Chemistry*, 160, 357–364. https://doi.org/10.1016/j.foodchem.2014.03.081

Wu, M., Si, M., Li, X., Song, L., Liu, J., Zhai, R., … Wang, Z. (2019). PbCOP1.1 contributes to the negative regulation of anthocyanin biosynthesis in pear. *Plants*, *8*(2), 1–12. https://doi.org/10.3390/plants8020039

Xu, F., Cao, S., Shi, L., Chen, W., Su, X., & Yang, Z. (2014). Blue light irradiation affects anthocyanin content and enzyme activities involved in postharvest strawberry fruit. *Journal of Agricultural and Food Chemistry*, *62*(20), 4778–4783. https://doi.org/10.1021/jf501120u

Yang, J., Li, B., Shi, W., Gong, Z., Chen, L., & Hou, Z. (2018). Transcriptional activation of anthocyanin biosynthesis in developing fruit of blueberries (*Vaccinium corymbosum* L.) by Preharvest and Postharvest UV Irradiation. *Journal of Agricultural and Food Chemistry*, *66*(42), 10931–10942. https://doi.org/10.1021/acs.jafc.8b03081

Zhai, R., Liu, X. T., Feng, W. T., Chen, S. S., Xu, L. F., Wang, Z. G., … Ma, F. W. (2014). Different biosynthesis patterns among flavonoid 3-glycosides with distinct effects on accumulation of other flavonoid metabolites in pears (*Pyrus bretschneideri* rehd.). *PLoS ONE*, *9*(3). https://doi.org/10.1371/journal.pone.0091945

Zhang, Y., Jiang, L., Li, Y., Chen, Q., Ye, Y., Zhang, Y., … Tang, H. (2018). Effect of red and blue light on anthocyanin accumulation and differential gene expression in strawberry (*Fragaria* × *ananassa*). *Molecules*, *23*(4), 1–17. https://doi.org/10.3390/molecules23040820

Zhou, Y., & Singh, B. R. (2002). Red light stimulates flowering and anthocyanin biosynthesis in American cranberry. *Plant Growth Regulation*, *38*(2), 165–171. https://doi.org/10.1023/A:1021322418740

Zhu, L., Liu, X., Tan, J., & Wang, B. (2013). Influence of harvest season on antioxidant activity and constituents of rabbit eye blueberry (*Vaccinium ashei*) leaves. *Journal of Agricultural and Food Chemistry*, *61*(47), 11477–11483. https://doi.org/10.1021/jf4035892

Zifkin, M., Jin, A., Ozga, J. A., Irina Zaharia, L., Schernthaner, J. P., Gesell, A., … Peter Constabel, C. (2012). Gene expression and metabolite profiling of developing highbush blueberry fruit indicates transcriptional regulation of flavonoid metabolism and activation of abscisic acid metabolism. *Plant Physiology*, *158*(1), 200–224. https://doi.org/10.1104/pp.111.180950

Zoratti, L., Sarala, M., Carvalho, E., Karppinen, K., Martens, S., Giongo, L., … Jaakola, L. (2014). Monochromatic light increases anthocyanin content during fruit development in bilberry. *BMC Plant Biology*, *14*(1), 1–10. https://doi.org/10.1186/s12870-014-0377-1

Zorzi, M., Gai, F., Medana, C., Aigotti, R., Morello, S., & Peiretti, P. G. (2020). Bioactive compounds and antioxidant capacity of Small Berries. *Foods*, *9*, *623*, 1-13.

Figure Legends

Fig 1. Effect of light spectral qualities on skin coloration after 2nd and 5th day of observation from detached berries **(A, B)** ripening in petri plates (expressed in percentages from ± SE of 3 replicates of 50 berries from each treatment). 'Control' represent the samples treated with normal white light (W) and under dark conditions (D). Berry skin coloration after 7 days of light treatment in detached berries **(C)**.

Fig 2. Total soluble polyphenols of detached and attached berries expressed as mg catechin (CAT) equivalent 100 g^{-1} DW (dry weight) **(A)**. Total monomeric anthocyanins expressed as mg cyanidin-3-glucoside (CYA-3-GLU) equivalent 100 g^{-1} DW **(B)**. Total flavonoids expressed as quercetin (QUE) equivalent 100g^{-1} DW **(C)**. Ferric reducing/antioxidant power (FRAP) antioxidant activity assay expressed as FE (II) mmol 100g^{-1} DW **(D)**. Different letters indicate significance between the light treatments when measured using ANOVA with pairwise comparisons ($p \leq 0.05$).

Fig 3. Concentrations of anthocyanins in mg 100g^{-1} DW (dry weight) quantified by LC-MS from fully ripe berries harvested from bush **(A)** and from detached conditions **(B)** under spectral light treatment. The amounts are expressed in average of three replicates ± SE from glucoside, galactoside and arabinoside-type derivatives from each class of anthocyanin compounds. Asterisks indicate significance between the light treatments when measured using ANOVA with pairwise comparisons (*$p \leq 0.05$, **$p \leq 0.01$). The distribution of anthocyanin constituents shared from all the five classes from each experimental setup in response to a major positively affected light treatment (Red and Blue) is represented as pie charts. The distribution of red light affected anthocyanin profile in attached berries **(C)** and blue light affected anthocyanin profile in detached berries **(D)**.

Fig 4. Concentrations of flavonols under different light treatments, myricetin 3-glucoside **(A)**, laricitrin 3-glucuronide **(B)**, quercetin-3-arabinopyranoside **(C)**, syringetin 3-glucuronide **(D)**, gallocatechin **(E)**, and procyanidin B2 dimer **(F)** compounds in mg $100g^{-1}$ DW (dry weight) quantified using LC-MS from detached berries and fully ripe berries from bush at the end of light treatment. The amounts are expressed in average of three replicates ± SE. Asterisks indicate significance between the light treatments when measured using ANOVA with pairwise comparisons (* $p \leq 0.05$, ** $p \leq 0.01$, *** $p \leq 0.001$) 'nd'-not detected.

Fig 5. Effect of light spectral treatment on gene expression of early flavonoid biosynthetic genes in attached berries from bushes **(A)** and from detached berries **(B)**, chalcone synthase (*VmCHS*), dihydroflavonol 4-reductase (*VmDFR*), flavonoid 3′ hydroxylase (*VmF3'H*), flavonoid 3′5′ hydroxylase (*VmF3'5'H*). The expression levels are normalized to the housekeeping gene *VmGAPDH* (glyceraldehyde 3-phosphate dehydrogenase) or actin. Error bars represents ±SE of three biological replicates and significant differences between control and light treatments were analyzed by comparison of means using student's t-test (indicated in asterisks*) with p-value ≤ 0.05.

Fig 6. Effect of light spectral treatment on gene expression of late flavonoid biosynthetic genes and key regulatory genes in attached berries from bushes **(A)** and from detached berries **(B)**, anthocyanidin synthase (*VmANS*), anthocyanidin 3-O-glucosyltransferase (*VmUFGT*), MYB transcription factors (*VmMYBA1*, *VmMYBPA1.1*). The expression levels are normalized to the housekeeping gene *VmGAPDH* (glyceraldehyde 3-phosphate dehydrogenase) or actin. Error bars represents ±SE of three biological replicates and significant differences between control and light treatments were analyzed by comparison of means using student's t-test (indicated in asterisks*) with p-value ≤ 0.05.

Fig 7. Effect of light spectral treatment on gene expression of photomorphogenesis related genes in attached berries from bushes **(A)** and from detached berries **(B)**, constitutive photomorphogenic 1 (*VmCOP1a*, *VmCOP1b)*, elongated hypocotyl 5 (*VmHY5*). The expression levels are normalized to the housekeeping gene *VmGAPDH* (glyceraldehyde 3-phosphate dehydrogenase) or actin. Error bars represents ±SE of three biological replicates and significant differences between control and light treatments were analyzed by comparison of means using student's t-test (indicated in asterisks*) with p-value ≤ 0.05.

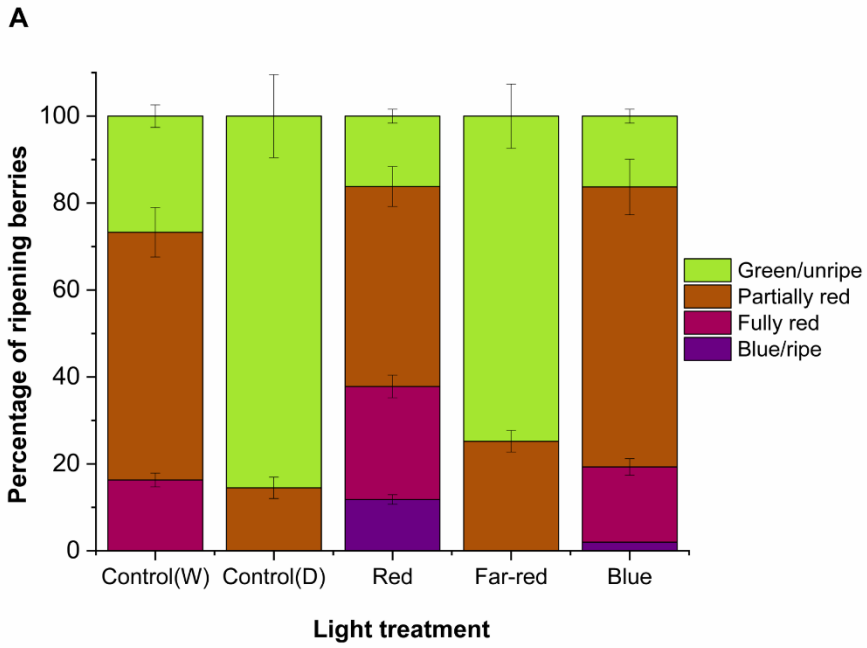
A
Percentage of ripening berries
100
80
60
40
20
0
Control(W)
Control(D)
Red
Far-red
Blue
Light treatment
Green/unripe
Partially red
Fully red
Blue/ripe

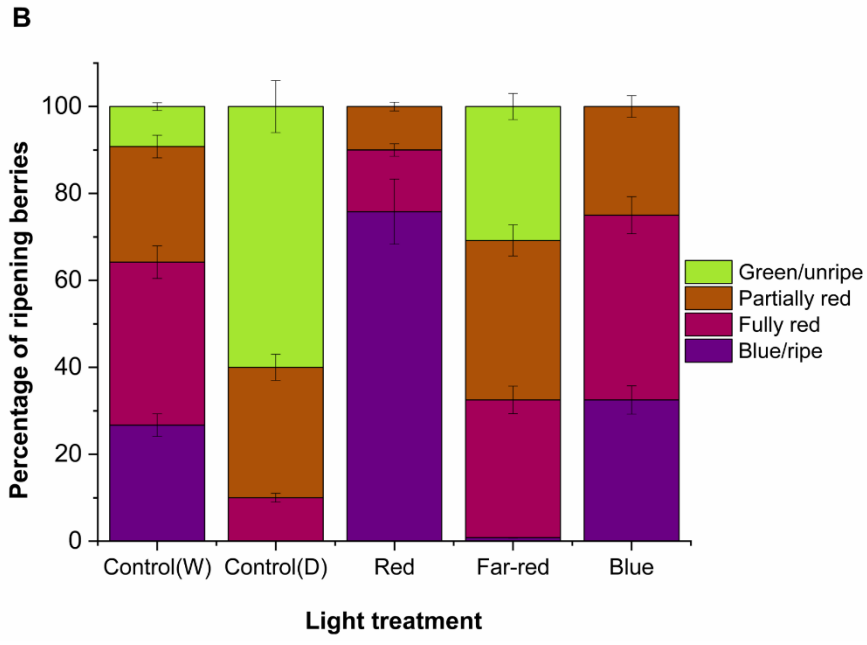
B
Percentage of ripening berries
100
80
60
40
20
0
Control(W)
Control(D)
Red
Far-red
Blue
Light treatment
Green/unripe
Partially red
Fully red
Blue/ripe

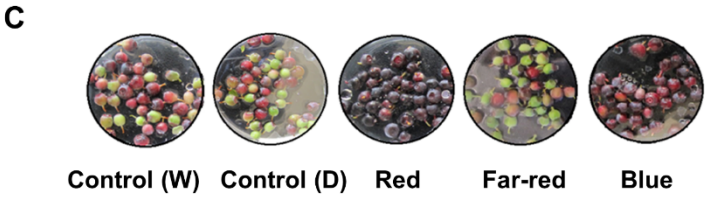
C
Control (W)
Control (D)
Red
Far-red
Blue

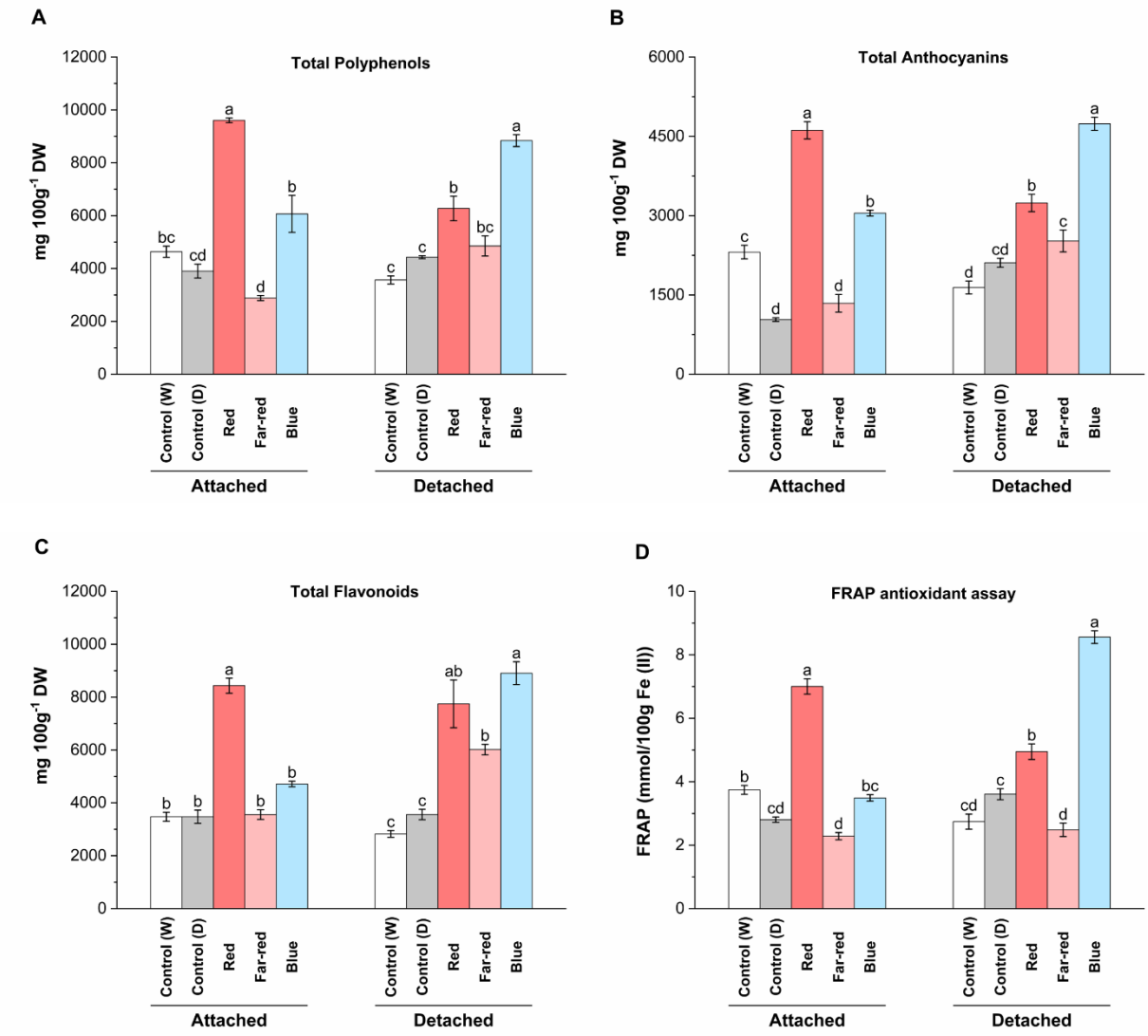
A
Total Polyphenols
mg 100g-1 DW
12000
10000
8000
6000
4000
2000
0
bc
cd
a
d
b
c
c
b
bc
a
Control (W)
Control (D)
Red
Far-red
Blue
Attached
Detached
B
Total Anthocyanins
mg 100g-1 DW
6000
4500
3000
1500
0
c
d
a
d
b
d
cd
b
c
a
C
Total Flavonoids
mg 100g-1 DW
12000
10000
8000
6000
4000
2000
0
b
b
a
b
b
c
c
ab
b
a
D
FRAP antioxidant assay
FRAP (mmol/100g Fe (II))
10
8
6
4
2
0
b
cd
a
d
bc
cd
c
b
d
a

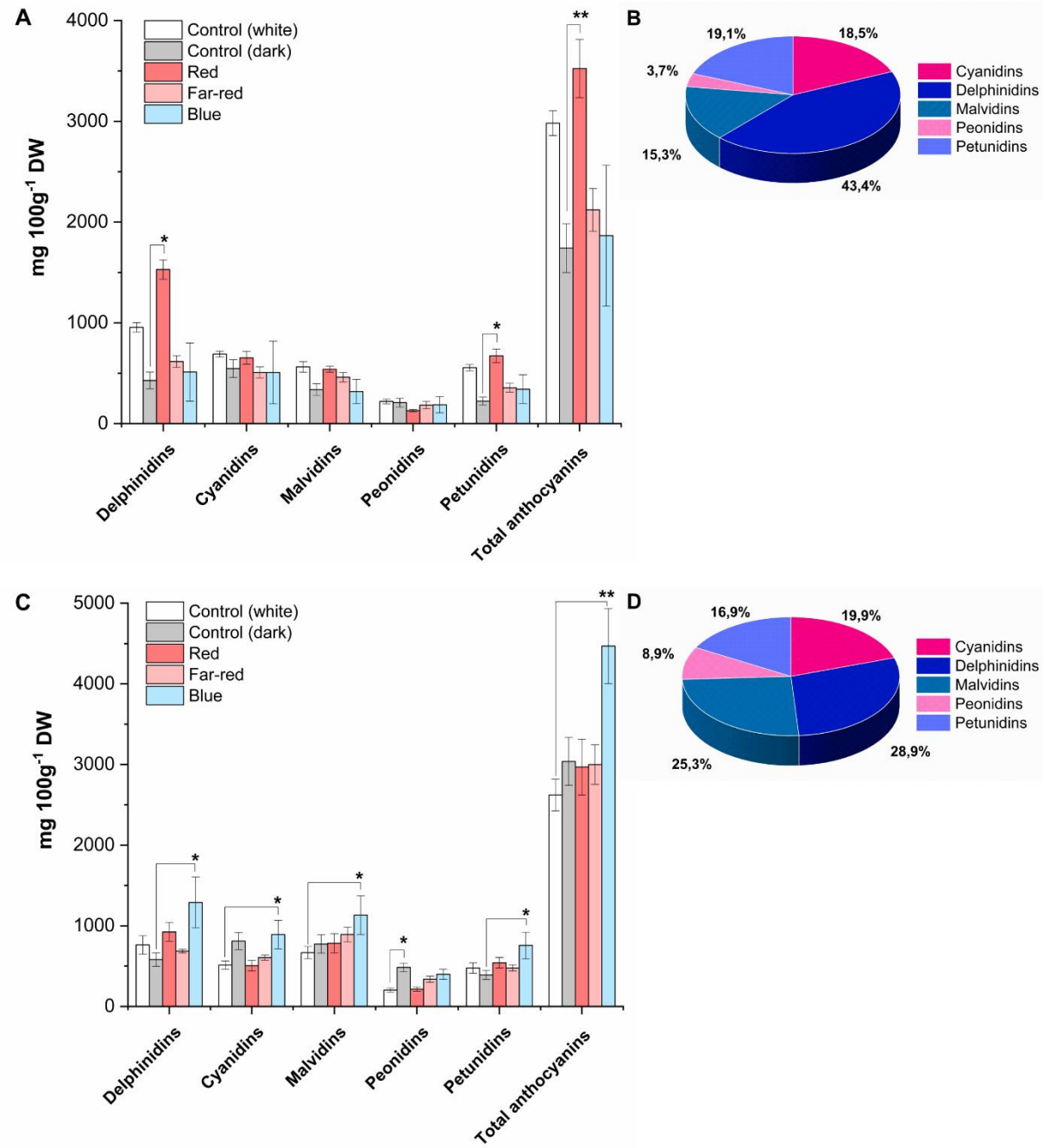
A
B
C
D
Control (white)
Control (dark)
Red
Far-red
Blue
mg 100g-1 DW
Delphinidins
Cyanidins
Malvidins
Peonidins
Petunidins
Total anthocyanins
19,1%
18,5%
3,7%
15,3%
43,4%
16,9%
19,9%
8,9%
25,3%
28,9%

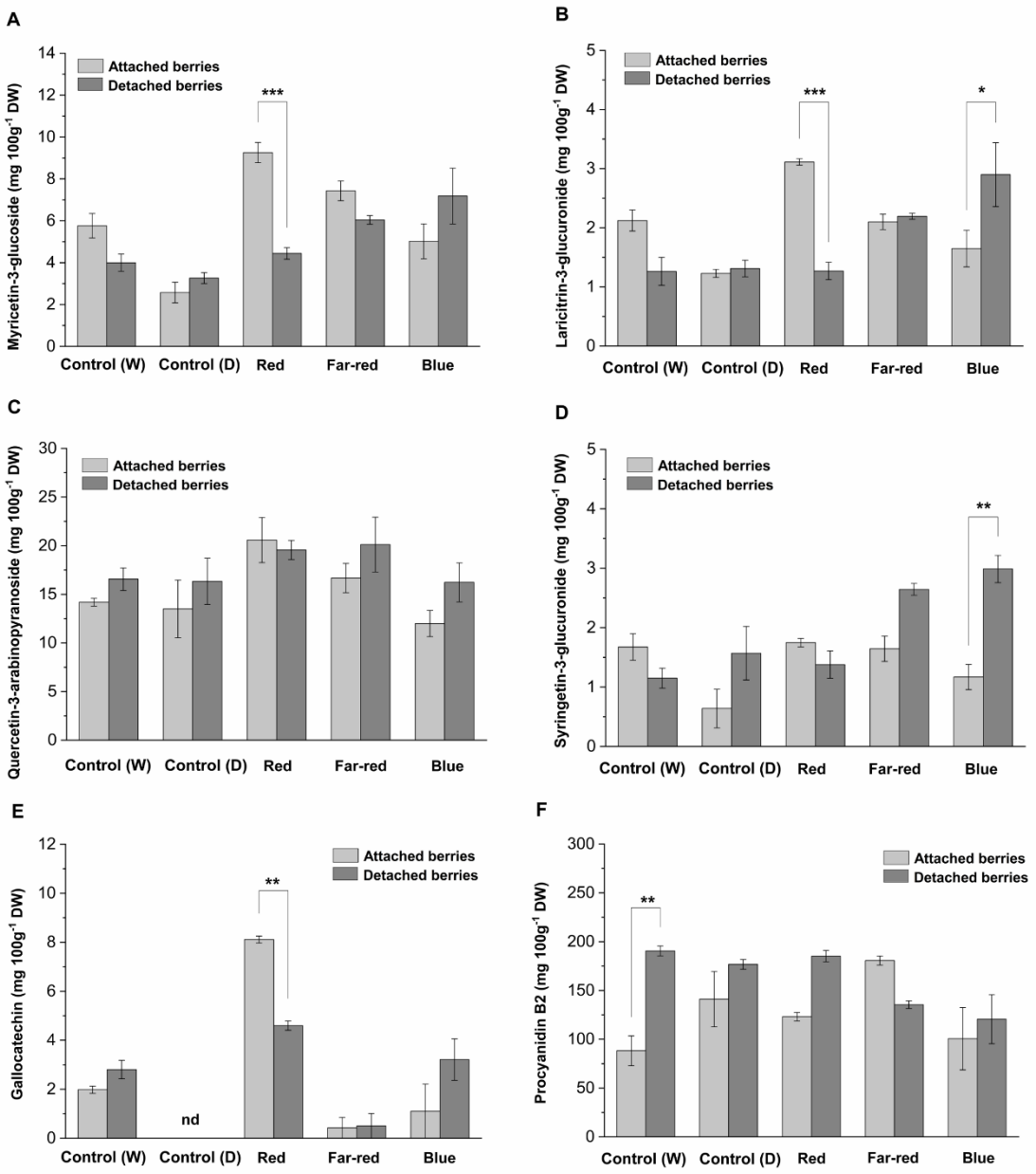
A
Myricetin-3-glucoside (mg 100g-1 DW)
Attached berries
Detached berries
***
Control (W)
Control (D)
Red
Far-red
Blue
B
Laricitrin-3-glucuronide (mg 100g-1 DW)
Attached berries
Detached berries
***
*
Control (W)
Control (D)
Red
Far-red
Blue
C
Quercetin-3-arabinopyranoside (mg 100g-1 DW)
Attached berries
Detached berries
Control (W)
Control (D)
Red
Far-red
Blue
D
Syringetin-3-glucuronide (mg 100g-1 DW)
Attached berries
Detached berries
**
Control (W)
Control (D)
Red
Far-red
Blue
E
Gallocatechin (mg 100g-1 DW)
Attached berries
Detached berries
**
nd
Control (W)
Control (D)
Red
Far-red
Blue
F
Procyanidin B2 (mg 100g-1 DW)
Attached berries
Detached berries
**
Control (W)
Control (D)
Red
Far-red
Blue

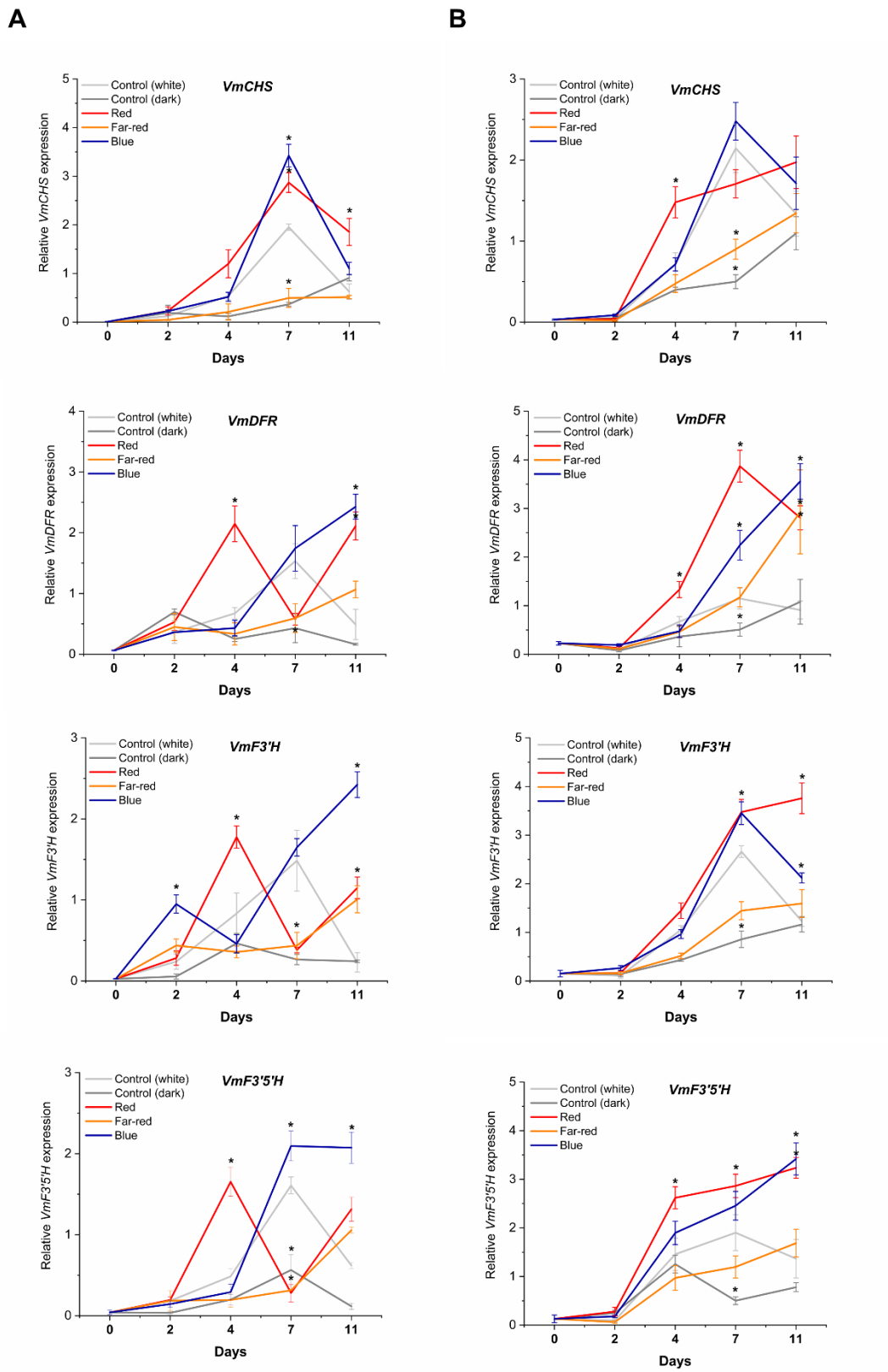
A
B
Control (white)
Control (dark)
Red
Far-red
Blue
VmCHS
VmDFR
VmF3'H
VmF3'5'H
Relative VmCHS expression
Relative VmDFR expression
Relative VmF3'H expression
Relative VmF3'5'H expression
Days
0
2
4
7
11

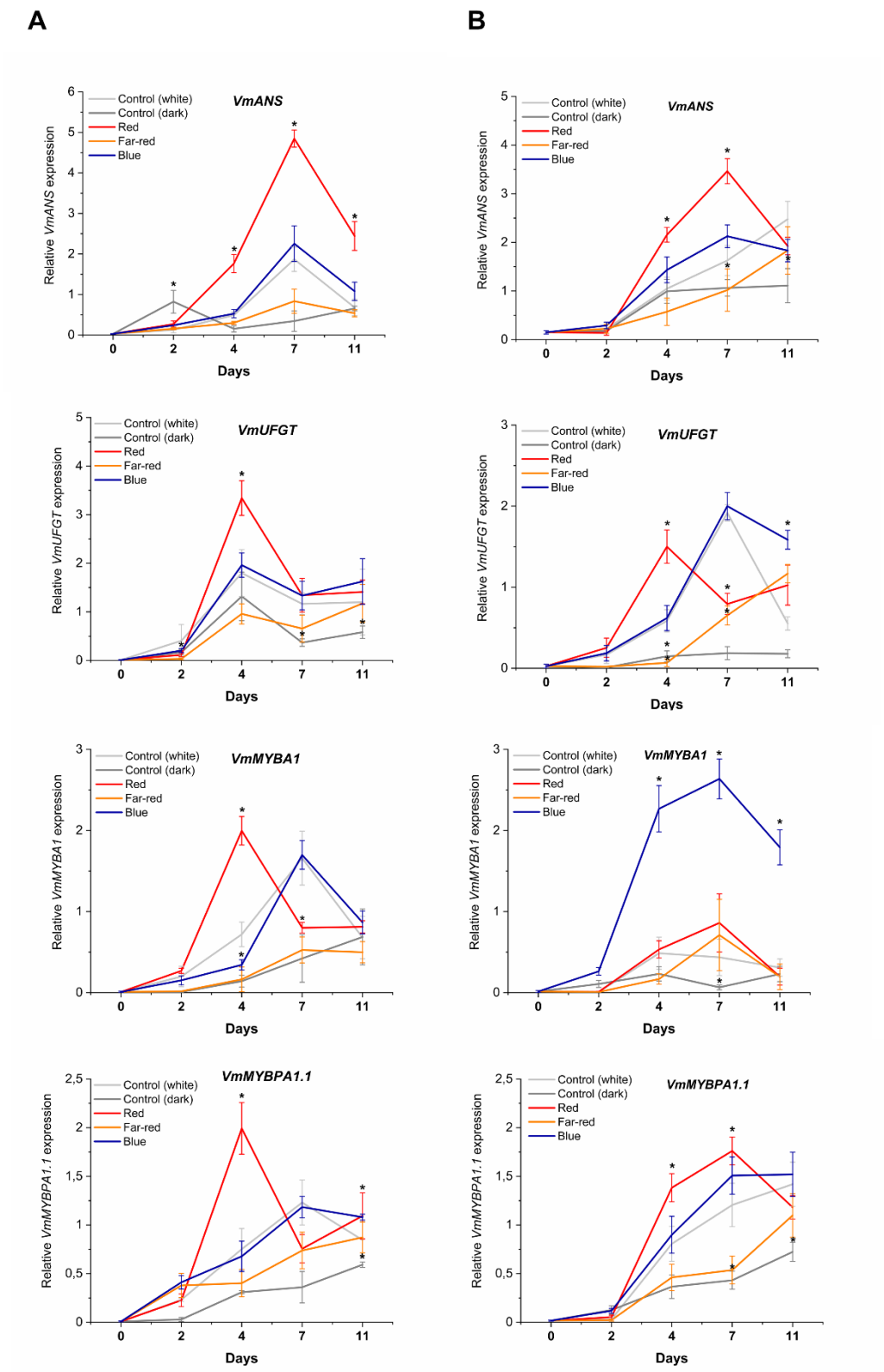
A
B
VmANS
VmUFGT
VmMYBA1
VmMYBPA1.1
Control (white)
Control (dark)
Red
Far-red
Blue
Days
Relative VmANS expression
Relative VmUFGT expression
Relative VmMYBA1 expression
Relative VmMYBPA1.1 expression

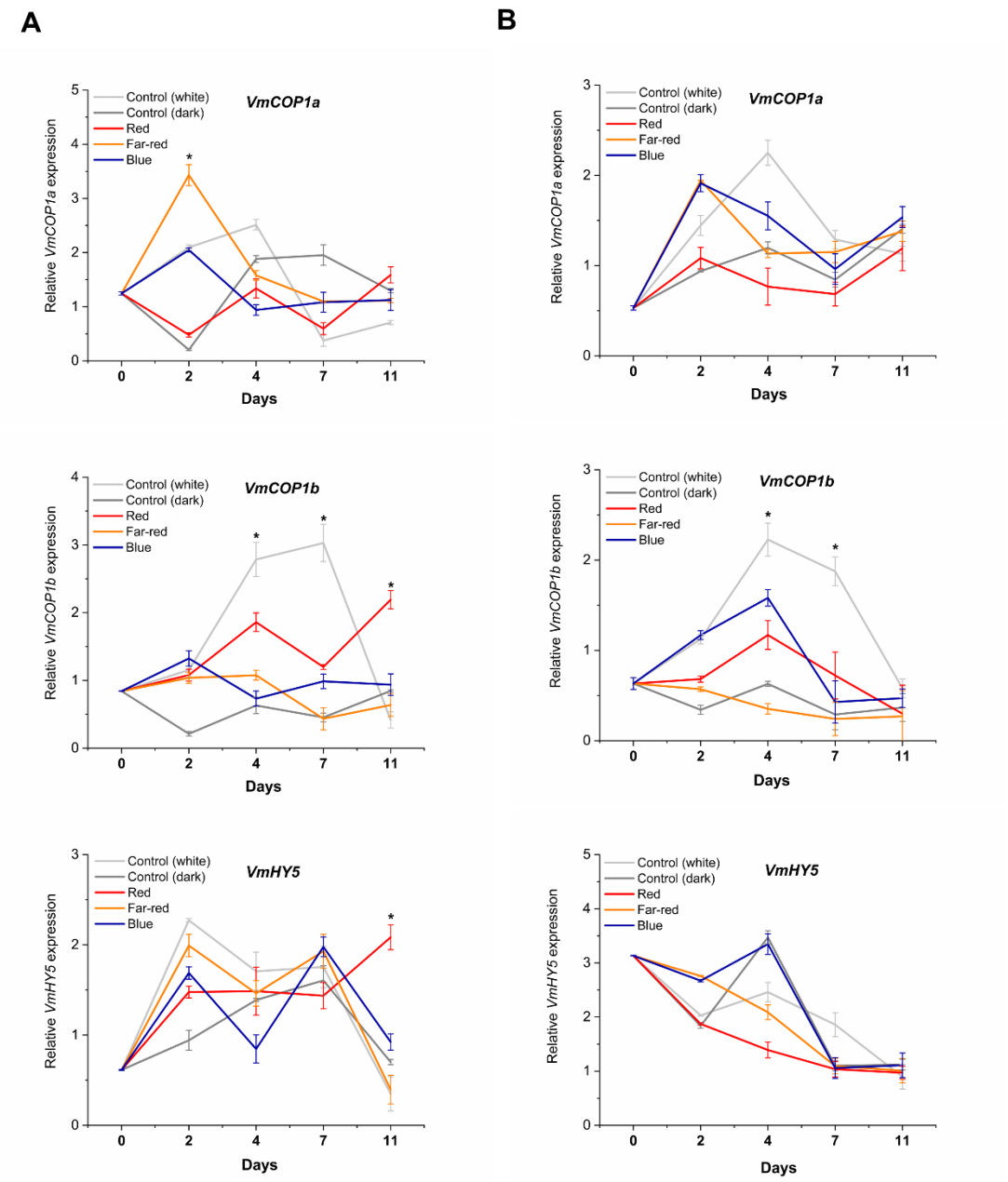
A
B
Control (white)
Control (dark)
Red
Far-red
Blue
VmCOP1a
VmCOP1b
VmHY5
Relative VmCOP1a expression
Relative VmCOP1b expression
Relative VmHY5 expression
Days
0
2
4
7
11
*

Paper 3

Insights into sugar metabolism during bilberry (*Vaccinium myrtillus* L.) fruit development

Amos Samkumar[1*], Katja Karppinen[1], Binita Dhakal[1], Inger Martinussen[2], Laura Jaakola[1,2]

[1]Department of Arctic and Marine Biology, UiT The Arctic University of Norway, Tromsø, Norway

[2]Norwegian Institute of Bioeconomy Research, Ås, Norway

*Corresponding author. E-mail: amos.s.premkumar@uit.no

Abstract

Bilberry is regarded as one of the best natural sources of anthocyanins and is widely explored for its health-beneficial compounds. Besides anthocyanins, one of the major attributes that determines the berry quality is the accumulation of sugars that provide sweetness and flavor to the ripening fruit. In this study, we have identified 25 sugar metabolism related genes in bilberry that are categorized into invertases, hexokinases, fructokinases, sucrose synthases and sucrose phosphatases. The results indicate that various isoforms of the identified genes express differentially suggesting that they might have specialized functions. The highest sugar content was found in fully-ripe berries with fructose and glucose dominating the composition with low sucrose amounts. The related enzyme activities across four berry developmental stages were further analyzed to understand the molecular mechanism of sugar accumulation. The activity of the invertases in the cell wall and vacuolar spaces tend to increase rapidly towards ripe berries. Amylase activity involved in starch metabolism was not detected in unripe berries and was only found at very low rate in ripe berries. Sucrose resynthesizing enzymes showed higher activity upon early ripening and had the highest activity in ripe berries. Interestingly, we found that continuous red and blue light supplemental irradiation triggered starch degradation by up-regulating both α- and β amylases, and contrasting differential expression pattern across sucrose, galactose and sugar-alcohol metabolism were found. Both enzymological and transcriptional data in the present study provide new understanding on the sugar metabolism during bilberry fruit development having major effect on the fruit quality.

Keywords: *Vaccinium myrtillus*, bilberry, sugar metabolism, sucrose, glucose, fructose, starch

1. Introduction

Carbohydrates are primarily formed during photosynthesis being the main energy source for plant growth and development (Rolland et al., 2006). They comprise of simple building units of monosaccharides (glucose, fructose, galactose), which can be combined through glycosidic bonds to form complex molecules such as disaccharides (sucrose), oligosaccharides (stachyose, raffinose) polysaccharides (starch) and derived sugar-alcohols (Hu et al., 2016; Moing, 2000). Glucose, fructose and sucrose are classified as soluble sugars. Starch being the non-soluble sugar that accumulates in storage tissues such as plastids and can be utilized only as reserve energy source (Cho et al., 2020; Wang et al., 2013). In addition to being precursors for energy yielding processes, the soluble sugars have been identified as signaling molecules in various plant metabolic processes and known to be involved in stress and defense responses (Tauzin & Giardina, 2014). During plant development, the soluble sugars are transported from photosynthetic-source tissues, such as leaves, towards sink tissues such as fruit, root and shoot (Hammond & White, 2008). In fruits, the amount and type of sugars accumulating during the ripening improve sweetness and flavor of fruit, thus, affecting to the quality of fleshy fruits (Borsani et al., 2009). In most fleshy fruits, glucose, fructose, and sucrose constitute more than 99% of sugar content followed by trace amounts of other minor carbohydrates and sugar-alcohols.

Sucrose is the major sugar which is transported to sink tissues via phloem during fruit development. In fruit tissues, sucrose is either hydrolyzed to hexoses, such as glucose and fructose, by the invertases or converted to fructose and UDP-glucose by sucrose synthase (SS) (Verma et al., 2011). A schematic representation of the identified bilberry sugar metabolism genes is shown in Fig. 1. Three types of invertases are known to be involved in sucrose hydrolysis and degradation. A neutral invertase (NINV), which is predominantly localized in cytosol and two acid invertases, a soluble invertase bound to vacuoles (VINV) and an insoluble form found in the cell wall (CWINV) has been shown to be involved in plant sugar metabolism (Ruan et al., 2010). The cleaved hexoses from sucrose, i.e., glucose and fructose, found in extracellular space are further phosphorylated into glucose-6-phosphate (G6P), fructose-6-phosphate (F6P) by hexokinase (HK) and fructokinase (FK), respectively. These hexose phosphates are the precursors in energy-yielding glycolysis process leading towards the citric acid (TCA) cycle (Granot et al., 2013). The cleaved sugars from hydrolysis of sucrose into UDP-glucose and F6P by SS can be further involved in sucrose resynthese by sucrose phosphate synthase (SPS) and sucrose phosphate phosphatase (SPP). The degradation of sucrose and resynthesis, which is known as ‘futile sucrose recycle’ is critical for accumulation of fruit sugars and thus playing a key role in fruit development (Nguyen-Quoc & Foyer, 2001).

Sugars being the primary determinants of fruit quality also vary in its composition and accumulation across fruit crops. In climacteric fruits such as apples and tomatoes, a gradual increase of sugar content can be seen towards fruit maturation (Li et al., 2012; Nguyen-Quoc & Foyer, 2001), whereas in non-

climacteric fruits such as grapes and strawberries, a rapid accumulation of sugars is reported only at later stages of ripening. (Akšić et al., 2019; Zhu et al., 2017). Some of the earlier studies on sugar metabolism related to fruit ripening have mainly focused only on few genes or isoforms and are not very comprehensive (Dai et al., 2016; Zhu et al., 2017).

Apart from flavor enhancement, the roles of sugars in fruit development are diverse. Galactose, another important hexose sugar found comparatively only in very low amounts in fleshy fruits, has a major role in the reduction of cell-wall loosening during fruit ripening (Althammer et al., 2020; Brummell, 2006). Unlike sucrose metabolism, galactose pathway in plants is poorly understood. Galactose moieties are often associated with production of raffinose-type oligosaccharides including stachyoses in cell wall localized polysaccharides, which are derived from sucrose metabolism (Gangl & Tenhaken, 2016). Furthermore, sugar alcohols such as sorbitol, myo-inositol and galactinols are synthesized by α-galactosyltransferases (α-gal), and they are known to be involved in protecting fruit tissues from dehydration by maintaining the cellular turgor pressure (Loescher, 1987). The hexose interconversion reactions in these pathways are usually mediated by UDP-glucose-pyrophosphorylases (UDPG-PP), phosphoglucoisomerases (PGI) and phosphoglucomutases (PGM) enzymes (Decker & Kleczkowski 2019; Fig. 1). Some studies have shown the correlation of insoluble starch accumulation and soluble sugar content in ripe fruits (Cho et al., 2020). However, the breakdown of starch by α-amylase and β-amylase could also contribute well towards significant increase in sugar content at later stages of fruit development (Souleyre et al., 2004).

Bilberry (*Vaccinium myrtillus* L.) is an important wild berry species native to Northern Eurasian regions gaining worldwide economic importance due to high levels of anthocyanins accumulating during fruit ripening (Pires et al., 2020). In *Vaccinium* berries, the sugars are mostly accumulating at later stages of ripening upon pigmentation. Also, the glycoside residues in bilberry anthocyanin compounds are mostly of glucoside, galactoside and arabinoside derivatives (Kähkönen et al., 2003; Karppinen et al., 2018). Earlier, we have shown that specific light wavelengths such as red and blue light can improve anthocyanin accumulation in bilberries (Samkumar et al., 2021), but further information on sugar metabolism, transport and signaling is lacking. Red and blue light wavelengths could selectively induce sugar metabolism as evidenced by some of the recent studies in tomato and lettuce crops (Chen et al., 2019; Li et al., 2017).

The current study aims to shed light on sugar biosynthesis and metabolism in developing bilberries through analysis of the sugar content, related gene expression and enzyme activity assays. The study also highlights the role of spectral light quality, specifically the effect of red and blue light on sugar metabolism identified from light-treated bilberry transcriptome dataset. The results provide deeper understanding on the relationship between sugar metabolism and fruit ripening in bilberry by adding

further knowledge towards improving economic value of small berries, fruit quality, marketability and could also accelerate *Vaccinium* breeding programs in future.

2. Materials and methods

2.1 Plant materials

Wild bilberry fruits were collected from forest stands in Oulu (65°01' N, 25°28' E), Finland and Tromsø (69°71' N, 19°41' E), Norway. The samples were kept in -80°C until RNA and enzyme extraction. The berry samples were collected at four different developmental stages of bilberry; small unripe green berries (S2), large unripe green berries (S3), ripening purple berries (S4) and fully ripe blue-colored berries (S5) as previously described (Karppinen et al., 2013).

The earlier published transcriptome dataset from red, blue, and light treated bilberry fruits was utilized in this study (Samkumar et al., 2021). The raw reads can be retrieved from the Bio Project ID PRJNA747684 from NCBI-SRA database. The top differentially expressed genes (DEGs) were analyzed and subjected to KEGG pathway enrichment analysis using Blast2GO software suite and all the genes classified under sugar metabolic pathways were filtered out and further analyzed. The S5 berries from the light treatments were collected for analysis of the sugar content.

2.2 Identification of sugar metabolism genes

Genes encoding the major groups of sugar metabolism enzymes corresponding to CWINV, NINV, VINV, FK, SS, SPP and SPS were retrieved from transcriptome shotgun assembly (TSA) sequence databases of *Vaccinium virgatum* (Qi et al., 2019) and transcriptomes of *Vaccinium myrtillus* (Nguyen et al., 2018; Samkumar et al., 2021).

2.3 Phylogenetic analysis

Multiple sequence alignments of deduced amino acid sequences were performed using EMBL-EBI, Clustal Omega program (https://www.ebi.ac.uk/Tools/msa/clustalo/). To analyze the common relationship between the sugar-enzyme families and across fruit-crop species, phylogenetic analysis was performed from the CLUSTAL-aligned sequences. The unrooted phylogenetic tree was constructed using MEGA X software package (Kumar et al., 2018) using the maximum-likelihood method with bootstrap test value set to 500 replicates in a poisson-distributed model.

2.4 RNA extraction and qRT-PCR analysis

The frozen berries were ground to a fine powder under liquid nitrogen using mortar and pestle. Total RNA was isolated from approximately 120 mg tissue powder by using Spectrum Plant Total RNA kit (Sigma-Aldrich, St. Louis, MO, USA) following the manufacturer's instructions. The residual DNA was eliminated with on-column digestion using DNase I (Sigma-Aldrich). The RNA was qualified and quantified using a Nanodrop (Thermo Fischer Scientific, Waltham, MA, USA). First-strand cDNA was synthesized using Invitrogen Superscript IV reverse transcriptase (Thermo Fisher Scientific) using 4 µg of total RNA according to manufacturer's instructions.

Real-time quantitative reverse transcription PCR (qRT-PCR) analysis was performed in C1000 Thermal cycler (CFX96 Real-Time System; Bio-Rad, Hercules, California, USA) and using SSOFast EvaGreen-SYBR supermix (Bio-Rad) in 15 µl volume per reaction. The PCR conditions were 95°C for 30 sec followed by 40 cycles at 95°C for 5 sec, and 60°C for 10 sec. The program was further followed by a melt-curve analysis ranging from 65°C to 95°C with an increment of 0.5°C every cycle. All analyses were performed in three biological replicates. The results were analyzed using CFX connect software (Bio-Rad) using $2^{(-\Delta\Delta Cq)}$ method. The relative expression levels were normalized with either *GAPDH* (glyceraldehyde-3-phosphate dehydrogenase) or *Actin* housekeeping genes with similar results. Primer sequences for genes used in this study are listed in Table S2.

2.5 Enzyme activity assays

For enzyme activity assays, we used a slightly modified extraction protocol as previously described by Xie et al. (2009). Approximately 1g of freshly grounded fruit tissues with 1:8 (w/v) of extraction buffer containing 50 mM HEPES-NaOH (pH 7.5), 10 mM $MgCl_2$, 2.5 mM DTT, 1.0 mM EDTA, 0.05% (v/v) Triton X-100, 0.1% (w/v) BSA, 0.1% β-merchaptoethanol, and 2% w/v polyvinylpolypyrrolidone (PVPP). The homogenate was centrifuged at 12,000 g for 15 min to obtain the supernatant. The crude extract was then dialyzed using a cellulose tubing (dialysis membrane with molecular cut-off 14,000 Da; Sigma-Aldrich) for 16 h with 25 mM HEPES-NaOH (pH 7.5) and 0.25 mM disodium-EDTA dialysis buffer. The insoluble pellet was homogenized two times of 10 ml extraction buffer and then resuspended in 3 ml of 50 mM HEPES-NaOH (pH 7.5) and 0.5 mM disodium-EDTA. The pellets were further washed with 200 ml extraction buffer (1:40 v/v) without PVPP to assay the insoluble CWINV. All the extracts were transferred in pre-chilled vials and the analyses were carried out at 0-4°C. The enzyme activities were measured in proportional to the amount of corresponding sugar released to the reaction time.

Activity of VINV and NINV were measured according to Lowell et al. (1989). Amount of 0.3 ml of enzyme extract was incubated for 40 min at 37°C with 80 mM K_3PO_4-acetate (pH 4.5) and 500 mM sucrose in a total volume of 1 ml. The reaction was stopped at 30 min by adding 600 µl of 1% (w/v) 3,5

dinitro salicylic acid (DNS) and boiling for 5 min. Absorbance was read at 540 nm in a spectrophotometer (Smart Spec; Bio-Rad, Hercules, California, USA). CWINV activity assay was carried out from the extracts of insoluble pellets washed with extraction buffer without PVPP. The activity of invertases was expressed as amount of glucose (µmol) produced h^{-1} g^{-1} of sample fresh weight (FW).

SPS and SS activity were measured according to Zhang et al. (2011). The reaction solution consists of 0.5 M HEPES-NaOH (pH 7.5), 0.14 M $MgCl_2$, 0.028 M disodium EDTA, 0.112 M fructose-6-phosphate (F6P) and 0.042 M uridine diphosphate glucose (UDP-G). Amount of 85 µl of crude enzyme extract was mixed with 55 µl of reaction solution. The mixture was then incubated for 40 min at 37°C and then the reaction was terminated by adding 70 µl of 1.0 M NaOH. Non-reacted F6P was degraded by keeping samples in 100°C for 10 min. After cooling, 0.25 ml of resorcinol solution (w/v dissolved in 95% ethanol) and 0.75 ml of 35% HCl (v/v) were added into the mixture and the tubes were incubated at 80°C for 8 min. SS and SPS were measured the same way except by replacing of F6P with 0.084 M fructose in reaction mixtures. The amount of sucrose produced was calculated from the standard curve derived from sucrose standard concentrations and the absorbance values measured at 520 nm were expressed as µmol of sucrose generated h^{-1} g^{-1} FW.

Starch degradation activity by α-amylase and β-amylase were measured according to Hagenimana et al. (1994). Amount of 0.25 ml of 100 mM phosphate buffer (pH 6.0), 0.25 ml of enzyme extract and 0.5 ml of 1% (g ml^{-1}) starch solution were mixed together. The reaction mixtures were pre-incubated for 5 min at 40°C and terminated by adding 1 ml of 0.4 M NaOH. The generated reducing sugars were determined by DNS reagent based on Miller (1959). For α-amylase activity, we followed the same procedure, but the enzyme extract was pre-incubated at 15 min at 70°C to deactivate β-amylase. The activity of β-amylase was determined by the difference in total amylase and α-amylase activity and expressed as amount of maltose produced h^{-1} g^{-1} FW.

2.6 Measurement of sugar content

Part of the berry samples ground for RNA extraction were dried in a freeze dryer (Virtis benchtop-K; SP Scientific, Gardiner, NY, USA). The dried sample powder of 0.1 g was extracted with 12 ml water containing 0.12 g PVPP in an orbital shaker for 1.5 h. The extracts were centrifuged at 4500 g for 10 min and the supernatant was filtered using a 0.2 µm filter (Merck-Millipore, NJ, USA) and stored in -20°C until used for sugar content analysis.

Total sugar content was analyzed according to the phenol-sulfuric acid method described by Nielsen et al. (2010). Amount of 100 µl of the sample was added with 1.9 ml of water to make it a 2-ml sample volume followed by 0.05 ml of 80 % of phenol. Samples were mixed vigorously. After constant shaking, 5 ml of sulfuric acid was added to the sample mixture. The samples were incubated in room temperature

for 10 min and the tubes were kept at 25°C for 10 min. Finally, the absorbance was read at 490 nm and quantified against a glucose standard curve.

Individual soluble sugars were analyzed using Sucrose/D-Glucose/D-Fructose assay kit (R-biopharm, Darmstadt, Germany). All samples were analyzed in triplicates and the absorbances were measured at 340 nm with the spectrophotometer. The absorbance difference for each sugar was calculated using the formula provided by the manufacturer.

2.7 Statistical analysis

The comparison of means from the concentrations of sugar were analyzed by one-way ANOVA. The means-comparison was followed by Tukey's post-hoc test. All the visualizations and ANOVA were performed in Origin pro software v2021b (OriginLab Corporation, Northampton, MA, USA).

3. Results and discussion

3.1 Sugar content during bilberry fruit development

The total sugar content analyzed by phenol-sulfuric acid method showed that the highest sugar levels were found in fully ripe S5 berries followed by the S4 berries, while the lowest sugar content was found on S3 berries (Table 1). The results were confirmed by the total amount of individual sugars. A recent study in strawberries has shown similar pattern of soluble sugar accumulation with a decrease in middle stage followed by an increase in later developmental stages (Wang et al., 2018).

From the individual soluble sugars quantification, the fructose concentration was slightly higher than glucose concentrations and the sucrose concentration was much lower than fructose and glucose (Table 1). In earlier studies, fructose was found to be the predominant sugar in bilberry fruits followed by glucose, and sucrose is found in relatively low amounts (Milivojević et al., 2012; Mikulic-Petkovsek et al., 2015; Uleberg et al., 2012). Fructose and glucose levels showed similar trends in concentration during ripening. In small unripe green fruit (S2), fructose and glucose concentration were measured at 80 mg g^{-1} DW and 70 mg g^{-1} DW, respectively, before decreasing nearly by two-fold at S3 stage, and then increasing by approximately 1.5 times at S4 stage. In the final maturation stage (S5), the fructose concentration was 225 mg g^{-1} DW and glucose concentration 161 mg g^{-1}. The sucrose concentration was 4 mg g^{-1} DW in S2 stage and increased slightly in later stages of fruit development and ripening (Table 1).

3.2 Identification and phylogenetic analysis of sugar metabolism related gene families in bilberry

The genes coding for sugar metabolism-enzyme families such as CWINV, VINV, NINV, HK, FK, SPP, SPS and SS were retrieved from the available transcriptome datasets on *Vaccinium* species. Altogether, 25 sugar metabolism pathway genes were identified; three isoforms of CWINV, two isoforms of VINV, five isoforms of NINV, five isoforms of HK, five isoforms of FK, two isoforms of SPP, four isoforms of SPS and four isoforms of SS. All the identified *V. virgatum* sequences, with their matching sequences from TSA database and corresponding bilberry sequences retrieved from SRA transcriptome datasets are presented in the Supplementary Table 1.

We used Plant-mSubP online tool to predict the subcellular localization of the invertases, as it is one of the differentiating factors to classify its types. It is performed to confirm the precise subcellular localization of identified genes belonging to invertases class based on signal peptides (Table S1). Although, it is widely believed that neutral invertases are only found in cytoplasm, a previous study has shown that it can be found on plastids also (Murayama and Handa, 2007). From our analysis, three isoforms were predicted; NINV 1,2 & 4, which are most likely to be present on plastids than in the cytoplasm. Another study showed that sucrose could enter inside plastids, but the metabolism of sucrose by invertases inside that organelle are relatively unknown (Gerrits et al., 2001).

A phylogenetic tree was constructed using sequences of *V. myrtillus* sugar genes with sequences from related fruit species such as apple, strawberry, peach and grapevine is shown for its evolutionary relationship (Fig, 2). The phylogenetic tree shows that HK and FK were grouped in similar branches from the main clade because of its similar phosphorylating nature of hexoses (Granot et al., 2014), whereas CWINV and VINV were grouped in the same branches considering both are acid invertases (Roitsch, & González, 2004). Likewise, SS and SPS were branched from the next major clade and NINV was found in the distant clade grouped together with SPP (Fig. 2).

3.3 Expression of sugar metabolism genes during bilberry fruit development

The relative gene expression levels of all identified gene isoforms were determined by using qRT-PCR during berry development. The expression pattern of all three isoforms of *CWINV* was different from one another (Fig. 3a). *VmCwINV1* expression was low in S3 and S4 fruits, but slightly higher in the ripening stage S5, whereas *VmCwINV2* showed 4 times higher expression in S3 than in the S2. In later stages of ripening (S4 and S5), there was no expression of the *VmCwINV2*. The *VmCwINV3* showed slightly lower expression in S3 than in S2, whereas it showed similar expression in S4 and again decreased its expression in fully ripe fruit (Fig. 3a). However, the expression of *VmCwINV3* did not vary significantly across the different fruit development and ripening stages (Fig. 3a). CWINVs are vital

during sink organs development such as fruit and play a major role in fruit setting (Ru et al., 2017). These are the key partitioning enzymes once the sucrose is transported from source tissues and upregulate the sink strength in fruits (Roitsch & González, 2004). From our results, we can infer that all these differently expressed isoforms of *CWINV* might have distinct functions at certain developmental stages.

The expression of *VmVINV1* showed increment from S3 to S5. *VmVINV1* had the highest expression in S5 (Fig. 3b). *VmVINV2* showed a 13-fold higher expression in ripening purple fruit, whereas the expression of *VmVINV2* decreased significantly in fully ripe blue fruit. The expression of *VmVINV2* was also found negligible in green unripe fruit stages (Fig. 3b). Since VINV determine the storage and resynthesis of sucrose in vacuoles at mature stages of fruit development (Hussain et al., 2001; Tang et al., 1999), we speculate that the increase in expression levels of two isoforms of *VINV*s at the ripening stages S4 and S5 could be responsible for maintaining the sugar balance in such organelles and in ripe bilberries.

The expression pattern of three isoforms of neutral invertases (*VmNINV1,2 & 3*) were similar among small green unripe fruit and large green unripe fruit. All three genes were slightly lower expressed in large green unripe fruit than in small green unripe fruit. *VmNINV1* had the highest expression in ripening red colored fruit (S4), and *VmNINV2* had the highest expression in blue-colored S5 fruit. *VmNINV3* had lower expression in S4 and expression of *VmNINV3* in the other three ripening stages was similar. *VmNINV4* had similar expression in S3 and S5 stages, and expression in these two stages were higher than in the small unripe green fruit (S2). *VmNINV5* also had much lower transcript levels in S4 and S5 fruit (Fig. 3c). A direct correlation of neutral invertases activity to that of fructose-to-glucose ratios has earlier been shown in fruits (Desnoues et al., 2014). Our results show that NINVs were expressed in all the developmental stages during bilberry fruit development. This indicates that higher NINV activity means an increase in fructose amounts in all developmental stages achieved by the segregation of sucrose in the cytoplasm (Ran et al., 2017).

The hexose phosphorylating enzymes, HKs and FKs, *VmHK1*, *VmHK2* and *VmHK4* isoforms were similarly expressed between developmental stages S2-S3. Afterwards, *VmHK2* increased expression rapidly and to some extent by *VmHK1* in stages 4 and 5, unlike other isoforms, which were not altered significantly (Fig. 4a). Glucose can only be phosphorylated by HKs, while fructose will be phosphorylated by both HKs and FKs, although the affinity towards fructose moieties will be higher in FKs (Granot, 2013). From our results, all the FKs, except *VmFK5* (*VmFK1,2,3 & 4*), rapidly increased expression after stage 2, and increased further with the highest expression level found on stage 3 berries. However, during late developmental stages 4 and 5, the expression levels fall down dramatically (Fig. 4b). The HKs and FKs are showing an interesting opposite expression pattern in early and late berry developmental stages (Fig. 4). The result suggests that an increase in fructose content can be attributed

by the interplay of FKs in the beginning of ripening and by both FKs and HKs at late berry developmental stages.

Finally, in regards with the sucrose metabolism enzymes, expression of *VmSPS1* increased in late stages, whereas, *VmSPS2* and *VmSPS3* expression in stages 4 and 5 was low. *VmSPS2* was highest in stage 3 berries (Fig. 5a). SPS is the key enzyme involved in the sucrose resynthesis and an increase in expression at the onset of ripening implies that sucrose is recycled actively, especially at S3 stage. It could also be correlated with the increase in sucrose content at same stage (Table 1), as previously shown in another study (Vimolmangkang et al., 2016). SPP did not show significant variation across developmental stages, except at S4 where *VmSPP1, VmSPP2* levels slightly increased (Fig. 5b). The only characterized and expressed sucrose synthase isoform *VmSS* was also higher in early berry development and tended to decrease lately (Fig. 5c). A similar trend was shown in kiwifruit ripening, where SS was shown to be involved in post sucrose-unloading pathways (Chen et al., 2017).

3.4 Sugar related enzyme activities across bilberry developmental stages

Enzyme activities of CWINV, VINV were not detected or were only found in very low levels in early developmental stages (S2, S3), but increased rapidly from S3 on with the highest activity found in S5 berries (Fig. 6). Generally, CWINVs are considered sink-specific enzyme, which should be involved in sucrose unloading very early in berry development, but some studies have shown that gene expression and enzyme activities of CWINVs are lower in fruits and may not be directly related in apoplastic sucrose unloading in the beginning of ripening (Li et al., 2012). Contrastingly, NINV activity was found early in S2 berries and then the activity increased later at fully ripe S5 berries (Fig. 6). Activities of both sucrose metabolism enzymes SS and SPS were also detected in unripe berries and those tend to increase only at later stages. Both of these enzymes have an opposite enzyme activity at S3, which might be the critical stage in sucrose resynthesis occurring in bilberry fruits (futile cycle). SPS activity was highest in S3 whereas SS activity was lowest at the same stage (Fig. 6). Our results are consistent with earlier studies, as previously demonstrated that SS activities are often higher than NINVs as the former produces reversible conversion and better homeostasis in sink tissues (Moscatello et al., 2011). SS is also likely to be involved in starch accumulation in plastids at the beginning of fruit ripening (Ross et al., 1994). However, degradation of starch occurs during late berry development in amyloplasts. The activities of both of the starch-degrading amylases (α, β amylases), were only found increased in fully ripe berries at S5, and not detected in other stages of bilberry fruit development (Fig. 6).

3.5 Effect of light spectral quality in bilberry sugar metabolism

Sugar concentrations of glucose and fructose were significantly higher in red light treatment (165 and 210 mg g^{-1} DW, respectively), when compared with control (Fig. 7b). Blue light also slightly increased glucose and fructose content in ripe berries but was not found significantly different (141 and 166 mg g^{-1} DW). Sucrose levels were found to be very low across the light treatments (2-3.5 mg g^{-1} DW) and they were not found to be significantly affected by the supplemental light treatments (Fig. 7b).

The top DEGs obtained between the control and light treatments (red, blue) were visualized and shown as heatmap with log2-fold changes (Log2 FC) (Fig. 7a). Both light treatments up-regulated α-amylase and β-amylases, which are the key genes involved in starch degradation in plastids (Fig. 7a). Red light up-regulated β-amylase levels up to 3-folds, which indicates that maltose levels have been elevated inside amyloplasts, which subsequently can be converted to other hexoses such as glucose, thus adding sweetness or flavor to the fully ripe fruit (Xiao et al., 2018). Blue light down-regulated the hexose inter-conversion enzymes involved in galactose metabolism such as phosphoglucomutase (PGM), α-galactosyltransferse (α-gal) and UDP-glycopyrophophorylase (UDPG-PP) (Fig. 7a). On the other hand, red light upregulated α-galactosyltransferse gene, which is likely to be involved in deriving sugar alcohols. Other key enzymes arising from galactose metabolism, such as galactinol synthase (GS), UDP-galactose epimerase (UGE) and raffinose synthase (RFS), were also up-regulated in red light treatment (Fig. 7a). Comparatively, blue light up-regulated hexose phosphorylating enzymes such as HK, FK and PFK genes more than red light. The VINV were up-regulated by both light treatments (Fig. 7a). The result suggests that the degradation of sucrose to hexoses, which was highly upregulated in response to light treatment was mostly occurring in vacuolar spaces by VINVs than in the cytosol by the NINVs (Rabot et al., 2014). Likewise, it is also evidenced by the NINVs, which are lowly expressed under light treatments. All the CWINV were down-regulated under light treatments. The result is consistent with the earlier studies which have shown that CWINV activities are reduced under abiotic stress during fruit set and are the most targeted during altered circadian rhythm (Liu et al., 2016; Proels & Hückelhoven, 2014). Sucrose enzymes such as SS and SPP were up-regulated under red-light whereas, SPP and SPS were down-regulated under blue light (Fig. 7a).

Conclusion

In the current study, we have identified and analyzed the sugar metabolism encoding genes in bilberry across fruit developmental stages through enzyme activities and related gene expression. The results shown that the gene expression and enzyme activities of acid invertases were low in the beginning of bilberry development, and detected rapid increases in the expression of the enzyme genes producing irreversible sucrose conversions at later stages. Our results indicate that SS is most likely the key enzyme

involved in the reversible sucrose conversions, as both its activity and expression levels were found consistent across all the four bilberry developmental stages. All the invertases, hexose-kinases and sucrose resynthesizing enzymes at the last ripening stage contributed to the final accumulation of sugars in fully ripe berries, where fructose and glucose were found as the most abundant sugars. In response to light spectral quality, we have shown that both red and blue supplemental light irradiation trigger degradation of starch, which is stored in amyloplasts, and likely contributes to the increase in hexoses content. In addition, both light qualities have negative impact on CWINV, but the up-regulation in both hexose-kinases and vacuolar invertases are responsible for the increase in glucose and fructose content under red light. Further, red light increased sugar concentrations of bilberries. This study provides the first comprehensive report on bilberry sugar metabolism, and provides an ideal platform towards further functional genomics studies on improving the berry fruit quality.

Acknowledgments

The authors would like to thank Leidulf Lund for the technical help in setting up light experiments at the Phytotron facility at UiT The Arctic University of Norway. The work was financially supported by NordPlant (NordForsk grant no. 84597).

Author contributions

LJ and KK conceptualized the project. AS performed the enzyme activity assays, analyzed the data, and wrote the manuscript. BD and KK performed the gene expression analyses. KK with contribution of BD quantified the sugar content. LJ, KK and IM contributed to the editing and proofreading of the manuscript draft. All authors have read and approved the manuscript.

Conflict of interest

The authors declare that they have no conflicts and competing interests.

References

Akšić, M. F., Tosti, T., Sredojević, M., Milivojević, J., Meland, M., & Natić, M. (2019). Comparison of sugar profile between leaves and fruits of blueberry and strawberry cultivars grown in organic and integrated production system. *Plants*, 8(7). https://doi.org/10.3390/plants8070205

Althammer, M., Blöchl, C., Reischl, R., Huber, C. G., & Tenhaken, R. (2020). Phosphoglucomutase is not the target for galactose toxicity in plants. *Frontiers in plant science*, 11(February), 1–9. https://doi.org/10.3389/fpls.2020.00167

Borsani, J., Budde, C. O., Porrini, L., Lauxmann, M. A., Lombardo, V. A., Murray, R. ... Lara M.V. (2009). Carbon metabolism of peach fruit after harvest: Changes in enzymes involved in organic acid and sugar level modifications. *Journal of Experimental Botany*, 60(15), 1823–1837.

Brummell, D. (2006). Cell wall disassembly in ripening fruit. *Functional Plant Biology*, 33(2), 103. doi: https://doi.org/110.1071/fp05234

Chen, C., Yuan, Y., Zhang, C., Li, H., Ma, F., & Li, M. (2017). Sucrose phloem unloading follows an apoplastic pathway with high sucrose synthase in *Actinidia* fruit. *Plant Science*, 255, 40–50. https://doi.org/10.1016/j.plantsci.2016.11.011

Chen, X. li, Wang, L. chun, Li, T., Yang, Q. chang, & Guo, W. zhong. (2019). Sugar accumulation and growth of lettuce exposed to different lighting modes of red and blue LED light. *Scientific Reports*, *9*(1), 1–10. https://doi.org/10.1038/s41598-019-43498-8

Cho, Y. G., & Kang, K. K. (2020). Functional analysis of starch metabolism in plants. *Plants*, 9(9), 1–6. https://doi.org/10.3390/plants9091152

Dai, Z., Wu, H., Baldazzi, V., van Leeuwen, C., Bertin, N., Gautier, H., … Génard, M. (2016). Inter-species comparative analysis of components of soluble sugar concentration in fleshy fruits. *Frontiers in Plant Science*, 7 (May2016), 1–12. https://doi.org/10.3389/fpls.2016.00649

Decker, D., & Kleczkowski, L. A. (2019). UDP-sugar producing pyrophosphorylases: Distinct and essential enzymes with overlapping substrate specificities, providing de novo precursors for glycosylation reactions. *Frontiers in Plant Science*, 9(January). https://doi.org/10.3389/fpls.2018.01822

Desnoues, E., Gibon, Y., Baldazzi, V., Signoret, V., Génard, M., & Quilot-Turion, B. (2014). Profiling sugar metabolism during fruit development in a peach progeny with different fructose-to-glucose ratios. *BMC Plant biology*, 14(1), 12–14. https://doi.org/10.1186/s12870-014-0336-x

Gangl, R., & Tenhaken, R. (2016). Raffinose family oligosaccharides act as galactose stores in seeds and are required for rapid germination of Arabidopsis in the dark. *Frontiers in Plant Science*, 7(July2016), 1–15. https://doi.org/10.3389/fpls.2016.01115

Granot, D, Kelly, G Stein, O, David-Schwartz, R. (2014) Substantial roles of hexokinase and fructokinase in the effects of sugars on plant physiology and development, *Journal of Experimental Botany*, Volume 65, Issue 3, March 2014, Pages 809–819, https://doi.org/10.1093/jxb/ert400

Granot, D., David-Schwartz, R., & Kelly, G. (2013). Hexose kinases and their role in sugar-sensing and plant development. *Frontiers in plant science*, 4(MAR), 1–17. https://doi.org/10.3389/fpls.2013.00044

Hagenimana, V., Vézina, L.-P, & Simard, R. E. (1994). Sweetpotato α- and β-Amylases: Characterization and Kinetic Studies with Endogenous Inhibitors. *Journal of Food Science*, *59*(2), 373–376. doi:https://doi.org/10.1111/j.1365-2621.1994.tb06970.x

Hao-Ran, W., Jia-Yu, Y., Tong-Tong, Z., Na, C., Sheng, H., Rui, Z., & Si-Qiong, X. (2017). Relationship between neutral invertase activity and sugar contents in tomato fruit and its functional prediction analysis. *Biotechnology journal international*, 20(1), 1–6. https://doi.org/10.9734/bji/2017/37195

Hu, W., Sun, D. W., Pu, H., & Pan, T. (2016). Recent Developments in Methods and Techniques for Rapid Monitoring of Sugar Metabolism in Fruits. *Comprehensive Reviews in Food Science and Food Safety*, 15(6), 1067–1079. https://doi.org/10.1111/1541-4337.12225

Husain, S. E., Thomas, B. J., Kingston-Smith, A. H., & Foyer, C. H. (2001). Invertase protein, but not activity, is present throughout development of *Lycopersicon esculentum* and *L. pimpinellifolium* fruit. *New Phytologist*, 150(1), 73–81. https://doi.org/10.1046/j.1469-8137.2001.00064.x

Jia, H., Wang, Y., Sun, M., Li, B., Han, Y., Zhao, Y., … Jia, W. (2013). Sucrose functions as a signal involved in the regulation of strawberry fruit development and ripening. *New Phytologist*, 198(2), 453–465. https://doi.org/10.1111/nph.12176

John P. Hammond, Philip J. White. (2008) Sucrose transport in the phloem: integrating root responses to phosphorus starvation, *Journal of Experimental Botany*, Volume 59, Issue 1, January, Pages 93–109, https://doi.org/10.1093/jxb/erm221

Kähkönen, M. P., Heinämäki, J., Ollilainen, V., & Heinonen, M. (2003). Berry anthocyanins: Isolation, identification and antioxidant activities. *Journal of the Science of Food and Agriculture*, 83(14), 1403–1411. https://doi.org/10.1002/jsfa.1511

Karppinen, K., Hirvelä, E., Nevala, T., Sipari, N., Suokas, M., & Jaakola, L. (2013). Changes in the abscisic acid levels and related gene expression during fruit development and ripening in bilberry (*Vaccinium myrtillus* L.). *Phytochemistry*, 95, 127-134. doi: https://doi.org/10.1016/j.phytochem.2013.06.023

Karppinen, K., Tegelberg, P., Häggman, H., & Jaakola, L. (2018). Abscisic acid regulates anthocyanin biosynthesis and gene expression associated with cell wall modification in ripening bilberry (*Vaccinium myrtillus* L.) fruits. *Frontiers in Plant Science*, 9(August), 1–17. https://doi.org/10.3389/fpls.2018.01259

Li, M., Feng, F., & Cheng, L. (2012). Expression patterns of genes involved in sugar metabolism and accumulation during apple fruit development. *PLoS ONE*, 7(3). https://doi.org/10.1371/journal.pone.0033055

Li, Y., Xin, G., Wei, M., Shi, Q., Yang, F., & Wang, X. (2017). Carbohydrate accumulation and sucrose metabolism responses in tomato seedling leaves when subjected to different light qualities. *Scientia horticulturae*, *225*(March), 490–497. https://doi.org/10.1016/j.scienta.2017.07.053

Liu, Y. H., Offler, C. E., & Ruan, Y. L. (2016). Cell wall invertase promotes fruit set under heat stress by suppressing ROS-independent cell death. *Plant Physiology*, 172(1), 163–180. https://doi.org/10.1104/pp.16.00959

Loescher, W. (1987). Physiology and metabolism of sugar alcohols in higher plants. *Physiologia plantarum*, 70(3), 553-557. doi: https://doi.org/10.1111/j.1399-3054.1987.tb02857.x

Lowell, C. A., Tomlinson, P. T., & Koch, K. E. (1989). Sucrose-Metabolizing Enzymes in Transport Tissues and Adjacent Sink Structures in Developing Citrus Fruit. *Plant Physiology*, *90*(4), 1394–1402. https://doi.org/10.1104/pp.90.4.1394

Mikulic-Petkovsek, M., Schmitzer, V., Slatnar, A., Stampar, F., & Veberic, R. (2015). A comparison of fruit quality parameters of wild bilberry (Vaccinium myrtillus L.) growing at different locations. *Journal of the Science of Food and Agriculture*, 95(4), 776–785. https://doi.org/10.1002/jsfa.6897

Milivojević, J., Maksimović, V., Dragišić Maksimović, J., Radivojević, D., Poledica, M., & Ercisli, S. (2012). A comparison of major taste-and health-related compounds of Vaccinium berries. *Turkish journal of biology*, 36, 738-745. doi: https://doi.org/10.3906/biy-1206-39

Miller, G. L. (1959). Use of Dinitrosalicylic Acid Reagent for Determination of Reducing Sugar. *Analytical chemistry*, 31(3), 426–428. https://doi.org/10.1021/ac60147a030

Moing, A. (2000). Sugar alcohols as carbohydrate reserves in some higher plants. *Developments in crop science*, 337-358. doi: https://doi.org/10.1016/s0378-519x(00)80017-3

Moscatello, S., Famiani, F., Proietti, S., Farinelli, D., & Battistelli, A. (2011). Sucrose synthase dominates carbohydrate metabolism and relative growth rate in growing kiwifruit (*Actinidia deliciosa*, cv Hayward). *Scientia Horticulturae*, *128*(3), 197–205. https://doi.org/10.1016/j.scienta.2011.01.013

Murayama, S., & Handa, H. (2007). Genes for alkaline/neutral invertase in rice: Alkaline/neutral invertases are located in plant mitochondria and also in plastids. *Planta*, 225(5), 1193–1203. https://doi.org/10.1007/s00425-006-0430-x

Nguyen, N., Suokas, M., Karppinen, K., Vuosku, J., Jaakola, L., & Häggman, H. (2018). Recognition of candidate transcription factors related to bilberry fruit ripening by de novo transcriptome and qRT-PCR analyses. *Scientific reports*, 8(1), 1–12. https://doi.org/10.1038/s41598-018-28158-7

Nguyen-Quoc, B., & Foyer, C. (2001). A role for 'futile cycles' involving invertase and sucrose synthase in sucrose metabolism of tomato fruit. *Journal of experimental botany*, 52(358), 881-889. doi: https://doi.org/10.1093/jexbot/52.358.881

Nielsen, S. S. (2010). Phenol-Sulfuric Acid Method for Total Carbohydrates. In S. S. Nielsen (Ed.), *Food Analysis Laboratory Manual* (pp. 47-53). Boston, MA: Springer US.

Pires, T. C. S. P., Caleja, C., Santos-Buelga, C., Barros, L., & Ferreira, I. C. F. R. (2020). Vaccinium myrtillus L. Fruits as a Novel Source of Phenolic Compounds with Health Benefits

and Industrial Applications - A Review. *Current pharmaceutical design*, 26(16), 1917–1928. https://doi.org/10.2174/1381612826666200317132507

Proels, R. K., & Hückelhoven, R. (2014). Cell-wall invertases, key enzymes in the modulation of plant metabolism during defence responses. *Molecular plant pathology*, 15(8), 858–864. https://doi.org/10.1111/mpp.12139

Qi X, Ogden EL, Ehlenfeldt MK, Rowland LJ. (2019) Dataset of de novo assembly and functional annotation of the transcriptome of blueberry (*Vaccinium* spp.). *Data Brief*. Aug 12;25:104390.

Rabot, A., Portemer, V., Péron, T., Mortreau, E., Leduc, N., Hamama, L., … Le Gourrierec, J. (2014). Interplay of sugar, light and gibberellins in expression of Rosa hybrida vacuolar invertase 1 regulation. *Plant and Cell Physiology*, 55(10), 1734–1748. https://doi.org/10.1093/pcp/pcu106

Roitsch, T., & González, M. C. (2004). Function and regulation of plant invertases: sweet sensations. *Trends in Plant Science*, 9(12), 606–613. https://doi.org/10.1016/j.tplants.2004.10.009

Rolland, F., Baena-Gonzalez, E., & Sheen, J. (2006). Sugar sensing and signaling in plants: conserved and novel mechanisms. *Annual review of plant biology*, 57, 675–709. https://doi.org/10.1146/annurev.arplant.57.032905.105441

Ross, H., Davies, H., Burch, L., Viola, R., & McRae, D. (1994). Developmental changes in carbohydrate content and sucrose degrading enzymes in tuberising stolons of potato (*Solanum tuberosum*). *Physiologia Plantarum*, 90(4), 748-756. doi: https://doi.org/10.1111/j.1399-3054.1994.tb02533.x

Ruan, Y. L., Jin, Y., Yang, Y. J., Li, G. J., & Boyer, J. S. (2010). Sugar input, metabolism, and signaling mediated by invertase: roles in development, yield potential, and response to drought and heat. *Molecular plant*, 3(6), 942–955. https://doi.org/10.1093/mp/ssq044

Samkumar, A., Jones, D., Karppinen, K., Dare, A. P., Sipari, N., Espley, R. V., … Jaakola, L. (2021). Red and blue light treatments of ripening bilberry fruits reveal differences in signalling through abscisic acid-regulated anthocyanin biosynthesis. *Plant Cell and Environment*, 44(10), 3227-3245. https://doi.org/10.1111/pce.14158

Smeekens S. 2000. Sugar induced signal transduction in plants. *Annual Review of Plant Physiology and Plant Molecular Biology* 51:49–81.

Souleyre, E., Iannetta, P., Ross, H., Hancock, R., Shepherd, L., & Viola, R. et al. (2004). Starch metabolism in developing strawberry (Fragaria x ananassa) fruits. *Physiologia Plantarum*, 121(3), 369-376. doi: https://doi.org/10.1111/j.0031-9317.2004.0338.x

Kumar, S., Stecher, G., Li, M., Knyaz, C & Tamura, K (2018) MEGA X: Molecular Evolutionary Genetics Analysis across computing platforms. *Molecular biology and evolution* 35:1547-1549

Tang, G. Q., Lüscher, M., & Sturm, A. (1999). Antisense repression of vacuolar and cell wall invertase in transgenic carrot alters early plant development and sucrose partitioning. *Plant Cell*, 11(2), 177–189. https://doi.org/10.1105/tpc.11.2.177

Tauzin, A. S., & Giardina, T. (2014). Sucrose and invertases, a part of the plant defense response to the biotic stresses. *Frontiers in plant science*, 5(JUN), 1–8. https://doi.org/10.3389/fpls.2014.00293

Uleberg, E., Rohloff, J., Jaakola, L., Trôst, K., Junttila, O., Häggman, H., & Martinussen, I. (2012). Effects of temperature and photoperiod on yield and chemical composition of northern and southern clones of bilberry (*Vaccinium myrtillus* L.). *Journal of agricultural and food chemistry*, 60(42), 10406–10414. https://doi.org/10.1021/jf302924m

Verma, A.K.; Upadhyay, S.K.; Verma, P.C.; Solomon, S.; Singh, S.B (2011). Functional analysis of sucrose phosphate synthase (SPS) and sucrose synthase (SS) in sugarcane (*Saccharum*) cultivars. *Plant Biology*., 13, 325–332.

Vimolmangkang, S., Zheng, H., Peng, Q., Jiang, Q., Wang, H., Fang, T., … Han, Y. (2016). Assessment of sugar components and genes involved in the regulation of sucrose accumulation in peach fruit. Journal of agricultural and food chemistry, 64(35), 6723–6729. https://doi.org/10.1021/acs.jafc.6b02159

Wan, H., Wu, L., Yang, Y., Zhou, G., & Ruan, Y.-L. (2018). Evolution of Sucrose Metabolism: The Dichotomy of Invertases and Beyond. *Trends in Plant Science*, 23(2), 163-177. doi: https://doi.org/10.1016/j.tplants.2017.11.001

Wang, K., Shao, X., Gong, Y., Zhu, Y., Wang, H., & Zhang, X. et al. (2013). The metabolism of soluble carbohydrates related to chilling injury in peach fruit exposed to cold stress. *Postharvest biology and technology*, 86, 53-61. doi: https://doi.org/10.1016/j.postharvbio.2013.06.020

Wang, S., Song, M., Guo, J., Huang, Y., Zhang, F., Xu, C., … Zhang, L. (2018). The potassium channel FaTPK1 plays a critical role in fruit quality formation in strawberry (*Fragaria* × *ananassa*). *Plant Biotechnology Journal*, 16(3), 737–748. https://doi.org/10.1111/pbi.12824

Xiao, Y. Y., Kuang, J. F., Qi, X. N., Ye, Y. J., Wu, Z. X., Chen, J. Y., & Lu, W. J. (2018). A comprehensive investigation of starch degradation process and identification of a transcriptional activator MabHLH6 during banana fruit ripening. *Plant Biotechnology Journal*, 16(1), 151–164. https://doi.org/10.1111/pbi.12756

Xie, Z. Sen, Li, B., Forney, C. F., Xu, W. P., & Wang, S. P. (2009). Changes in sugar content and relative enzyme activity in grape berry in response to root restriction. *Scientia Horticulturae*, 123(1), 39–45. https://doi.org/10.1016/j.scienta.2009.07.017

Zhang, X. M., Dou, M. A., Yao, L., Du, L. Q., Li, J. G., & Sun, G. M. (2011). Dynamic analysis of sugar metabolism in different harvest seasons of pineapple (*Ananas comosus* L. (Merr.)). *African Journal of Biotechnology*, *10*(14), 2716–2723. https://doi.org/10.5897/ajb10.1284

Zhu, X., Zhang, C., Wu, W., Li, X., Zhang, C., & Fang, J. (2017). Enzyme activities and gene expression of starch metabolism provide insights into grape berry development. *Horticulture Research*, *4*(1), 1–16. https://doi.org/10.1038/hortres.2017.18

Figures and legends

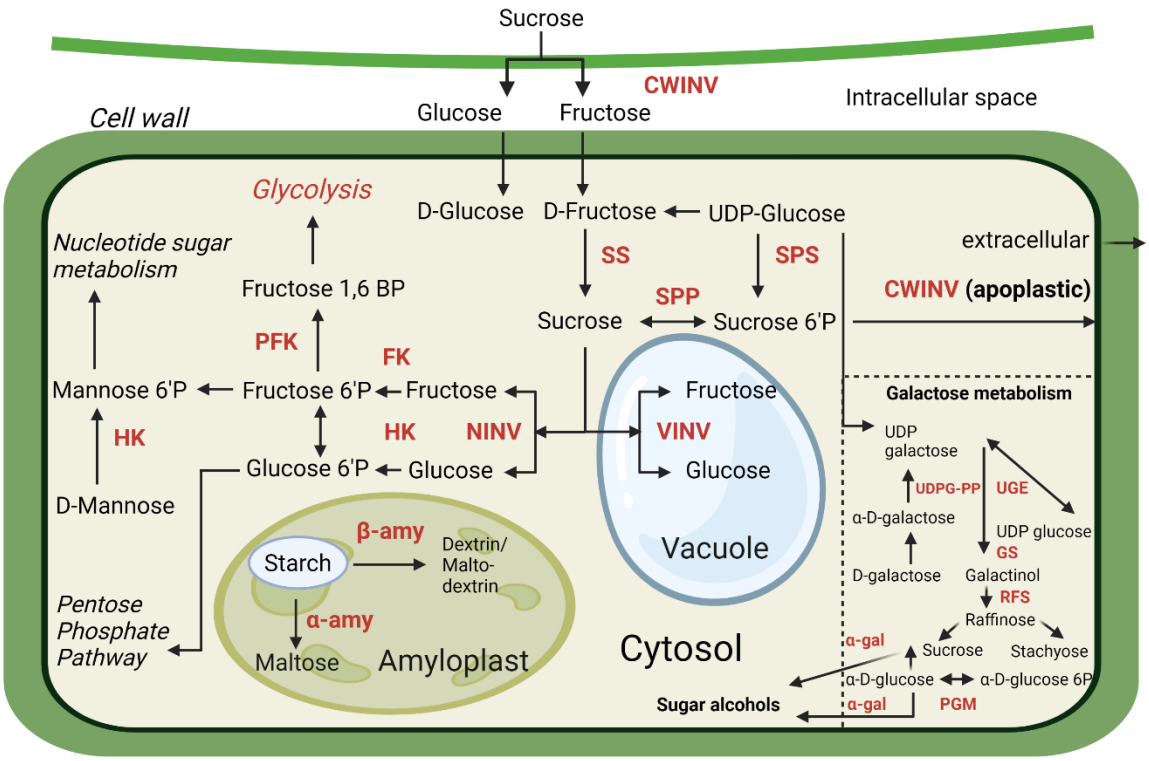

Fig. 1 Schematic representation of sugar metabolism. The key genes discussed in this study are highlighted in red color. *CwINV*, cell wall invertase; *VINV*, vacuolar invertase; *NINV*, neutral invertase; *FK*, fructokinase, *HK*, hexokinase; *SS*, sucrose synthase; *SPS*, sucrose phosphate synthase; *SPP*, sucrose phosphate phosphatase; *α-amy*, α-amylases; *β-amy*, β-amylases. A simple minor pathway presentation of the galactose metabolism and the key genes involved is also shown.

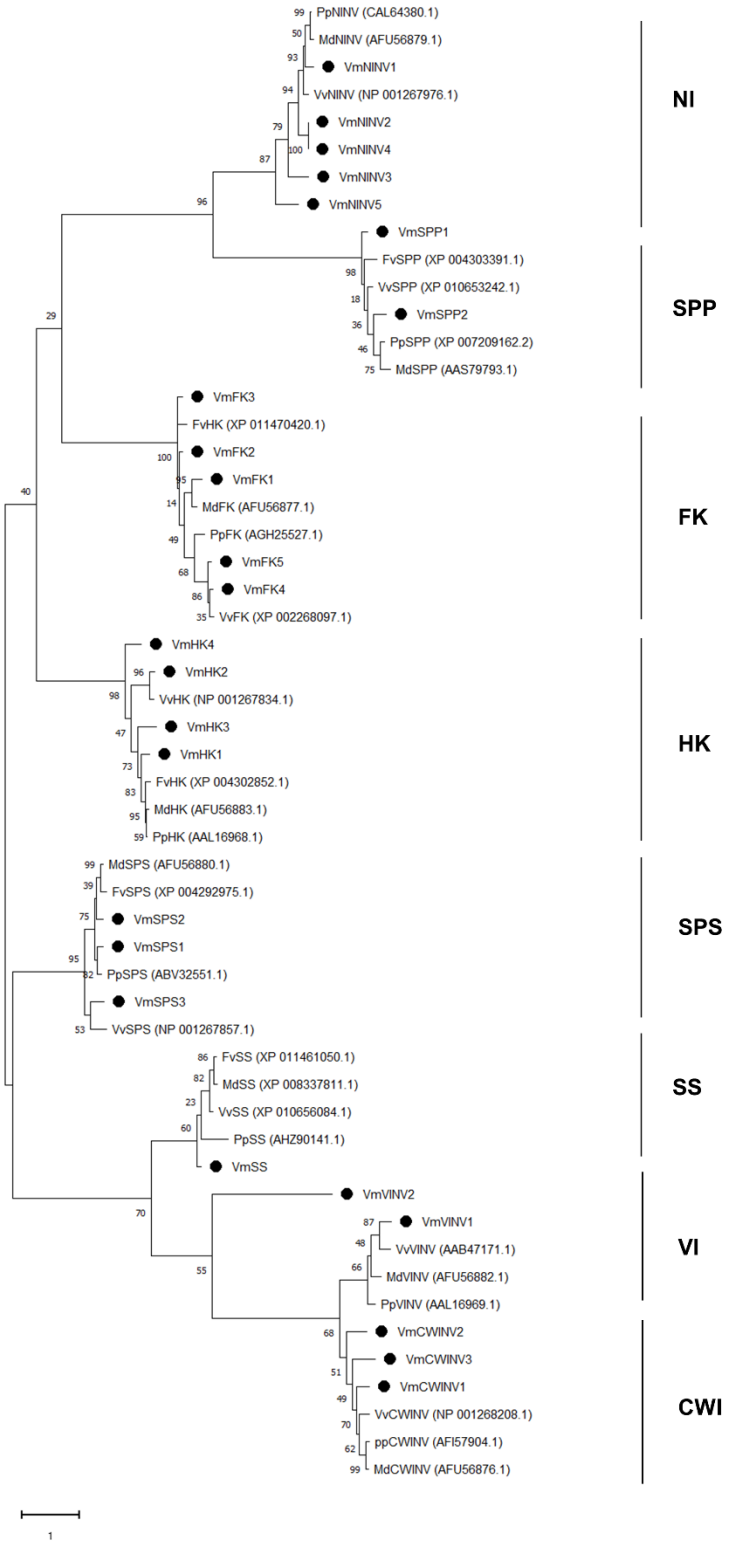
PpNINV (CAL64380.1)
MdNINV (AFU56879.1)
VmNINV1
VvNINV (NP 001267976.1)
VmNINV2
VmNINV4
VmNINV3
VmNINV5
VmSPP1
FvSPP (XP 004303391.1)
VvSPP (XP 010653242.1)
VmSPP2
PpSPP (XP 007209162.2)
MdSPP (AAS79793.1)
VmFK3
FvHK (XP 011470420.1)
VmFK2
VmFK1
MdFK (AFU56877.1)
PpFK (AGH25527.1)
VmFK5
VmFK4
VvFK (XP 002268097.1)
VmHK4
VmHK2
VvHK (NP 001267834.1)
VmHK3
VmHK1
FvHK (XP 004302852.1)
MdHK (AFU56883.1)
PpHK (AAL16968.1)
MdSPS (AFU56880.1)
FvSPS (XP 004292975.1)
VmSPS2
VmSPS1
PpSPS (ABV32551.1)
VmSPS3
VvSPS (NP 001267857.1)
FvSS (XP 011461050.1)
MdSS (XP 008337811.1)
VvSS (XP 010656084.1)
PpSS (AHZ90141.1)
VmSS
VmVINV2
VmVINV1
VvVINV (AAB47171.1)
MdVINV (AFU56882.1)
PpVINV (AAL16969.1)
VmCWINV2
VmCWINV3
VmCWINV1
VvCWINV (NP 001268208.1)
ppCWINV (AFI57904.1)
MdCWINV (AFU56876.1)
NI
SPP
FK
HK
SPS
SS
VI
CWI
1

Fig. 2 Phylogenetic analysis of bilberry sugar metabolism-related genes. The identified bilberry gene isoforms are highlighted with black circles. The sequences were classified into seven enzyme groups in corresponding subclades, neutral invertases (NI), cell wall invertases (CWI), vacuolar invertases (VI), hexokinases (HK), fructokinases (FK), sucrose phosphate phosphatases (SPP), sucrose synthases (SS) and sucrose phosphate synthases (SPS), respectively. Numbers in forks represents… Bar represents… Fv, *Fragaria vesca*; Md, *Malus × domestica*; Pp, *Prunus persica*; Vv, *Vitis vinifera*; Vm, *Vaccinium myrtillus.*

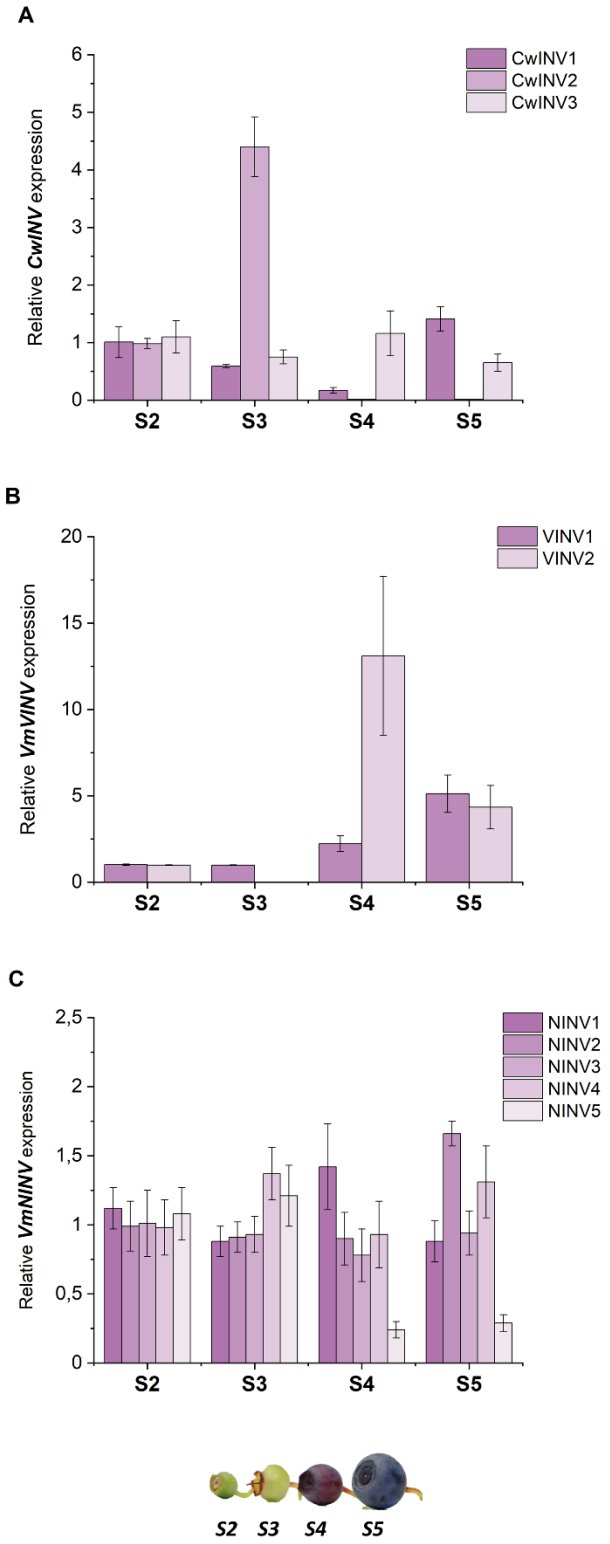

Fig. 3 Relative expression of invertase genes during bilberry fruit development. The relative expression levels of A) *CWINV*, (B) *VINV* and (C) *NINV* were quantified by qRT-PCR. The expression level of gene isoforms was normalized to the level of *VmGAPDH*. S2, small unripe green fruit; S3, large unripe green fruit; S4, ripening purple fruit; S5, fully ripe blue fruit. All the values are means of four biological replicates ± SEM.

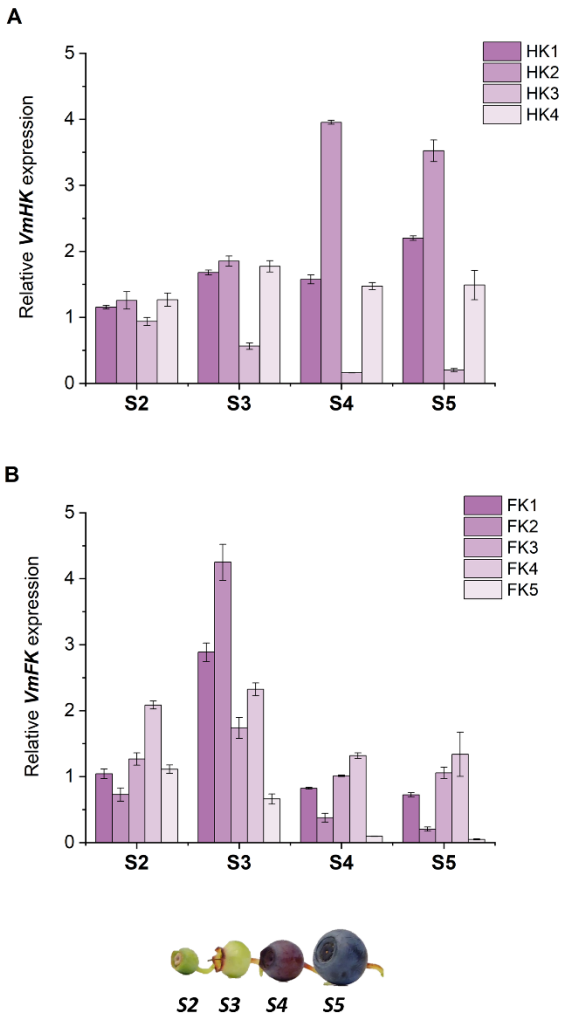

Fig. 4 Relative expression of (A) HK and (B) FK genes during bilberry fruit development. The relative expression levels of genes were quantified by qRT-PCR. The expression level of every gene isoform was normalized to the level of *VmGAPDH*. S2, small unripe green fruit; S3, large unripe green fruit; S4, ripening purple fruit; S5, fully ripe blue fruit. All the values are means of four biological replicates ± SEM.

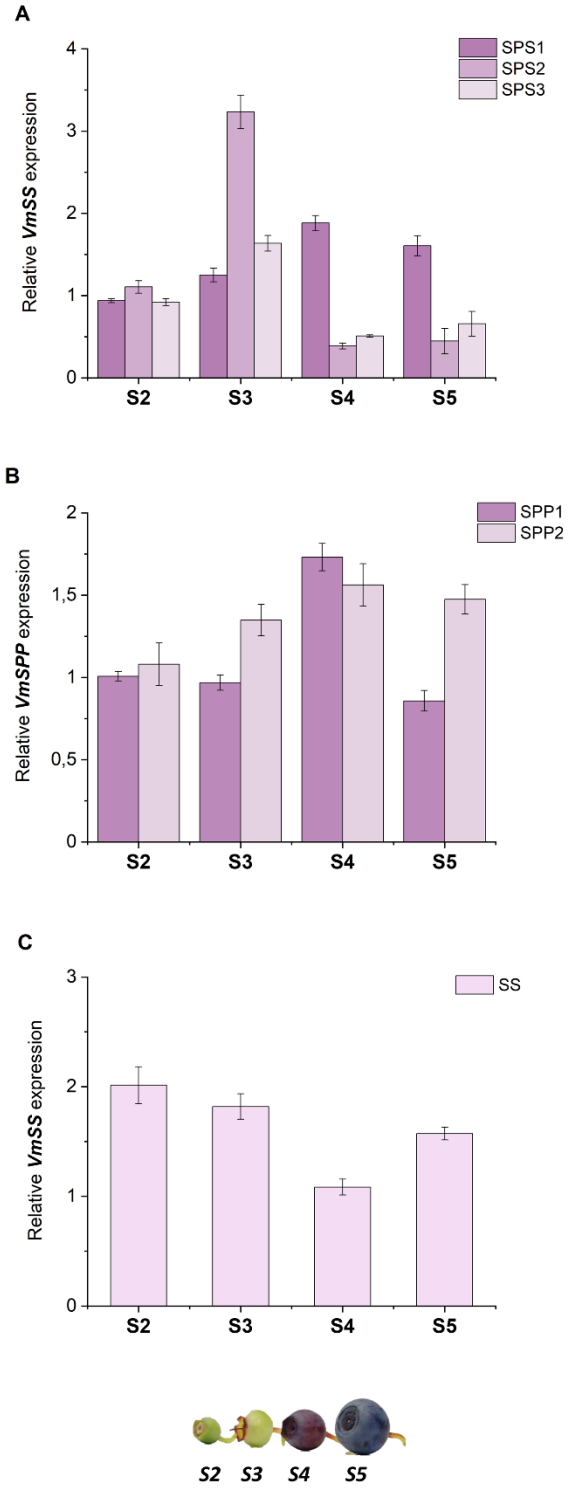

Fig. 5 Relative expression of the sucrose metabolism genes SPS, (A) SPP, (B) SS (C) during bilberry fruit development. The relative expression levels of each gene were quantified by qRT-PCR. The expression level of gene isoforms was normalized to the level of *VmGAPDH*. S2, small unripe green fruit; S3, large unripe green fruit; S4, ripening purple fruit; S5, fully ripe blue fruit. All the values are means of four biological replicates ± SEM.

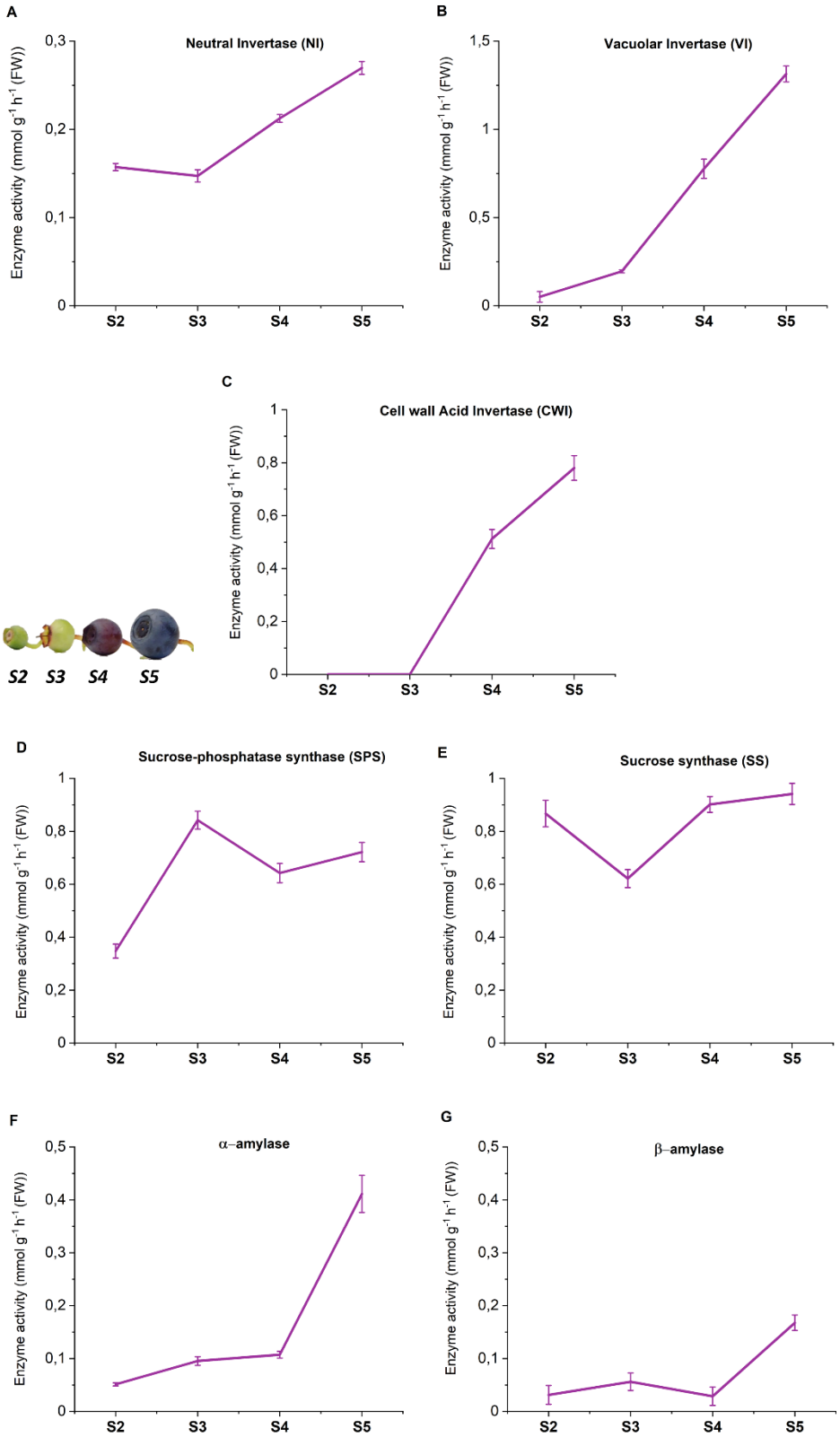
A
Neutral Invertase (NI)
Enzyme activity (mmol g-1 h-1 (FW))
0,3
0,2
0,1
0
S2
S3
S4
S5
B
Vacuolar Invertase (VI)
Enzyme activity (mmol g-1 h-1 (FW))
1,5
1
0,5
0
S2
S3
S4
S5
C
Cell wall Acid Invertase (CWI)
Enzyme activity (mmol g-1 h-1 (FW))
1
0,8
0,6
0,4
0,2
0
S2
S3
S4
S5
S2
S3
S4
S5
D
Sucrose-phosphatase synthase (SPS)
Enzyme activity (mmol g-1 h-1 (FW))
1
0,8
0,6
0,4
0,2
0
S2
S3
S4
S5
E
Sucrose synthase (SS)
Enzyme activity (mmol g-1 h-1 (FW))
1
0,8
0,6
0,4
0,2
0
S2
S3
S4
S5
F
α–amylase
Enzyme activity (mmol g-1 h-1 (FW))
0,5
0,4
0,3
0,2
0,1
0
S2
S3
S4
S5
G
β–amylase
Enzyme activity (mmol g-1 h-1 (FW))
0,5
0,4
0,3
0,2
0,1
0
S2
S3
S4
S5

Fig.6 Changes in enzyme activities related to sucrose and starch metabolism during bilberry fruit development. The enzyme activities were expressed in amounts of corresponding sugar released per hour from fresh weight (FW) used in each assay. The values represent mean ± SEM of four biological replicates. S2, small unripe green fruit; S3, large unripe green fruit; S4, ripening purple fruit; S5, fully ripe blue fruit.

A

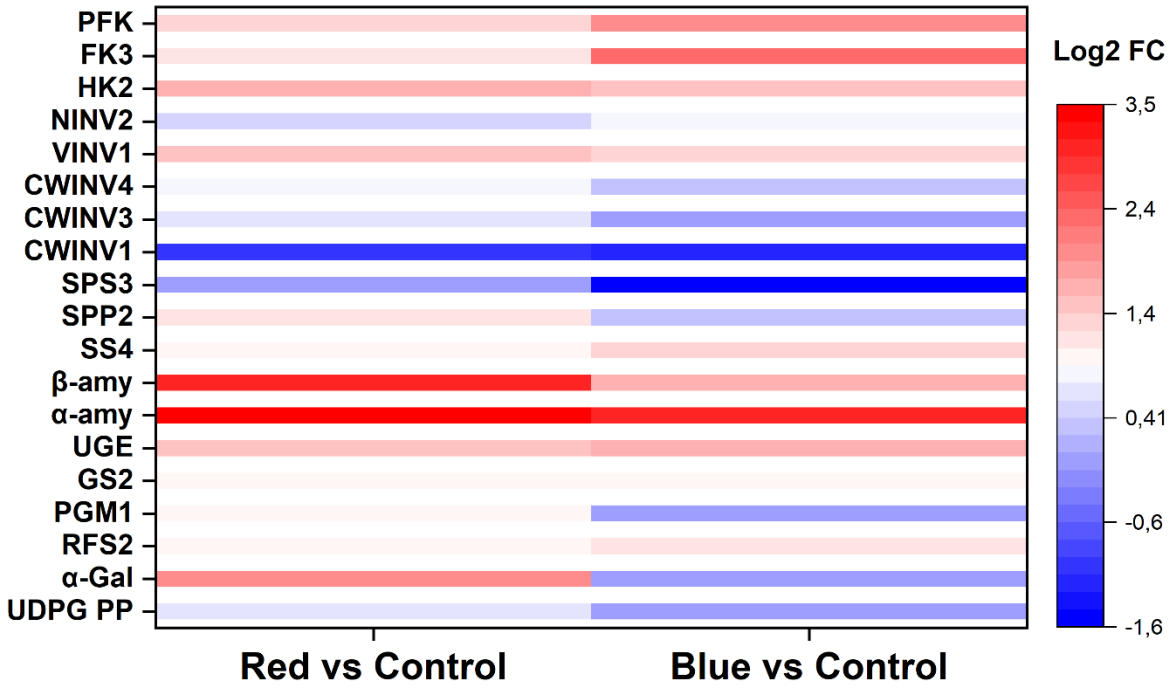
PFK
FK3
HK2
NINV2
VINV1
CWINV4
CWINV3
CWINV1
SPS3
SPP2
SS4
β-amy
α-amy
UGE
GS2
PGM1
RFS2
α-Gal
UDPG PP
Red vs Control
Blue vs Control
Log2 FC
3,5
2,4
1,4
0,41
-0,6
-1,6

B

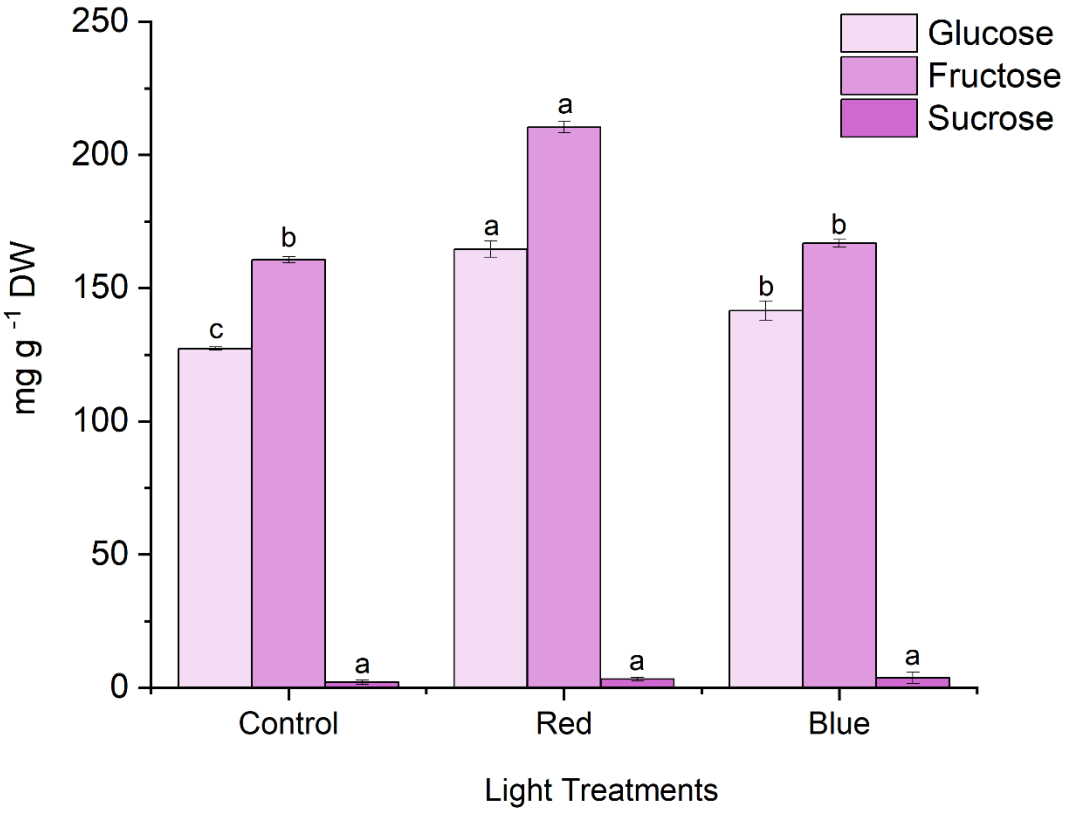
Glucose
Fructose
Sucrose
mg g -1 DW
250
200
150
100
50
0
a
b
c
a
a
a
b
b
a
Control
Red
Blue
Light Treatments

Fig.7 Differentially expressed genes (DEGs) related to sugar metabolism and sugar content in response to spectral light qualities. (A) The associated DEGs from red and blue light vs. control were represented in color code boxes based on log2 fold changes. Red light treatment is shown on left and blue light treatment on the right side of the box. Gene names: *Phosphofructokinases (PFK), fructokinases (FK), hexokinases (HK), neutral invertases (NINV), vacuolar invertases (VI), cell wall invertases (CWINV), sucrose phosphate synthases (SPS), sucrose phosphate phosphatases (SPP), sucrose synthases (SS), α-amy*, α-amylases; *β-amy*, β-amylases, *UDP-galacturonate 4-epimerase (UGE), galactinol synthase (GS), phosphoglucomutase (PGM), raffinol synthase (RFS), α- galactosidases (α- gal), UDP glucose7galactose pyrophosphorylases (UDPG PP),* (B) Sugar content in light-treated bilberry samples. The values (mg g^{-1}) represent mean ± SEM of biological and technical replicates. Different letters denote significant differences among light treatments analyzed by one-way ANOVA followed by Tukey's post hoc test (p-value <0.05).

Table. 1 Quantification of sugar content during bilberry fruit developmental with two different methods (Phenol-sulfuric method and Sucrose/D-Glucose/ D-Fructose assay kit). The values are mean of three biological replicates ± SEM and expressed in mg g^{-1} of dry weight (DW). S2, small unripe green fruit; S3, large unripe green fruit; S4, ripening purple fruit; S5, fully ripe blue fruit.

Ripening stages of bilberry	**Glucose content (mg g^{-1})**	**Frutose content (mg g^{-1})**	**Sucrose content (mg g^{-1})**	**Total Sugar content (mg g^{-1})**	**Total Sugar content (Phenol-sulfuric method) (mg g^{-1})**
Stage 2	70.06 ± 0.26	78.04 ± 0.38	4.57 ± 0.22	152.67 ± 0.86	135.63±6.73
Stage 3	35.90 ± 0.77	47.29 ± 1.29	7. 48 ± 0.54	90.67 ± 2.60	87.56±2.73
Stage 4	101.11 ± 3.45	123.69 ± 4.94	7.97 ± 0.38	232.77 ± 8.77	214.55±13.84
Stage 5	165.76 ± 4.06	227.55 ± 2.17	4.55 ± 0.19	397.86 ± 6.42	333.36±13.78

Appendix

Supplementary data (Paper 1)

Red and blue light treatments of ripening bilberry fruits reveal differences in signaling through ABA regulated anthocyanin biosynthesis

Amos Samkumar[1], Dan Jones[2], Katja Karppinen[1], Andrew P. Dare[2], Nina Sipari[3], Richard V. Espley[2], Inger Martinussen[4], Laura Jaakola[1,4]

[1]Department of Arctic and Marine Biology, UiT The Arctic University of Norway, Tromsø, Norway

[2]The New Zealand Institute for Plant & Food Research Ltd., Auckland, New Zealand

[3]Viikki Metabolomics Unit, Organismal and Evolutionary Biology Research Programme, Faculty of Biological and Environmental Sciences, University of Helsinki, Finland

[4]Norwegian Institute of Bioeconomy Research, Ås, Norway

Number of figures: 9

Number of tables: 10

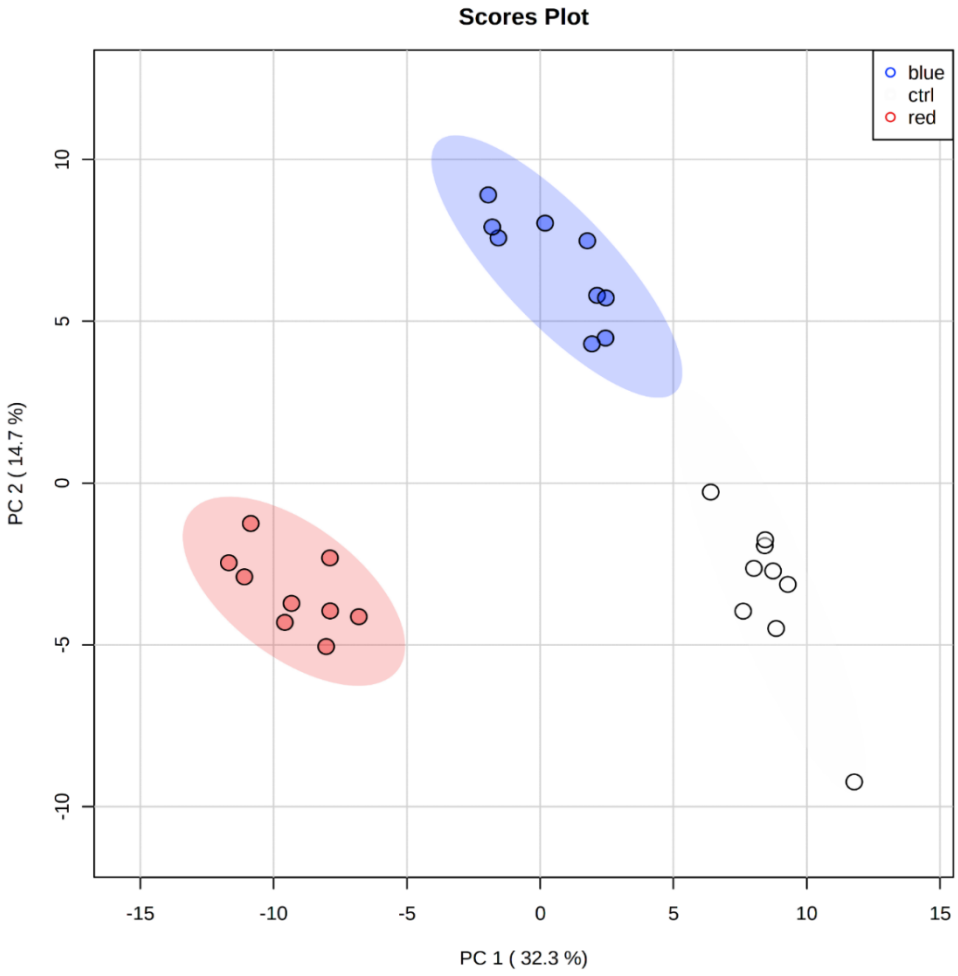

Supplementary figure S1. Principal component analysis (PCA) lot of the three sample groups (control, blue and red; n= 9) from metabolic profiling analysis with UPLC-HDMS. Color codes indicate the different sample groups

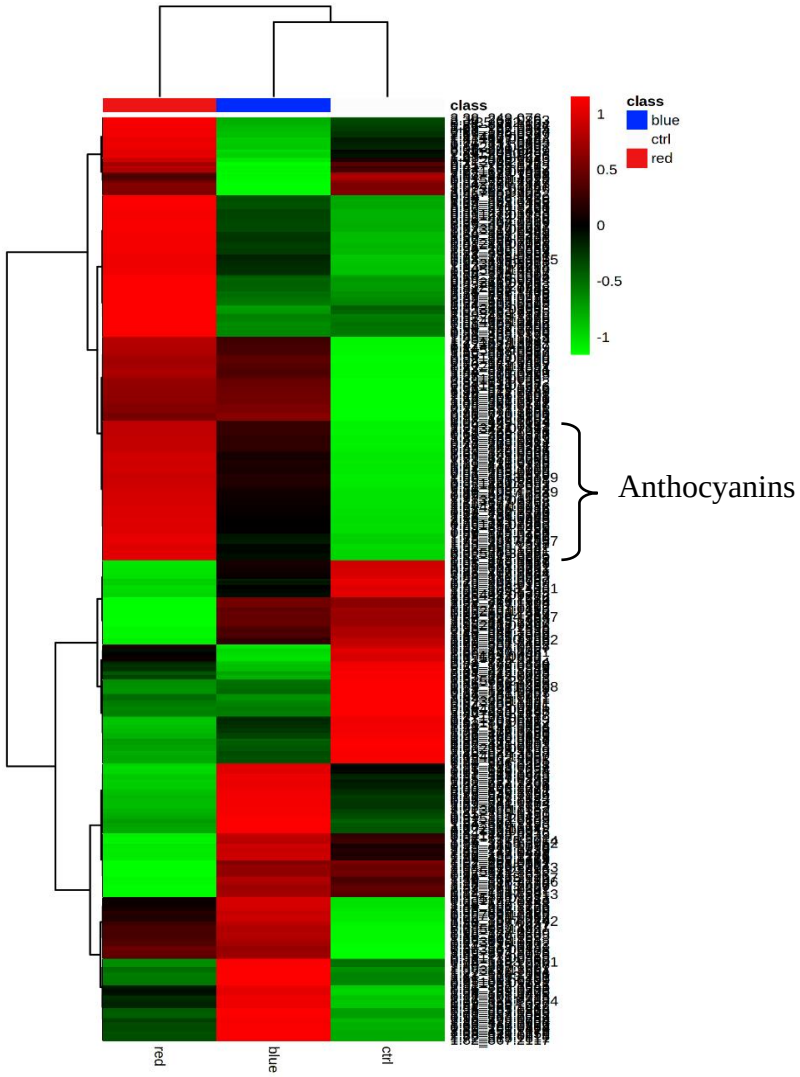

Supplementary figure S2. Heat map analysis of metabolic profiling data (average) with UPLC-HDMS. Color codes indicate different sample groups.

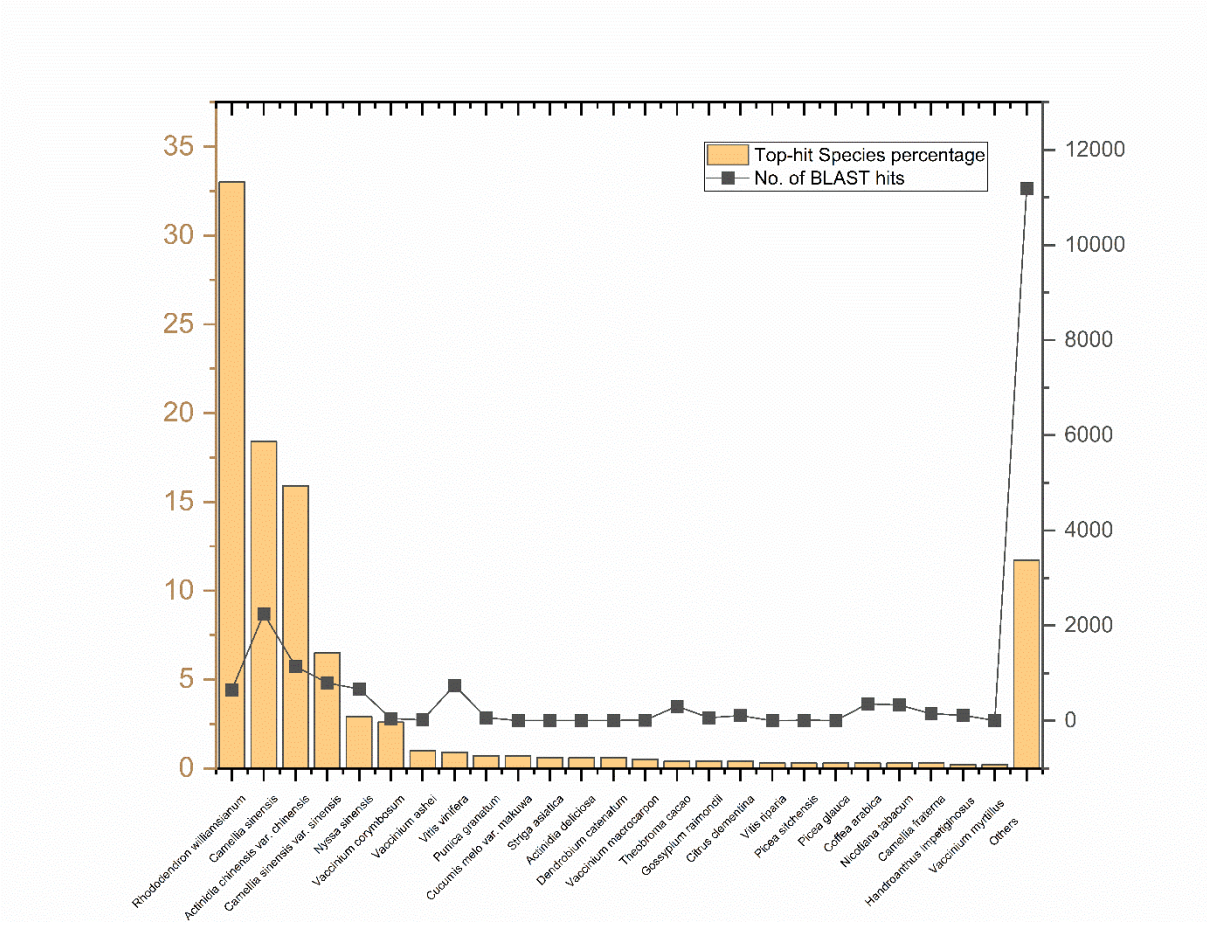

Supplementary figure S3. BLAST search distribution among top 25-species, the top-hit species were expressed as percentage and in bars whereas the corresponding number of search hits in terms of sequences were visualized as line-graph.

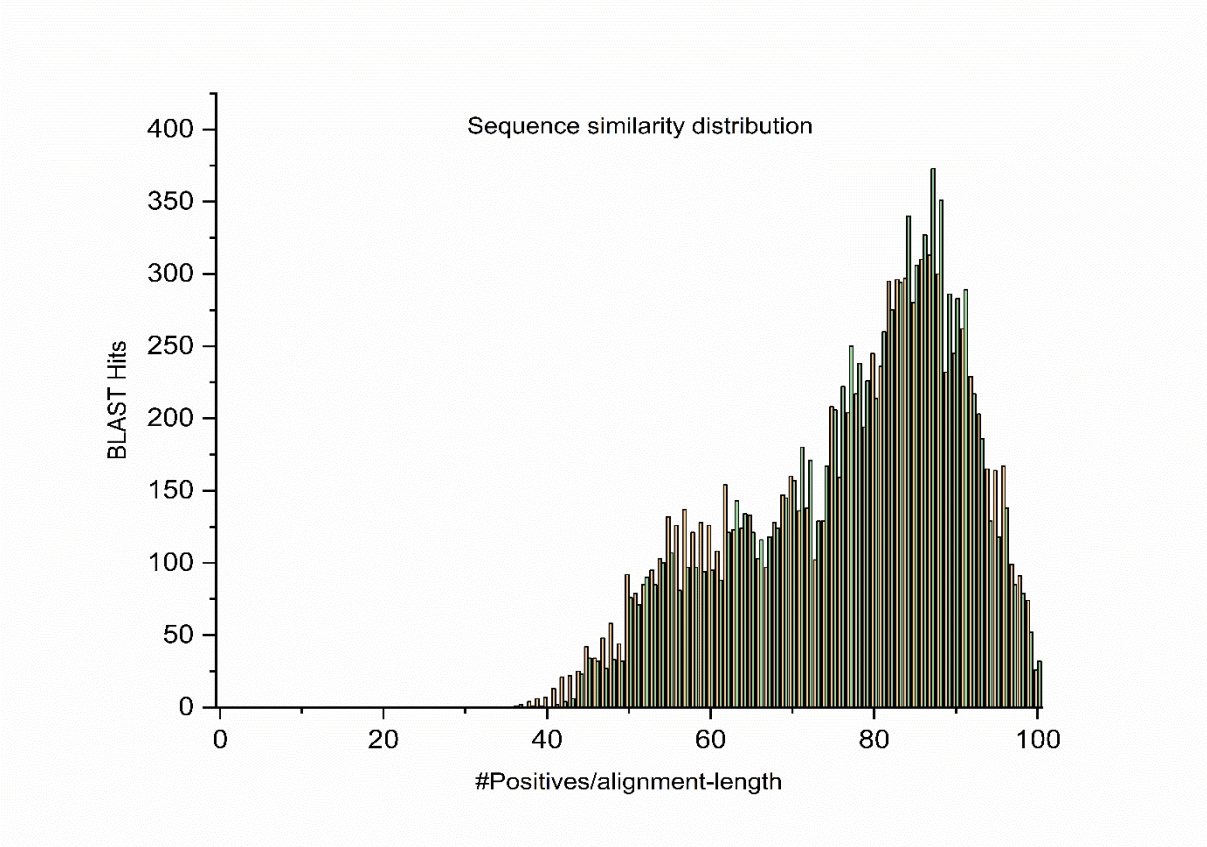

Supplementary figure S4. Sequence similarity distribution of BLAST hits among the top 500 DEGs analyzed by Blast2GO suite.

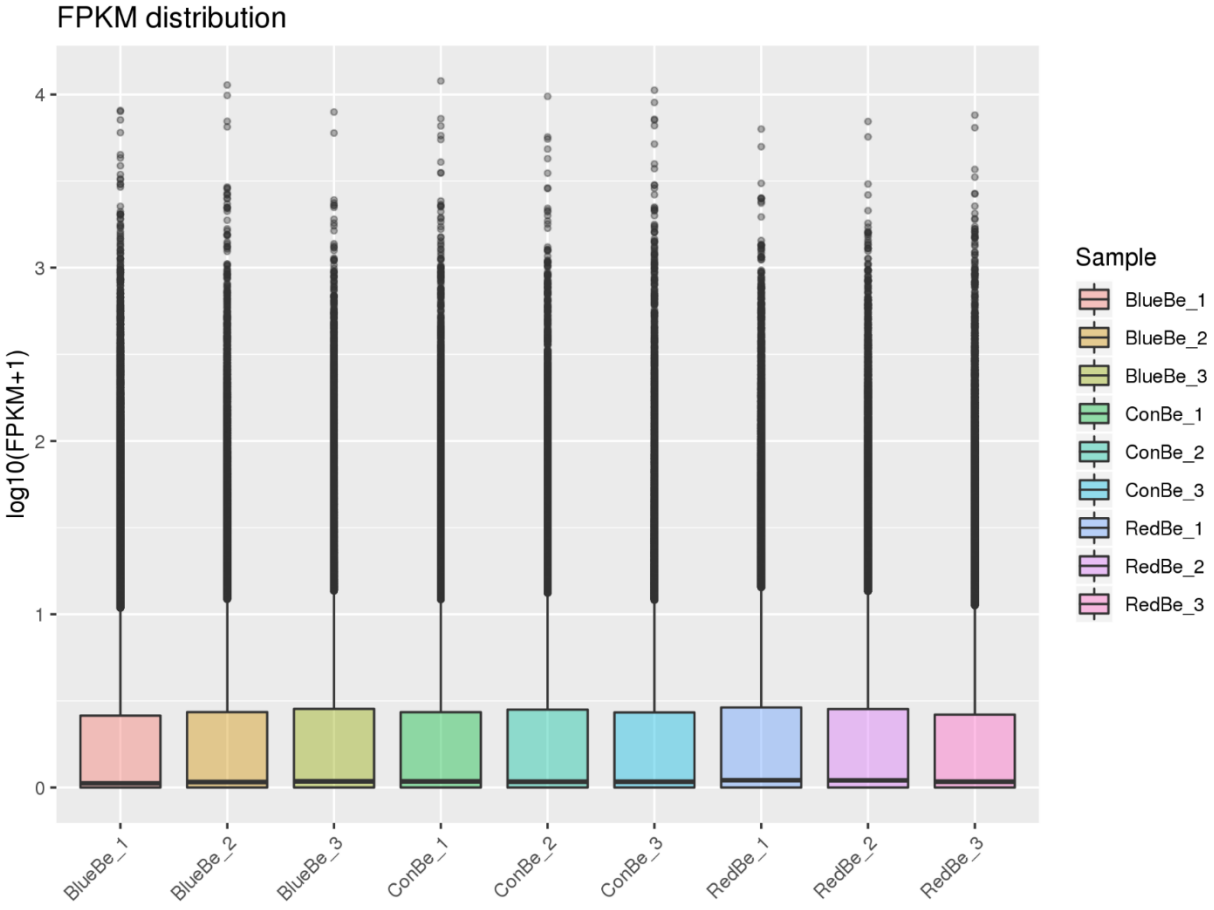

Supplementary figure S5. Gene expression box plot from all the samples under different conditions based on fragments per kilobase of transcript sequence per millions base pairs sequenced (FPKM) distribution. (The sample codes correspond to replicates of berry samples from light treatments)

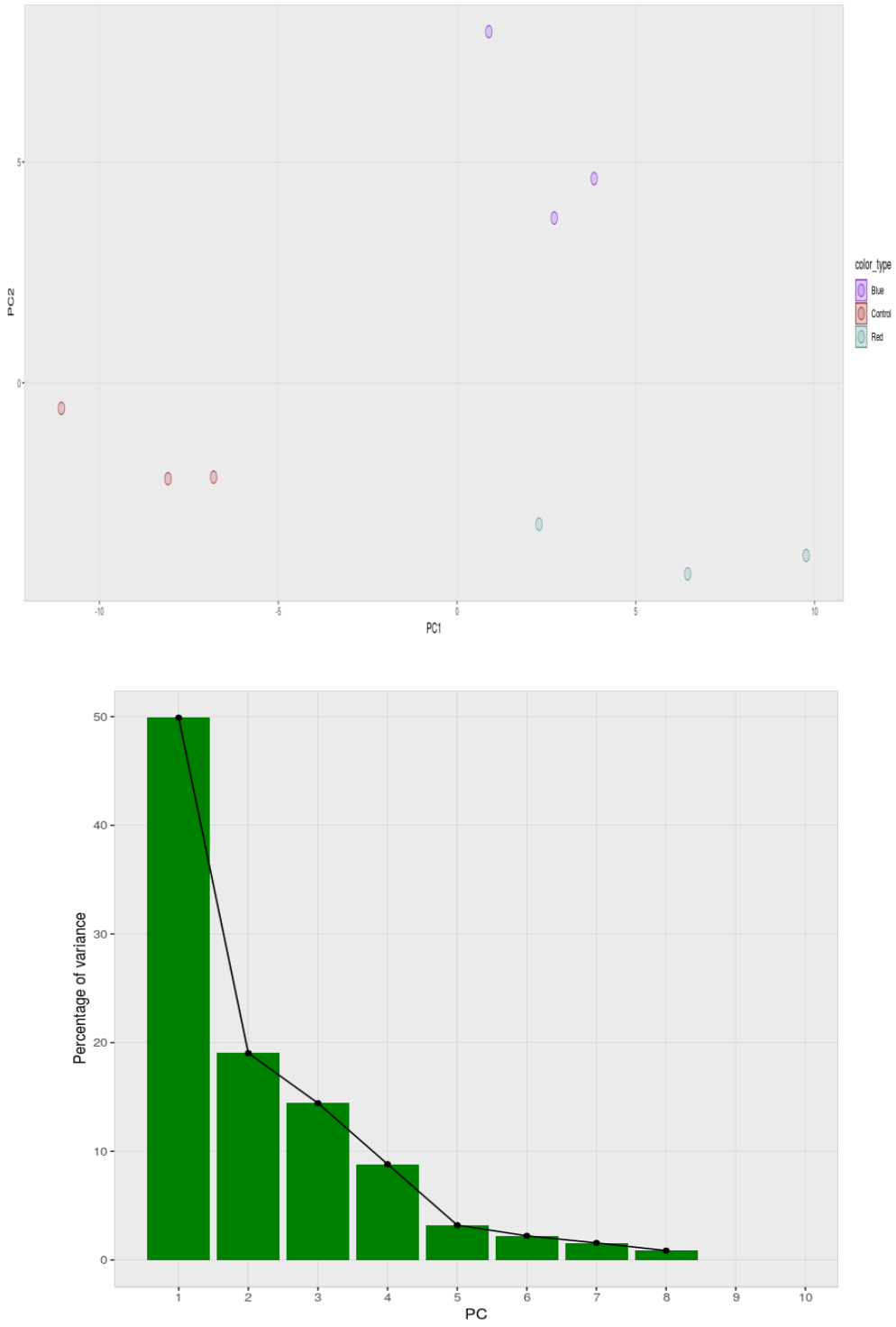

Supplementary figure S6. Principal component analysis (PCA) plot for all the analyzed RNA-seq samples as a QC method before differential expression analysis using DESeq2. The clustering of samples is based on the type of light treatment as indicated in color codes and the percentage of variance between the components are shown next to it.

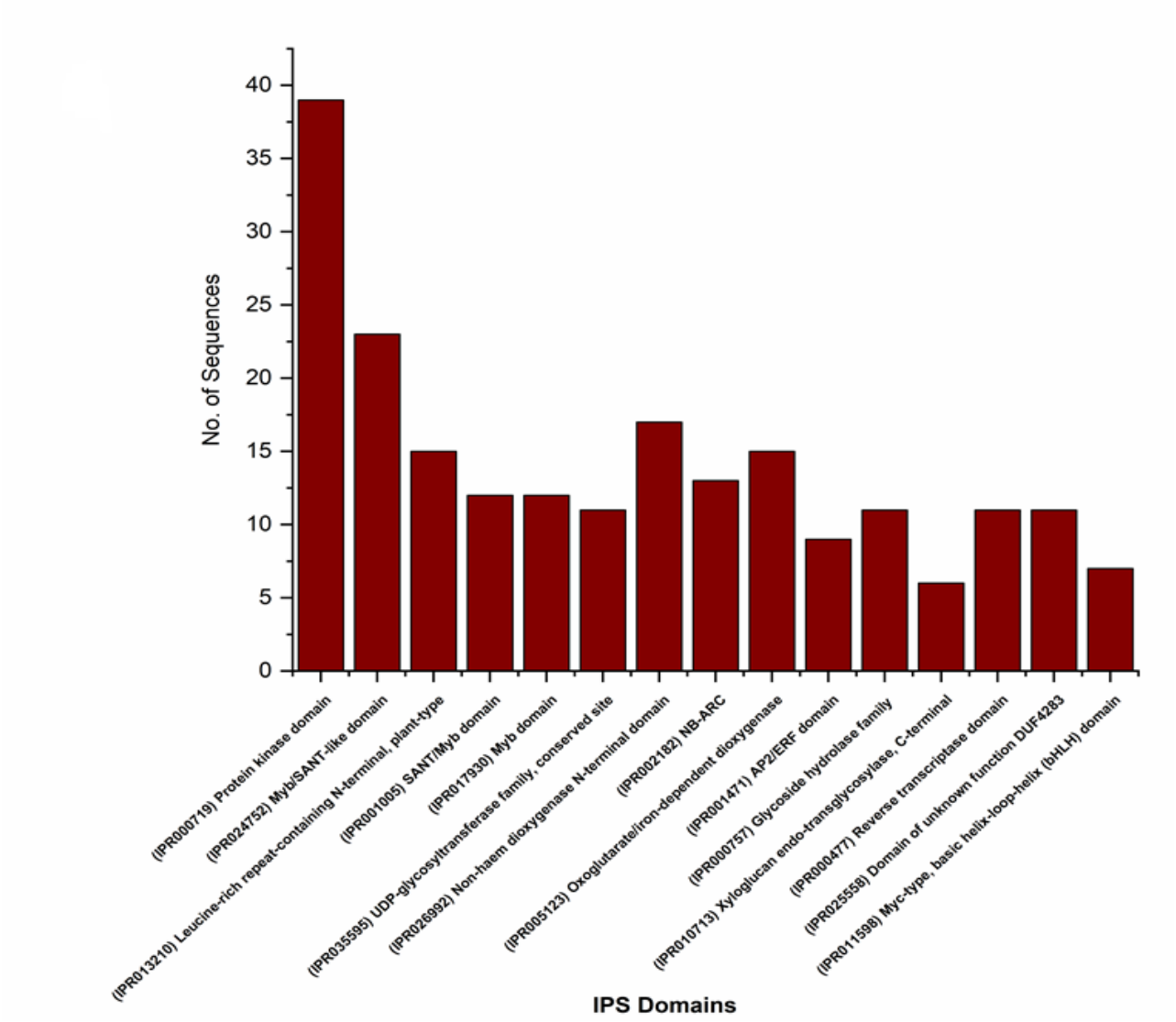

Supplementary figure S7. InterproScan protein domain families identified from the top differentially expressed genes (DEGs)

Supplementary figure S8. List of transcription factor families (TF) identified from DEGs, size of the bars represents the number of unigenes assigned to TFs as provided in scale chart

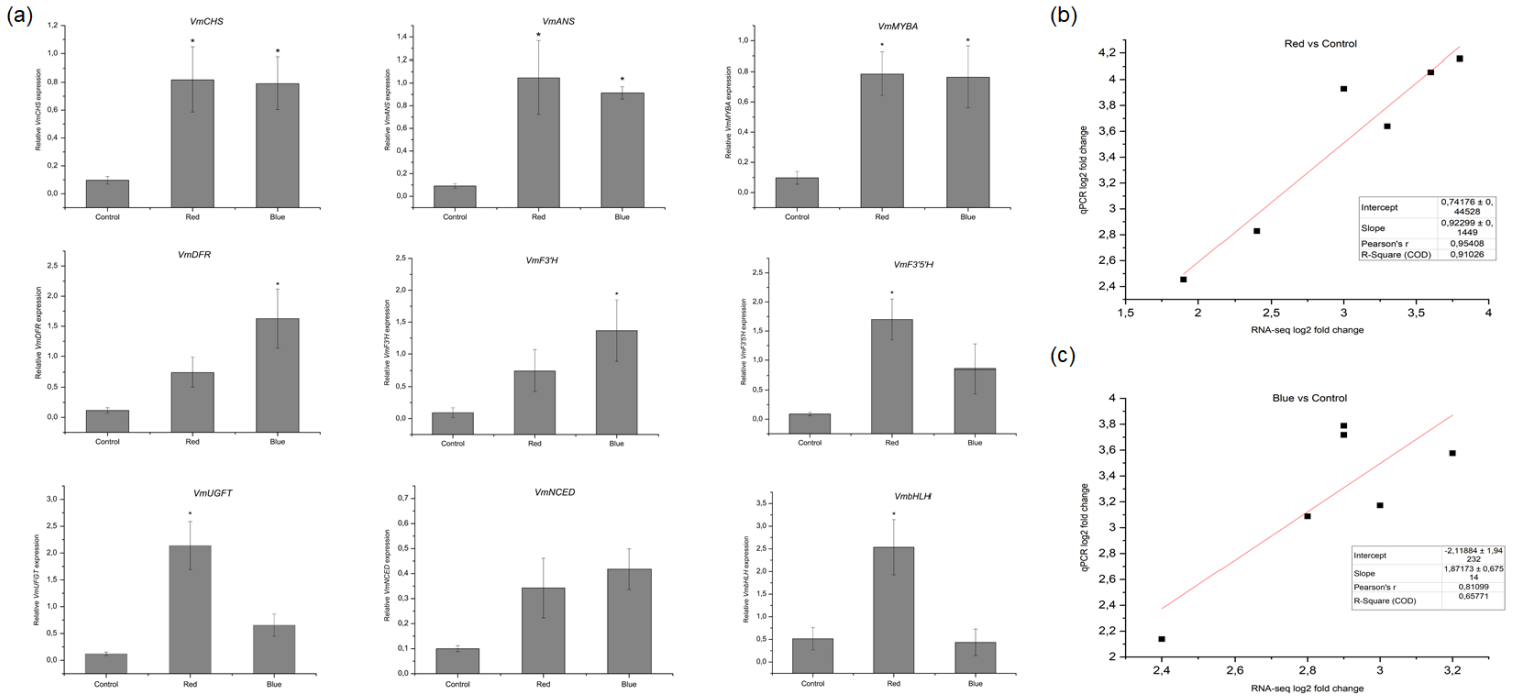

Supplementary figure S9. qRT-PCR analysis of key genes and validation of DEGs by Pearson's linear correlation (**a**) qRT-PCR analysis of bilberry flavonoid biosynthetic genes (*VmCHS, VmANS, VmDFR, VmUFGT, VmF3'H, VmF3'5'H),* transcription factors (*VmMYBA1, VmbHLH*) and Carotenoid-ABA pathway gene (*VmNCED*). Error bars represent standard error (±SE) of minimum 3 biological replicates, significant differences between control and light treatments were analyzed by comparison of means using student's t-test (indicated in asterisks) with p-value ≤ 0.05. (**b, c**) Pearson's linear correlation plot of comparison between select key gene expression results from qPCR and DEGs from RNA-seq dataset expressed in log2fold changes.

Supplementary table S1. List of primers used in qRT-PCR analysis

Gene	Forward primer sequence	Reverse primer sequence
VmCHS	CCAAGGCCATCAAGGAATG	TGATACATCATGAGTCGCTTCAC
VmANS	GCAACTCTTCTACGAGGGCAAA	CCTGTGGAGAATGCTCTTGCAC
VmMYBA	CTCGACCACAAACCTTGTCCA	GCCTCCTCATTTGATCCGTCA
VmDFR	GAAGTGATCAAGCCGACGAT	ATCCAAGTCGCTCCAGTTGT
VmF3'H	TTCTTCGACACCCGAAAGTC	TCGAACCCTTTGGAATGAAG
VmF3'5'H	GATTGCGTGGATGGACTTACA	AAATCTGGGTTCCCTTTACGC
VmUFGT	CATCCAAACCCTGTTCCCATCC	TCATCCCTGCCTTCAAGCTCTC
VmNCED	GCTCAAATCCACCATGATAGCC	GACCATCCAACGGTATTTCCAC
VmbHLH	CAGGTGCAGGTGTCGATTATAG	CCGTTGTCTTTCACCTTAGCTC
VmGAPDH	CAAACTGTCTTGCCCCACTT	CAGGCAACACCTTACCAACA
VmActin	TTCCCTGGGATTGCTGATAG	GGTCTTGGCAATCCACATCT

Supplementary table S2: Concentration of different classes of anthocyanins (mg $100g^{-1}$ DW) quantified by UHPLC in fully ripe bilberries at the end of spectral light treatment (4^{th} week). The amounts are expressed in average of three replicates ± standard error. Different letters indicate significant differences analyzed by one-way ANOVA followed by Turkey's post-hoc analysis of comparative means (p-value <0.05) of each compound between the light treatments

Anthocyanin compounds	Control	Red	Blue
Delphinidin 3-galactoside	428 ± 41 ^{b}	929 ± 24 ^{a}	269 ± 193 ^{b}
Delphinidin 3-glucoside	394 ± 40	587 ± 20	365 ± 122
Cyanidin 3-galactoside	249 ± 11	332 ± 5	203 ± 184
Delphinidin 3-arabinoside	507 ± 38 ^{b}	1077 ± 31 ^{a}	210 ± 176 ^{b}
Cyanidin 3-glucoside	254 ± 14	231 ± 2.7	311 ± 114
Petunidin 3-galactoside	129 ± 9.5 ^{ab}	237 ± 7.3 ^{a}	81 ± 55 ^{b}
Cyanidin-3-arabinoside	244 ± 8.1	347 ± 3.7	159 ± 139
Petunidin 3-glucoside	256 ± 22	328 ± 11	246 ± 88
Petunidin 3-arabinoside	105 ± 6.3 ^{b}	204 ± 8 ^{a}	50.7 ± 34 ^{b}
Peonidin 3-glucoside	100 ± 9.2	68 ± 1.1	118 ± 44
Malvidin 3-galactoside	74 ± 7.5 ^{ab}	98 ± 4.7 ^{a}	50 ± 22 ^{b}
Malvidin 3-glucoside	254 ± 23	232 ± 8.1	193 ± 73
Malvidin 3-arabinoside	66.8 ± 4.7 ^{ab}	93.7 ± 4.9 ^{a}	37.7 ± 14.3 ^{b}
Total anthocyanins	**3060.8**	**4763.7**	**2293.4**

Supplementary table S3. Summary of raw reads after Illumina sequencing and QC analysis report

QC summary	Control	Red	Blue
Total raw reads	70,627,656	82,253,205	78,192,227
Total clean reads	69,827,226	81,424,244	77,450,097
Error rate	0.03%	0.03%	0.03%
Q20	97.77%	97.80%	97.68%
Q30	93.81%	93.85%	93.62%
GC Content	48.14%	47.43%	47.77%
Avg Phred score	>36	>36	>36

Supplementary table S4. Transcriptome assembly completeness assessment by BUSCO analysis between the assemblies constructed using Trinity

BUSCOs (Embryophyta (ODB_9)		**Genome-guided *de novo* assembly**	**Combined assembly**
Complete BUSCOs (C)		1331 (96.8%)	1339 (97.4%)
Complete and single copy BUSCOs (S)		1288 (93.7%)	1310 (95.3%)
Complete and duplicated BUSCOs (D)		43 (3.1%)	29 (2.1%)
Fragmented BUSCOs (F)		20 (1.5%)	15 (1.1%)
Missing BUSCOs (M)		24 (1.7%)	21 (1.5%)
Total BUSCO groups searched	**1375**		

Supplementary table S5. List of significantly enriched KEGG metabolic pathways in **'Red light'** treatment using *Vitis vinifera* as reference organism for obtaining the KEGG orthology (KO) annotation terms. Gene ratio represents the ratio of differentially expressed genes to the total number of genes corresponds to concerned pathway whereas Bg ratio corresponds to ratio of all genes in background KEGG database

KEGG ID	Description	Gene ratio	Bg ratio	p-value	p-adj
vvi01100	Metabolic pathways	1054|2282	2006|4927	2.02046082748e-43	2.3235299516e-41
vvi01110	Biosynthesis of secondary metabolites	699|2282	1182|4927	4.41257915734e-40	2.53723301547e-38
vvi01230	Biosynthesis of amino acids	186|2282	225|4927	1.37613369984e-21	5.27517918271e-20
vvi01200	Carbon metabolism	172|2282	253|4927	2.0884448757e-14	6.00427901763e-13
vvi03050	Proteasome	44|2282	50|4927	1.02425966773e-06	2.35579723578e-05
vvi00010	Glycolysis / Gluconeogenesis	76|2282	120|4927	2.40166281985e-06	4.60318707138e-05
vvi00940	Phenylpropanoid biosynthesis	108|2282	196|4927	3.18228508723e-06	5.22803978617e-05
vvi04144	Endocytosis	85|2282	143|4927	4.0743939677e-06	5.85694132857e-05
vvi00630	Glyoxylate and dicarboxylate metabolism	52|2282	72|4927	6.83914203788e-06	8.73890371507e-05
vvi00030	Pentose phosphate pathway	40|2282	48|4927	7.64664673469e-06	8.79364374489e-05
vvi01210	2-Oxocarboxylic acid metabolism	46|2282	61|4927	1.03956439536e-05	0.000108681732243
vvi00561	Glycerolipid metabolism	48|2282	67|4927	1.75775540018e-05	0.000168451559184
vvi00130	Ubiquinone and other terpenoid-quinone biosynthesis	34|2282	41|4927	3.83486039464e-05	0.000339237650295
vvi00500	Starch and sucrose metabolism	112|2282	225|4927	6.12047733096e-05	0.000502753495043
vvi01212	Fatty acid metabolism	43|2282	62|4927	7.99883957754e-05	0.000613244367611
vvi00260	Glycine, serine and threonine metabolism	45|2282	68|4927	0.000121770324234	0.00087522420543
vvi00052	Galactose metabolism	39|2282	57|4927	0.000205017924833	0.0013868859621
vvi00620	Pyruvate metabolism	51|2282	86|4927	0.000326151912135	0.00208374832753
vvi00330	Arginine and proline metabolism	38|2282	58|4927	0.000454525824262	0.00274992210082
vvi04146	Peroxisome	45|2282	74|4927	0.000478247321881	0.00274992210082
vvi00051	Fructose and mannose metabolism	38|2282	59|4927	0.000576896704941	0.00315919624135
vvi00250	Alanine, aspartate and glutamate metabolism	31|2282	44|4927	0.000620661383442	0.00324436632254

vvi00460	Cyanoamino acid metabolism	40|2282	65|4927	0.000807867156483	0.00403933578242
vvi00900	Terpenoid backbone biosynthesis	34|2282	52|4927	0.000905302045375	0.00433790563409
vvi00071	Fatty acid degradation	29|2282	42|4927	0.0011470454973	0.00527640928759
vvi00040	Pentose and glucuronate interconversions	49|2282	89|4927	0.00141100978635	0.00624100482426
vvi00062	Fatty acid elongation	27|2282	39|4927	0.00162543749999	0.00692315972219
vvi04933	AGE-RAGE signaling pathway	16|2282	17|4927	0.0018058170509	0.00741674860189
vvi04075	Plant hormone signal transduction	121|2282	280|4927	0.00224339836764	0.00889623490616
vvi00562	Inositol phosphate metabolism	31|2282	50|4927	0.00272259398802	0.00984258965178
vvi04120	Ubiquitin mediated proteolysis	61|2282	123|4927	0.002746471275	0.00984258965178
vvi04070	Phosphatidylinositol signaling system	34|2282	57|4927	0.00278140451637	0.00984258965178
vvi00053	Ascorbate and aldarate metabolism	26|2282	39|4927	0.00285683611374	0.00984258965178
vvi04626	Plant-pathogen interaction	106|2282	242|4927	0.00290998302748	0.00984258965178
vvi00511	Other glycan degradation	17|2282	21|4927	0.00383861698153	0.0126125986536
vvi04141	Protein processing in endoplasmic reticulum	93|2282	210|4927	0.00396090822234	0.0126529012658
vvi01040	Biosynthesis of unsaturated fatty acids	19|2282	26|4927	0.00504551204607	0.0156819968999
vvi00280	Valine, leucine and isoleucine degradation	31|2282	54|4927	0.00627913345052	0.0190026407055
vvi00073	Cutin, suberine and wax biosynthesis	18|2282	25|4927	0.00696847670084	0.020548072323
vvi00670	One carbon pool by folate	15|2282	19|4927	0.00754293534357	0.0211570137685
vvi00340	Histidine metabolism	15|2282	19|4927	0.00754293534357	0.0211570137685
vvi00640	Propanoate metabolism	24|2282	39|4927	0.00829797143829	0.022720636081
vvi00350	Tyrosine metabolism	31|2282	56|4927	0.00916805852705	0.0245192262933
vvi00520	Amino sugar and nucleotide sugar metabolism	66|2282	147|4927	0.010732102637	0.0280498137103
vvi04145	Phagosome	45|2282	93|4927	0.0124441654234	0.031801756082
vvi00710	Carbon fixation in photosynthetic organisms	33|2282	63|4927	0.0132017506798	0.0330043766996
vvi00531	Glycosaminoglycan degradation	12|2282	15|4927	0.0151563333583	0.036808689914
vvi00600	Sphingolipid metabolism	18|2282	28|4927	0.0153636270945	0.036808689914

Supplementary table S6. List of significantly enriched KEGG metabolic pathways in **'Blue light'** treatment using *Vitis vinifera* as reference organism for obtaining the KEGG orthology (KO) annotation terms. Gene ratio represents the ratio of differentially expressed genes to the total number of genes corresponds to concerned pathway whereas Bg ratio corresponds to ratio of all genes in background KEGG database

KEGG ID	Description	Gene ratio	Bg ratio	p-value	p-adj
vvi01110	Biosynthesis of secondary metabolites	457|1413	1182|4927	1.19046941626e-39	1.42856329951e-37
vvi01100	Metabolic pathways	655|1413	2006|4927	1.03523043028e-37	6.2113825817e-36
vvi01230	Biosynthesis of amino acids	122|1413	225|4927	1.09742214956e-19	4.38968859824e-18
vvi00360	Phenylalanine metabolism	57|1413	62|4927	9.08833439806e-17	2.72650031942e-15
vvi00400	Phenylalanine, tyrosine and tryptophan biosynthesis	45|1413	49|4927	1.55090123185e-13	3.72216295645e-12
vvi01200	Carbon metabolism	105|1413	253|4927	2.09379565344e-11	4.18759130688e-10
vvi00940	Phenylpropanoid biosynthesis	86|1413	196|4927	1.53225055192e-10	2.62671523187e-09
vvi03010	Ribosome	113|1413	338|4927	8.0089067863e-08	1.20133601794e-06
vvi00010	Glycolysis / Gluconeogenesis	54|1413	120|4927	1.94784273183e-07	2.59712364244e-06
vvi00350	Tyrosine metabolism	32|1413	56|4927	1.33396819048e-06	1.46725181756e-05
vvi00020	Citrate cycle (TCA cycle)	31|1413	53|4927	1.34498083276e-06	1.46725181756e-05
vvi01210	2-Oxocarboxylic acid metabolism	29|1413	61|4927	5.71205709816e-05	0.000571205709816
vvi00620	Pyruvate metabolism	36|1413	86|4927	6.50568863661e-05	0.000600525104918
vvi00190	Oxidative phosphorylation	53|1413	152|4927	8.48551636608e-05	0.000699179140576
vvi04626	Plant-pathogen interaction	75|1413	242|4927	8.7397392572e-05	0.000699179140576
vvi00260	Glycine, serine and threonine metabolism	30|1413	68|4927	0.00012342778759	0.000925708406927
vvi03040	Spliceosome	53|1413	159|4927	0.000213084880904	0.00150412857109
vvi04144	Endocytosis	48|1413	143|4927	0.000361720299096	0.00241146866064
vvi00130	Ubiquinone and other terpenoid-quinone biosynthesis	20|1413	41|4927	0.000599382596521	0.00378557429382
vvi00900	Terpenoid backbone biosynthesis	23|1413	52|4927	0.000706879249436	0.00424127549662
vvi00230	Purine metabolism	48|1413	150|4927	0.000851974511428	0.00486842577959
vvi01212	Fatty acid metabolism	25|1413	62|4927	0.00121824179554	0.00664495524841
vvi00520	Amino sugar and nucleotide sugar metabolism	46|1413	147|4927	0.00156191056815	0.00814909861646
vvi00480	Glutathione metabolism	40|1413	124|4927	0.00194048839404	0.00962474284891
vvi04933	AGE-RAGE signaling	11|1413	17|4927	0.00200515476019	0.00962474284891
vvi00071	Fatty acid degradation	18|1413	42|4927	0.00336287580171	0.0155209652386
vvi00052	Galactose metabolism	22|1413	57|4927	0.00356064800314	0.0158251022362

vvi03050	Proteasome	20|1413	50|4927	0.00385871261329	0.0165373397712
vvi00500	Starch and sucrose metabolism	61|1413	225|4927	0.00517719790465	0.0209265430594
vvi00030	Pentose phosphate pathway	19|1413	48|4927	0.00523163576485	0.0209265430594
vvi02010	ABC transporters	12|1413	25|4927	0.00787714714586	0.0304921825001
vvi00760	Nicotinate and nicotinamide metabolism	9|1413	16|4927	0.00980704107238	0.0367764040214
vvi00950	Isoquinoline alkaloid biosynthesis	13|1413	30|4927	0.0110022574834	0.0400082090307
vvi00261	Monobactam biosynthesis	6|1413	8|4927	0.0134418346477	0.0474417693447

Supplementary table S7. List of significantly enriched top 500 differentially expressed genes (DEGs) identified from **'Red light'** treatment with corresponding unigene IDs and its associated KEGG metabolic pathways

Metabolic pathway	Transcript / UniGene ID	Pathway ID	Enzyme category with EC code
Phenylpropanoid biosynthesis	TRINITY_GG_4529_c0_g1_i1,TRINITY_DN9091_c0_g1_i1, TRINITY_DN5507_c0_g1_i4, TRINITY_DN9284_c0_g4_i3, TRINITY_DN3121_c0_g1_i11,TRINITY_DN1681_c0_g1_i1, TRINITY_GG_18165_c1_g1_i3,TRINITY_DN11312_c0_g1_i1, TRINITY_DN11605_c0_g2_i1	map00940	ec:1.14.14.91 - 4-monooxygenase, ec:3.2.1.21 - gentiobiase, ec:2.3.1.133 - O-hydroxycinnamoyltransferase, ec:6.2.1.12 - ligase, ec:1.11.1.7 - lactoperoxidase, ec:2.1.1.104 - O-methyltransferase
Flavonoid biosynthesis	TRINITY_GG_4529_c0_g1_i1, TRINITY_DN412_c2_g1_i3, TRINITY_DN5507_c0_g1_i4, TRINITY_DN10833_c0_g2_i1, TRINITY_DN3902_c0_g1_i5, TRINITY_DN112_c3_g2_i1, TRINITY_GG_19334_c0_g1_i1,TRINITY_DN64714_c1_g1_i1, TRINITY_DN11605_c0_g2_i1	map00941	ec:1.14.14.91 - 4-monooxygenase, ec:1.14.20.4 - synthase, ec:2.3.1.133 - O-hydroxycinnamoyltransferase, ec:5.5.1.6 - isomerase, ec:1.1.1.219 - 4-reductase, ec:1.14.11.9 - 3-dioxygenase, ec:2.3.1.74 - synthase, ec:2.1.1.104 - O-methyltransferase
Starch and sucrose metabolism	TRINITY_DN2892_c2_g1_i2, TRINITY_DN9091_c0_g1_i1, TRINITY_DN14485_c0_g1_i2, TRINITY_DN13224_c0_g2_i1, TRINITY_DN13559_c0_g1_i1, TRINITY_GG_5009_c0_g1_i1, TRINITY_DN6766_c1_g1_i8, TRINITY_DN2422_c1_g2_i5, TRINITY_GG_12379_c19_g1_i3	map00500	ec:2.4.1.15 - synthase (UDP-forming), ec:3.2.1.21 - gentiobiase, ec:3.2.1.4 - endo-1,4-beta-D-glucanase, ec:5.3.1.9 - isomerase, ec:3.1.3.12 - trehalose 6-phosphatase, ec:3.6.1.9 - diphosphatase, ec:2.4.1.12 - synthase (UDP-forming)
Galactose metabolism	TRINITY_DN4248_c1_g1_i9, TRINITY_DN3131_c0_g2_i2, TRINITY_DN22219_c0_g2_i1	map00052	ec:5.1.3.2 - 4-epimerase, ec:3.2.1.23 - lactase (ambiguous)
Fructose and mannose metabolism	TRINITY_DN111141_c0_g1_i1	map00051	ec:4.1.2.13 - aldolase
Vitamin B6 metabolism	TRINITY_DN22170_c0_g1_i1	map00750	ec:1.2.3.1 - oxidase

Terpenoid backbone biosynthesis	TRINITY_DN162_c3_g1_i2, TRINITY_DN162_c3_g2_i1, TRINITY_DN4167_c0_g1_i1, TRINITY_DN1034_c1_g1_i3	map00900	ec:1.1.1.34 - reductase (NADPH), ec:1.3.1.83 - diphosphate reductase, ec:1.17.7.1 - synthase (ferredoxin)
Ubiquinone and other terpenoid-quinone biosynthesis	TRINITY_GG_4529_c0_g1_i1, TRINITY_DN9284_c0_g4_i3	map00130	ec:1.14.14.91 - 4-monooxygenase, ec:6.2.1.12 - ligase
Monoterpenoid biosynthesis	TRINITY_DN10057_c1_g1_i1	map00902	ec:1.14.19.62 - synthase
Diterpenoid biosynthesis	TRINITY_DN6826_c1_g1_i1	map00904	ec:1.14.11.13 - 2beta-dioxygenase
Drug metabolism - cytochrome P450	TRINITY_GG_8402_c1_g1_i1, TRINITY_DN2833_c0_g1_i3, TRINITY_DN955_c5_g1_i3, TRINITY_DN8870_c1_g1_i1, TRINITY_DN22170_c0_g1_i1, TRINITY_DN164_c0_g1_i2	map00982	ec:2.5.1.18 - transferase, ec:1.2.3.1 - oxidase, ec:1.2.1.5 - dehydrogenase [NAD(P)+]
Metabolism of xenobiotics by cytochrome P450	TRINITY_GG_8402_c1_g1_i1, TRINITY_DN2833_c0_g1_i3, TRINITY_DN955_c5_g1_i3, TRINITY_DN8870_c1_g1_i1, TRINITY_DN164_c0_g1_i2	map00980	ec:2.5.1.18 - transferase, ec:1.2.1.5 - dehydrogenase [NAD(P)+]
Stilbenoid, diarylheptanoid and gingerol biosynthesis	TRINITY_GG_4529_c0_g1_i1, TRINITY_DN5507_c0_g1_i4, TRINITY_DN11605_c0_g2_i1	map00945	ec:1.14.14.91 - 4-monooxygenase, ec:2.3.1.133 - O-hydroxycinnamoyltransferase,
Tropane, piperidine and pyridine alkaloid biosynthesis	TRINITY_GG_10501_c37_g1_i1	map00960	ec:2.1.1.104 - O-methyltransferase ec:2.6.1.1 - transaminase
Isoquinoline alkaloid biosynthesis	TRINITY_GG_897_c9_g1_i1, TRINITY_GG_10501_c37_g1_i1	map00950	ec:1.10.3.1 - oxidase, ec:2.6.1.1 – transaminase

Supplementary table S8. List of significantly enriched top 500 differentially expressed genes (DEGs) identified from **'Blue light'** treatment with corresponding unigene IDs and its associated KEGG metabolic pathways

Metabolic pathway	Transcript / UniGene ID	Pathway ID	Enzyme category with EC code
Flavonoid biosynthesis	TRINITY_GG_2790_c18_g1_i1,TRINITY_GG_4529_c0_g1_i1, TRINITY_DN5507_c0_g1_i4, TRINITY_DN412_c2_g1_i3, TRINITY_DN10833_c0_g2_i1, TRINITY_DN3902_c0_g1_i5, TRINITY_DN1306_c0_g2_i1, TRINITY_DN112_c3_g2_i1, TRINITY_DN10794_c0_g1_i2,TRINITY_GG_19334_c0_g1_i1, TRINITY_DN64714_c1_g1_i1, TRINITY_DN43095_c0_g2_i1, TRINITY_DN11605_c0_g2_i1	map00941	ec:1.14.14.91 - 4-monooxygenase, ec:2.3.1.133 - O-hydroxycinnamoyltransferase, ec:1.14.20.4 - synthase, ec:5.5.1.6 - isomerase, ec:1.1.1.219 - 4-reductase, ec:1.14.11.9 - 3-dioxygenase, ec:2.3.1.74 - synthase, ec:2.3.1.170 - synthase, ec:2.1.1.104 - O-methyltransferase
Phenylpropanoid biosynthesis	TRINITY_GG_2790_c18_g1_i1, TRINITY_GG_4529_c0_g1_i1, TRINITY_DN5507_c0_g1_i4, TRINITY_DN1194_c0_g1_i2, TRINITY_DN6706_c0_g2_i1, TRINITY_DN9284_c0_g4_i3, TRINITY_GG_18165_c1_g1_i3, TRINITY_DN11605_c0_g2_i1, TRINITY_DN1194_c0_g1_i2	map00940	ec:1.14.14.91 - 4-monooxygenase, ec:2.3.1.133 - O-hydroxy-cinnamoyltransferase, ec:4.3.1.24 - ammonia-lyase, ec:2.1.1.68 - O-methyltransferase, ec:6.2.1.12 - ligase, ec:1.11.1.7 - lactoperoxidase, ec:2.1.1.104 - O-methyltransferase, ec:4.3.1.25 - ammonia-lyase
Stilbenoid, diarylheptanoid and gingerol biosynthesis	TRINITY_GG_2790_c18_g1_i1, TRINITY_GG_4529_c0_g1_i1, TRINITY_DN5507_c0_g1_i4, TRINITY_DN11605_c0_g2_i1	map00945	ec:1.14.14.91 - 4-monooxygenase, ec:2.3.1.133 - O-hydroxycinnamoyltransferase, ec:2.1.1.104 - O-methyltransferase
Starch and sucrose metabolism	TRINITY_DN6766_c1_g1_i8, TRINITY_DN3452_c0_g2_i5, TRINITY_DN13224_c0_g2_i1, TRINITY_DN7755_c0_g1_i5, TRINITY_DN2422_c1_g2_i5	map00500	ec:3.6.1.9 - diphosphatase, ec:3.2.1.28 - trehalase, ec:3.2.1.4 - endo-1,4-beta-D-glucanase, ec:2.4.1.12 - synthase (UDP-forming)
Fructose and mannose metabolism	TRINITY_DN43095_c0_g2_i1	map00051	ec:1.1.1.21 - reductase

Pentose and glucuronate interconversions	TRINITY_DN3757_c0_g1_i2, TRINITY_DN11563_c0_g1_i7, TRINITY_DN43095_c0_g2_i1, TRINITY_DN43095_c0_g2_i1	map00040	ec:3.1.1.11 - pectin demethoxylase, ec:3.2.1.15 - pectin depolymerase (ambiguous), ec:1.1.1.2 - dehydrogenase (NADP+), ec:1.1.1.21 - reductase
Galactose metabolism	TRINITY_DN4248_c1_g1_i9, TRINITY_DN22219_c0_g2_i1, TRINITY_DN3131_c0_g2_i2, TRINITY_DN43095_c0_g2_i1	map00052	ec:5.1.3.2 - 4-epimerase, ec:3.2.1.23 - lactase (ambiguous), ec:1.1.1.21 - reductase
Biosynthesis of various secondary metabolites	TRINITY_DN427_c0_g1_i4	map00997	ec:2.3.1.30 - O-acetyltransferase
Riboflavin metabolism	TRINITY_DN6766_c1_g1_i8	map00740	ec:3.6.1.9 - diphosphatase
Biotin metabolism	TRINITY_DN12383_c0_g1_i1, TRINITY_DN8408_c0_g2_i2	map00780	ec:2.8.1.6 - synthase, ec:1.1.1.100 - reductase
Retinol metabolism	TRINITY_GG_3724_c0_g1_i1	map00830	ec:1.14.14.1 - monooxygenase
Terpenoid backbone biosynthesis	TRINITY_DN1034_c1_g1_i3, TRINITY_DN162_c3_g2_i1	map00900	ec:1.17.7.1 - synthase (ferredoxin), ec:1.1.1.34 - reductase (NADPH)
Ubiquinone and other terpenoid-quinone biosynthesis	TRINITY_GG_2790_c18_g1_i1, TRINITY_GG_4529_c0_g1_i1, TRINITY_DN9284_c0_g4_i3	map00130	ec:1.14.14.91 - 4-monooxygenase, ec:6.2.1.12 - ligase
Metabolism of xenobiotics by cytochrome P450	TRINITY_DN955_c5_g1_i3, TRINITY_GG_3724_c0_g1_i1, TRINITY_DN19075_c0_g2_i2	map00980	ec:2.5.1.18 - transferase, ec:1.14.14.1 - monooxygenase, ec:3.3.2.9 - epoxide hydrolase
Drug metabolism - cytochrome P450	TRINITY_DN955_c5_g1_i3, TRINITY_GG_3724_c0_g1_i1	map00982	ec:2.5.1.18 - transferase, ec:1.14.14.1 - monooxygenase

Tropane, piperidine and pyridine alkaloid biosynthesis	TRINITY_DN27193_c0_g2_i6, TRINITY_GG_10501_c37_g1_i1	map00960	ec:1.4.3.21 - oxidase, ec:2.6.1.1 - transaminase
Isoquinoline alkaloid biosynthesis	TRINITY_DN27193_c0_g2_i6, TRINITY_GG_10501_c37_g1_i1	map00950	ec:1.4.3.21 - oxidase, ec:2.6.1.1 - transaminase
Geraniol degradation	TRINITY_DN521_c0_g2_i4	map00281	ec:4.2.1.17 - hydratase
Ascorbate and aldarate metabolism	TRINITY_DN4199_c0_g3_i1	map00053	ec:1.10.3.3 - oxidase
Folate biosynthesis	TRINITY_DN43095_c0_g2_i1	map00790	ec:1.1.1.21 - reductase

Supplementary table S9. List of Differentially expressed genes (DEGs) analyzed in the study, Unigene ID represents corresponding Trinity assembly generated IDs and also the IDs obtained from reference mapped transcripts with *V.corymbosum* reference transcriptome. Log2 fold changes (log2FC) values used to indicate the change in expression levels of red and blue light treatment against control samples.

Gene	Unigene ID	Red log2FC	Blue log2FC	Base mean	p-value
PAL	TRINITY_DN1194_c0_g1_i2	3,16	3,09	2534.96	1.13559771093187e-08
4CL	TRINITY_DN9284_c0_g4_i3	2,65	3,14	2070.30	1.33363802497801e-13
C4H	TRINITY_GG_4529_c0_g1_i1	3,5	3,37	470.32	7.76866368268588e-15
CCoAOMT	TRINITY_DN11605_c0_g2_i1	3,1	3,49	8025.26	2.09571120946705e-23
cPOD	TRINITY_GG_18165_c1_g1_i3	2	2,4	366.76	2.52011275196023e-21
POD	TRINITY_DN11312_c0_g1_i1	1,6	1,7	9936.44	9.01410106372537e-22
POD	TRINITY_DN1681_c0_g1_i1	1,6	1,6	580.06	4.0730169338204e-11
CHS	TRINITY_DN64714_c1_g1_i1	3	3,09	1180.98	1.98781438543831e-13
CHS	TRINITY_GG_19334_c0_g1_i1	3,3	3	32561.01	4.90411932338327e-18
CHI	TRINITY_DN10833_c0_g2_i1	3,1	2,2	7121.16	2.88941152579967e-19
F3H	TRINITY_DN112_c3_g2_i1	3,1	2,6	22390.27	1.2163904073052e-10
DFR	TRINITY_DN3902_c0_g1_i5	1,9	2,4	15968.18	1.1127216873835e-15
ANS	TRINITY_DN412_c2_g1_i3	3	3,2	37495.82	1.05179438749397e-18
UFGT	TRINITY_GG_9245_c7_g1_i1	3,6	2,4	647.23	5.27567333184581e-10
F3'H	TRINITY_GG_9118_c0_g1_i1	2,4	2,9	11570.81	2.62097320073997e-15
F3'5'H	TRINITY_GG_2771_c11_g1_i1	3,8	2,8	3535.49	1.43532258680869e-09
PYL4	TRINITY_DN103928_c0_g1_i1	-0.02	0.07	15.92	0.969677240209893

PYL5	TRINITY_DN96921_c0_g1_i1	0	-3.74	0.9064	0.264504724804651
PYL8	TRINITY_DN19749_c0_g3_i1	0.80	-2.88	3.1609	0.664603017328677
bHLH68	TRINITY_DN16132_c0_g1	0.50	0.20	278.65	0.0300788637756759
bHLH147	TRINITY_DN5976_c1_g2	1.42	1.83	111.54	0.000146563441493589
bHLH137	TRINITY_DN25907_c3_g1	0.88	0.24	2.6492	0.55977173505464
bHLH130	TRINITY_DN7885_c0_g3	0.32	0.50	433.14	0.138909863419285
bHLH6(MYC2)	TRINITY_DN6043_c1_g1	1.84	1.13	91.00	1.61439024505516e-06
bHLH79	TRINITY_DN789_c4_g1	1.11	0.23	178.88	0.00023622127850259
SPL9	TRINITY_DN11723_c0_g2	-0.38	0.25	6.5630	0.849016521808505
SPL14	TRINITY_DN9692_c0_g2	-0.13	0.28	1915.66	0.256844310472337
ELF3	TRINITY_DN485_c0_g1	0.30	-0.3	868.02	0.21049324888455
ABI5	TRINITY_DN3274_c0_g2	0.07	0.31	541.40	0.682294589209716
MYBPA2.3	TRINITY_DN12151_c0_g1	1.32	0.72	197.98	6.32204955757876e-06
MYB5a	TRINITY_DN2950_c1_g1	1.10	0.25	155.07	0.000147278498507948
MYBC2.4	TRINITY_DN7597_c2_g1	2.46	1.02	144.99	6.18628212863232e-13
MYBPA2.1	TRINITY_DN36527_c0_g2	0.75	0.91	432.29	0.000512413027327003
MYBPA3	TRINITY_DN83973_c0_g1	1.91	-0.43	496.83	1.54976749540082e-16
MYBC2	TRINITY_DN23081_c0_g1	0.78	0.96	5433.02	5.21008725831344e-05
MYBPA1.1	TRINITY_DN2372_c0_g1	3.06	0.33	26.697	0.000135023261440509
MYBA1	TRINITY_DN7565_c0_g1	0.97	0.66	206.05	0.00018214423889815
AGL15	TRINITY_DN95420_c0_g1	0.10	-0.27	78.82	0.790148245441992
AGL80	TRINITY_DN39475_c2_g1	0.52	-0.37	4.2490	0.794528615241529

AGL21	TRINITY_DN25951_c0_g1	2.08	-1.71	1.013	0.544613532853483
AGL62	TRINITY_DN5737_c0_g1	0.51	-0.85	38.68	0.455745051748257
DEF21	TRINITY_DN141586_c0_g1	1.16	1.99	0.3449	0.772366204989313
AGL80	TRINITY_DN136367_c0_g1	3.47	-0.52	1.500	0.211077069545803
AGL61	TRINITY_GG_8890_c0_g1	0.61	0,40	4.251	0.649514325042815
MADS8	TRINITY_GG_8911_c9_g1	0.54	0.0	81.308	0.117122913801785
MADS2	TRINITY_GG_14930_c16_g1	1.08	1.73	4.686	0.172339586292708
AGL36	TRINITY_GG_16958_c5_g1	0.82	0.27	4.216	0.832603509601504
AGL8	TRINITY_GG_21414_c7_g1	0.95	1.28	147.76	1.23195261054432e-05
AGL103	TRINITY_DN14273_c0_g1	1.38	0.06	76.387	6.84958843452372e-05
MADS4	TRINITY_DN5696_c0_g1	0.02	-0.41	4848.73	0.0318818995798769
TM6	TRINITY_DN24624_c0_g1	0.25	-0.24	141.14	0.573965621733156
AGL104	TRINITY_DN2888_c0_g2	0.44	0.42	658.26	0.134361611879413
AGL11	TRINITY_DN7503_c0_g2	0.32	0.15	925.956	0.289945315866146
PHE2	TRINITY_DN9784_c0_g1	1.06	1.19	56.073	0.00818993887466707
EJ2	TRINITY_DN8782_c1_g2	0.00	-0.59	1553.64	0.00773395372372358
PHE2	TRINITY_DN77534_c0_g1	0.94	0.08	0.887	0.736696708724709
AGL62	TRINITY_DN40442_c0_g2	0.59	-0.38	32.827	0.261684955404918
MADS3	TRINITY_DN19671_c1_g1	0.54	-0.03	1571.01	0.0139756154344428

PSY	maker-VaccDscaff40-augustus-gene-261.26	1.03	1.36	0.00318472014252185
BCH	maker-VaccDscaff20-augustus-gene-17.33	1.41	2.53	0.00551524754353847
ZDS	maker-VaccDscaff31-snap-gene-199.32	1.01	0.0	0.000193070167856835
CYP450-BCH	maker-VaccDscaff29-augustus-gene-52.39	0.98	1.63	0.000206344276354788
LUT1	augustus_masked-VaccDscaff10-processed-gene-213.0	2.94	0	2.77225695012847e-05
ABA-8'hyd	maker-VaccDscaff47-augustus-gene-7.20	1.89	-1.42	0.00155443740615647
ABA-8'hyd	maker-VaccDscaff30-augustus-gene-239.28	1.75	-1.88	0.00024338545929852
NCED1	augustus_masked-VaccDscaff5-processed-gene-375.4	2.84	1.42	6.12345481869073e-09
NCED2	augustus_masked-VaccDscaff8-processed-gene-51.4	2.76	1.69	1.97724995875247e-10
NCED3	augustus_masked-VaccDscaff1-processed-gene-398.3	1.84	1.22	0.00180227049894788
PHYB	maker-VaccDscaff5-augustus-gene-14.24	1.15	0	0.000481855855030434
COP1	maker-VaccDscaff5-augustus-gene-212.35	1.76	-1.55	0.000202697305224461
CRY2	maker-VaccDscaff26-augustus-gene-28.22	0	1.9	0.000696468547543756
ELF3	maker-VaccDscaff25-snap-gene-13.33	1.22	0	0.00504026741037277
PRR5	maker-VaccDscaff20-augustus-gene-6.43	-1.85	1.71	0.872645955273502
CK2α	maker-VaccDscaff23-snap-gene-302.37	1.49	1.85	0.00010135944984272
FT	maker-VaccDscaff17-augustus-gene-209.31	0	2.84	0.000715164095418072
STX1-4	snap_masked-VaccDscaff39-processed-gene-265.17	0.87	-1.45	0.000723775461031569
STX5	augustus_masked-VaccDscaff30-processed-gene-264.6	2.44	1.71	6.17863290548414e-07

STX6	maker-VaccDscaff28-snap-gene-311.50	0.67	0		6.17863290548414e-07
STX7	maker-VaccDscaff30-augustus-gene-302.32	1.49	0		6.32552208809001e-05
STX16	maker-VaccDscaff2-augustus-gene-326.19	0.9	0		0.000425068587827104
Bos1	maker-VaccDscaff28-snap-gene-93.28	2.12	1.72		6.17863290548414e-07
Gos1	maker-VaccDscaff16-augustus-gene-227.28	1.68	0		0.000436017008759363
Ykt6	maker-VaccDscaff37-augustus-gene-275.24	1.52	0		6.000079411515e-05
Syp7	maker-VaccDscaff10-snap-gene-227.21	1.65	1.79		0.00106698165174146
Sec20	maker-VaccDscaff41-snap-gene-166.28	1.18	0		0.000632509215119724
Sec22	maker-VaccDscaff27-snap-gene-334.44	1.22	1.33		0.000269214174128016
ABC	maker-VaccDscaff27-snap-gene-325.31 / maker-VaccDscaff27-snap-gene-78.27	2.27	-2.5		1.23375747176032e-24
HY5	maker-VaccDscaff39-snap-gene-182.31	0.96	-0.87		0.000742615247188214
MATE efflux	TRINITY_DN6830_c0_g1	-2.49	-2-26	476.48	3.26979036798978e-25
MATE efflux	TRINITY_DN5394_c0_g2	-2.48	-1.62	1529.10	3.9585080445247e-14
MATE efflux	TRINITY_DN5202_c0_g1	1.59	0.92	466.39	6.99225449632855e-11
GSTF12	TRINITY_DN2833_c0_g1_i3	1.82	0.72	925	6.99357e-129
GSTT1	TRINITY_DN955_c5_g1_i3	1.21	0.92	1071	1.10917e-119

Supplementary table S10. List of MBW complex (MYBs, bHLH and WD-40) transcription factor families from bilberry and their corresponding unigene IDs identified from the online PlantTFCat tool

Transcription factor family	Transcript / Unigene ID	Interproscan domain ID
bHLH	TRINITY_DN6043_c1_g1_i2, TRINITY_DN4567_c0_g1_i3, TRINITY_DN789_c4_g1_i1, TRINITY_GG_6055_c0_g1_i1, TRINITY_DN14804_c1_g1_i2, TRINITY_DN14378_c0_g1_i2, TRINITY_DN25455_c0_g1_i1, TRINITY_DN6085_c0_g1_i1, TRINITY_DN16474_c0_g1_i1, TRINITY_DN30998_c0_g1_i1, TRINITY_DN4018_c0_g2_i1, TRINITY_GG_17951_c0_g1_i1, TRINITY_DN16301_c1_g1_i2, TRINITY_GG_22982_c6_g1_i1, TRINITY_DN398_c1_g1_i5, TRINITY_DN3836_c2_g1_i4, TRINITY_DN4786_c0_g2_i1, TRINITY_DN5792_c0_g4_i1, TRINITY_DN5957_c0_g1_i1, TRINITY_DN15043_c0_g1_i1, TRINITY_DN11562_c0_g1_i2, TRINITY_DN1108_c0_g5_i2, TRINITY_DN27689_c0_g1_i4	IPR011598
WD-40	TRINITY_DN5929_c0_g1_i1, TRINITY_DN7980_c0_g1_i1, TRINITY_DN7980_c0_g1_i1, TRINITY_DN19010_c0_g1_i1, TRINITY_GG_22935_c7_g1_i1, TRINITY_GG_7965_c0_g1_i1, TRINITY_GG_20136_c0_g1_i1, TRINITY_GG_5675_c0_g1_i1, TRINITY_DN11429_c0_g1_i13, TRINITY_DN9428_c2_g1_i1, TRINITY_GG_13342_c6_g1_i4, TRINITY_DN5724_c0_g1_i1, TRINITY_GG_15476_c0_g1_i2, TRINITY_DN75621_c0_g1_i1, TRINITY_DN75621_c0_g1_i1, TRINITY_DN75621_c0_g1_i1, TRINITY_GG_17409_c0_g1_i10, TRINITY_GG_17409_c0_g1_i10, TRINITY_GG_8315_c5_g1_i1, TRINITY_DN8991_c0_g1_i1, TRINITY_GG_15350_c0_g1_i2 TRINITY_DN1920_c0_g1_i1, TRINITY_GG_5621_c44_g1_i9, TRINITY_DN6112_c0_g1_i7	IPR001680, IPR001841, IPR017986, IPR019775, IPR000210, IPR011333, IPR015943
MYB **MYB/SANT** **MYB-HB like**	TRINITY_DN45038_c0_g1_i1, TRINITY_DN1852_c0_g1_i5 TRINITY_DN197_c1_g6_i1, TRINITY_DN197_c1_g1_i1, TRINITY_DN29014_c0_g1_i1, TRINITY_DN13284_c0_g1_i1, TRINITY_DN13284_c0_g1_i1 TRINITY_DN2719_c0_g1_i10, TRINITY_DN2372_c0_g1_i10, TRINITY_DN197_c1_g6_i1, TRINITY_DN14067_c0_g2_i2, TRINITY_GG_24282_c4_g1_i1, TRINITY_DN6140_c0_g1_i1, TRINITY_DN2451_c0_g1_i10TRINITY_DN2451_c0_g1_i10, TRINITY_DN7060_c5_g1_i1,	IPR001005, IPR015495, IPR017877 IPR006447, IPR009057, IPR017884,

	TRINITY_DN197_c1_g1_i1, TRINITY_DN19359_c0_g1_i1, TRINITY_DN5307_c0_g1_i2, TRINITY_GG_637_c8_g1_i7, TRINITY_GG_12318_c1_g1_i1TRINITY_GG_22921_c3_g1_i1, TRINITY_DN10709_c0_g1_i1, TRINITY_DN33909_c0_g2_i7, TRINITY_DN29014_c0_g1_i1, TRINITY_DN13284_c0_g1_i1, TRINITY_DN13284_c0_g1_i1, TRINITY_DN5573_c0_g1_i3 TRINITY_DN17117_c0_g1_i2, TRINITY_DN5738_c0_g1_i10, TRINITY_GG_4910_c3_g1_i1, TRINITY_DN11767_c0_g1_i4, TRINITY_DN3930_c5_g1_i2, TRINITY_DN2889_c0_g1_i1, TRINITY_GG_17611_c36_g1_i1, TRINITY_DN23081_c0_g1_i1, TRINITY_DN6289_c0_g1_i4, TRINITY_DN7565_c0_g1_i2, TRINITY_DN68146_c0_g2_i1	IPR017930 IPR001005, IPR006447, IPR009057, IPR017884, IPR017930, IPR017877 IPR015495

Supplementary data (Paper 2)

Flavonoid biosynthesis is differentially altered in detached and naturally ripening attached bilberries in response to spectral light quality

Amos Samkumar[1], Katja Karppinen[1], Tony K. McGhie[2], Richard V. Espley[3], Inger Martinussen[4], Laura Jaakola[1,4]

[1]Department of Arctic and Marine Biology, UiT The Arctic University of Norway, Tromsø, Norway

[2]The New Zealand Institute for Plant & Food Research Ltd., Palmerston North, New Zealand

[3]The New Zealand Institute for Plant & Food Research Ltd., Auckland, New Zealand

[4]Norwegian Institute of Bioeconomy Research, Ås, Norway

Number of figures: 2

Number of tables: 3

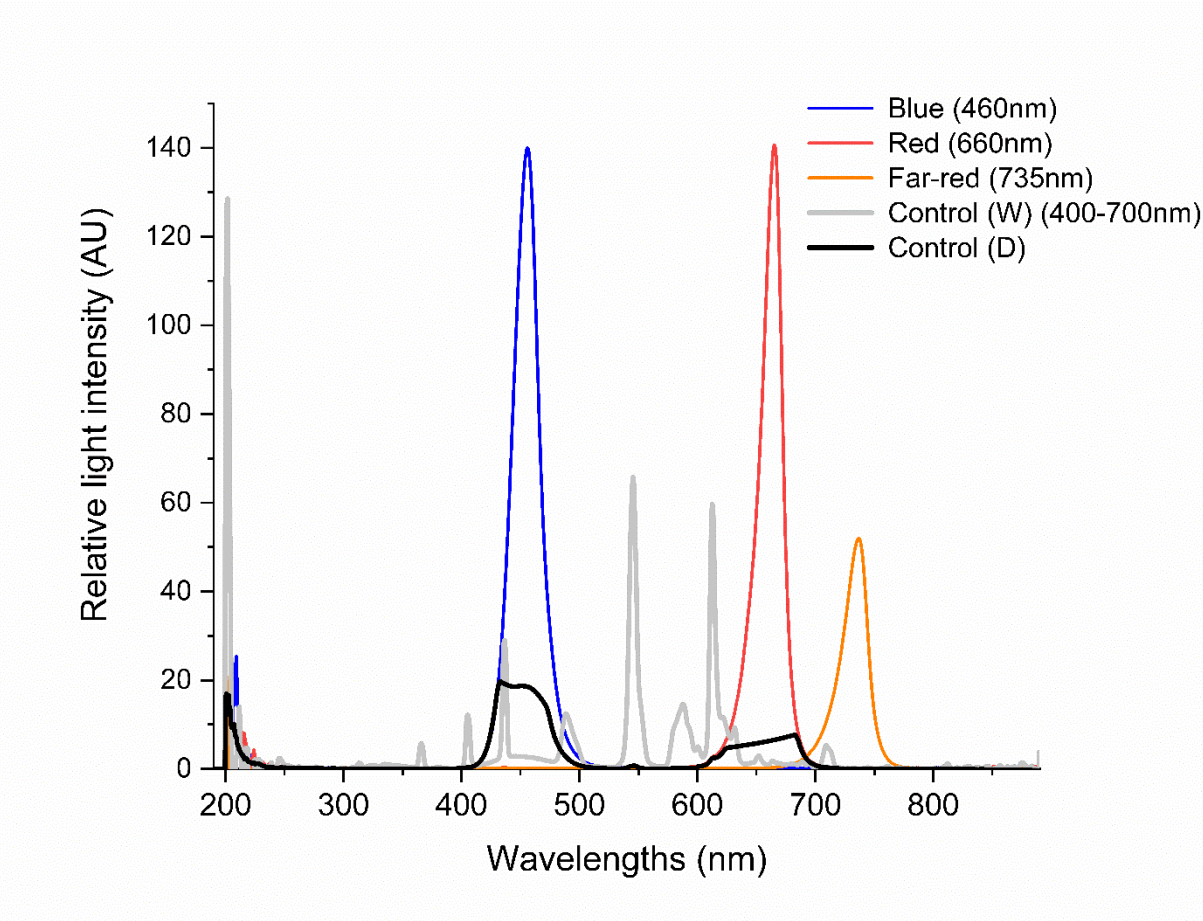

Fig S1. Supplemental blue (460 nm), red (660 nm) and far-red (735nm) light treatments provided for bilberry plants by Heliospectra LED lamps alongside control (400-700 nm). Relative intensities of light spectra from the treatments expressed in arbitrary units (AU).

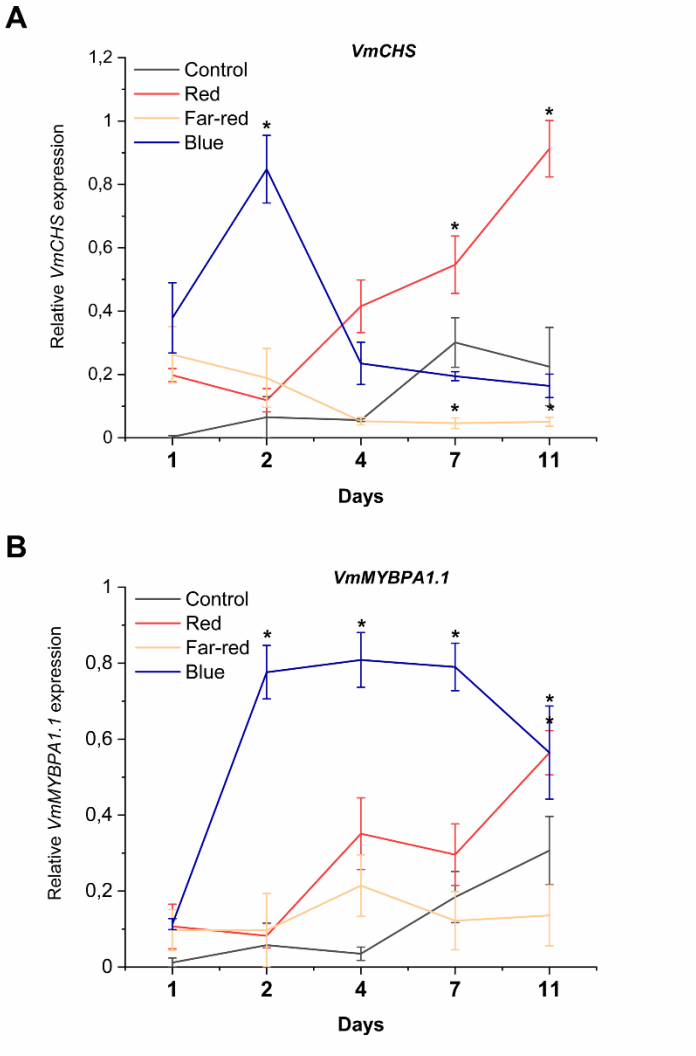

Fig S2. Effect of light spectral treatment on gene expression of a major flavonoid biosynthetic gene and a regulatory gene in bilberry leaves, Chalcone synthase (*VmCHS*) **(A)**, R2R3-MYB transcription factor (*VmMYBPA1.1*) **(B)**. The expression levels are normalized to the reference gene *VmGAPDH* (Glyceraldehyde 3-phosphate dehydrogenase). Error bars represents ±SE of three biological replicates and significant differences between control and light treatments were analyzed by comparison of means using student's t-test (indicated in asterisks*) with p-value ≤ 0.05.

Supplementary table S1. List of primers used in qRT-PCR analysis

Gene	Forward primer sequence	Reverse primer sequence
VmCHS	CCAAGGCCATCAAGGAATG	TGATACATCATGAGTCGCTTCAC
VmANS	GCAACTCTTCTACGAGGGCAAA	CCTGTGGAGAATGCTCTTGCAC
VmMYBA1	CTCGACCACAAACCTTGTCCA	GCCTCCTCATTTGATCCGTCA
VmDFR	GAAGTGATCAAGCCGACGAT	ATCCAAGTCGCTCCAGTTGT
VmF3'H	TTCTTCGACACCCGAAAGTC	TCGAACCCTTTGGAATGAAG
VmF3'5'H	GATTGCGTGGATGGACTTACA	AAATCTGGGTTCCCTTTACGC
VmUFGT	CATCCAAACCCTGTTCCCATCC	TCATCCCTGCCTTCAAGCTCTC
VmMYBPA1.1	GGACATTCAACGCCAATCTGGT	CGGCAAAGGAATCCAACTGAAG
VmCOP1a	GGAAAATTTGCCGATTCGTA	GATCCGGCATCTTCATCAGT
VmCOP1b	TGAGAAATGTCAGCCAACCA	CTCTAAATGTGCGCAGTGGA
VmHY5	GGGAGGAAGTAAGGTCCAAATG	TATAGGGTTACCGGGAGGAATG
VmGAPDH	CAAACTGTCTTGCCCCACTT	CAGGCAACACCTTACCAACA
VmActin	TTCCCTGGGATTGCTGATAG	GGTCTTGGCAATCCACATCT

Supplementary table S2: Concentration of different classes of anthocyanin compounds (mg $100g^{-1}$ DW) quantified by LC-MS in fully ripe bilberries at the end of spectral light treatment from both experimental setups. The amounts are expressed in average of three replicates ± SE. DEL-Delphinidins, CYA-Cyanidins, MAL-Malvidins, PEO-Peonidins, PET-Petunidins; GLU-Glucoside, GAL-Galactoside, ARA-Arabinoside. Different letters indicate significant difference from pairwise comparison by ANOVA followed by Tukey's post-hoc test (p-value=0.05).

	Attached berries					Detached berries				
	Control (W)	**Control (D)**	**Far-Red**	**Red**	**Blue**	**Control (W)**	**Control (D)**	**Far-Red**	**Red**	**Blue**
DEL_GLU	274±15.32^{a}	151±31.66^{a}	204±15.09^{a}	387±6.68^{a}	227±71.25^{a}	178±32.76^{a}	177±20.25^{a}	170±10.26^{a}	213±37.12^{a}	397±130.32^{a}
DEL_GAL	279±13.72^{ab}	126±27.79^{b}	193±16.53^{b}	542±23.36^{a}	146±103.39^{b}	166±24.35^{a}	151±17.42^{a}	164±9.17^{a}	205±33.17^{a}	385±122.66^{a}
DEL_ARA	402±18,23^{ab}	151±23.29^{b}	219±26.66^{b}	600±66.65^{a}	139±114.33^{b}	419±56.90^{a}	253±46.23^{a}	353±3.77^{a}	506±46.72^{a}	508±61.99^{a}
	955	**428**	**616**	**1529**	**512**	**763**	**581**	**687**	**924**	**1290**
CYA_GLU	247±12.23^{a}	194±30.20^{a}	195±26.51^{a}	175±19.17^{a}	248±81.08^{a}	154±16.94^{a}	296±31.15^{a}	197±15.78^{a}	137±16.53^{a}	294±78.10^{a}
CYA_GAL	236±10.64^{a}	147±27.04^{a}	158±21.64^{a}	230±30.13^{a}	147±133^{a}	126±7.64^{a}	225±24.99^{a}	164±9.77^{a}	117±11.19^{a}	264±68.69^{a}
CYA_ARA	207±4.95^{a}	205±31.05^{a}	154±7.74^{a}	248±14.29^{a}	112±95.70^{a}	233±26.54^{a}	289±50.10^{a}	244±8.72^{a}	251±37.52^{a}	333±29.79^{a}
	690	**546**	**507**	**653**	**507**	**513**	**810**	**605**	**505**	**891**
MAL-GLU	321±25.53^{a}	221±40.35^{a}	279±14.34^{a}	278±13.76^{a}	204±66.50^{a}	279±37.86^{a}	393±43.72^{a}	366±48.13^{a}	325±53.19^{a}	549±142.45^{a}
MAL-GAL	118±14.44^{a}	47±10.63^{a}	79±10.80^{a}	128±7.20^{a}	62±31.65^{a}	97±9.43^{b}	124±16.46^{ab}	145±20.23^{ab}	116±15.68^{b}	228±49.98^{a}
MAL-ARA	124±12.53^{a}	69±7.49^{a}	102±21.63^{a}	134±9.39^{a}	52±22.20^{a}	292±28.53^{a}	257±53.57^{a}	381±23.34^{a}	343±49.79^{a}	355±46.97^{a}
	563	**337**	**460**	**540**	**318**	**668**	**774**	**892**	**784**	**1132**
PEO-GLU	156±15.84^{a}	145±32.63^{a}	133±25.13^{a}	79±7.24^{a}	145±51.3^{a}	123±17.55^{b}	309±31.65^{a}	199±24.81^{ab}	123±15.78^{b}	255±40.37^{ab}
PEO-GAL	34±4.43^{a}	28±7.91^{a}	26±5.48^{a}	23±1.59^{a}	23±18.5^{a}	24±2.99^{b}	69±10.04^{a}	45±6.55^{ab}	25±3.23^{b}	64±10.83^{ab}
PEO-ARA	29±3.04^{a}	35±2.69^{a}	24±5.90^{a}	27±2.10^{a}	19±10.7^{a}	55±6.70^{b}	105±13.32^{a}	94±6.89^{ab}	65±6.62^{b}	80±12.66^{ab}
	219	**208**	**183**	**129**	**187**	**202**	**483**	**338**	**213**	**399**
PET-GLU	282±16.72^{a}	126±25.56^{a}	197±23.57^{a}	288±27.62^{a}	218±64.4^{a}	200±34.56^{a}	189±24.61^{a}	205±25.12^{a}	214±31.92^{a}	363±102.61^{a}
PET-GAL	121±5.72^{ab}	40±8.59^{b}	70±9.10^{ab}	173±15.76^{a}	63±39.5^{b}	76±10.20^{a}	62±8.55^{a}	77±7.13^{a}	84±10.90^{a}	165±46.88^{a}
PET-ARA	152±8.52^{ab}	57±5.89^{b}	88±11.30^{b}	212±23.34^{a}	60±39.1^{b}	200±19.11^{ab}	139±22.81^{b}	195±4.98^{ab}	244±22.19^{a}	228±14.91^{ab}
	555	**223**	**355**	**673**	**341**	**476**	**390**	**477**	**542**	**756**

Supplementary table S3: Concentration polyphenolic compounds (mg $100g^{-1}$ DW) quantified by LC-MS in fully ripe bilberries at the end of spectral light treatment from both experimental setups. The amounts are expressed in average of three replicates ± SE. Que-Quercetin, Mye-Myricetin, Lar-Laricitrin, Syr-Syringetin; glu-glucoside/glucuronide, rha-rhamnoside, gal-galactoside, ara-arabinopyranoside. 1S-3R-(1S,3R)-3-(beta-D-glucopyranosyloxy)-1-methylbutyl (2E)-3-(4-hydroxyphenyl) prop-2-enoate), Caff-4-glu-(E)-caffeoyl 4-glucoside, 5caff-shik-5-O-caffeoylshikimic acid, Chlor acid/Z-Chloro/Neo-chlor-(Z)/neo/Chlorogenic acid, p-tran.cou-p-trans-coumaroyl monotropein, Catechin/Epicatech/Gallocatc -Epicatechin/Gallocatachin, Procya B1/B2/C2 - Procyanidin B1/B2/C2, Nandin-A-Nandinaside A.
Different letters indicate significant difference from pairwise comparison by ANOVA followed by Tukey's post-hoc test (p-value=0.05).

	Attached berries					Detached berries				
	Control (W)	**Control (D)**	**Far-Red**	**Red**	**Blue**	**Control (W)**	**Control (D)**	**Far-Red**	**Red**	**Blue**
Myr-3-glu	5.76±0.58^{b}	2.57±0.49^{c}	7.43±0.47^{ab}	9.26±0.48^{a}	5.02±0.83^{bc}	4.00±0.41^{b}	3.26±0.25^{b}	6.04±0.20^{ab}	4.44±0.27^{ab}	7.18±1.33^{a}
Que-3-ara	14.19±0.40^{a}	13.49±2.96^{a}	16.67±1.50^{a}	20.58±2.32^{a}	11.99±1.34^{a}	16.56±1.15^{a}	16.33±2.37^{a}	20.11±2.81^{a}	19.56±0.98^{a}	16.23±2.00^{a}
Que-3-rha	7.95±1.63^{a}	1.39±0.73^{c}	2.76±0.14^{bc}	5.88±0.40^{ab}	7.68±0.98^{a}	2.54±1.22^{a}	3.03±0.58^{a}	3.88±0.72^{a}	3.44±0.41^{a}	2.32±0.86^{a}
Syr-3-gal	10.16±1.28^{a}	7.19±1.01^{a}	7.33±0.95^{a}	6.85±0.43^{a}	10.18±1.78^{a}	6.91±0.24^{c}	19.38±2.54^{a}	13.77±1.09^{ab}	7.84±1.19^{bc}	16.38±0.59^{a}
Syr-3-glu	1.67±0.22^{a}	0.64±0.32^{a}	1.65±0.21^{a}	1.75±0.06^{a}	1.17±0.21^{a}	1.15±0.16^{c}	1.57±0.45^{bc}	2.64±0.09^{ab}	1.38±0.22^{c}	2.99±0.23^{a}
Lar-3-gal	11.67±0.21^{ab}	5.80±0.74^{b}	6.94±0.52^{b}	10.58±0.67^{ab}	13.42±1.99^{a}	4.30±0.42^{b}	9.03±1.16^{ab}	6.61±0.65^{ab}	4.63±0.68^{ab}	10.54±2.61^{a}
Lar-3-glu	2.12±0.17^{ab}	1.23±0.06^{b}	2.10±0.12^{ab}	3.11±0.05^{a}	1.65±0.30^{b}	1.26±0.23^{b}	1.31±0.14^{b}	2.19±0.05^{ab}	1.27±0.14^{b}	2.90±0.53^{a}
Que-3-gal	47.79±1.20^{a}	52.12±8.6^{a}	53.84±4.1^{a}	64.19±8.2^{a}	37.4±11^{a}	46.88±5.02^{a}	51.81±7.16^{a}	60.28±7.08^{a}	52.85±3.34^{a}	48.29±3.31^{a}
Que-3-glu	82.41±3.19^{a}	85.82±17.4^{a}	109.45±1.^{a}	118.01±6.5^{a}	77.6±3.9^{a}	145.24±9.7^{ab}	107.03±2.1^{b}	130.53±7.0^{ab}	159.42±6.33^{a}	110.90±11.1^{b}
Total Flavonols	**183.72**	**170.25**	**208.17**	**240.21**	**166.17**	**228.84**	**212.75**	**246.05**	**254.83**	**217.73**
1S-3R	125.7±8^{a}	159.8±25.2^{a}	131.6±10.8^{a}	170.7±8.69^{a}	215.4±15^{a}	336.0±7.2^{a}	286.4±8.5^{abc}	181.2±14.5^{c}	324.3±50.9^{ab}	210.4±43.3^{bc}
Caff-4-glu	128.6±21^{b}	178.8±32^{ab}	275.8±17.2^{a}	99.5±8.41^{b}	128.2±32.3^{b}	68.3±5.1^{b}	197.2±34.37^{a}	124.3±3.92^{ab}	67.0±1.42^{b}	52.0±8.67^{b}
5Caff-shik	13.8±1.5^{bc}	11.0±1.9^{bc}	27.0±2.68^{a}	6.1±0.12^{c}	17.3±2.16^{b}	21.5±0.4^{a}	13.7±1.48^{ab}	14.5±3.2^{ab}	21.5±0.59^{a}	9.1±1.78^{b}
Chlor acid	190.5±7.2^{a}	284.6±67^{a}	276.7±16.4^{a}	174.9±3.71^{a}	303.8±20.49^{a}	370.1±35^{ab}	423.8±3.10^{s}	265.2±4.19^{ab}	368.0±69.9^{ab}	201.8±70^{b}

Z-Chloro	12.4±2.96^{a}	25.0±7.28^{a}	27.2±0.59^{a}	16.2±0.62^{a}	14.0±4.22^{a}	31.1±1.2^{ab}	43.5±1.58^{a}	25.2±1.47^{ab}	42.5±8.15^{a}	19.4±6.08^{b}
Neo-chlor	4.0±0.23^{a}	5.1±2.55^{a}	5.5±0.77^{a}	4.0±0.28^{a}	7.3±0.07^{a}	8.7±0.25^{a}	7.2±1.16^{a}	4.9±0.44^{a}	8.0±1.35^{a}	5.2±0.60^{a}
p-tran.cou	1049.3±65^{ab}	493.9±77.7^{c}	1268.0±104^{a}	760.8±76^{bc}	861.6±100^{abc}	1252.3±147^{a}	737.8±102^{b}	854.3±23.2^{ab}	1190.7±138^{ab}	711.8±92.1^{b}
Epicatech	56.12±11^{a}	96.91±21.1^{a}	108.09±1.39^{a}	76.62±3.93^{a}	53.99±27.8^{a}	110.78±4.43^{a}	103.15±7.34^{a}	74.40±2.93^{a}	119.13±2.17^{a}	74.10±4.1^{a}
Catechin	0.72±0.7^{b}	1.77±0.2^{ab}	1.62±0.02^{ab}	4.07±0.12^{a}	1.07±1^{b}	3.13±0.14^{a}	1.35±0.68^{a}	1.18±0.59^{a}	3.25±0.32^{a}	2.71±0.4^{a}
Procya B1	0.00^{a}	1.09±1^{a}	3.04±0.27^{a}	1.12±1^{a}	0.72±0.7^{a}	5.07±0.20^{a}	2.74±0.48^{a}	3.02±0.40^{a}	5.12±0.76^{a}	2.36±1.43^{a}
Procya B2	88.19±15^{b}	141.10±28^{ab}	180.66±4.5^{a}	123.10±4.3^{ab}	100.57±32^{ab}	190.53±5.04^{a}	176.73±4.98^{a}	135.43±3.99^{a}	185.15±5.8^{a}	120.62±25.1^{a}
Procya C1	35.93±6.1^{b}	59.41±16^{ab}	83.39±3.3^{a}	48.71±0.29^{ab}	26.41±15.7^{b}	86.24±2.06^{a}	62.82±6.18^{a}	55.06±0.43^{a}	77.53±5.99^{a}	45.55±11.71^{a}
Gallocatec	1.98±0.1^{b}	0.00^{b}	0.42±0.4^{b}	8.11±0.14^{a}	1.10±1^{b}	2.80±0.3^{ab}	0.00^{c}	0.51±0.5^{bc}	4.60±0.18^{a}	3.21±0.84^{a}
Nandin A	66.55±6.7^{a}	100±18^{a}	61.16±8^{a}	40.08±2.94^{a}	44.16±5.87^{a}	91.79±12.8^{b}	190.25±41.5^{a}	103.73±3.37^{b}	113.26±16^{ab}	70.15±6.1^{b}
Leuco-cyanidin	22.53±4.2^{a}	28.91±10.2^{a}	34.37±1.6^{a}	51.26±0.28^{a}	26.87±23^{a}	39.69±5.03^{a}	41.38±2.58^{a}	33.42±3.29^{a}	43.13±3.15^{a}	50.63±8.65^{a}

Supplementary data (Paper 3)

Insights into sugar metabolism during bilberry (*Vaccinium myrtillus* L.) fruit development

Amos Samkumar[1], Katja Karppinen[1], Binita Dhakal[1], Inger Martinussen[2], Laura Jaakola[1,2]

[1]Department of Arctic and Marine Biology, UiT The Arctic University of Norway, Tromsø, Norway

[2]Norwegian Institute of Bioeconomy Research, Ås, Norway

Number of tables: 2

Supplementary Table 1. The Identified sugar metabolism genes from *V.myrtillus* fruit. The corresponding sequences are retrieved from *V.virgatum* and their TSA (Transcriptome Shotgun Assembly) IDs are provided in the following column. The gene query matches with the highest similarity and its corresponding transcript and unigene IDs from the two *V. myrtillus* transcriptomes datasets were shown in the next two columns. The homologous genes with other related species are shown in next column with identities expressed in percentages. The last column represents the subcellular localization of all the identified isoforms of invertases using Plant mSub-P tool. The likelihood scores for cellular localization are shown in brackets in the range of 1 (NA-not applicable).

Gene name	Sequence_ID from TSA Database (*V. virgatum*)	SRA_ID (*V.myrtillus*) and identity match (%)	Unigene_ID (*V.myrtillus)* and identity match (%)	Related species identity match (%)	Sub-Cellular localization (Plant-mSubP)
Cell wall invertase 1 (CWINV1)	GGAB01072872.1	729392 (97%)	TRINITY_DN2977_c2_g1_i2 (98%)	*NC034011(P. persica)* (66%)	Cell wall (0.7)
Cell wall invertase 2 (CWINV2)	GGAE01109889.1	976747 (97%)	TRINITY_DN58605_c0_g1_i1 (98%)	*NW021025375(C. sinensis)* (82%)	Cell wall (0.9)
Cell wall invertase 3 (CWINV3)	GGAE01121540.1	1364501 (99%)	TRINITY_DN17376_c0_g1_i10 (96%)	*NC012010(V. vinifera)* (64%)	Cell wall (0.3)
Neutral invertase 1 (NINV1)	GGAE01022874.1	1523998 (99%)	TRINITY_DN2901_c0_g1_i1 (99%)	*KF718860(C. sinensis)* (84%)	Plastid (0.5)
Neutral invertase 2 (NINV2)	GGAE01119103.1	783733 (95%)	TRINITY_DN7461_c0_g1_i1 (93%)	*CM014052(M. domestica)* (76%)	Plastid (0.6)
Neutral invertase 3 (NINV3)	GGAE01011826.1	1386518 (99%)	TRINITY_GG_15949_c0_g1_i1 (99%)	*NC_012012(V. vinifera)* (79%)	Cytoplasm (0.2)
Neutral invertase 4 (NINV4)	GGAE01062287.1	1278054 (98%	TRINITY_DN141831_c0_g1_i1 (100%)	*KP053405(C. sinensis)* (88%)	Plastid (0.6)
Neutral invertase 5 (NINV5)	GGAE01030565	1057615 (99%)	TRINITY_GG_11522_c76_g1_i1 (90%)	*NC034016(P. persica)* (86%)	Cytoplasm (0.2)

Vacuolar invertase 1 (VINV1)	GGAE01006295.1	505506 (97%)	TRINITY_DN4663_c0_g1_i3 (78%)	*KU884473(C. sinensis)* (76%)	Vacuole (0.7)
Vacuolar invertase 2 (VINV2)	GGAB01063390.1	1675652 (98%)	TRINITY_DN4663_c0_g1_i3 (97%)	*NC012022.3(V. vinifera)* (67%)	Vacuole (0.7)
Hexokinase 1 (HK1)	GGAE01107266.1	1301214 (100%)	TRINITY_DN381_c0_g3_i3 (99%)	*NC034015(P. persica)* (83%)	NA
Hexokinase 2 (HK2)	GGAE01118471.1	1529550 (99%)	TRINITY_DN381_c0_g3_i3 (85%)	*AM456450.2 (V. vinifera)* (83%)	NA
Hexokinase 3 (HK3)	GGAE01031242.1	-	TRINITY_DN6805_c0_g2_i7 (99%)	*JN118545.1(V. vinifera)* (82%)	NA
Hexokinase 4 (HK4)	GGAB01088020.1	1137583 (99%)	TRINITY_DN6900_c1_g1_i3 (99%)	*NC041799(M. domestica)* (72%)	NA
Fruktokinase 1 (FK1)	GGAE01074415.1	1269317 (100%)	TRINITY_GG_25277_c0_g1_i1 (98%)	*NW021026114(C. sinensis)* (78%)	NA
Fruktokinase 2 (FK2)	GGAB01032707.1	1052446 (98%)	TRINITY_DN1834_c1_g3_i2 (99%)	*XM008378279(M. domestica)* (84%)	NA
Fruktokinase 3 (FK3)	GGAB01048669.1	232383 (97%)	TRINITY_DN28664_c0_g2_i3 (99%)	*JX067537(A. chinensis)* (85%)	NA
Fruktokinase 4 (FK4)	GGAB01032403.1	1177935 (99%)	TRINITY_GG_8267_c0_g1_i1 (98%)	*JX067535(A. chinensis)* (90%)	NA
Fruktokinase 5 (FK5)	GGAB01084714.1	1423238 (96%)	TRINITY_GG_983_c0_g1_i1 (97%)	*NC012011(V. vinifera)* (86%)	NA
Sucrose synthase (SS)	GGAE01053339	826437 (97%)	TRINITY_GG_1104_c141_g1_i1 (99%)	*NC041805(M. domestica)* (77%)	NA
Sucrose-phosphate phosphatase 1 (SPP1)	GGAE01112488.1	664663 (99%)	TRINITY_DN6169_c0_g1_i1 (99%)	*AY509994(A. chinensis)* (87%)	NA
Sucrose-phosphate phosphatase 2 (SPP2)	GGAB01063835.1	1470994 (96%)	TRINITY_DN43187_c0_g1_i1 (98%)	*NC012014.3(V. vinifera)* (68%)	NA

Sucrose-phosphate synthase 1 (SPS1)	GGAE01109516.1	554516 (99%)	TRINITY_GG_21764_c3_g1_i1 (99%)	*AF318949(A. chinensis)* (85%)	NA
Sucrose-phosphate synthase 2 (SPS2)	GGAB01078977.1	324571 (99%)	TRINITY_GG_1633_c14_g1_i2 (99%)	*NC012017(V. vinifera)* (78%)	NA
Sucrose-phosphate synthase 3 (SPS3)	GGAE01036876.1	1146340 (97%)	TRINITY_GG_12565_c121_g1_i1 (99%)	*ONI28760.1(P. persica)* (82%)	NA

Supplementary Table 2. List of primers used in qRT-PCR analysis.

Gene	**Forward primer sequence**	**Reverse primer sequence**
VmCWINV1	GTGGACCGAAGCCAAACAACCT	GCCCAGTCTTCGATGTCTCGAT
VmCWINV2	CTCTGATGCAACCAGTTCCTCT	CTCCTGAGGGAAAGCTTCTTGT
VmCWINV3	GGCTTCAGTCGTTTCCAAGMC	CCACCCTTGAGCTCTGTATCAT
VmVINV1	TGATGACCTCTTGAAGGGTTGG	AGCAGGGAATTCAGTACCGTTC
VmVINV2	TTGCTCAAGGAGGGAGAACAGT	TATAAGCCGAGTCCATCGACCA
VmNINV1	GGCCTGCATTAAGATGAAGAGG	TTCCCTACAAATCTCCCACTGC
Vm NINV2	GAAGTCCTAGACCCAGATTTCG	CCAGTTACCTTCCCATAAGCAC
Vm NINV3	GAAGGCGAGGAGTGGAGAATTA	TGCGTCTCTCGGCTATCTTAAC
Vm NINV4	CCGTTAGACAGTTGGCCTGAAT	TCCTCCCAGTACAGCAAAGAAG
Vm NINV5	GAGTGGTTAAGCGTCTTCATGC	TCCATTCAGGGAGAGAATCAGG
VmFK1	GCACAACTAGCTGAGGATGACA	ATTGCACCTCTCTCCTTGACAG
VmFK2	CTGAAGGGTCAGATGGTTGCAGA	AATGCATCACCAGCACCAGTCG
VmFK3	TTTACCAGGACGAGGAGCGATT	CTTTCGTCGGTAAGGCAGGAAT
VmFK4	ACCGCTGATGAACTCAATCTCG	ACCTCCATCGCCTTTAAGTGAG
VmFK5	CCAGGCTGAAGTGATAAAGGTG	CACCAATGGTCACAAGGAGAAG
VmHK1	GGAGGCAGATACTACGACTCAA	AGGTAGTAGACCATGCCACTTG
VmHK2	GGGCACTCTCGTTAAATGGACA	CACACGCATATCGAGACCAACT
VmHK3	TGTCTGCCCTGGTCAATGAT	TACTCTGGCATCCATGTCC

VmHK4	GAAGTTGAGAAGAACGGTCGTG	GATTTCAGTCACGGCTTCATCC
VmSPS1	GGCATGGTCAAAGGGTGTTCTA	CTCCTCAACGCTGGGAATTTAC
VmSPS2	AGGAGGCTTTAATCCTGTGGAC	CGGAAGACTCACCTTCTGAGTT
VmSPS3	GAGCTGCTTAGAACAGCTGGAA	CTTCGCTTCTGCATTGGTGTAG
VmSPP1	AGCACTAAGTCTTCCGTCCTGT	TGACTTGATCTACCCACACTCG
VmSPP2	GTTTGACAAGTGGGAGCTGTCT	ATACGAGCCCATCTGGTACTTC
VmSS	CGGGGTCTCTGGTTTTCACAT	CCCGTACAAAGATCCCATGTTC
VmGAPDH	CAAACTGTCTTGCCCCACTT	CAGGCAACACCTTACCAACA
VmActin	TTCCCTGGGATTGCTGATAG	GGTCTTGGCAATCCACATCT